

Aus dem Bereich Biologie
der Medizinischen Fakultät der Universität des Saarlandes, Homburg/Saar,
und dem
Institut für Immunologie, Centre de Recherche Public de la Santé, Luxembourg

Vorbereitungsmaßnahmen gegen Influenza A Virus:
Charakterisierung von NS Gen-Reassortanten und der antiviralen
Wirksamkeit tanninreicher Pflanzenextrakte

Influenza A Virus Preparedness: Characterization of NS Gene
Reassortants and the Antiviral Efficacy of Tannin-rich Plant Extracts

Dissertation

zur Erlangung des Grades des Doktors der Naturwissenschaften
der Medizinischen Fakultät
der UNIVERSITÄT DES SAARLANDES

2014

vorgelegt von

Linda Theisen

Geb. am 11. März 1984 in Bad Pyrmont

Declaration of Previous Publication

Parts of this thesis are in preparation for publication or have been published as follows:

Linda L. Theisen, Sandra Gohrbandt, Sophie A. Kirschner, Aurélie Sausy, Regina Brunnhöfer, Jürgen Stech, Claude P. Muller; Characterization of pandemic H1N1/2009 influenza A virus reassortants carrying heterologous NS genes reveals a role of a naturally occurring NS1 five amino acid deletion in host gene regulation. In preparation.

Linda L. Theisen, Claude P. Muller (2012), EPs® 7630 (Umckaloabo®), an extract from *Pelargonium sidoides* roots, exerts anti-influenza virus activity *in vitro* and *in vivo*, Antiviral Research 94: 147–56.

Linda L. Theisen, Clemens A. J. Erdelmeier, Gilles A. Spoden, Fatima Boukhallouk, Aurélie Sausy, Luise Florin, Claude P. Muller (2014), Tannins from *Hamamelis virginiana* bark extract: Characterization and improvement of the antiviral efficacy against influenza A virus and human papillomavirus, PLOS ONE 9: e88062.

Index of Contents

Declaration of Previous Publication	I
Index of Contents	II
Index of Figures	VI
Index of Tables	VII
Index of Amino Acids.....	VIII
Index of Abbreviations.....	IX
1 Abstract (German and English).....	1
1.1 Zusammenfassung	2
1.2 Abstract.....	5
2 Introduction	8
2.1 Influenza A Virus	9
2.1.1 Classification and nomenclature	9
2.1.2 Genomic organization and encoded proteins	9
2.1.3 Viral life cycle	11
2.2 The IAV NS1 protein	13
2.2.1 Structure and localization of NS1	13
2.2.2 Functions of NS1	13
2.3 IAV strain variability	18
2.3.1 The basis of strain variability: point mutations and reassortments	18
2.3.2 Host species and host range restriction	19
2.3.3 IAV strains circulating in humans, birds and swine.....	21
2.3.4 Reverse genetics: a tool to generate <i>in vitro</i> mutants and reassortants	27
2.4 Antiviral prevention, treatment and resistance	30
2.4.1 Vaccination.....	30
2.4.2 Currently marketed antiviral drugs and antiviral resistance.....	31
2.4.3 Antiviral drugs in development and novel strategies	32

2.4.4	NS1-based vaccine and antiviral approaches	33
2.4.5	Tannin- and pseudotannin-based antiviral approaches	34
2.5	Objectives of the study	37
3	Materials	39
3.1	Animals.....	40
3.2	Cells.....	40
3.2.1	Cell lines.....	40
3.2.2	Cell culture media	41
3.3	Viruses.....	41
3.3.1	Wild type viruses.....	41
3.3.2	Recombinant influenza viruses	42
3.3.3	Virus growth media.....	43
3.4	Bacteria.....	43
3.4.1	Bacteria strains	43
3.4.2	Bacteria growth media	43
3.5	Antiviral drugs and plant extracts.....	44
3.6	Solutions, chemicals, reagents.....	44
3.7	Enzymes.....	47
3.8	Antibodies.....	47
3.9	Commercial Kits.....	47
3.10	Buffers.....	48
3.11	DNA: Plasmids and primers	49
3.11.1	Plasmids	49
3.11.2	Primers	50
3.12	Instruments.....	55
3.13	Software	56
4	Methods.....	57
4.1	Construction of IAV pH1N1, NS reassortants and NS mutants by reverse genetics	58
4.1.1	Reverse genetics plasmid construction and isolation.....	58
4.1.2	Virus rescue from plasmids.....	63

4.2	Virus culture and quantification of rescued and wild type viruses.....	63
4.2.1	Cultivation of cell lines	63
4.2.2	Expansion of influenza virus stocks.....	63
4.2.3	TCID50 determination	64
4.2.4	Viral growth kinetics	64
4.3	Investigation of the antiviral host response to different NS1 proteins	64
4.3.1	Determination of cytokine mRNA and pre-mRNA levels by real-time PCR	64
4.3.2	PCR array	65
4.3.3	Luciferase reporter assays	65
4.3.4	IFN resistance assay	66
4.4	Antiviral drug testing	66
4.4.1	Antiviral drug testing <i>in vitro</i>	66
4.4.2	Antiviral drug testing <i>in vivo</i>	70
4.5	Statistical methods	71
5	Results and Discussion	72
5.1	Characterization of pandemic H1N1/2009 IAV reassortants carrying heterologous NS genes reveals a role of a naturally occurring NS1 five amino acid deletion in host gene regulation.....	73
5.1.1	Results	75
5.1.2	Discussion	89
5.2	EPs® 7630 (Umckaloabo®), an extract from <i>Pelargonium sidoides</i> roots, exerts anti-influenza virus activity <i>in vitro</i> and <i>in vivo</i>	93
5.2.1	Results	94
5.2.2	Discussion	105
5.3	Tannins from <i>Hamamelis virginiana</i> bark extract: Characterization and improvement of the antiviral efficacy against influenza A virus	108
5.3.1	Results	110
5.3.2	Discussion	122

6	Conclusions and perspectives	126
7	References	129
8	Annexe	154
8.1	Publications	155
8.2	Conference participations:	156
8.2.1	Oral presentations.....	156
8.2.2	Posters	157
8.3	Acknowledgements	158
	Curriculum vitae.....	160

Index of Figures

Figure 1: Structure of an IAV virus particle	10
Figure 2: The IAV life cycle	12
Figure 3: Inhibition of type I IFN induction by NS1.	14
Figure 4: Inhibition of downstream type I IFN signalling by NS1.	15
Figure 5: Inhibition of general host cell gene expression by NS1.	16
Figure 6: The basis of IAV strain variability: point mutations and reassortments.	18
Figure 7: The IAV host range	19
Figure 8: The genetic origin of the pandemic and seasonal IAV strains from 1918-2009	22
Figure 9: The genetic origin of the pandemic H1N1 (2009).....	23
Figure 10: IAV rescue by reverse genetics	28
Figure 11: Reverse genetics system by Stech et al. used in this study.....	29
Figure 12: Examples of tannin and pseudotannin structures from <i>Hamamelis virginiana</i>	35
Figure 13: Fitness of NS reassortants <i>in vitro</i>	76
Figure 14: Pathogenicity of NS reassortants <i>in vivo</i>	77
Figure 15: NS1 sequence analysis.....	78
Figure 16: Fitness of NS aa 80-84 deletion/insertion mutants <i>in vitro</i>	79
Figure 17: Effect of NS reassortment and aa 80-84 deletion/insertion on IFN- β expression. .	81
Figure 18: Effect of NS reassortment and aa 80-84 deletion/insertion on cytokine mRNA expression.....	82
Figure 19: Effect of NS reassortment and aa 80-84 deletion/insertion on expression of 84 genes involved in the human antiviral host response.....	83
Figure 20: Effect of NS reassortment and aa 80-84 deletion/insertion on general host gene expression.....	87
Figure 21: Effect of NS reassortment and aa 80-84 deletion/insertion on pre-mRNA expression.....	88
Figure 22: Cytotoxicity and antiviral efficacy of EPs® 7630 <i>in vitro</i>	95
Figure 23: Anti-IAV mechanism of EPs® 7630.	97
Figure 24: Anti-IAV activity of tannins from EPs® 7630.....	99

Figure 25: Structures of EPs® 7630 constituents with anti-IAV activity.....	100
Figure 26: Anti-IAV activity of EPs® 7630 <i>in vivo</i>	103
Figure 27: Toxicity of EPs® 7630 <i>in vivo</i>	104
Figure 28: Antiviral activity of Hamamelis bark extract.	111
Figure 29: Anti-IAV activity of UF-concentrate.....	114
Figure 30: Anti-IAV activity of Hamamelis tannins.....	116
Figure 31: Effect of bark extract and UF-concentrate on different IAV life cycle steps.	117
Figure 32: IAV preincubation with Hamamelis extracts or individual compounds.	119
Figure 33: Cell preincubation with Hamamelis extracts or individual compounds.	120
Figure 34: Cytotoxicity or unspecific host cell receptor inhibition of Hamamelis extracts or individual compounds.	121

Index of Tables

Table 1: Human antiviral host response PCR array data	84
Table 2: Cytotoxic and anti-IAV activities of catechin monomers, dimers and oligo-/polymers present in EPs® 7630	101
Table 3: Cytotoxic and anti-IAV activities of Hamamelis extracts	110
Table 4: Cytotoxic and anti-IAV activities of hydrolysable tannins and pseudotannins	112
Table 5: Cytotoxic and anti-IAV activities of Hamamelis extracts and UF-fractions	113
Table 6: Hemagglutination and neuraminidase inhibition of Hamamelis extracts, UF-fractions and individual compounds	118

Index of Amino Acids

Single letter code	Amino acid
A	Alanine
C	Cysteine
D	Aspartic acid
E	Glutamic acid
F	Phenylalanine
G	Glycine
H	Histidine
I	Isoleucine
K	Lysine
L	Leucine
M	Methionine
N	Asparagine
P	Proline
Q	Glutamine
R	Arginine
S	Serine
T	Threonine
V	Valine
W	Tryptophane
X	Undefined amino acid
Y	Tyrosine

Index of Abbreviations

Abbreviation	Full name
2'5'-OAS	2'5'-oligoadenylate synthase
aa	Amino acid
ATF2	Activating transcription factor 2
BSA	Bovine serum albumin
CC50	Half maximal cytotoxic concentration
cDNA	Complementary deoxyribonucleic acid
CHAPS	3-[(3-cholamidopropyl)dimethylammonio]-1-propanesulfonate
CPSF30	Cleavage and polyadenylation specificity factor 30
cRNA	Complementary ribonucleic acid
Ct	Cycle threshold
del	Deletion of five amino acids (TIASV) on position 80-84 of NS1
DMEM	Dulbecco's modified Eagle medium
DMSO	Dimethylsulfoxide
DNA	Deoxyribonucleic acid
dNTP	Deoxyribonucleotidetriphosphate
dsRNA	Double stranded ribonucleic acid
DTT	Dithiotreitol
EC50	Half maximal antiviral concentration
EDTA	Ethylenediaminetetraacetic acid
e.g.	Exempli gratia / for example
EGCG	Epigallocatechin gallate
eIF2 α	Eukaryotic translation initiation factor 2 α
EMEM	Eagle's minimum essential medium
ERK	Extracellular-signal-regulated kinases
FBS	Fetal bovine serum
GFP	Green fluorescent protein
HA	Hemagglutinin
HaCaT	Human adult low-calcium high-temperature, nonvirally transformed keratinocytes
HEPES	2-[4-(2-hydroxyethyl)piperazin-1-yl]ethanesulfonic acid
HIC50	Half maximal hemagglutination inhibiting concentration
HIV	Human immunodeficiency virus
H5N1	Highly pathogenic avian influenza virus
IAV	Influenza A virus
IFN	Interferon
IL	Interleukin

ins	Insertion of five amino acids (TIASV) on position 80-84 of NS1
IRF	Interferon regulatory factor
I κ B- α	NF κ B inhibitor α
Jak	Janus kinase
kDa	Kilodalton
LB	Luria Broth
LPAIV	Low pathogenic avian influenza virus
M	Matrix gene segment
M1/2	Matrix protein 1/2
MDCK	Madin-Darby canine kidney
MEK	Mitogen-activated protein kinase kinase
MES	2-(N-morpholino)ethanesulfonic acid
MLD50	Half maximal mouse lethal dose
MOI	Multiplicity of infection
mRNA	Messenger ribonucleic acid
MUNANA	2'-(4-methylumbelliferyl)- α -D-N-acetylneuraminic acid
n.d.	Not detectable
NA	Neuraminidase
ND	Not determined
NEP	Nuclear export protein
NF κ B	Nuclear factor kappa-light-chain-enhancer of activated B cells
NIC50	Half maximal neuraminidase inhibiting concentration
NLRP3	NOD-like receptor family, pyrin domain containing 3
NOD	Nucleotide-binding oligomerization domain-containing protein
NP	Nucleoprotein
NS	Nonstructural gene segment
NS1/2/3	Nonstructural protein 1/2/3
OD	Optical density
PA	Polymerase acidic
PABPII	PolyA binding protein II
PB1	Polymerase basic 1
PB2	Polymerase basic 2
PBS	Phosphate buffered saline
PCR	Polymerase chain reaction
Pen/Strep	Penicillin / streptomycin
PG	Polymerization grade
PGE	Pyrogallol equivalents
pH1N1	Pandemic H1N1 (2009)
pi	Post infection
PKR	Protein kinase RNA activated
polyA	Polyadenylate
polyI:C	Polyinosinic:polycytidylic acid
RANTES	Regulated on activation, normal T cell expressed and secreted

RIG-I	Retinoic acid inducible gene I
RLU	Relative luminescent units
RNA	Ribonucleic acid
RNase L	Latent RNase
rpm	Revolutions per minute
SDS	Sodium dodecyl sulfate
SI	Selectivity index
SOC	Super optimal broth with catabolite repression
ST	Swine fetal testis cells
STAT	Signal transducer and activator of transcription
T _a	Annealing temperature
TAE	Tris acetate EDTA
TBS	Tris buffered saline
TCID ₅₀	Half maximal tissue culture infectious dose
TNF	Tumor necrosis factor
TPCK	L-1-tosylamido-2-phenylethyl chloromethylketone
UF	Ultrafiltration
UF-conc.	Ultrafiltration concentrate
UF-filt.	Ultrafiltration filtrate
vRNA	Viral ribonucleic acid
vRNP	Viral ribonucleoprotein
wt	Wildtype
XTT	2,3-Bis(2-methoxy-4-nitro-5-sulfohenyl)-2H-tetrazolium-5-carboxanilide

Abbreviations of human antiviral factors determined in the PCR array are explained in Table 1, Section 5.1.1.4.

1 Abstract (German and English)

1.1 Zusammenfassung

Saisonale Influenza-Epidemien verursachen bis zu 500 000 Todesfälle jährlich und belasten die öffentliche Gesundheit erheblich. Zusätzlich zu saisonalen Epidemien kann Influenza A Virus (IAV) weltweite Pandemien verursachen, wie zuletzt 2009 die sogenannte „Schweinegrippe“. Im Jahr 2012 wurde zum ersten Mal ein hochpathogenes Vogelgrippevirus des Subtyps H5 im Labor hergestellt, welches zwischen Frettchen, dem gängigen Tiermodell für menschliche Ansteckung, übertragen werden kann. Ein Vogelgrippestamm des Subtyps H7N9 entstand 2013 in China und infizierte in diesem Jahr über 130 Menschen. Diese Beispiele zeigen die Notwendigkeit effektiver und umfassender Vorbereitungsmaßnahmen gegen IAV, bestehend unter anderem aus der Überwachung aktueller Virusstämme, Prävention, Risikomanagementstrategien und der Bereitstellung ausreichender medikamentöser Behandlungsmöglichkeiten.

Eine effektive Vorbereitungsmaßnahme gegen IAV ist eine gründliche Charakterisierung früherer und aktueller Virusstämme, da hierdurch eine schnelle und korrekte Reaktion auf neue Stämme erleichtert wird. Im ersten Teil der vorliegenden Dissertation wurden NS Reassortanten des pandemischen H1N1 Stammes (pH1N1) revers-genetisch konstruiert und charakterisiert. pH1N1 entstand 2009 als pandemisches Virus. Es zirkuliert heutzutage als saisonaler humaner Stamm, wurde aber auch in Schweinen oder Vögeln nachgewiesen. Dies birgt das Risiko, dass pH1N1 Reassortanten mit aktuellen aviären, porzinen oder humanen Stämmen bildet. Das Nicht-Strukturprotein NS1 ist ein viraler Virulenzfaktor mit der Hauptfunktion, die antivirale Immunantwort des Wirts zu hemmen. Acht Reassortanten, welche NS Gene humaner, aviärer oder porziner Stämme in Kombination mit den restlichen Genen von pH1N1 tragen, wurden revers genetisch hergestellt. pH1N1 erwies sich als sehr empfänglich für NS Gene verschiedener Wirtsspezies: 6 von 8 Reassortanten waren nur minimal in ihrer Replikation in A549 Zellen beeinträchtigt. Interessanterweise waren jedoch pH1N1 Reassortanten mit NS Genen hochpathogener aviärer IAV-Stämme des Subtyps H5N1 in A549 und DF-1 Zellen sowie *in vivo* stark replikationsinhibiert. Sequenzvergleiche des NS1 Proteins von stark und schwach in A549 replizierenden Reassortanten zeigten eine Deletion von fünf Aminosäuren auf Position 80-84. Diese Deletion kommt bei den meisten aktuellen H5N1 Stämmen vor, im Gegensatz zu nicht-H5 Stämmen. Die Deletion der Aminosäuren 80-84 im NS1 Protein von pH1N1 beeinträchtigte die virale Replikation *in*

vitro, was die Abwesenheit dieser Deletion bei fast allen natürlich vorkommenden nicht-H5 Stämmen erklären könnte. Mechanistisch zeigte sich bei NS1 Proteinen aus pH1N1 eine höhere generelle Expression von Wirtsgenen als bei NS1 Proteinen aus hochpathogenen H5N1 Stämmen. Auch der Deletion der Aminosäuren 80-84 konnte eine (zuvor unbekannte) Rolle in der Regulierung der generellen Expression von Wirtsgenen zugewiesen werden. Diese Regulierung findet möglicherweise auf dem Niveau der prä-mRNA Reifung statt.

Die hohe Replikationsfähigkeit der meisten in Teil 1 konstruierten NS Reassortanten, sowie die Vielzahl an natürlich vorkommenden Reassortments und Punktmutationen verdeutlichen die hohe Variabilität von IAV. Diese Variabilität ist die Grundlage für Resistenzen gegen antivirale Substanzen. Daher werden neue, effektive antivirale Wirkstoffe benötigt.

Aus diesem Grund wurde im zweiten Teil dieser Studie ein tanninreicher Pflanzenextrakt aus *Pelargonium sidoides* DC, EPs® 7630 (Umckaloabo®), welcher bereits zur Behandlung akuter Bronchitis zugelassen ist, auf seine antivirale Wirksamkeit untersucht. EPs® 7630 zeigte eine dosisabhängige Aktivität gegen mehrere IAV Stämme. Es hemmte eine frühe Etappe im viralen Lebenszyklus, beispielsweise die Rezeptorinteraktion, aber auch die Neuraminidaseaktivität. EPs® 7630 war nicht viruzid, denn eine Präinkubation des Virus (im Gegensatz zur Präinkubation der Wirtszelle) hemmte die Infektivität nicht. Weiterhin verursachte EPs® 7630 keine Resistenzen über vier Viruspassagen. Kondensierte Tannine und Pseudotannine wurden als antiviral aktive Inhaltsstoffe identifiziert. Die molekulare Kettenlänge beeinflusste die antivirale Aktivität, denn Mono- und Dimere waren weniger wirksam als Oligo- und Polymere. Allerdings waren auch die Monomere Gallocatechin und Epigallocatechin antiviral wirksam. Inhalativ appliziertes EPs® 7630 verbesserte signifikant Überleben und Krankheitsverlauf von IAV-infizierten Mäusen, was erstmals Anhaltspunkte zum Nutzen von EPs® 7630 zur Behandlung von IAV-Infektionen *in vivo* liefert.

Diese Daten bestätigen und detaillieren die antivirale Aktivität von Tanninen gegen IAV. Allerdings kommen verschiedene Tanninklassen und -strukturen oft zusammen in Pflanzenextrakten vor, obwohl sie sich in ihrer antiviralen Wirksamkeit unterscheiden können. Trotzdem gibt es nur wenige systematische Vergleichsuntersuchungen der Struktur-Wirkungs-Beziehungen gegen IAV. Ein besseres Verständnis der antiviralen Wirksamkeit verschiedener Tanninstrukturen gegen IAV ist wichtig um pflanzliche antivirale Arzneimittel erfolgreich zu entwickeln und zu verbessern.

Im dritten Teil dieser Studie wurde *Hamamelis virginiana* L. als Modellpflanze gewählt, da sie reich an verschiedenen gutcharakterisierten Tanninen und Pseudotanninen ist. Hamamelis Rindenextrakt, Fraktionen angereichert mit Tanninen verschiedener Molekulargewichte oder einzelne Tannine/Pseudotannine mit definierter Struktur wurden auf ihre Wirksamkeit gegen IAV getestet. Der Rindenextrakt war gegen verschiedene IAV Stämme wirksam, unter anderem gegen den 2013 erstmals aufgetretenen aviären H7N9 Stamm. Fraktionen mit Tanninen bestimmter Molekulargewichte wurden von Kollaborationspartnern durch die einfache und reproduzierbare Methode der Ultrafiltration hergestellt. Eine mit hochmolekularen kondensierten Tanninen angereicherte Fraktion zeigte die beste Wirksamkeit. Dieses Ultrafiltrations-Konzentrat und der Rindenextrakt inhibierten frühe Etappen des viralen Lebenszyklus am stärksten, beeinflussten aber auch die Neuraminidaseaktivität. Interessante Unterschiede im Wirkmechanismus konnten zwischen verschiedenen (Pseudo)tanninstrukturen gezeigt werden: hochmolekulare kondensierte Tannine und die ebenfalls hochmolekulare Gerbsäure hemmten sowohl die Interaktion mit dem viralen Rezeptor als auch die Neuraminidaseaktivität. Hingegen inhibierten die getesteten niedermolekularen Stoffe (< 500 g/mol) nur die Neuraminidaseaktivität aber nicht die Rezeptorinteraktion. Generell schien die Hemmung der Neuraminidase wenig zur antiviralen Wirksamkeit beizutragen. Interessanterweise waren die hochmolekulare Fraktion sowie der unfraktionierte Rindenextrakt effektiver als alle isolierten Einzelstoffe.

Zusammenfassend leistet diese Dissertation einen Beitrag zu verschiedenen Aspekten der Vorsorge gegen IAV, nämlich zur Charakterisierung von aktuellen und möglicherweise zukünftig auftretenden Stämmen, sowie zur Entwicklung antiviraler Arzneien. Es wurde eine zuvor unbekannte Funktion einer natürlich auftretenden Deletion von fünf Aminosäuren im NS1 Protein identifiziert, nämlich die Regulation der antiviralen Immunantwort der Wirtszelle. Die Erkenntnis, dass pH1N1 die meisten getesteten humanen, aviären und porzinen NS Gensegmente ohne nennenswerten Replikationsverlust aufnahm, zeigt die Notwendigkeit zur Überwachung von pH1N1 NS Reassortanten. Schließlich wurde die antivirale Wirksamkeit von EPs® 7630, einem tanninreichen Pflanzenextrakt mit Zulassung zur Behandlung von akuter Bronchitis, *in vitro* und *in vivo* gezeigt. Die erstellten Struktur-Wirkungs-Beziehungen von Tanninen und Pseudotanninen aus *Pelargonium sidoides* und *Hamamelis virginiana* sind von Interesse zur Entwicklung und Verbesserung antiviraler pflanzlicher Arzneien.

1.2 Abstract

Seasonal influenza virus epidemics causing up to 500 000 deaths each year represent a substantial public health burden. In addition to seasonal epidemics, influenza A virus (IAV) can cause global pandemics, as evidenced by the swine-origin influenza virus in 2009. The recent creation of a highly pathogenic avian influenza H5 subtype virus that efficiently transmits between ferrets in the laboratory increases concerns about the acquisition of human-to-human transmission of highly pathogenic strains. Avian H7N9 recently emerged in China and infected more than 130 people in 2013. Such examples highlight the need for effective IAV preparedness, including IAV surveillance, prevention, risk management strategies and sufficient treatment options.

A prerequisite for effective IAV preparedness is a thorough characterization of past and circulating IAV strains, since it facilitates a prompt reaction to newly emerging strains. In the first part of the present study, pandemic H1N1 (pH1N1) NS gene reassortants were constructed by reverse genetics and characterized. pH1N1 emerged as a pandemic IAV in 2009 and continues to circulate nowadays as a seasonal strain. Besides infecting humans, pH1N1 has also been detected in swine or birds. Thus, there is a considerable risk of developing new reassortants with other co-circulating avian, swine or human strains. The viral non-structural protein 1 (NS1) is a key player in inhibiting the antiviral immune response and a known virulence factor. By reverse genetics, eight reassortants carrying NS genes of human, avian or swine strains in the genetic background of pH1N1 were constructed. pH1N1 was highly permissive to NS genes from various host species, showing only minor fitness losses in 6 out of 8 reassortants on A549 cells. However, introduction of NS from highly pathogenic avian influenza virus (HPAIV) H5N1 attenuated the virus on A549 and DF-1 cells and *in vivo*. NS1 sequence comparisons revealed a five amino acid deletion in position 80-84 that is also found in most contemporary H5N1 strains, but hardly ever in non-H5 subtypes. Deletion of positions 80-84 in pH1N1 NS1 attenuated viral replication *in vitro*, possibly explaining the absence of this deletion in virtually all naturally occurring non-H5 strains. Mechanistically, NS1 from pH1N1 allowed higher general host gene expression than NS1 from HPAIV H5N1. Importantly, a previously unknown role in the regulation of the general host gene expression was attributed to the deletion of amino acids 80-84. This regulation occurs possibly at the level of pre-mRNA maturation.

The high viral fitness of several pH1N1 NS reassortants created in Part 1 of the study, as well as naturally occurring reassortments and point mutations show the high variability of IAV strains and therefore their propensity to antiviral resistance. Thus, new safe and effective antiviral drugs are needed. Two classes of drugs are currently licensed for the treatment of IAV infections, namely neuraminidase and matrix protein inhibitors, preventing release of new virions from the infected host cell or viral uncoating, respectively. Development of antivirals targeting a different step of the viral life cycle would be especially advantageous.

Therefore in the second part of this study, a tannin-rich extract from *Pelargonium sidoides* DC, EPs® 7630 (Umckaloabo®), which is licensed to treat acute bronchitis, was investigated for its antiviral effects. EPs® 7630 showed dose-dependent activity against several IAV strains. It inhibited an early step of influenza infection and impaired viral hemagglutination as well as neuraminidase activity. EPs® 7630 was not virucidal, as virus preincubation (unlike cell preincubation) did not influence infectivity. Importantly, EPs® 7630 showed no propensity to resistance development *in vitro*. Condensed tannins and pseudotannins were identified as the active principle and structure-activity relations were investigated. Chain length influenced antiviral activity, as monomers and dimers were less effective than oligo- and polymers. Importantly, gallicocatechin and its stereoisomer epigallocatechin exert antiviral activity also in their monomeric form. In addition, EPs® 7630 administered by inhalation significantly improved survival and illness of influenza-infected mice, demonstrating the benefit of EPs® 7630 in treatment of influenza.

These data have confirmed and specified the antiviral activity of tannin-rich plant extracts and selected tannins. However, different classes and molecular weights of tannins are often found together in plant extracts, and may differ in their antiviral activities. Nevertheless, there are only few systematic comparisons of their anti-IAV structure-activity relations. A better understanding of the antiviral activity of different tannin structures against IAV is warranted to optimize plant-based antivirals.

In the third part of this study, *Hamamelis virginiana* L. was chosen as a model plant, since it is rich in different tannins that have been previously well characterized. We compared the anti-IAV effect of *Hamamelis virginiana* bark extract, fractions enriched in tannins of different molecular weights and individual tannins of defined structures, including pseudotannins. The bark extract was active against different IAV strains, including the

recently emerged avian H7N9 strain. Fractions enriched in tannins of different molecular weights were produced by a collaborator using ultrafiltration, a simple, reproducible and easily upscalable method. A highly potent fraction enriched in high molecular weight condensed tannins was identified as the best performing antiviral candidate. This ultrafiltration concentrate and the bark extract inhibited early and, to a minor extent, later steps in the IAV life cycle. Interesting mechanistic differences between tannin structures were observed: high molecular weight tannin containing extracts and tannic acid (1702 g/mol) inhibited both IAV receptor binding and neuraminidase activity. In contrast, the tested low molecular weight compounds (< 500 g/mol) inhibited neuraminidase but not hemagglutination. Average molecular weight of the compounds seemed to positively correlate with receptor binding (but not neuraminidase) inhibition. In general, neuraminidase inhibition seemed to contribute little to the antiviral activity. Importantly, antiviral use of the ultrafiltration fraction enriched in high molecular weight condensed tannins and, to a lesser extent, the unfractionated bark extract was preferable over individual isolated compounds.

In summary, this study contributes to different aspects of IAV preparedness, namely to the characterization of current and possibly emerging IAV strains and to the development and optimization of antivirals. Briefly, a previously unknown role of a naturally occurring NS1 five amino acid deletion in the regulation of the antiviral host response was identified. Also, the finding that pH1N1 reassorted with most of the tested human, avian and swine NS gene segments without a major loss in fitness highlights the need for IAV surveillance of NS reassortants. Finally, antiviral activity of EPs® 7630, a tannin-rich plant extract already licensed for acute bronchitis treatment, was demonstrated *in vitro* and *in vivo*. The established antiviral structure-activity relations of tannins and pseudotannins from *Pelargonium sidoides* and *Hamamelis virginiana* are of interest for developing and improving plant-based antivirals.

2 Introduction

2.1 Influenza A Virus

2.1.1 Classification and nomenclature

Influenzavirus A, B, C, *Thogotovirus*, *Isavirus* and *Quarantavirus* are genera of the *Orthomyxoviridae* family (International Committee on Taxonomy of Viruses 2012). Influenza A virus strains are classified into different subtypes by their surface proteins hemagglutinin and neuraminidase (HxNx). To date, 18 HA subtypes and 11 NA subtypes have been identified (Tong et al. 2013). Influenza strains are named by the following systematic: influenza type/host species (except if human)/country or city of isolation/identification number/year of isolation (HxNx), for example A/Luxembourg/43/2009 (H1N1) for a human strain or A/swan/Germany/R65/2006 (H5N1) for a non-human strain.

2.1.2 Genomic organization and encoded proteins

Influenza A viruses (IAVs) are enveloped, negative-sensed, single-stranded RNA viruses (Fig. 1). Both filamentous and spherical forms, the latter with a diameter of roughly 100 nm, have been described (Mosley & Wyckoff 1946, Fujiyoshi et al. 1994, Rossman & Lamb 2011). IAVs carry eight RNA gene segments, namely the polymerase basic 2 (PB2), polymerase basic 1 (PB1), polymerase acidic (PA), hemagglutinin (HA), nucleoprotein (NP), neuraminidase (NA), matrix (M) and non-structural (NS) segment. The first 13 nucleotides on the 5' and the first 12 nucleotides on the 3' ends of the viral RNAs (vRNAs) are highly conserved between IAV genes and strains and constitute the IAV promoter (Skehel & Hay 1978, Lamb & Horvath 1991).

The eight gene segments can code for up to 15 proteins, depending on the IAV strain. HA, NA and the ion channel M2 are located on or in the viral membrane, which is derived from the host cell membrane. The nucleoprotein NP and the polymerase proteins PB2, PB1 and PA are located inside of the virus. They associate to all viral RNAs and thereby form the viral ribonucleoprotein complexes (vRNPs). M1 underlies the viral envelope. While NS2 (also called nuclear export protein, NEP) has been detected in the virus particle and in infected host

cells (Richardson & Akkina 1991), NS1 is exclusively expressed in infected host cells (Lazarowitz et al. 1971, Hale et al. 2008).

Some viral gene segments code for more than one protein. M codes for M1 and M2, due to different splice variants. NS codes for NS1, a key player in the inhibition of the antiviral host response (see Section 2.2.2, (Garcia-Sastre et al. 1998)), and NS2, involved in nuclear export of viral genes (O'Neill et al. 1998). NS1 mRNA is much more abundant than NS2 mRNA (Lamb et al. 1980). Recently, NS3 was discovered as a third splice variant (Selman et al. 2012), but its function is unknown so far. PB1 has been shown to encode, in addition to the PB1 protein, up to two accessory proteins by using an alternative open-reading frame or start codon: PB1-F2 (Chen et al. 2001) and PB1-N40 (Wise et al. 2009). While data on PB1-N40 are still scarce, it is known that PB1-F2 is not expressed by every IAV strain (Zell et al. 2007), but constitutes a virulence factor (Zamarin et al. 2006). Very recently, two more proteins have been identified to be encoded by the PA or M gene, namely PA-X (Jagger et al. 2012) and M42 (Wise et al. 2012).

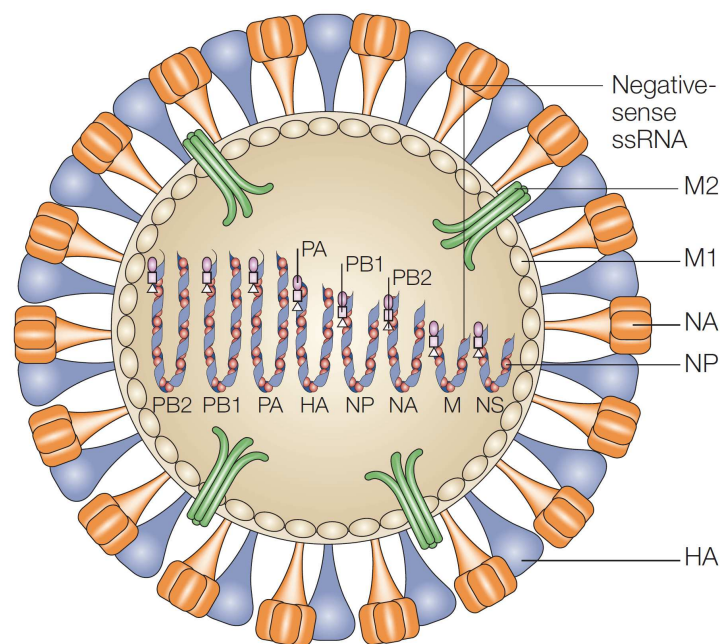


Figure 1: Structure of an IAV virus particle. NS2, NS3, PB1-F2, PB1-N40, PA-X and M42 are not shown due to unclear localization in the virus particle or strain-dependent existence. Reprinted by permission from Macmillan Publishers Ltd: Nature Reviews Microbiology (Horimoto & Kawaoka 2005), copyright 2005. <http://www.nature.com/nrmicro/journal/v3/n8/full/nrmicro1208.html>

2.1.3 Viral life cycle

The IAV life cycle, which takes about eight hours, is schematically represented in Figure 2. After cleavage of the full length precursor protein HA0 into its subunits HA1 and HA2 by trypsin- or subtilisin-like proteases (Klenk et al. 1975, Bertram et al. 2010), IAV can bind to its host cell receptor, sialic acid (Weis et al. 1988, Ge & Wang 2011), by its surface glycoprotein HA1. This binding triggers endocytosis of the virus particle. Endosomal acidification by the vacuolar-dependent ATPase mediates a conformational change of HA, which allows fusion of HA2 with the endosomal membrane and release of vRNPs into the cytosol (Maeda & Ohnishi 1980, Maeda et al. 1981, Hamilton et al. 2012). Import of H⁺ ions into the virus particle by the ion channel M2 is also needed for viral uncoating, as it disrupts interactions between M1 and vRNPs (Bui et al. 1996). Unbound vRNPs can then be transported into the nucleus via an active mechanism through nuclear pore complexes (Martin & Helenius 1991). Viral uncoating from the endosome occurs with a half time of roughly 25 min after attachment, nuclear import of these cytosolic vRNPs was detected within 10 min (Martin & Helenius 1991).

In the nucleus, negative-sense vRNA is transcribed by the viral polymerase complex (PB2, PB1 and PA) into both (+)mRNA and (+)complementaryRNA (cRNA). Viral mRNA synthesis starts with the so-called 'cap-snatching': PB2 binds capped cellular pre-mRNA (Guilligay et al. 2008) and PA cleaves its cap (7-methylguanosin-triphosphate) (Dias et al. 2009). Subsequently, the cap is used as a primer to transcribe the nascent viral mRNA from the vRNA template (Krug 1981, Plotch et al. 1981), and a polyA tail is added to the 3'end by stuttering of the polymerase complex at a stretch of 5-7 uridines (Luo et al. 1991, Zheng et al. 1999). Cap and polyA tail are essential for nuclear export, protection of mRNA against degradation and translation initiation (Wahle & Rügsegger 1999, Decroly et al. 2012). Since IAV snatches the cap from cellular mRNAs, their nuclear export is inhibited. mRNA of viral gene segments such as M or NS is partly spliced using the cellular splicing machinery (Lamb & Choppin 1979, Inglis & Brown 1981, Engelhardt & Fodor 2006). In addition to the viral (+)mRNA which serves as a template for protein translation, (+)cRNA is generated to form the transcription template for synthesis of new (-)vRNA.

The different vRNAs in helical hairpin structure associate with viral NP and the polymerase complex to form vRNPs and are exported from the nucleus, mediated by M1 and NS2 (Boulo

et al. 2007). M1, able to associate with both vRNPs and lipid membranes, mediates recruitment of viral components to the cell membrane and is the driving force for the subsequent budding of new virions (Gómez-Puertas et al. 2000, Nayak et al. 2004). Budding occurs by membrane bending at lipid raft domains of the apical membrane of polarized cells (Nayak et al. 2004). The virions are at first bound to the host cell membrane by interaction of HA and sialic acid (Seto & Rott 1966, Wagner et al. 2002). They are released by NA which cleaves sialic acids from the host cell (Gottschalk 1957). This also prevents re-infection of the same cell, as well as self-aggregation of viral particles, since sialic acids are also cleaved from glycoproteins on the virus surface (Palese et al. 1974, Palese & Compans 1976). The involvement of NS1 in the viral life cycle will be described in more detail in the following Section 2.2.

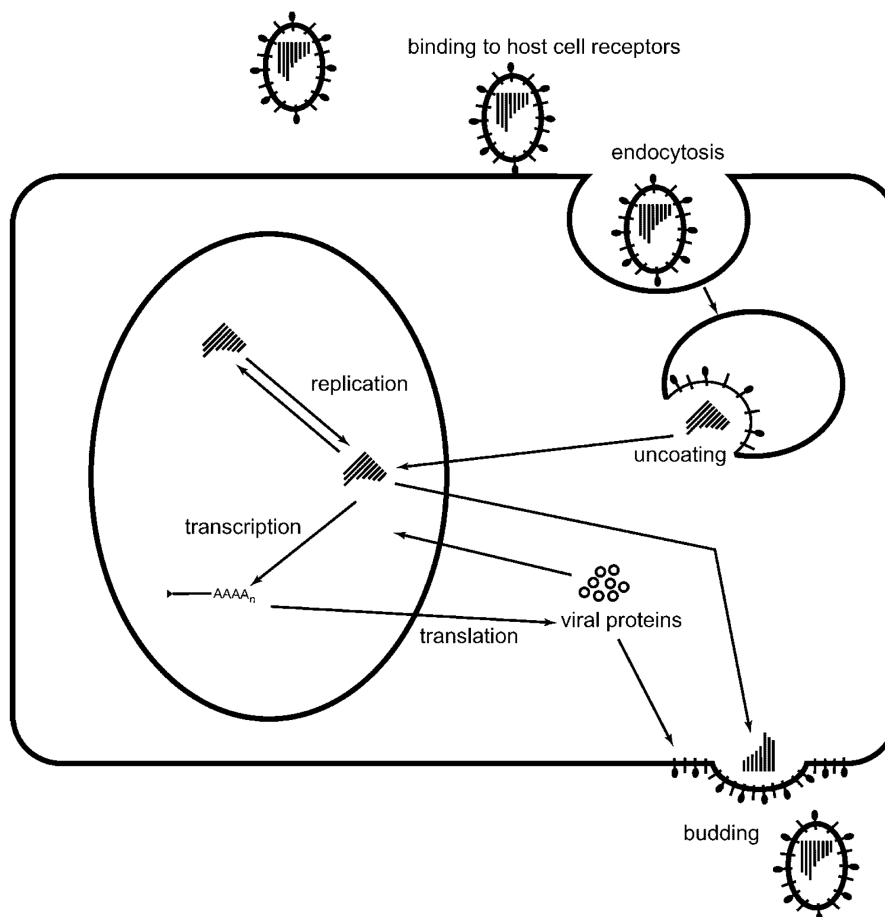


Figure 2: The IAV life cycle. After binding of viral hemagglutinin to its host cell receptor, endocytosis of the viral particle is triggered and leads to viral uncoating. Viral RNA is imported into the nucleus, where both replication of vRNA and transcription of mRNA take place. After nuclear export, viral mRNA is translated in to proteins, which are assembled with viral RNPs into new virus particles. Progeny virions bud from the host cell membrane and are released by neuraminidase-mediated cleavage. (Engelhardt & Fodor 2006), copyright 2006, John Wiley & Sons, Ltd.

2.2 The IAV NS1 protein

2.2.1 Structure and localization of NS1

NS1 is encoded by the unspliced IAV gene segment 8. It generally has a length of 230 amino acids (aa) and a molecular mass of 26 kDa, but some strains have C-terminal deletions or insertions yielding a protein of 202-237 aa (Hale et al. 2008, Dundon & Capua 2009). It occurs as a dimer (Nemeroff et al. 1995, Bornholdt & Prasad 2006) and is divided into an N-terminal RNA-binding domain (aa 1-73) (Qian et al. 1995) and a C-terminal effector domain (aa 74-237) (Bornholdt & Prasad 2006) mainly involved in protein-protein interactions.

NS1 is a non-structural protein, meaning that it is not expressed in the virus particle itself (Lazarowitz et al. 1971). However, NS1 is expressed early after infection (Shapiro et al. 1987), as it is needed to inhibit the antiviral host response and allow viral replication early after infection (Hale et al. 2008, Moltedo et al. 2009). NS1 has at least one nuclear localization signal (Greenspan et al. 1988) and one nuclear export signal (Li, Yamakita, et al. 1998). It can be found both in the nucleus and in the cytoplasm of the host cell (Krug & Etkind 1973, Greenspan et al. 1988).

2.2.2 Functions of NS1

NS1 is a multifunctional protein and mainly works as a key player in blocking the host's innate immune response (Hale et al. 2008, Ehrhardt et al. 2010). Upon infection, IAV triggers the innate immune response, such as the release of cytokines attracting immune cells. Among these, type I interferons (especially IFN- α/β) are the most important antiviral mediators, regulating the expression of several hundred genes (DeVeer et al. 2001). Type I interferons are inhibited by NS1, which was discovered when an NS1-deficient IAV induced high IFN expression in infected host cells (Garcia-Sastre et al., 1998). While this virus was attenuated in IFN competent systems, it replicated well in IFN deficient systems such as Vero cells or STAT1^{-/-} mice. Meanwhile, several ways how NS1 favours viral gene expression over host cell gene expression have been described. Importantly, as described in the next Sections (2.2.2.1-2.2.2.4), NS1 inhibits both pre-transcriptional and post-transcriptional host gene expression and induces preferential translation of viral mRNAs.

2.2.2.1 Inhibition of type I IFN induction by NS1

IAV infection of a host cell is detected by pattern recognition receptors such as the Toll-like receptor 3/7 (Lund et al. 2004, Guillot et al. 2005), the NOD-like receptor NLRP3 (Thomas et al. 2009, Ichinohe 2010) or the retinoic acid inducible gene I (RIG-I), which subsequently trigger signalling cascades and lead to the induction of antiviral host factors. While no direct effect of NS1 has been shown on Toll-like receptors or NLRP3 so far, NS1 is well characterized in limiting the activation of RIG-I (Fig. 3).

The RIG-I signalling cascade is triggered by RIG-I binding to 5'-triphosphorylated short RNAs (Hornung et al. 2006, Pichlmair et al. 2006, Baum et al. 2010). Instead of the initial proposition that NS1 sequesters dsRNA away from RIG-I (Talon et al. 2000), NS1 forms a complex with RIG-I (Pichlmair et al. 2006, Mibayashi et al. 2007) and inhibits RIG-I activation by Tripartite motif-containing protein 25 or, strain-specifically, Riplet ubiquitin-ligases (Gack et al. 2009, Rajsbaum et al. 2012). Consequently, downstream transcription factors of the RIG-I cascade like IRF-3/7, NF κ B or ATF2/c-Jun cannot induce expression of IFN- β and other host factors any longer (Dixit & Kagan 2013).

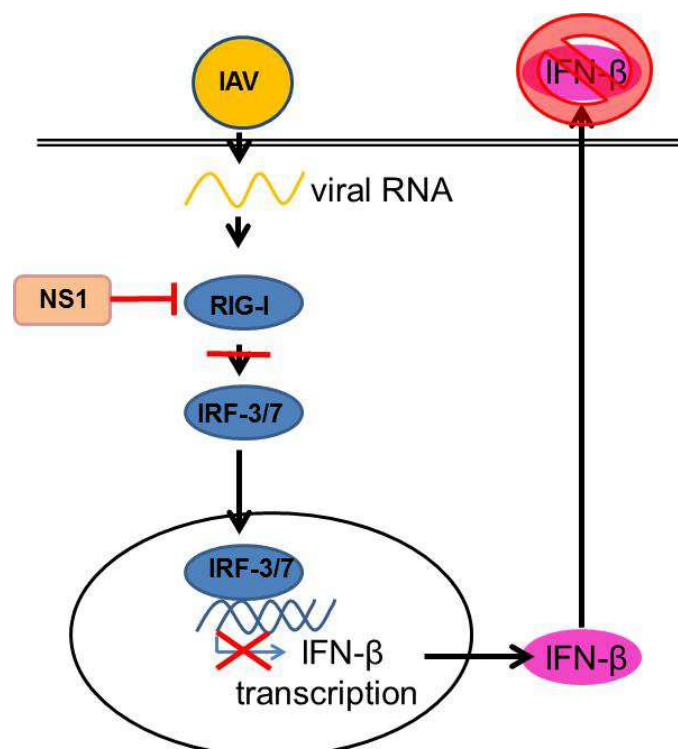


Figure 3: Inhibition of type I IFN induction by NS1. NS1 inhibits activation of RIG-I by viral RNA and thereby the downstream IRF3/7 signalling cascade and induction of IFN- β transcription.

2.2.2.2 Inhibition of downstream type I IFN signalling by NS1

Additionally to decreasing type I IFN induction, NS1 also inhibits downstream IFN signalling (Fig. 4). Upon binding of its receptor, IFN activates the Jak-STAT signalling pathway (Platanias 2005) which leads to induction of an intracellular antiviral state. NS1 inhibits at least two of the induced interferon-stimulated genes, namely protein kinase RNA activated (PKR) and 2'5'-oligoadenylate synthase (2'5'-OAS).

Upon sensing of dsRNA or partially complementary viral RNA, PKR phosphorylates the eukaryotic translation initiation factor 2 α (eIF2 α), which leads to a generalized translation shutoff in the infected host cell (Roberts et al. 1976, Gale & Katze 1998, Hatada et al. 1999). NS1 prevents PKR activation by direct PKR binding (Tan & Katze 1998, Li et al. 2006). Finally, NS1 also sequesters dsRNA away from 2'5'-OAS (Min & Krug 2006). Thereby, the 2'5'-OAS-mediated activation of latent RNase (RNaseL) which would cleave viral RNA (Hovanessian 1991), is inhibited.

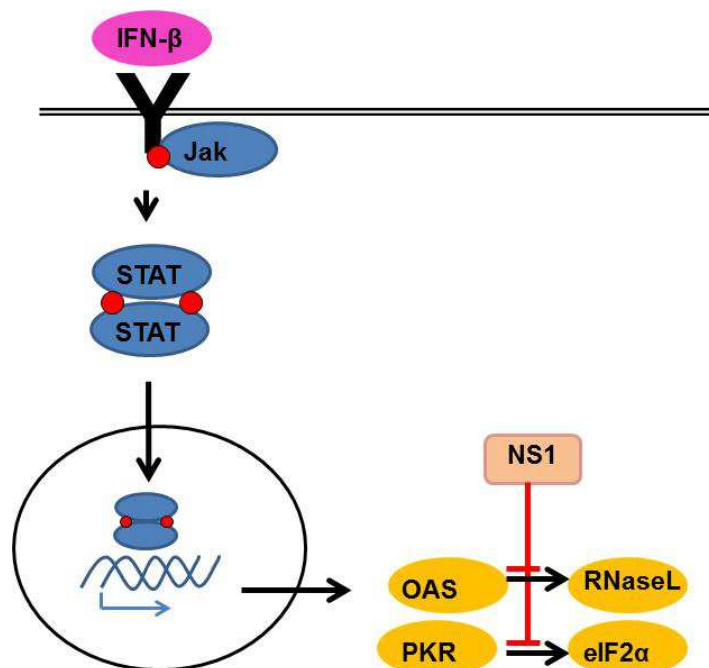


Figure 4: Inhibition of downstream type I IFN signalling by NS1. Secreted IFN- β induces an antiviral state via Jak-STAT signalling. The effect of the resulting antiviral factors 2'5'-OAS and PKR is inhibited by NS1.

2.2.2.3 Inhibition of general host cell gene expression by NS1

NS1 can confer a general block of host gene expression by inhibiting cellular pre-mRNA maturation (Fig. 5) and nuclear export. NS1 inhibits pre-mRNA maturation by binding to cleavage and polyadenylation specificity factor 30 (CPSF30) (Nemeroff et al. 1998) and polyA binding protein II (PABP2) (Chen et al. 1999). CPSF30 is required for cleavage of cellular pre-mRNAs, allowing addition of short (approximately 10 nucleotides) polyA tails by the cellular polyA polymerase, which can then be elongated in the presence of PABP2 (Wahle & Kühn 1997). Thus, NS1 blocks polyadenylation of cellular pre-mRNA, an essential step required for nuclear export (Nemeroff et al. 1998, Zhao et al. 1999). NS1 also interacts with proteins of the mRNA nuclear export machinery (Satterly et al. 2007). Thus, NS1 induces retention of cellular pre-mRNA and mRNA in the nucleus, which results in rapid RNA degradation (Katze & Krug 1984). Interestingly, NS1 does not inhibit viral mRNA polyadenylation because this process is independent of the cellular polyadenylation machinery. The polyA tail is added to viral mRNA by the viral polymerase (Luo et al. 1991).

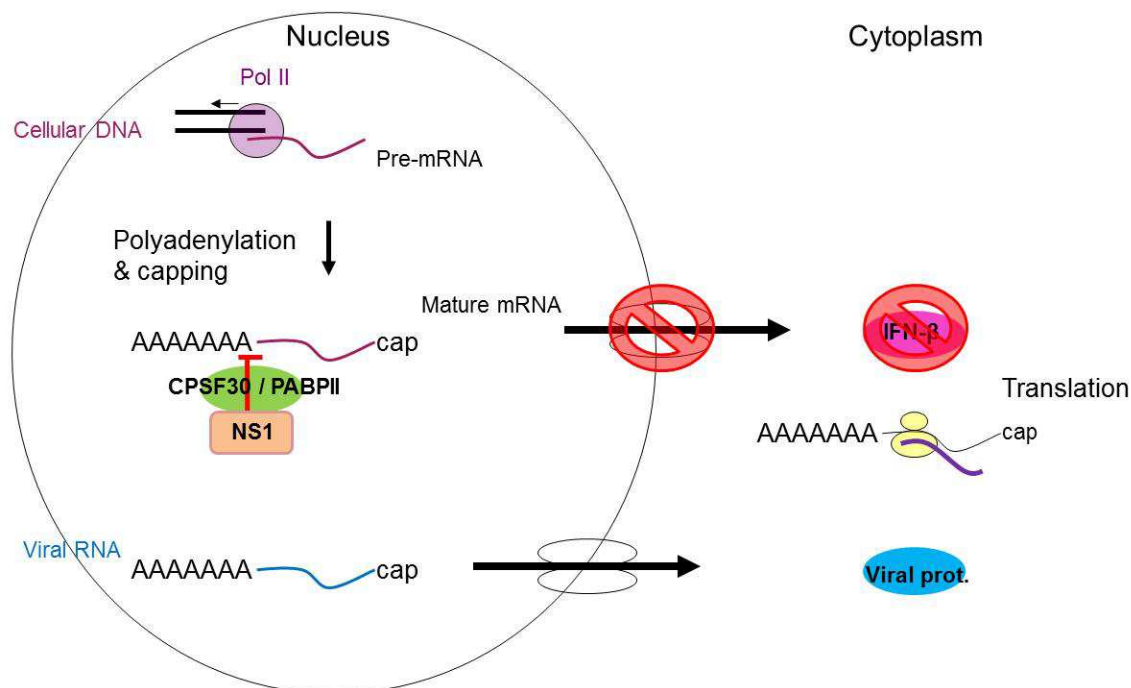


Figure 5: Inhibition of general host cell gene expression by NS1. NS1 inhibits polyadenylation of cellular pre-mRNA by binding to CPSF30 and/or PABP2, resulting in nuclear retention of immature pre-mRNAs. Viral RNA polyadenylation is independent of the cellular machinery and exported into the cytoplasm, where translation to viral proteins takes place.

2.2.2.4 Enhancement of viral mRNA translation by NS1

NS1 stimulates translation of viral proteins rather than cellular proteins. This mechanism is mediated by the IAV 5' untranslated region, which is bound by NS1 to enhance translation initiation (Garfinkel & Katze 1993, de la Luna et al. 1995). NS1 also interacts with proteins involved in translation, such as the human Staufen protein (Falcón et al. 1999), the eukaryotic translation initiation factor 4 subunit GI (Aragón et al. 2000) and polyA binding protein I (Burgui 2003). Thereby, NS1 is believed to mediate interaction of viral mRNA 5' untranslated regions with the cellular translation machinery, leading to selective translation enhancement of viral mRNAs over cellular mRNAs.

2.2.2.5 Strain-dependency of the NS1 functions

The effect of NS1 on the antiviral host response is strain specific since the strength of the distinct antiviral mechanisms described above greatly varies between strains. To name only a few examples, NS1 proteins of H1N1 A/Puerto Rico/8/34, H5N1 A/Hong Kong/483/97 or pandemic H1N1 IAVs inefficiently bind CPSF30 (Twu et al. 2007, Kochs et al. 2007, Hale et al. 2010). NS1 from the H3N2 A/Udorn/72 strain binds CPSF30 but is unable to prevent the induction of IFN- β transcription (Kuo et al. 2010). The combination of such effects leads to differential induction of antiviral responses and differential viral fitness. Therefore, NS1 is considered a virulence factor (Tscherne & Garcia-Sastre 2011), while its contribution to virulence varies between different IAV strains.

2.3 IAV strain variability

2.3.1 The basis of strain variability: point mutations and reassortments

IAV mutates frequently due to its viral polymerase, which lacks proof-reading activity. During transcription, point mutations arise and can contribute to differential viral fitness or changed antigenic properties (“antigenic drift”). Also, due to the segmented nature of the genome, co-infection of the same host cell with different IAV viruses can result in an exchange of gene segments and lead to a novel IAV with different properties (reassortment, or “antigenic shift” if HA or NA are involved, Fig. 6).

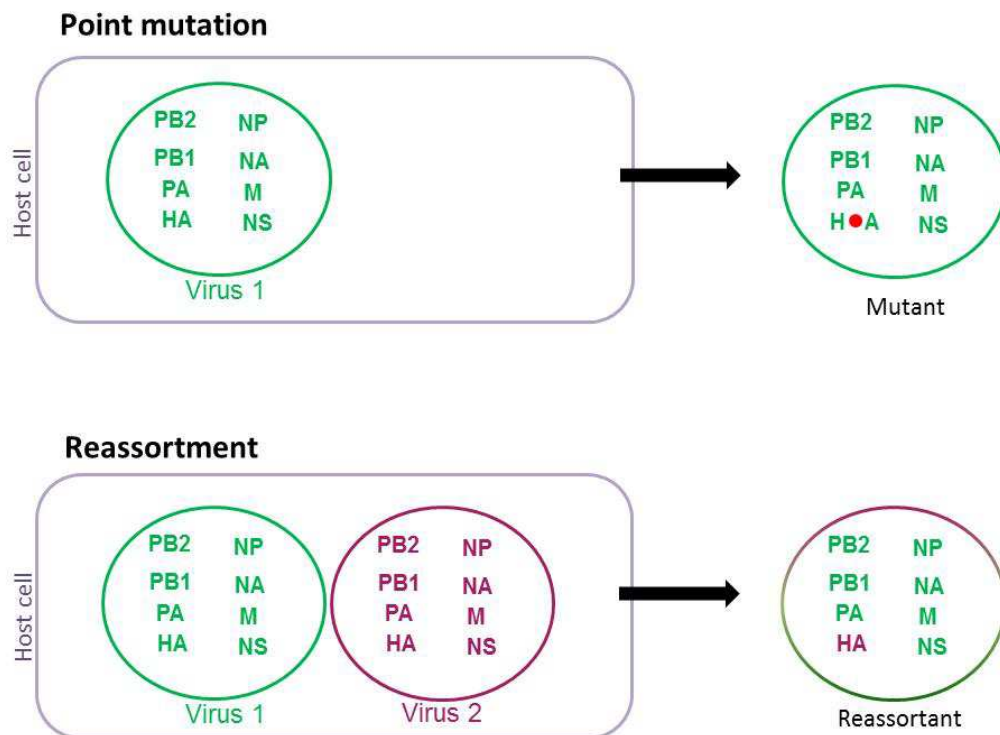


Figure 6: The basis of IAV strain variability: point mutations and reassortments. The red dot indicates a point mutation.

2.3.2 Host species and host range restriction

With the exception of H17N10 and H18N11 (Tong et al. 2012, 2013), all HA and NA subtypes have been detected in wild birds (Solorzano et al. 2007) and phylogenetic analysis showed that viral NP from a large variety of hosts evolved from an avian ancestor (Gorman et al. 1990). Thus, wild aquatic birds are considered the main reservoir of IAV (Slemons et al. 1974, Webster et al. 1992). However, IAV infects a wide range of host species and has been detected e.g. in humans, domestic poultry, swine, dogs, cats, horses, whales, seals or bats (Hinshaw et al. 1986, Shinya et al. 2010, Anthony et al. 2012, Tong et al. 2012) (Fig. 7). IAVs can cross the species barrier and either cause transient infections or establish new stable lineages, as it has happened in humans (currently circulating strains: H1N1, H3N2), swine (H1N1, H1N2, H3N2; (Kuntz-Simon & Madec 2009)) or horses (H3N8, (Daly et al. 2011)). In general, establishment of stable lineages in a new host species is a rather rare event subject to extensive host adaptation.

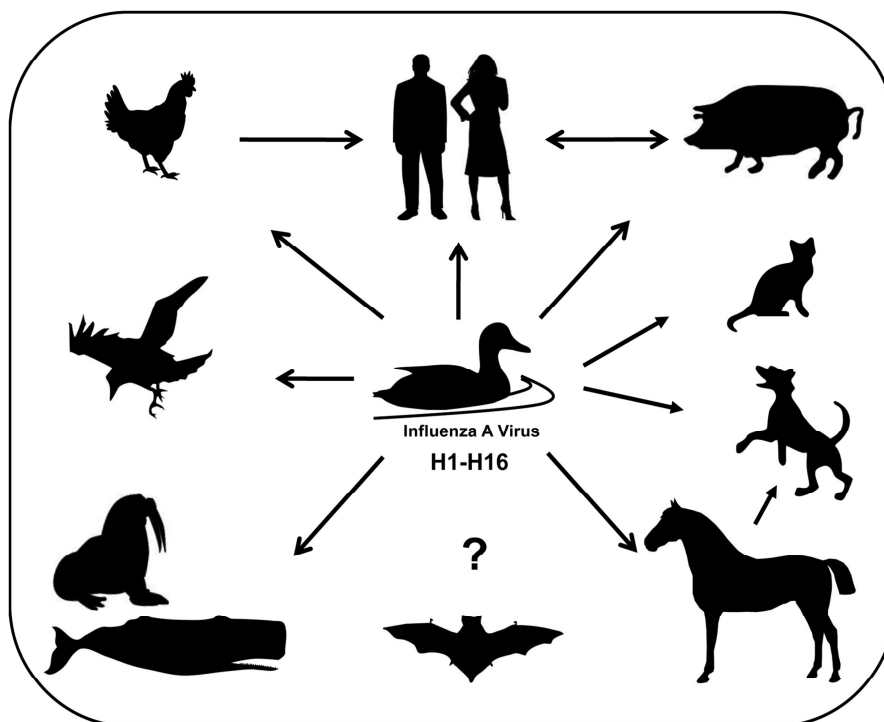


Figure 7: The IAV host range. While all H1 to H16 hemagglutinin subtypes have been detected in wild waterfowl, the IAV main animal reservoir, several other species can be infected from the main reservoir or another host. Infection can lead to transient illness or establishment of new stable lineages. IAVs of subtype H17 and H18 have recently been detected in bats, but their relationship to IAVs from other host species is not clear yet. From (Mänz, Schwemmler, et al. 2013), reprinted with permission from ASM.

2.3.2.1 Viral proteins involved in host range restriction

In general, all IAV proteins can impact on the replicative ability in a certain host species, but for some, their importance has been widely described. An important determinant of the host range is the viral HA protein, which mediates binding of the virus to its host cell receptor, sialic acid. HA from avian strains preferably binds to sialic acid linked to the neighbouring galactose by an α 2,3-bond, while HA from human strains prefers α 2,6-linked sialic acid (Rogers & Paulson 1983, Matrosovich et al. 1997). α 2,6-linked sialic acid is more prevalent in the human upper respiratory tract and α 2,3-linked sialic acid prevails in birds. The difficulty to reach the human lower airways harbouring also α 2,3-linked sialic acid may explain that avian IAVs sporadically infect humans after close contact to infected birds, but do not transmit naturally from human to human (Shinya et al. 2006).

Interestingly, swine carry both α 2,3- and α 2,6-linked sialic acids in their respiratory tract, making them susceptible to avian and human IAV strains (Ito et al. 1998). They were proposed to function as a “mixing vessel” for avian and human strains (Ito et al. 1998), since reassortment easily occurs upon parallel infection with two IAV strains. In addition, it was shown that upon replication in swine, avian-like IAVs can acquire the ability to recognize human receptors (Ito et al. 1998), emphasizing the role of swine for the generation of novel human-pathogenic IAV strains.

The “mixing vessel” theory is also supported by studies on another viral protein, NP. A temperature sensitive NP mutant could only be rescued in an avian but not in a human genetic IAV background, while in a swine background, both successful and unsuccessful rescues occurred (Scholtissek et al. 1985, Scholtissek 1990). In addition, NP from all analysed species can be phylogenetically classified into exclusively the avian or human branch, but pig NPs were the only ones to belong to either the avian or human branch (Gammelin et al. 1990).

The different components of the polymerase have also been shown to play a role in host adaptation (Mänz, Schwemmler, et al. 2013). Especially, the involvement of PB2 residue 627 is widely established. Here, lysine (found in currently circulating human strains and some H5N1 strains isolated from humans) instead of glutamic acid (found in avian isolates) confers a replicative advantage in mammalian cells (Subbarao et al. 1993).

Different studies have shown a role of NS1 in host adaptation. For example, when an allele A NS was exchanged with a strictly avian allele B NS in a human IAV background, the reassortant was attenuated in squirrel monkeys (Treanor et al. 1989). Also, carrying NS of the human 1918 pandemic H1N1 in the background of a mouse adapted H1N1 (A/WSN/33), the reassortant lost its ability to kill mice (Basler et al. 2001). In addition, NS1 strain-specifically inhibits the antiviral innate immune response, which can impact on its replicative ability.

2.3.3 IAV strains circulating in humans, birds and swine

2.3.3.1 Human IAV strains: Past pandemics and currently circulating strains

Pandemics can be distinguished from epidemics by affecting a large geographical area (often worldwide) and a high percentage of the population. There are several prerequisites for an IAV strain to become pandemic (World Health Organization 2009a): A new IAV strain must be able to (1) infect humans, (2) cause serious disease, (3) spread efficiently from human to human and (4) encounter an immunologically naïve population. While human pandemics have been described already in the Middle Ages, they could be attributed to influenza since at least the 18th century (Beveridge 1991). In the last 100 years, there have been five pandemics due to IAV strains whose origins are depicted in Figures 8 and 9.

In 1918-1919, the most devastating IAV pandemic known to date, the “Spanish influenza”, killed about 50 million worldwide (Johnson & Mueller 2002). The corresponding H1N1 strain was completely sequenced and reconstructed in 2005 and is believed to be of entirely avian origin (Taubenberger et al. 2005, Tumpey et al. 2005). H1N1 from 1918 continued to circulate in humans until its replacement by the next pandemic strain.

In 1957, an H2N2 strain known as “Asian influenza” emerged by reassortment of the circulating 1918-derived H1N1 with HA (H2), NA (N2) and PB1 genes of avian origin (Scholtissek et al. 1978, Kawaoka et al. 1989, Oxford 2000). The pandemic killed more than one million people (Potter 2001), evolved into a seasonal virus and completely disappeared in 1968.

In 1968, a reassortment of H2N2 with avian HA (H3) and PB1 led to emergence of an H3N2 strain (Webster & Laver 1972, Kawaoka et al. 1989), the “Hong Kong influenza”. This pandemic was milder than the previous two, which was attributed to the presence of

antibodies against N2, from the previous 1957 H2N2 strain (Schulman & Kilbourne 1969). “Hong Kong influenza”-derived strains still circulate in humans today as seasonal H3N2.

In 1977, the H1N1 that disappeared in 1957 re-emerged and caused the “Russian influenza” pandemic. As sequence comparison revealed very little difference to the H1N1 strains circulating in 1950, the pandemic was possibly due to an accidental release of a virus frozen for many years (Nakajima et al. 1978). Strains derived from this virus circulated up to 2009.

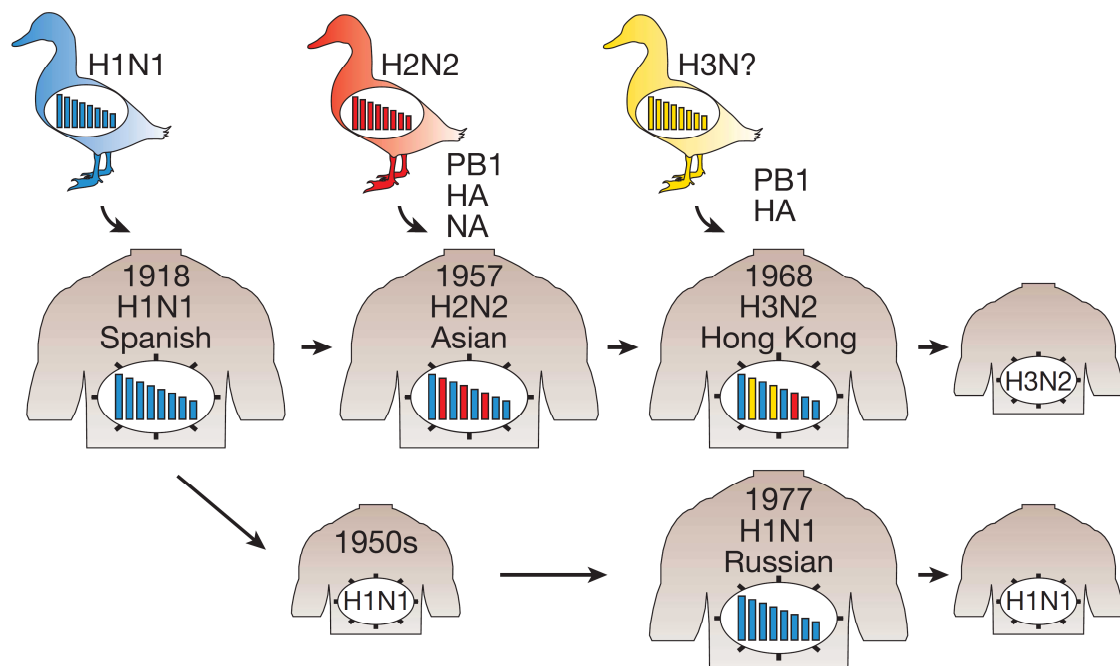


Figure 8: The genetic origin of the pandemic and seasonal IAV strains from 1918-2009. While the 1918 pandemic IAV was of avian origin, in 1957 genes from circulating 1918-derived H1N1 reassorted with avian HA, NA and PB1 genes. This H2N2 strain then reassorted with avian HA and PB1 genes in 1968 to an H3N2 strain, whose derivatives still circulate today as seasonal IAVs. 1918-strain derived H1N1 circulating in the 50's was “reactivated” by an unknown mechanism in 1977 and gave rise to the seasonal H1N1 that circulated until it was replaced by “swine influenza” pH1N1 in 2009. Reprinted by permission from Macmillan Publishers Ltd: Nature, (Neumann et al. 2009) copyright 2009. <http://www.nature.com/nature/journal/v459/n7249/full/nature08157.html>

In March/April 2009, the first human cases of the so-called “swine influenza” (or pandemic influenza/2009, pH1N1) emerged in Mexico and the USA (Ginsberg et al. 2009, Perez-Padilla et al. 2009), followed by a rapid global spread of the virus. The strain originated by a reassortment of NA and M gene segments from Eurasian swine IAV and the remaining genes from American triple reassortant H1N2. Precisely, HA, NP and NS genes were ultimately derived from classical swine IAV, PB2 and PA from avian strains and PB1 from human H3N2 (Garten et al. 2009, Smith et al. 2009) (Fig. 9, see Section 2.3.3.4. for description of the different swine influenza lineages). So far, it is unknown in which species the reassortment occurred, although a reassortment in swine seems likely (Smith et al. 2009). The disease was milder than initially expected and the mortality was estimated to be around 280 000 people within the first twelve months of the pandemic (Dawood et al. 2012). The strain became established in humans and still co-circulates with H3N2 and influenza B. Importantly, it replaced the previously seasonal H1N1 in 2010, possibly because it elicits antibodies against the highly conserved HA stalk region (Pica et al. 2012).

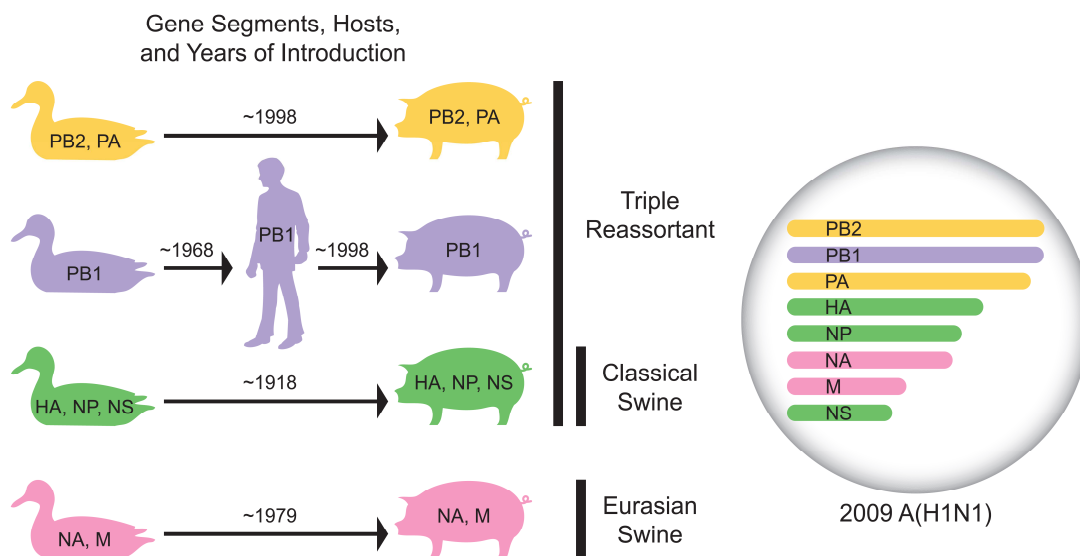


Figure 9: The genetic origin of the pandemic H1N1 (2009). All gene segments were ultimately derived from avian IAV strains. PB1 passed from birds to humans, before forming a triple reassortant with PB2, PA, HA, NP and NS in swine. NA and M were derived from Eurasian swine strains. From (Garten et al. 2009), reprinted with permission from AAAS.

2.3.3.2 Avian IAV strains

Avian influenza widely circulates in birds: 16 of the 18 known HA subtypes and 9 of the 11 NA subtypes have been detected (Solorzano et al. 2007, Tong et al. 2012, 2013). They are divided into highly and low pathogenic subtypes based on their pathogenicity in chickens, which is determined by the amino acid sequence on their hemagglutinin cleavage site. Cleavage of HA0 into HA1 and HA2 is required for IAV infectivity (Klenk et al. 1975). LPAIVs have a monobasic HA cleavage site (R↓X) and can be cleaved by trypsin-like proteases (Lazarowitz et al. 1973, Klenk & Garten 1994). Those are confined to the respiratory and gastrointestinal tract, which accounts for local infections. HPAIVs are characterized by a polybasic HA cleavage site, carrying several arginine or lysine residues. Thereby, a cleavage motif (R-X-R/K-R↓X) (Vey et al. 1992) for furin, a ubiquitous member of the subtilisin-like protease family, is created (Stieneke-Gröber et al. 1992), and HA can be cleaved throughout the complete host organism, inducing systemic infection (Mo et al. 1997, Garten & Klenk 1999).

It has been shown that LPAIV can evolve into HPAIV (García et al. 1996, Ito et al. 2001). So far, only subtypes H5 and H7 naturally occur as highly pathogenic phenotype. However, a polybasic cleavage site has been artificially inserted also into LPAIV H2, H4, H6, H8 and H14 rendering it highly pathogenic in chicken (Munster et al. 2010, Veits et al. 2012). Inversely, insertion of a polybasic cleavage site alone is not always sufficient to create a highly pathogenic phenotype (Stech et al. 2009, Gohrbandt et al. 2011).

The past or present circulation of roughly all IAV subtypes in birds highlights the enormous avian IAV gene pool. This diversity is caused by the frequent gene reassortments and mutations that occur in birds during asymptomatic intra- and interspecies infection. Moreover, dissemination is facilitated by short distance fecal-oral transmission in wetlands (Ito et al. 1995) and long distance transport of viruses by migratory birds (Olsen et al. 2006). The highly diverse IAV strains from the avian reservoir pose a threat for human IAV infection.

2.3.3.3 Human infections with avian influenza

Outbreaks of HPAIV frequently occur in domestic poultry and humans can be infected, mostly upon close contact with sick animals (van Kerkhove et al. 2011). Since HPAIV H5N1 so far showed a mortality rate of about 60% in humans (World Health Organization 2013a) the risk of human infections is of particular concern. In 1997 occurred the first major human HPAIV H5N1 outbreak in Hong Kong, involving 18 infections and 6 deaths (Subbarao 1998, Tam 2002). The virus had an HA closely related to an avian H5N1 isolated in 1996 on a Chinese goose farm (Xu et al. 1999), while the internal genes were derived from avian H9N2 (Guan et al. 1999). After massive poultry culling, no more human outbreaks were observed for years, but the virus continued to circulate in the avian reservoir (Li et al. 2004) and distinctive mutations emerged. A deletion of 20 amino acids in the neuraminidase stalk domain was linked to viral adaptation to chicken (Guan et al. 2002) and mutation of positions 103 (L to F) and 106 (I to M) in NS1 induced tighter binding to CPSF30 (Twu et al. 2007), linked to a stronger repression of the antiviral host response. The biological function of a deletion of amino acid 80-84 in NS1 is unknown so far but has been linked to higher virulence of H5N1 HPAIV (Long et al. 2008).

In 2003, the first two human cases were observed again in China (Peiris et al. 2004). Between 2004 and 2012, 610 human cases were observed, mostly throughout Southeast Asia, China and Egypt (World Health Organization 2013a). It has been shown experimentally that HPAIV H5N1 can acquire airborne transmission from ferret to ferret, the IAV animal model considered closest to human. This was achieved by targeted mutagenesis of 3 amino acids involved in mammalian adaptation along with serial passaging in ferret lungs (Herfst et al. 2012) or by selection of randomly introduced mutations for α -2,6-linked sialic acid affinity along with reassortment of HPAIV HA with internal genes from pandemic H1N1 from 2009 (Imai et al. 2012). Although sustained human-to-human transmission has not occurred naturally so far, HPAIV H5N1 is regarded as a pandemic threat.

In addition to H5, there have also been human infections with HPAIV H7 strains, such as H7N3 (Tweed et al. 2004) and H7N7 (Fouchier et al. 2004). In general, H7 strains induce milder symptoms in humans, including conjunctivitis or influenza-like illness, although fatalities have occurred (Fouchier et al. 2004).

For LPAIV, generally mild human infections with mostly H9N2 or H7 subtypes have been reported (Peiris et al. 1999, Butt et al. 2005, Ostrowsky et al. 2012). However, from February to May 2013, there have been over 130 cases of human infection with a novel low pathogenic avian H7N9 strain in China, showing a mortality rate of about 30% (World Health Organization 2013b). Only sporadic new cases were reported from May to September 2013, this decrease being possibly linked to the closure of wet markets (Wang et al. 2014). From October 2013, the second important wave of new cases has started over the winter season, counting 74 new cases until January 21, 2014 (World Health Organization 2014). This highlights the need for ongoing vigilance. However, control of H7N9 is difficult, since contrarily to HPAIV H5N1, H7N9 does generally not cause clinical signs in poultry. Not all patients had contact with birds and limited, but no sustained human-to-human transmission was observed so far (Qi et al. 2013, Li et al. 2013). H7N9 was created by reassortment of H7 and N9 of avian strains with internal genes from avian H9N2 (Kageyama et al. 2013, Gao, Cao, et al. 2013, Chen et al. 2013).

2.3.3.4 Swine IAV strains

The subtypes H1N1, H1N2 and H3N2 currently circulate as stable lineages in swine. In general, swine IAV strains are distinguished into American and European lineages, which differ in their origin. American H1N1 (also called classical H1N1) is a descendant of the 1918 pandemic H1N1 and was first described in 1931 (Shope 1931). European (or Eurasian) H1N1 appeared in 1979 and is completely derived of an avian strain (Pensaert et al. 1981), while European H3N2 and H1N2 have appeared through several reassortments and carry genes of both avian and human origin (Kuntz-Simon & Madec 2009). American H3N2 emerged in 1997 mostly as triple reassortants, carrying human, avian and swine genes (Zhou et al. 1999), followed by H1N2 in 1998, a reassortant of American swine H3N2 and classical H1N1 (Olsen 2002). Since the emergence of pandemic H1N1 in swine in 2009, the virus has been detected in pigs worldwide and led to several reassortments (Vijaykrishna et al. 2010, Ducatez et al. 2011). In particular, since 2011, there have been more than 300 human cases of generally mild illness caused by a reassortant of US H3N2 carrying the M gene segment of pandemic H1N1 from 2009 (Centers for Disease Control and Prevention 2013a). These cases mostly occurred upon contact with swine at agricultural fairs, but some cases of limited human-to-human transmission have been reported (Centers for Disease Control and Prevention 2011, 2012a). Also previously there have been occasional infections of humans with swine IAVs, mostly after contact with infected animals (van Reeth 2007).

2.3.4 Reverse genetics: a tool to generate *in vitro* mutants and reassortants

In contrast to “conventional” genetics, where the genetic base of a particular phenotype is investigated, reverse genetics allows investigation of a phenotype arising from a defined genetic constellation. Since their first use in 1989 (Luytjes et al. 1989), reverse genetics have evolved to the technique of choice to investigate precise IAV mutations or reassortments (Neumann & Kawaoka 2002).

Transfection of negative-sense IAV RNA does not lead to infectious virus, because it cannot be translated into viral proteins in the absence of viral polymerase. The first attempts to generate IAV from cloned cDNA relied on transfection of the *in vitro* transcribed vRNA of interest mixed with purified PB2, PB1, PA and NP proteins to create functional vRNPs (Luytjes et al. 1989, Enami et al. 1990, Seong & Brownlee 1992). For expression of the remaining genes, co-infection with a helper IAV virus was needed. This, however, required subsequent selection of the virus of choice over the helper virus. The system has gone through several improvements, e.g. the use of plasmids containing the gene of interest in negative orientation under control of a polymerase I promoter (Neumann et al. 1994). RNA polymerase I usually transcribes ribosomal RNA, devoid of 5' cap and 3' polyA, and is therefore suitable to produce vRNA. This system makes *in vitro* transcription and polymerase/NP purification unnecessary.

Nowadays, the reverse genetics approach allows the generation of an IAV virus of choice entirely from cloned cDNA, without the need for a helper virus. This was first achieved by transfecting eight vRNA expressing plasmids under the control of a polymerase I promoter and four protein expressing plasmids (PB2, PB1, PA, NP) (Fodor et al. 1999, Neumann et al. 1999). In order to reduce the number of transfected plasmids from twelve to eight, bidirectional plasmids encoding both vRNA from a polymerase I promoter in negative sense and mRNA from a polymerase II promoter in positive sense were developed (Hoffmann et al. 2000) (Fig. 10). In a mixed culture of HEK293T cells, which are easily transfectible, and MDCK cells, which support high-titer growth of IAV, the virus of choice is efficiently rescued.

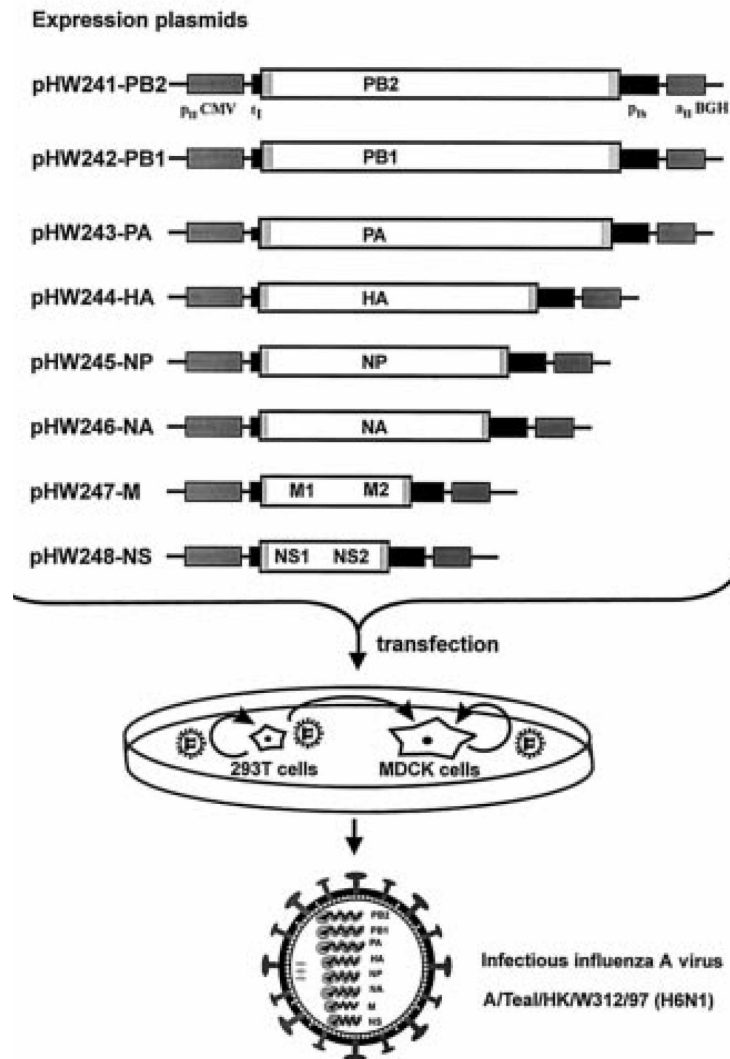


Figure 10: IAV rescue by reverse genetics using the method of Hoffmann et al. Eight bidirectional expression plasmids encoding both (-)vRNA and (+)mRNA of each IAV gene segment are co-transfected into a mixed culture of easily transfectible HEK293T cells and MDCK cells which support growth of the resulting virus to high titers. From (Hoffmann et al. 2000), copyright The National Academy of Sciences.

We use the system of Hoffmann et al., (Hoffmann et al. 2000) with improvements developed by Stech (Stech et al. 2008). The improved system does not depend on restriction sites to insert IAV segments into the plasmids. It uses a modified QuikChange PCR based on a megaprimer containing the IAV segment of interest between regions complementary to the plasmid (Fig. 11). This megaprimer anneals to the complementary plasmid sequences and is then elongated from its 3'-end by a proof-reading polymerase. Therefore, this method allows even cloning of viral segments of unknown sequence. It also contains the selection marker *ccdB*, which is toxic for bacteria due to inhibition of the bacterial topoisomerase II.

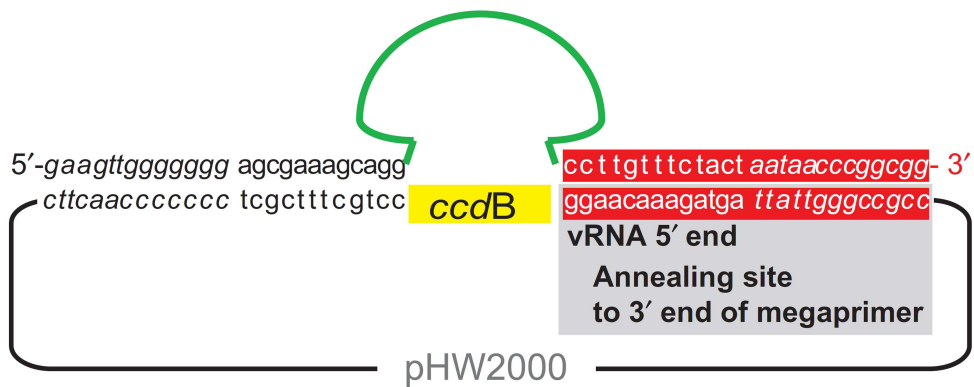


Figure 11: Reverse genetics system by Stech et al. used in this study. Annealing of the megaprimer containing the IAV segment (green) and plasmid-complementary regions (in italics) to the plasmid pHW2000, containing a negative selection marker (ccdB, yellow) and sequences complementary to the IAV conserved regions (normal type). Adapted from (Stech et al. 2008), copyright 2008, Oxford University Press.

2.4 Antiviral prevention, treatment and resistance

Worldwide, IAV causes around three to five million cases of severe illness and up to 500 000 deaths each year (World Health Organization 2009b). Hospitalizations are often required for the elderly and people with underlying medical conditions, which underlines the need for effective vaccines and drugs. Due to the large extent of antigenic drift and sporadic events of antigenic shift, a single vaccination does not confer immunity over decades such as for other viruses that are less prone to mutations, and resistance to antivirals may rapidly develop.

2.4.1 Vaccination

So far, the yearly seasonal influenza vaccine requires annual reformulation due to variability of the circulating strains. It is composed of the IAV H1N1, H3N2 and influenza B strain that are estimated to be the most prevalent during the targeted season. Yearly influenza vaccination is recommended for the elderly, people with underlying medical conditions, healthcare personnel and lately also for children aged 6-59 months and pregnant women (World Health Organization 2013c). Traditionally, a trivalent inactivated vaccine is used by intramuscular injection. However, since 2003 (Flumist®, USA) or 2011 (Fluenz®, Europe) intranasally administered live attenuated influenza vaccines are available for healthy people between 2 and 49 (Flumist®) or 2 and 18 (Fluenz®) years of age (Carter & Curran 2011, European Medicines Agency 2012). Also quadrivalent vaccines have been approved. They contain an H1N1, H3N2 and two instead of only one influenza B strain, corresponding to the two circulating influenza B lineages.

Lately, serious effort is put into the development of a so-called “universal influenza vaccine”, which targets epitopes conserved between different influenza strains and should therefore make annual reformulation and vaccination unnecessary. Promising candidate antigens are the stem region of hemagglutinin (Steel et al. 2010, Wang et al. 2010), the M2 ectodomain (Fiers et al. 2009) or NP (Altstein et al. 2006) either administered alone or in combination with each other or other antigens (Adar et al. 2009; Gao et al. 2013).

2.4.2 Currently marketed antiviral drugs and antiviral resistance

While vaccination remains the method of choice for prevention of IAV infection, there is a need for antivirals for the treatment of IAV infections, especially if they require hospitalization or if the patient has underlying medical conditions (Centers for Disease Control and Prevention 2013b). Also, upon emergence of a novel IAV strain, development of an effective vaccine can take months. For the treatment of influenza, two classes of antivirals are currently marketed, namely the neuraminidase inhibitors (oseltamivir/Tamiflu®, zanamivir/Relenza®) and the M2 channel inhibitors or adamantanes (amantadine/Symmetrel®, rimantadine/Flumadine®).

The latter have been approved by the Food and Drug Administration in 1966 or 1994, respectively, block the M2 ion channel of influenza A (but not influenza B) viruses, and thereby inhibit viral uncoating (Pinto & Lamb 2007). However, widespread resistances emerged, which have been attributed mainly to an S31N mutation of the M2 protein, but also other mutations have been described (Gu et al. 2013). Since the 2005/2006 season, H3N2 strains have demonstrated to be nearly completely resistant to adamantanes (Bright et al. 2006, Centers for Disease Control and Prevention 2013c), just as the other currently circulating influenza A strain, the formerly pandemic H1N1 which emerged in 2009 (Centers for Disease Control and Prevention 2013c). Therefore, the use of adamantanes against IAV is no longer recommended. Recently, there has been progress in early development of inhibitors of the mutated M2 channel (Baldi et al. 2013, Wang et al. 2013). However, their potential as clinically used antivirals remains to be determined.

Neuraminidase inhibitors block the cleavage of sialic acid bound to viral hemagglutinin and thereby the release of newly formed virions from their host cell. Zanamivir was discovered by rational design based on the neuraminidase's crystal structure (von Itzstein et al. 1993) and has been approved by the Food and Drug Administration in 1999. While zanamivir must be administered by inhalation due to low oral bioavailability (Cass et al. 1999), oseltamivir can be administered perorally. Indeed, oseltamivir carboxylate was discovered in 1997 (Kim et al. 1997), but its use as an ethylester prodrug made peroral application possible (Li et al. 1998).

Oseltamivir resistance is mostly mediated by a H274Y point mutation in the viral neuraminidase, which disrupts binding of the drug to its binding pocket (Moscona 2009). This mutation does not abolish binding to zanamivir. Due to a low resistance rate in currently

circulating influenza strains (> 98% of the H1N1 strains were sensitive in 2012) (Centers for Disease Control and Prevention 2012b), oseltamivir and zanamivir are the primary antiviral agents recommended to date. Nevertheless, sporadic clusters resistant to neuraminidase inhibitors have emerged (Baz et al. 2009, van der Vries et al. 2010) and even showed limited transmission (Hurt et al. 2011, Lackenby et al. 2011). The example of seasonal H1N1, which disappeared in 2009 with the emergence of pandemic H1N1, shows how rapidly oseltamivir resistance can develop. While before 2007, the number of oseltamivir resistant strains was minimal (Monto et al. 2006, Lackenby et al. 2008), up to 99% of seasonal H1N1 strains were resistant to oseltamivir in the 2008/2009 season (Centers for Disease Control and Prevention 2009, Sheu et al. 2011). These examples of emerged resistance highlight the need for new, effective antiviral drugs.

2.4.3 Antiviral drugs in development and novel strategies

Due to their high mutational rate, influenza viruses are likely to develop resistances against virtually any antiviral agent over time. Therefore, it is important to develop several parallel antiviral strategies, targeting different viral or host cell proteins. Some approaches have advanced into clinical phase II or III.

New developments in neuraminidase inhibitors concern both intravenous applications and long-acting drugs. With intravenous zanamivir, oseltamivir and peramivir, three candidates of intravenous neuraminidase inhibitors are in clinical development, with the goal to achieve rapid and high plasma concentrations. Laninamivir octanoate is the long-acting prodrug form of laninamivir, which is structurally related to zanamivir, and is administered by inhalation (Yamashita et al. 2009).

Antivirals targeting other viral proteins are also clinically developed. T-705 (favipiravir), after addition of a ribofuranosyl triphosphate by the host cell machinery, inhibits the viral polymerase (Furuta et al. 2009). Nitrazoxanide is already in use against protozoa such as cryptosporidium (Rossignol et al. 2006). More recently, its anti-influenza efficacy was discovered, as it posttranscriptionally blocks hemagglutinin maturation (Rossignol et al. 2009).

Rather than targeting viral proteins, it can be beneficial to target host cell proteins needed for viral replication. Indeed, host cell proteins are less prone to mutations, making appearance of

resistances less likely. DAS181 is a sialidase that removes both α 2,6- and α 2,3-linked sialic acids from the host cells, in a way that viral attachment is abolished (Malakhov et al. 2006). It was recently evaluated in a phase II clinical trial for inhalative administration (Moss et al. 2012).

In addition, there are numerous attempts to block host cell proteins that are in a less advanced stage, such as inhibition of the MEK/ERK pathway (Pleschka et al. 2001), the vacuolar ATPase (Müller et al. 2011) or the NF κ B pathway (Wurzer et al. 2004) to name only a few. Other approaches involve the use of antibodies, siRNAs or immunomodulators. Also combinations of established antivirals have shown beneficial synergistic effects *in vitro* and *in vivo* (Nguyen et al. 2010, Smee et al. 2010).

2.4.4 NS1-based vaccine and antiviral approaches

Since NS1 deficient or truncated IAVs are usually unable to suppress antiviral immune responses, they are often attenuated. This makes them interesting candidates for the development of live attenuated influenza vaccines. Mice or ferrets could be successfully protected from viral challenge by intranasal vaccination with IAVs expressing no NS1 or C-terminally truncated NS1 (Talon et al. 2000, Falcón et al. 2005, Romanova et al. 2009). Safety and immunogenicity of an NS1 deletion mutant were demonstrated in clinical phase I/II studies (Wacheck et al. 2010, Mössler et al. 2013).

NS1 has also shown potential as an antiviral drug target. Inhibition of NS1 using DNA aptamers (Woo et al. 2013) or human single chain antibody fragments (Yodsheewan et al. 2013) impaired viral replication and upregulated the antiviral immune response. Different drug screenings have identified compounds that inhibit the effect of NS1 on innate immunity (Basu et al. 2009) or its binding to RNA (Maroto et al. 2008, Cho et al. 2012). The screen of Basu et al., led to identification of two compounds, JJ3297 (Walkiewicz et al. 2011) and NSC125044 or derivatives (Jablonski et al. 2012) which inhibited IAV replication. Also administration of the CPSF30 domains F2F3 which outcompetes NS1 binding to CPSF30 attenuated IAV (Twu et al. 2006).

Interestingly, one study identified epigallocatechin gallate (EGCG) as an inhibitor of NS1 binding to RNA (Cho et al. 2012), suggesting a role of this pseudotannin with known antiviral activity in counteracting NS1.

2.4.5 Tannin- and pseudotannin-based antiviral approaches

Antimicrobial activity has been demonstrated for many plant extracts, while active compounds mostly belong to the phenolics (Cowan 1999). An important group of antimicrobial phenolics are the tannins. Tannins are secondary plant metabolites defined by their ability to precipitate protein, which is dependent on the tannin's molecular weight.

Tannins are subdivided into three classes: hydrolysable tannins, non-hydrolysable or condensed tannins (also known as proanthocyanidins (Haslam 2007)) and phlorotannins, which are only found in brown algae (Hagerman 1992). Hydrolysable tannins are based on gallic or ellagic acid moieties (gallic acid moiety highlighted in blue on Fig. 12), while condensed tannins are based on flavan structures (highlighted in red on Fig. 12), and phlorotannins on phloroglucinol. Figure 12 shows examples of hydrolysable and condensed tannins as well as their low molecular weight (< 500 g/mol) non-precipitating moieties such as gallic acid or catechins, which are also referred to as pseudotannins.

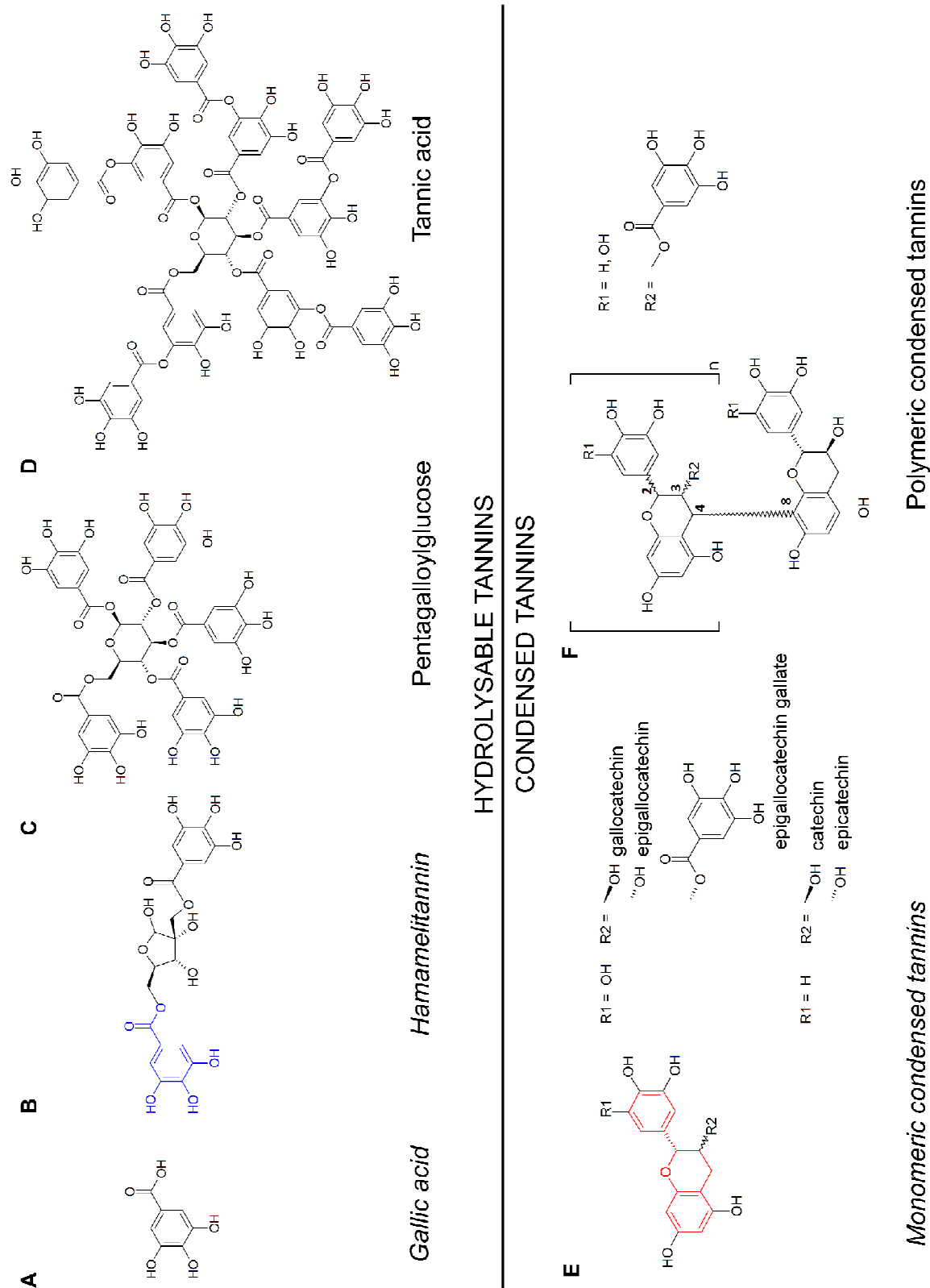


Figure 12: Examples of tannin and pseudotannin structures from *Hamamelis virginiana*. (D) tannic acid represented with 10 galloylation units, (E) monomeric pseudotannins with highlighted flavan unit, (F) polymeric condensed tannins as described by (Dauer et al. 2003). Pseudotannins having low or no protein precipitating activity (and molecular weights < 500 g/mol) are shown in italics.

As a rule of thumb, tannins with molecular weights from 500-3000 g/mol usually precipitate proteins (Wagner 1999). Their binding affinity and ability to precipitate proteins depends, in addition to the tannin's molecular weight, also on protein size and structure, as well as on reaction conditions (pH, temperature, solvent, time) (Hagerman 1992, Sarni-Manchado et al. 1999, Frazier et al. 2010). Soluble or insoluble complexes can be reversibly formed (Hagerman 1992, Li & Hagerman 2013). Tannins are multidentate ligands, binding to proteins mainly by hydrophobic interactions and hydrogen bonds (Hagerman 1992, Haslam 1996, Jöbstl et al. 2006). In addition to this rather unspecific binding, also highly specific binding, for example of EGCG to the human immunodeficiency virus (HIV) glycoprotein 120 binding pocket of the CD4 T-cell receptor has been demonstrated (Williamson et al. 2006).

Tannin- and pseudotannin-rich extracts have received some attention as antibacterial compounds. For example, cranberry extract inhibited adhesion of P-fimbriated *Escherichia coli* to uroepithelial cells (Howell et al. 1998), apple peel extract impaired the attachment of *Helicobacter pylori* *in vitro* and *in vivo* (Pastene et al. 2010) and a root extract from *Pelargonium sidoides*, EPs® 7630, prevented attachment of group A streptococci to epithelial cells (Janecki et al. 2011). In addition, the efficacy of (pseudo)tannin-rich extracts has been shown against various viruses, including IAV (Droebner et al. 2007, Haidari et al. 2009), herpes simplex virus (Erdelmeier et al. 1996, Schnitzler et al. 2008) or HIV (Notka et al. 2004).

More specifically, anti-infective properties of isolated condensed and hydrolysable tannins have been demonstrated. For example, EGCG has shown activity against *Streptococcus pyogenes* (Hull Vance et al. 2011) and staphylococci (Ikigai et al. 1993) and also inhibited hepatitis C virus (Ciesek et al. 2011), HIV (DeBruyne et al. 1999, Nance & Shearer 2003) or IAV (Song et al. 2005). Gallic and tannic acid inhibited IAV growth in embryonated eggs (Carson & Frisch 1953) and pentagalloylglucose influenced IAV infectivity and budding (Liu et al. 2011).

These examples show the established antimicrobial activity of (pseudo)tannins and (pseudo)tannin rich extracts. However, more insight into structure-activity relations is needed in order to develop new and improve existing antivirals against influenza. This can be obtained by direct systematic comparison of a large variety of (pseudo)tannin structures.

2.5 Objectives of the study

A thorough characterization of past and circulating IAV strains is indispensable for effective IAV risk management, because it can help rapid estimation of a new virus' fitness and potential danger. In **Part 1** of the study, pandemic H1N1 NS gene reassortants were characterized. pH1N1 nowadays circulates globally as a seasonal strain, together with H3N2 and influenza B strains. In addition to infecting humans, pH1N1 has also been found in other host species, such as swine or birds providing ample opportunities for gene reassortment. NS1 contributes to virulence, since its main role is impairment of the antiviral immune response. Using reverse genetics, a diverse panel of pH1N1 reassortants carrying NS genes from human, swine or bird strains was constructed, with the aim to:

- (i) characterize the viral fitness of the NS reassortants *in vitro* and *in vivo*;
- (ii) identify amino acids involved in viral fitness for use as pathogenicity markers;
- (iii) introduce the identified mutations into the pH1N1 backbone and characterize the viral fitness of the NS mutants *in vitro* and *in vivo*;
- (iv) characterize the potential differential effects of NS reassortants and mutants on the antiviral host response.

Reassortments and mutations occurring in nature and created in the laboratory (see Part 1 of this study) highlight that IAV strains are highly variable and thus prone to antiviral resistance. Therefore, the development of new safe and effective antivirals is of importance for public health.

In **Part 2** of the study, the antiviral efficacy of a tannin-rich plant extract from *Pelargonium sidoides* (EPs® 7630), having already a full marketing authorization for treatment of acute bronchitis, was tested with the aim to

- (i) demonstrate efficacy against IAV at non toxic concentrations *in vitro* and *in vivo*;
- (ii) elucidate the antiviral mechanism;
- (iii) test the propensity to induce viral resistance;
- (iv) determine the active compounds.

While selected tannins have shown anti-IAV efficacy, the corresponding plants mostly contain a multitude of different (pseudo)tannins at a time. It is important to better characterize and compare the anti-IAV activity of different tannin categories and structures, in order to select and extract the optimal antiviral tannin or composition of tannins.

In ***Part 3*** of the study, we used *Hamamelis virginiana*, a plant rich in different well characterized tannins, in order to:

- (i) compare the antiviral efficacies of Hamamelis bark extract, fractions enriched in tannins of different molecular weights and individual tannins and pseudotannins;
- (ii) define antiviral structure-activity relationships of (pseudo)tannins;
- (iii) investigate differences between distinct (pseudo)tannins regarding the antiviral mechanism.

3 Materials

In addition to those mentioned, also other product and company names may be trademarks TM or registered trademarks ®.

3.1 Animals

Pathogen-free female 7 week old BALB/c mice (Harlan, The Netherlands) were used for all experiments.

3.2 Cells

3.2.1 Cell lines

Cell line	Cell type	Source
HEK293T	Transformed human embryonic kidney cells	M. Lenk, Friedrich-Loeffler-Institut (D)
A549	Human adenocarcinomic alveolar epithelial cells	American Type Culture Collection
A549Luc	A549 cells expressing an IFN- β luciferase reporter gene	W. Barclay, Imperial College London (UK) (Hayman et al. 2006)
A549Slam	A549 cells expressing the Slam receptor	Y. Yanagi, Kyushu University (J) (Takeda et al. 2005)
DF-1	Chicken embryo fibroblasts	M. Lenk, Friedrich-Loeffler-Institut (D)
MDCK	Madin-Darby Canine kidney cells	American Type Culture Collection
ST	Swine fetal testis cells	M. Lenk, Friedrich-Loeffler-Institut (D)
VeroSlam	African green monkey kidney cells expressing the Slam receptor	Y. Yanagi, Kyushu University (J) (Ono et al. 2001)

3.2.2 Cell culture media

Cell line	Medium Composition
MDCK, ST	EMEM, 10% FBS, 25mM HEPES, 1% Pen/Strep
Vero/A549(Slam), DF-1	DMEM, 10% FBS, 1% Ultraglutamine, 1% Pen/Strep
A549Luc	DMEM, 10% FBS, 1% Ultraglutamine, 1% Pen/Strep, 2 mg/ml Geneticin® (G418)
HEK293T	DMEM, 10% FBS, 1% Ultraglutamine

3.3 Viruses

3.3.1 Wild type viruses

Virus/Subtype	Description	Source
IAV/H1N1	A/Puerto Rico/8/34	X. Saelens, VIB/Ghent University (B)
IAV/H1N1	A/Luxembourg/46/2009	M. Opp, Laboratoire National de Santé (L)
IAV/H1N1	A/Luxembourg/43/2009	M. Opp, Laboratoire National de Santé (L)
IAV/H1N1	A/Luxembourg/572/2008	M. Opp, Laboratoire National de Santé (L)
IAV/H1N1	A/Luxembourg/663/2008	M. Opp, Laboratoire National de Santé (L)
IAV/H1N1	A/swine/Iowa/H04Y52/2004	K. van Reeth, Ghent University (B)
IAV/H1N1	A/Swine/DE-NI/R819/2010	T. Harder, Friedrich-Loeffler-Institut (D)
IAV/H3N2	A/Swine/DE-NI/R494/2010	T. Harder, Friedrich-Loeffler-Institut (D)
IAV/H3N2	A/Luxembourg/01/2005	M. Opp, Laboratoire National de Santé (L)
IAV/H7N9	A/Anhui/01/2013	WHO Influenza Centre, National Institute for Medical Research, London (UK)
Adenovirus/V	ATCC reference strain	A. Heim, Hannover Medical School (D)
Measles	Schwarz strain/Rimevax	GlaxoSmithKline (B)

3.3.2 Recombinant influenza viruses

3.3.2.1 NS reassortants and aa 80-84 mutants

All the following recombinant viruses have seven background genes (PB2, PB1, PA, HA, NP, NA, M) from pH1N1 A/Luxembourg/43/2009:

Reassortant/mutant	NS gene from	NS1 mutations
pH1N1 wt	A/Luxembourg/43/2009 (H1N1)	none
H5-av	A/swan/Germany/R65/2006 (HPAIV H5N1)	none
H5-hum	A/Thailand/1(KAN-1)/2004 (HPAIV H5N1)	none
H5-LP	A/Teal/Germany/Wv632/2005 (LPAIV H5N1)	none
H9	A/Chicken/Emirates/R66/2002 (H9N2)	none
H1N1-swEU	A/Swine/DE-NI/R819/2010 (H1N1)	none
H3N2-swEU	A/Swine/DE-NI/R494/2010 (H3N2)	none
H1N1-swUS	A/Swine/Iowa/H04Y52/2004 (H1N1)	none
H3N2-seas	A/Luxembourg/01/2005 (H3N2)	none
PR8	A/Puerto Rico/8/34 (H1N1)	none
pH1N1 wt-del	A/Luxembourg/43/2009 (H1N1)	Deletion aa 80-84
PR8-del	A/Puerto Rico/8/34 (H1N1)	Deletion aa 80-84
H1N1-swEU-del	A/Swine/DE-NI/R819/2010 (H1N1)	Deletion aa 80-84
H5-av-ins	A/swan/Germany/R65/2006	Insertion aa 80-84
H5-hum-ins	A/Thailand/1(KAN-1)/2004	Insertion aa 80-84

3.3.2.2 NS splice mutants

All NS splice mutants are recombinant viruses with seven background genes (PB2, PB1, PA, HA, NP, NA, M) from pH1N1 A/Luxembourg/43/2009 and an NS gene from a strain of interest carrying an A to C nucleotide mutation at base pair 501. This mutation is silent on the amino acid level but results in a block of NS splicing. Thus, only the unspliced NS1 protein, but not the spliced NS2/NEP protein is expressed from the NS gene segment.

3.3.2.3 GFP reporter virus

Reporter virus	Description	Source
A/Puerto Rico/8/34-NS116-GFP	A/Puerto Rico/8/34 carrying a GFP open reading frame starting at amino acid 116	C. Kittel, AVIR Green Hills Biotechnology AG (A) (Kittel et al. 2004)

3.3.3 Virus growth media

Cell line	Virus growth medium composition
MDCK, ST	EMEM, 25 mM HEPES, 2 mg/ml BSA, 1% Pen/Strep, 2 µg/ml TPCK
A549, A549Luc	DMEM, 1% Ultraglutamine, 1% Pen/Strep, 0.2 µg/ml TPCK
DF-1	DMEM, 1% Ultraglutamine, 1% Pen/Strep, 0.5 µg/ml TPCK

3.4 Bacteria

3.4.1 Bacteria strains

Bacterial strain (chemically competent)	Source
OneShot® TOP10 <i>E. coli</i>	Life Technologies
XL1-Blue <i>E. coli</i>	Agilent

3.4.2 Bacteria growth media

LB medium

25g Luria Broth Base in 1L sterile water was autoclaved at 121°C for 15 min. If needed, the medium was supplemented with 100 µg/ml of ampicillin or 50 µg/ml of kanamycin before use.

LB agar

32g of LB agar in 1L sterile water was autoclaved at 121°C for 15 min. After 15-30min of cooling, 100µg/ml of ampicillin or 50 µg/ml of kanamycin were added and the agar was poured into 10cm petri dishes and kept at 4°C.

3.5 Antiviral drugs and plant extracts

Drugs provided by Dr. Willmar Schwabe GmbH	Drugs purchased at Sigma-Aldrich
Galocatechin	Gallic acid monohydrate
Epigallocatechin	Pentagalloylglucose
Epigallocatechin-(4β→8)-galocatechin	Hamamelitannin
Epigallocatechin-(4α→8)-epigallocatechin	Tannic acid
Galocatechin-(4β→8)-galocatechin	
Galocatechin-(4α→8)-epigallocatechin	
EPs® 7630	
EPs® 7630 oligo-/polymeric fraction	
Hamamelis bark extract	
Hamamelis leaf extract	
Hamamelis bark UF-concentrate	
Hamamelis bark UF-filtrate	

3.6 Solutions, chemicals, reagents

Compound	Company
0.05% Trypsin-Versene (EDTA)	Lonza
0.5% Trypsin-EDTA	Life Technologies
2-(<i>N</i> -morpholino)ethanesulfonic acid (MES)	Sigma-Aldrich
2-[4-(2-hydroxyethyl)piperazin-1-yl]ethanesulfonic acid (HEPES)	Lonza
2'-(4-methylumbelliferyl)-α-D-N-acetylneuraminic acid (MUNANA)	Sigma-Aldrich

3-[(3-cholamidopropyl)dimethylammonio]-1-propanesulfonate (CHAPS)	Sigma-Aldrich
Agar, extra pure, fine powder PhEur, BP	Merck
Ampicillin	Sigma-Aldrich
Bovine Serum Albumin (BSA)	Sigma-Aldrich
BSA Fraction V Solution (7.5%)	Lonza
Calcium Chloride (CaCl ₂)	Sigma-Aldrich
Dimethylsulfoxide (DMSO)	Sigma-Aldrich
DMEM 4,5g/L Glucose, 25mM HEPES, without L-Glutamine	Lonza
Dulbecco's Phosphate Buffered Saline (PBS)	Lonza
ECL Plex TM Fluorescent Rainbow Marker	GE Healthcare
EMEM with L-Glutamine	Lonza
Ethanol 96-100%	Merck
Ethylenediaminetetraacetic Acid (EDTA)	Sigma-Aldrich
Fetal Bovine Serum (FBS)	Lonza
Folin-Ciocalteu's Phenol Reagent	Sigma-Aldrich
Forene ® (isoflurane)	Abbott
GeneRuler 1kb plus DNA ladder	Fermentas
Geneticin® (G418)	Life Technologies
Glycerol	Sigma-Aldrich
Glycine	Sigma-Aldrich
Halt TM Protease Inhibitor Cocktail	Thermo Scientific
Hide powder	FILK Freiberg
Highly deionised formamide	Applied Biosystems
Human erythrocytes, type 0	Laboratoire National de Santé, Luxembourg
Hybond TM ECL blotting membrane	GE Healthcare
IGEPAL® CA-630	Sigma-Aldrich
Isopropanol	Sigma-Aldrich
Kanamycin	Sigma-Aldrich
L-1-tosylamido-2-phenylethyl chloromethylketone-(TPCK) trypsin	Sigma-Aldrich
LB Agar (Lennox L Agar)	Life Technologies
Lipofectamine TM 2000 Reagent	Life Technologies

Lipofectamine TM LTX with PLUS TM Reagent	Life Technologies
Luria Broth Base (LB)	Life Technologies
Magnesium Chloride (MgCl ₂)	Life Technologies
Methanol	Sigma-Aldrich
Nuclease Mix	GE Healthcare
Nucleotides (dNTPs)	Life Technologies
NuPAGE [®] 4-12% Bis-Tris gel	Life Technologies
NuPAGE [®] LDS sample buffer	Life Technologies
Opti-MEM [®] I Reduced Serum Medium with GLUTAMAX TM	Life Technologies
Penicillin/Streptomycin (Pen/Strep)	Lonza
Polyinosinic:polycytidylic acid (polyI:C)	Sigma-Aldrich
Pyrogallol	Sigma-Aldrich
Recombinant human TNF- α	R&D Systems
SeaKem [®] LE Agarose	Lonza
Sodium Carbonate (Na ₂ CO ₃)	Sigma-Aldrich
Sodium Dodecyl Sulfate (SDS)	Sigma-Aldrich
Sodium Hydroxide (NaOH)	Sigma-Aldrich
Staurosporine	Enzo Life Sciences
SYBR [®] Green nucleic acid stain	Molecular Probes
SYBR [®] Safe DNA Gel Stain	Life Technologies
Thiourea	Sigma-Aldrich
Tris-Base	Sigma-Aldrich
Tris-HCl	Sigma-Aldrich
Trypan Blue	Sigma-Aldrich
TWEEN [®] 20	Sigma-Aldrich
Ultraglutamine	Lonza
Universal type I interferon	PBL Interferon Source
Urea	Sigma-Aldrich
β -mercaptoethanol	Sigma-Aldrich

3.7 Enzymes

Enzyme	Source
DpnI	Takara
Phusion® High Fidelity DNA Polymerase	Bioke
Platinum® Taq DNA polymerase	Life Technologies
RNaseOUT™ Recombinant Ribonuclease Inhibitor	Life Technologies
SuperScript® III Reverse Transcriptase	Life Technologies

3.8 Antibodies

Antibody	Source
ECL Plex™ Goat- α -mouse IgG-Cy3	GE Healthcare
ECL Plex™ Goat- α -rabbit IgG-Cy5	GE Healthcare
Mouse anti- β -actin	Santa Cruz
Rabbit anti-I κ B- α (C-21)	Santa Cruz

3.9 Commercial Kits

Kit	Source
Big Dye® Terminator v3.1 Cycle Sequencing Kit	Life Technologies
Caspase-Glo® 3/7 Assay	Promega
Cell Proliferation Kit II (XTT, 2,3-Bis(2-methoxy-4-nitro-5-sulfophenyl)-2 <i>H</i> -tetrazolium-5-carboxanilide)	Roche Diagnostics
Human Antiviral Response PCR Array	Qiagen
Jetquick PCR Product Purification Spin Kit	Genomed
Luciferase Assay System	Promega
QIAamp® Viral RNA Mini Kit	Qiagen
QIAprep® Spin Midiprep Kit	Qiagen
QIAprep® Spin Miniprep Kit	Qiagen
QIAquick® Gel Extraction Kit	Qiagen
Renilla Luciferase Assay System	Promega
RNA 6000 Nano Total RNA Assay Kit	Agilent
RNase-Free DNase Set	Qiagen

RNeasy® Mini Kit	Qiagen
RT ² First Strand Kit	Qiagen

3.10 Buffers

Agarose gel electrophoresis buffers

1x TAE buffer

40mM	Tris
0.5mM	Sodium Acetate
10mM	EDTA
pH 7.8	

Neuraminidase inhibition assay buffers

1x Assay buffer

32.5mM	MES
4mM	CaCl ₂
pH 6.5	

Stop solution

0.14M	NaOH in 83% ethanol
-------	---------------------

Western blot buffers

CHAPS buffer

30mM	TrisCl
2M	Thiourea
7M	Urea
4%	CHAPS
1x	Protease inhibitor
1x	Nuclease mix
12%	Isopropanol
	H ₂ O

pH 8.5

Transfer buffer

2.92 g Glycine
 5.80 g Tris-Base
 200 ml Methanol
 1.88 ml 10% SDS
 Ad 1L H₂O

1x Tris Buffered Saline (TBS)

0.05M Tris-Base
 0.9% NaCl
 H₂O

pH 7.6

Blocking buffer

3% BSA
 0.3% TWEEN® 20
 1x TBS

3.11 DNA: Plasmids and primers

3.11.1 Plasmids

Material	Source
pHWSccdB	J. Stech, Friedrich Loeffler Institut (D)
NS from A/swan/Germany/R65/2006 in pHWS	J. Stech
NS from A/Thailand/1(KAN-1)/2004 in pHWS	J. Stech
NS from A/Teal/Germany/Wv632/2005 in pHWS	J. Stech
NS from A/Chicken/Emirates/R66/2002 in pHWS	J. Stech
pGL4.73	Promega
pIRES2-AcGFP1	Clontech

Primers	Eurogentec
Random hexamers	Life Technologies

3.11.2 Primers

3.11.2.1 Primer used to reverse transcribe extracted viral RNA (RT PCR)

Primer	Sequence 5'-3'
Uni 12	AGCAAAGCAGG

The primer is complementary to the conserved 3' region of IAV.

3.11.2.2 Primers used to insert viral gene segments into pHWSccdB

Primer	Sequence 5'-3'
pHW-PB2-F	<u>gaagtgggggggagcgaagcaggTC</u>
pHW-PB2-R	<u>ccgccgggttagtagaaacaaggTCGTTT</u>
pHW-PB1-F	<u>gaagtgggggggagcgaagcaggCAAAC</u>
pHW-PB1-R	<u>ccgccgggttagtagaaacaaggCATTT</u>
pHW-PA-F	<u>gaagtgggggggagcgaagcaggTAC</u>
pHW-PA-R	<u>ccgccgggttagtagaaacaaggTACTT</u>
pHW-HA-F	<u>gaagtgggggggagcaaaagcaggGG</u>
pHW-HA-R	Identical to pHW-NS-R
pHW-M-F	<u>gaagtgggggggagcaaaagcaggTAG</u>
pHW-M-R	<u>ccgccgggttagtagaaacaaggTAG</u>
pHW-NP-F	<u>gaagtgggggggagcaaaagcaggGTA</u>
pHW-NP-R	<u>ccgccgggttagtagaaacaaggGTATTTTT</u>
pHW-NA-F	<u>gaagtgggggggagcaaaagcaggAGT</u>
pHW-NA-R	<u>ccgccgggttagtagaaacaaggAGT</u>
pHW-M-F	<u>gaagtgggggggagcaaaagcaggTAG</u>
pHW-M-R	<u>ccgccgggttagtagaaacaaggTAG</u>
pHW-NS-F	<u>gaagtgggggggagcaaaagcaggGTG</u>
pHW-NS-R	<u>ccgccgggttagtagaaacaaggGTG</u>

Small letters designate nucleotides complementary to pHWSccdB. Underlined nucleotides designate conserved IAV promoter sequences. Capital letters designate IAV segment specific complementary nucleotides (Stech et al. 2008).

3.11.2.3 M13-tagged primers used to amplify cDNA for sequencing

Primer	Sequence 5'-3'
M13-21-PB2-F	tgtaaacgacggccagtTCATCTCGAGAGCAAAAGCAGGTC
M13-PB2-R	caggaaacagctatgaccATCTGTTCACAGTGGAAACAAGGTC
M13-21-PB1-F	tgtaaacgacggccagtTCATCTCGAGAGCAAAAGCAGGCA
M13-PB1-R	caggaaacagctatgaccATCTGTTCACAGTGGAAACAAGGCA
M13-21-PA-F	tgtaaacgacggccagtTCATCTCGAGAGCAAAAGCAGGTAC
M13-PA-R	caggaaacagctatgaccATCTGTTCACAGTGGAAACAAGGTAC
M13-21-HA-F	tgtaaacgacggccagtTCATCTCGAGAGCAAAAGCAGGGG
M13-HA-R	Identical to M13-21-NS-R
M13-21-NP-F	tgtaaacgacggccagtTCATCTCGAGAGCAAAAGCAGGGTA
M13-NP-R	caggaaacagctatgaccATCTGTTCACAGTAGAAACAAGGGTA
M13-21-NA-F	tgtaaacgacggccagtTCATCTCGAGAGCAAAAGCAGGAGT
M13-NA-R	caggaaacagctatgaccATCTGTTCACAGTAGAAACAAGGAGT
M13-21-M-F	tgtaaacgacggccagtTCATCTCGAGAGCAAAAGCAGGTAG
M13-M-R	caggaaacagctatgaccATCTGTTCACAGTAGAAACAAGGTAG
M13-21-NS-F	tgtaaacgacggccagtTCATCTCGAGAGCAAAAGCAGGGTG
M13-NS-R	caggaaacagctatgaccATCTGTTCACAGTAGAAACAAGGGTG

Small letters designate the M13-21-F or the M13-R sequence, respectively. Capital letters contain nucleotides complementary to the conserved IAV promoter, followed by IAV segment specific complementary nucleotides.

3.11.2.4 Untagged sequencing primers

Primer	Sequence 5'-3'
M13-21-F	TGTA AACGACGGCCAGT
M13-R	CAGGAAACAGCTATGACC
pHW-F	CTCACTATAGGGAGACCC
pHW-R	GAGGTATATCTTTCGCTCC
HA-736-F	AGRATGRACTATTACTGGAC
HA-1124-F	TGGATGGTAYGGTTAYCAYCA
HA-943-R	GAAAKGGGAGRCTGGTGTTTA
HA-1340-R	TTCTKCATTRTAWGTCCAAA
NA-536-F	GGTCAGCAAGCGCATGYCATGA
NA-941-F	TAGGATACATCTGCAGTGG

NA-501-R	ATCTTGAGTTGTATGGAGAGG
NA-740R	GGRCCATCGGTCATTATG
NA-1346-R	GCTGCTYCCRCTAGTCCAGAT
NP-513-F	TGGCATTCHAATTTRAATGAT
NP-925-F	CCTGCVTGTGYGTAWGGAC
NP-757-R	TTTGTGCAGCTGTTTGAAATTTYCCTTT
NP-1177-R	AAGCRATTTGTACYCCTCTAGT
NS-semicons-319-F	AGACTGGTTCATGCTCATGC
NS-semicons-637-F	ATACAGAGATTCGCTTGGAG
NS-semicons-329-R	TAGGCATGAGCATGAACCAG
NS-semicons-550-R	TGTTATCATTCCATTCAAGTCC
PA-702-F	TGCMTTGARAATTTTAGRACCTA
PA-1219-F	TGATGACTGCAAAGATGTTGG
PA-1787-F	ATGAARTGGGGAATGGAGATGAG
PA-756-R	TGAGAAAGCTTGCCCTCAATG
PA-1292-R	TCRCAKGCCTTGTTGAACTCATT
PA-1849-R	TCTCTTTGACAGAAGACTCG
PB1-711-F	TGAACACRATGACCAARGA
PB1-1177-F	AATACCAGCAGAAATGCTAGC
PB1-1532-F	GCYAATTTYAGCATGGAGCT
PB1-1830-F	TCTTCACATTCCTGAAGTCTGC
PB1-566-R	TCATGTTGTCTCTTACTCTCC
PB1-843-R	GTTCAAGCTTTTCRCAWATG
PB1-1278-R	TTGAACATGCCCATCATCATYCCAGG
PB1-1694-R	TTTGATGAACAATTGAAGAGCC
PB2-548-F	ACTGACAGCAGAGTCACAGC
PB2-713-F	CAAGCAGTRTRTACATTGAAGT
PB2-1140-F	ATTGATCCAGTTGATAGTAAGC
PB2-1447-F	CCAAGYACMGAGATGTCAATGAGA
PB2-1712-F	ACACTTATCAATGGATAATCAGG
PB2-816-R	GCTTTGRTCAAYATCRTCATT
PB2-1129R	TGGATCAATCTCCTGGTTGC
PB2-1509-R	GGAGTATTCATCYACACCCAT
PB2-2186-R	TTRCTCARTTCATTGATGCT

3.11.2.5 Mutagenesis primers

Mutagenesis primers for deletion or insertion of 5 amino acids on position 80-84 of NS1

Primer	Sequence 5'-3'
pH1N1 wt-del F	AGACACTTAGAATG CCTACTTCGCG
pH1N1 wt-del R	CGCGAAGTAGG CATTCTAAGTGTCT
H5-av-ins F	GCACTTAAAATG <u>ACAATTGCATCTGT</u> ACCAGCTTCACG
H5-av-ins R	CGTGAAGCTGGT <u>ACAGATGCAATTGTC</u> CATTTTAAGTGC
H5-hum-ins F	GCACTTAAAATG <u>ACAATTGCATCTGT</u> ACCGGCTTCACG
H5-hum-ins R	CGTGAAGCCGGT <u>ACAGATGCAATTGTC</u> CATTTTAAGTGC
H1N1-PR8-del F	AGGCACTTAAAATG CCTGCGTCGCGTTAC
H1N1-PR8-del R	GTAACGCGACGCAGG CATTTTAAGTGC
H1N1-swEU-del F	AGGCATTTAAACTA CCTACCTCACGCTATC
H1N1-swEU-del R	GATAGCGTGAGGTAGG TAGTTTAAATGCCT

|.designates the position of deletion of five amino acids at position 80-84 of NS1. Underlined letters designate the five amino acids (TIASV) inserted at position 80-84 of NS1.

Mutagenesis primers for generation of NS splice mutants

Primer	Sequence 5'-3'
pH1N1 wt-A501C F	TTACCTTCTCTTCC <u>CGG</u> ACATACTTATGAG
pH1N1 wt-A501C R	CTCATAAGTATGTCC <u>GGA</u> AAGAGAAGGTAA
H5-av and H1N1-swEU-A501C F	TTACCTTCTCTTCC <u>CGG</u> ACATACTAATGAG
H5-av and H1N1-swEU-A501C R	CTCATTAGTATGTCC <u>GGA</u> AAGAGAAGGTAA
H5-hum-A501C F	TTACCTTCTCTTCC <u>CGG</u> ACATACTGGTGAG
H5-hum-A501C R	CTCACCAGTATGTCC <u>GGA</u> AAGAGAAGGTAA
H5-LP-A501C F	TTACCTTCCCTTCC <u>CGG</u> ACATACTGATGAG
H5-LP-A501C R	CTCATCAGTATGTCC <u>GGA</u> AGGGAAGGTAA
H9 and H1N1-swEU-A501C F	TTACCTTCTCTTCC <u>CGG</u> ACATACTGATGAG
H9 and H1N1-swEU-A501C R	CTCATCAGTATGTCC <u>GGA</u> AAGAGAAGGTAA

A501C R		
H3N2-seas-A501C F	TTGCCTTCTTTTCC <u>C</u> GGACATACTATTGAG	
H3N2-seas-A501C R	CTCAATAGTATGTCC <u>G</u> GAAAAGAAGGCAA	
H3N2-swEU-A501C F	TTACCTTTTCTTCC <u>C</u> GGACATACTGATGAG	
H3N2-swEU-A501C R	CTCATCAGTATGTCC <u>G</u> GGAAGAAAAGGTAA	
H1N1-PR8 A501C F	TTGCCTTCTCTTCC <u>C</u> GGACATACTGCTGAG	
H1N1-PR8 A501C R	CTCAGCAGTATGTCC <u>G</u> GGAAGAGAAGGCAA	

The underlined letter designates the mutation at position 501. The same primers were used to introduce the splice mutation into 80-84 deletion or insertion mutants.

3.11.2.6 Real-time PCR primers and conditions for cytokine mRNA and pre-mRNA quantification

Cytokine		Primer sequence (5'-3')	Primers (μ M)	MgCl ₂ (mM)	T _a * (°C)
GAPDH	F	GAAGGTGAAGGTCGGAGTC	0.5	2.0	60
	R	GAAGATGGTGATGGGATTTTC			
IFN-β	F	GACGCCGCATTGACCATCTA	1.2	1.8	55.4
	R	CCTTAGGATTTCCACTCTGACT			
TNF-α	F	CTATCTGGGAGGGGTCTTCC	0.5	2.0	61
	R	GGTTGAGGGTGTCTGAAGGA			
RANTES	F	CGCTGTCATCCTCATTGCTA	0.5	1.8	61
	R	CTGGTCTCGAACTCCTGACC			
IP-10	F	GCATTCAAGGAGTACCTCT	1.0	1.8	56.5
	R	CCTTGCTAACTGCTTTCAG			
IL-1β	F	GACACATGGGATAACGAGGC	1.0	2.5	61
	R	ACGCAGGACAGGTACAGATT			
IL-6	F	GGCTTCTGAACCAGCTTGAC	0.2	3.8	62
	R	TCCTCTTTGTTGGGGATGTC			
GAPDH (pre-mRNA)	F	CTGGAAGGGCTTCGTATGAC	1	2	57
	R	GTAAAAGCAGCCCTGGTGA			
TNF-α (pre-mRNA)	F	CCCCAGGGACCTCTCTCTAA	1	2	57
	R	AAAGCTGAGACCCTTAAACTTCC			

RANTES	F	GCCAATGCTTGGTTGCTATT	1	2	57
(pre-mRNA)	R	ACAGTCATTGGGATGGGGTA			
IP-10	F	CTGTACGCTGTACCTGCATCA	1	2	57
(pre-mRNA)	R	TGGCATAACGCAGTTCTGAAG			
IL-6	F	TGGCTAGCATGTGGAGGAG	1	2	57
(pre-mRNA)	R	ACCACTGATCCGGTGGTGTA			

*T_a, annealing temperature

3.12 Instruments

Instrument	Source
ABI PRISM [®] 3130xl Genetic Analyzer	Applied Biosystems
Bioanalyzer 2100	Agilent
Biofuge [™] Stratos [™] Centrifuge	Heraeus
CFX 96 [™] real time PCR Cycler	Bio-Rad
Ecotron Incubator Shaker	Analisis
Electrophoresis Power Supply EV231	Consort
Fresco [™] 21 Centrifuge	Thermo Scientific
Gel tank, combs and casting form	Bioplastics
GENios Plus Fluorescence Reader	Tecan
HERAcell [®] 150 Incubator	Heraeus
IKA RCT Basic Magnetic Stirrer	IKA Labortechnik
Infinite [®] M200 Microplate reader	Tecan
InGenius Gel Bioimaging	Syngene
Mastercycler [®] Gradient PCR Cycler	Eppendorf
NanoDrop [®] ND-1000 Spectrophotometer	Isogen
PARI Boy [®] SX	PARI
Pellicon 2 Ultrafiltration Cassettes, C Screen	Millipore
Pico [™] 17 Centrifuge	Heraeus
Pro Flux M12 Tangential Flow Filtration System	Millipore
Precision Balance	Sartorius AG
SL40R Centrifuge	Thermo Scientific
SpectraMax Plus Microplate Reader	Molecular Devices
TH-5 Thermalert Monitoring Thermometer	Phymep

Thermomixer® Comfort Heating Block	Eppendorf
TissueLyser II	Qiagen
Trans-Blot® SD Semi-Dry Electrophoretic Transfer Cell	Bio-Rad
Transsonic TI-H-15 Ultrasonic Bath	Elma
Typhoon™ TRIO+ Scanner	GE Healthcare
UNO96 Thermal Cycler	VWR
Vortex-Genie 2	Scientific Industries
XCell SureLock™ Mini-Cell Electrophoresis System	Life Technologies

3.13 Software

Software	Source
BioEdit V7.2.3	http://www.mbio.ncsu.edu/bioedit/bioedit.html (Hall 1999)
Bio-Rad CFX Manager V3.0	Bio-Rad
FastPCR V5.2.28	PrimerDigital
Geneious V5.5.6	Biomatters
GeneSnap Image Acquisition	Syngene
ID-50 5.0	Spouge JL, http://www.ncbi.nlm.nih.gov/CBBresearch/Spouge/html_ncbi/html/index/software.html#1
RT ² Profiler PCR Array Data Analysis Package V4	Qiagen
SigmaPlot V12.3	Systat Software

If the software was updated during the course of the PhD studies, the newest version is indicated.

4 Methods

4.1 Construction of IAV pH1N1, NS reassortants and NS mutants by reverse genetics

4.1.1 Reverse genetics plasmid construction and isolation

The NS plasmids for A/Swan/Germany/R65/06 (H5N1), A/Thailand/1(KAN-1)/2004 (H5N1), A/Teal/Germany/Wv632/05 (H5N1) and A/Chicken/Emirates/R66/2002 (H9N2) were kindly provided by Dr. Jürgen Stech, Friedrich-Loeffler-Institut, Greifswald, Germany. All other plasmids were constructed from virus culture supernatant by the methods described in Sections 4.1.1.1-4.1.1.9.

4.1.1.1 Viral RNA extraction

Using the QIAamp® Viral RNA Mini Kit, viral RNA was extracted from 280 µl of culture supernatant according to the manufacturer's instructions and stored at -80°C.

4.1.1.2 Reverse transcription of viral RNA

The extracted viral RNA was reverse transcribed into cDNA using a universal primer (Uni 12) complementary to the 3' region conserved between influenza strains.

5.5 µl	H ₂ O
1 µl	dNTPs (10 mM)
1 µl	Uni 12 primer (40 mM)
5 µl	RNA

This mix was incubated for 5 min at 65°C to destroy RNA secondary structures, then kept on ice for at least 1min to allow primer annealing. Afterwards, the following mix was added:

2 µl	DTT (0.1 M)
4 µl	5x First Strand Buffer
0.5 µl	RNaseOUT™ RNase Inhibitor (40 U/ µl)
1 µl	SuperScript® III Reverse Transcriptase (200 U/µl)

The reaction was incubated at 55°C for 60-80 min for cDNA synthesis and then inactivated at 70°C for 15 min.

4.1.1.3 Specific amplification of viral gene segments with addition of vector-complementary regions

During this step, the different viral gene segments are amplified and at the same time, regions complementary to the pHWSccdB plasmid are added adjacent to the viral gene sequences. This allows subsequent insertion of the viral segment into pHWSccdB by a QuikChange-like PCR and is done by primers complementary on one side to the viral gene sequence flanked by the vector region directly next to the insertion site (Figure 11, for primers see Section 3.11.2.2).

71 µl	H ₂ O
20 µl	5x HF buffer
2 µl	dNTPs (10 mM)
2.5 µl	Primer F (20 µM)
2.5 µl	Primer R (20 µM)
1 µl	Phusion® High Fidelity DNA Polymerase (2 U/µl)
1 µl	cDNA

Temperature protocol:

98°C 30s	} 35 cycles
98°C 10s	
55°C 30s	
72°C 4min	
72°C 5min	
10°C 5min	

The above volumes were used 2 to 4 times in order to produce sufficient quantities of each segment for subsequent agarose gel purification. Amplified segments were cut and purified from a 1 % agarose gel using the QIAquick® Gel Extraction Kit according to the manufacturer's instructions.

4.1.1.4 Gel electrophoresis

For a medium size gel (14x12 cm), 1 g of agarose was heated in 100 ml TAE buffer in the microwave for 90 s. After a short cool down, 10 μ l of SYBR[®]Safe DNA Gel Stain were added and the gel was cast. After transfer of the solidified gel into the running chamber containing TAE buffer, 5 μ l of GeneRuler 1kb plus DNA ladder or 1 μ l of loading dye with 5 μ l of DNA sample were loaded and run at 130 V and 300 mA for 30-40 min. DNA was visualized by exposure to UV light and analysis by the Syngene gel documentation system.

4.1.1.5 Insertion of the IAV gene segment into pHWSccdB

During this step, the IAV gene segment is integrated into the pHWSccdB vector using the method of Stech (Stech et al. 2008). It anneals to pHWSccdB by its plasmid-complementary regions. The free 3' end is then used as a megaprimer to synthesize the sequence complementary to the rest of the plasmid.

Ad 50 μ l	H ₂ O
10 μ l	5x HF buffer
1 μ l	dNTPs (10 mM)
2 μ l	Phusion [®] High Fidelity DNA Polymerase (2 U/ μ l)
xx μ l	cDNA (200-300 ng)
xx μ l	pHWSccdB (50–100 ng)

Temperature protocol:

98°C 30s	} 35 cycles
98°C 10s	
48°C 1min	
72°C 5min 30s	
10°C 5min	

Selection of IAV segment-carrying plasmids over pHWSccdB is ensured by two mechanisms. First, the PCR product is digested with 20 U of DpnI at 37°C for 3 h. DpnI specifically digests bacterial methylated DNA (such as pHWSccdB, previously grown in *E. coli*), and therefore leads to selection of the unmethylated PCR product. Further, negative selection of remaining pHWSccdB is ensured in the following cloning steps by toxicity of ccdB to bacteria by inhibition of their topoisomerase II.

4.1.1.6 Plasmid mutagenesis

Mutations were introduced into the plasmids by site-directed mutagenesis according to the QuikChange method (Stratagene). This method uses complementary forward and reverse primers carrying the mutation of interest in their middle region and 11 to 16 nucleotides complementary to the plasmid on both extremities. Mutagenesis primers described in Section 3.11.2.5 were used as follows:

35 μ l	H ₂ O
10 μ l	5x HF buffer
1 μ l	dNTPs (10 mM)
1 μ l	Primer F (125 ng/ μ l)
1 μ l	Primer R (125 ng/ μ l)
1 μ l	Phusion® High Fidelity DNA Polymerase (2 U/ μ l)
1 μ l	Plasmid (100 ng/ μ l)

Temperature protocol:

98°C 30s	} 20 cycles
98°C 10s	
60°C 1min	
72°C 5min 30s	
10°C 5min	

Before transformation (Section 4.1.1.7), the PCR product is digested with 20 U of DpnI at 37°C for 3 h for selection of unmethylated PCR product over methylated original plasmid.

4.1.1.7 Transformation of chemically competent bacteria

Chemically competent *E. coli* XL1-Blue (100 μ l in presence of 1.7 μ l β -mercaptoethanol) or TOP10 (25-50 μ l) were incubated for 30 min on ice with 2-20 μ l of the DpnI digested plasmids. A heat shock for 30-45 s at 42°C was followed by an immediate 2 minute incubation on ice. 200 μ l SOC medium were added and the bacteria were incubated for 1 h at 37°C with orbital shaking. After a 1 min centrifugation at 1000 rpm, bacteria were resuspended in 50 μ l SOC and plated LB agar plates with ampicillin or kanamycin.

4.1.1.8 Plasmid preparations

After overnight incubation at 37°C, single clones were picked, expanded in 2.5 ml LB with antibiotics and used for minipreparation with the QIAprep® Spin Miniprep Kit according to the manufacturer's instructions. The QIAprep® Spin Midiprep Kit was used according to the manufacturer's instructions for isolation of large plasmid quantities from bacteria expanded in 50-100 ml LB with antibiotics. Plasmid concentrations were determined using the NanoDrop® ND-1000 spectrophotometer by measuring the absorption at 260 nm. The plasmid sequences were verified by Sanger sequencing.

4.1.1.9 Sequencing

Sanger sequencing was performed using the Big Dye® Terminator v3.1 Cycle Sequencing Kit on an ABI PRISM® 3130xl Genetic Analyzer according to the manufacturer's instructions. For sequencing of plasmids, 40-50 ng of DNA (midipreparation) or 3 µl of minipreparation were used per reaction.

Max. 5µl DNA template
1 µl Primer F or R (5µM)
1 µl Reaction mix BigDye 3.1
1.5 µl 5x buffer
ad 10 µl H₂O

Temperature protocol:

96°C 1min
96°C 10s
50°C 5s
60°C 2min
10°C 5min

} 30 cycles

The PCR product was purified according to the manufacturer's instructions by ethanol/EDTA precipitation. After heating for 5 min at 95°C, the samples were boiled again for 5 min at 95°C in 10 µl of highly deionized formamide and loaded on the sequencer. Sequences were analysed using Geneious Pro.

4.1.2 Virus rescue from plasmids

Recombinant virus rescues can be performed in HEK293T cells cultivated alone in suspension culture or in adherent mixed culture together with MDCK cells. Transfection of suspension cells is more efficient due to a higher accessible surface of the cells, while in adherent mixed cultures, MDCK cells can be directly infected by the virus released from HEK293T cells. Cells were overlaid with 4 ml virus growth medium devoid of trypsin and antibiotics. 1 µg of each of 8 or 7 (negative control) IAV plasmids was transfected using 20 µl of Lipofectamine™ 2000 in 480 µl Opti-MEM®. After 6 (suspension culture) or 6-16 h (adherent culture) of incubation, the medium was replaced by virus growth medium with 2 µg/ml of TPCK-treated trypsin and antibiotics and incubated for 24-48 h. 0.5-2 ml of supernatant were then used to infect new MDCK cells in 4 ml virus growth medium. After 72 h, the success of the rescue was monitored by assessment of the cytopathogenic effect and hemagglutinating activity of the supernatant. Identity of the rescued virus was controlled by RNA extraction (Section 4.1.1.1), reverse transcription (Section 4.1.1.2), amplification with selected primers from Sections 3.11.2.3/3.11.2.4 and Sanger sequencing (Section 4.1.1.9, 10 ng DNA) of at least the full NS gene. Rescued viruses were stored at -80°C.

4.2 Virus culture and quantification of rescued and wild type viruses

4.2.1 Cultivation of cell lines

The cell lines (see Section 3.2.1) were maintained in 175 cm² cell culture flasks in their respective culture media (see Section 3.2.2) at 37°C and 5% CO₂ in a humidified atmosphere. When approximately 90% confluence was reached, cells were washed with PBS and detached with 0.05% trypsin (or 0.5% for MDCK). Detached cells were taken up in growth medium, centrifuged at 1500 rpm for 3 minutes, resuspended in fresh growth medium and splitted at an appropriate ratio into a new cell culture flask.

4.2.2 Expansion of influenza virus stocks

MDCK cells were washed with PBS, overlaid with virus growth medium containing 2 µg/ml TPCK-trypsin and infected with different amounts of viral stocks. The cultures were

monitored daily and when > 70% cytopathogenic effect was observed, supernatants were harvested, centrifuged for 10 min at 1500 rpm, aliquoted and stored at -80°C.

4.2.3 TCID50 determination

The half maximal tissue culture infectious dose (TCID50) of IAV was determined on MDCK cells, adenovirus on A549 cells, measles virus on VeroSlam cells. Cells were incubated for 3 days at 37°C and 5% CO₂ with 3-fold serial dilutions of virus-containing supernatant. The cytopathogenic effect was scored and TCID50 was calculated by the ID-50 5.0 program.

4.2.4 Viral growth kinetics

A549, DF-1 or ST cells were incubated in at least triplicates for 1h in presence of 0.01 MOI of IAV and washed three times with PBS before addition of virus growth medium. TCID50 was determined in samples taken at 0, 8, 24, 48 and 72h post infection.

4.3 Investigation of the antiviral host response to different NS1 proteins

4.3.1 Determination of cytokine mRNA and pre-mRNA levels by real-time PCR

Using the RNeasy® Mini Kit according to the manufacturer's instructions, total RNA was extracted from A549 cells 24 h after infection with pH1N1 wt, the H5-av or the H5-hum reassortants or their aa 80-84 deletion/insertion mutants at a MOI of 1. Reverse transcription of mRNA was performed on 500 ng of total RNA using dT₂₀ primers. Pre-mRNA was reverse transcribed similarly but using random hexamers and DNase treated total RNA. Real time PCR was performed in biological triplicates and technical duplicates using SYBR® Green nucleic acid stain and the primers and conditions described in Section 3.11.2.6. Primers for pre-mRNA quantification were designed such that one primer (F or R) targets an exon and the other one an intron. Changes in gene expression were calculated using the $2^{-\Delta\Delta C_t}$ method (Livak & Schmittgen 2001).

4.3.2 PCR array

A549 cells were infected in triplicate with pH1N1 wt, the H5-hum reassortant or their aa 80-84 deletion/insertion mutants at a MOI of 1. After 24h, total RNA was extracted using the RNeasy® Mini Kit according to the manufacturer's instructions and DNA was removed by on-column DNase digestion. RNA integrity (RNA Integrity Number > 7) was verified using an RNA 6000 Nano Total RNA Assay on a Bioanalyzer 2100. cDNA was synthesized from 400 ng of RNA using the RT² First Strand Kit. Human Antiviral Response PCR Arrays were performed according to the manufacturer's instructions, followed by data analysis using the RT² Profiler PCR Array Data Analysis Package V4: changes in gene expression were calculated using the $2^{-\Delta\Delta Ct}$ method and significant differences using the Student's t-test (significance if $p < 0.05$). Genes with both average Ct values > 35 and genes with both average Ct values > 30 and $p < 0.05$ were excluded as recommended by the manufacturer.

4.3.3 Luciferase reporter assays

To monitor IFN- β expression after IAV infection, A549 cells stably expressing a firefly luciferase reporter plasmid under the control of an IFN- β promoter (IFN- β Luc, (Hayman et al. 2006)) were infected with a MOI of 3 of either NS reassortants or aa 80-84 mutants or transfected with 50 ng of polyI:C as a positive control. To monitor IFN- β expression after NS transfection, HEK293T cells were transfected with 0.25 μ g of the IFN- β reporter plasmid IFN- β Luc (Hayman et al. 2006) and 0.75 μ g of NS plasmid or empty vector using LipofectamineTM LTX and PLUSTM reagent. After 48h, IFN- β expression was stimulated by transfection with 0.2 μ g of polyI:C. Six hours after polyI:C transfection in the transfection experiments (or 8/24h after infection for the IAV infection experiments), the cells were washed with PBS and luminescence was read using the Luciferase Assay System according to the manufacturer's instructions on a Tecan Infinite® M200 plate reader.

To monitor the influence of NS on the general host gene expression, 0.75 μ g of NS-containing pHWS or pIRES2-AcGFP1 plasmid or the corresponding empty vector was co-transfected into HEK293T cells with 12.5 ng of pGL4.73, a plasmid encoding Renilla luciferase under control of a constitutively active SV40 promoter. Luminescence was read after 48h using the Renilla Luciferase Assay System according to the manufacturer's instructions.

4.3.4 IFN resistance assay

A549 cells were preincubated for 6h with 0 or 500 U/ml of universal type I interferon. The cells were infected (MOI 0.1) with pH1N1 wt, H5 NS reassortants or their respective aa 80-84 deletion/insertion mutants. After 1h, cells were washed and overlaid with fresh virus growth medium containing 0 or 500 U/ml of IFN. TCID₅₀ was determined in the supernatant 48h post infection.

4.4 Antiviral drug testing

4.4.1 Antiviral drug testing *in vitro*

4.4.1.1 Preparation of plant extracts, fractions and tannin-free extracts

All tannin-containing extracts and fractions were prepared and provided by Dr. Willmar Schwabe GmbH & Co. KG, Karlsruhe as dry powders after aqueous-ethanolic extraction and, if applicable, fractionation. Concentrations indicated designate dry extract weight per volume of solvent. The oligo-/polymeric fraction from EPs® 7630 was obtained by acetic elution from a SephadexLH20 chromatographic column (Vennat et al. 1992). To prepare Hamamelis ultrafiltration fractions, a Pro Flux M12 Tangential Flow Filtration System with Pellicon 2 ultrafiltration cassettes was used. EPs® 7630 dry extract was dissolved in PBS at 2 mg/ml (*in vitro* experiments), in 10% ethanol at 20 mg/ml (CC₅₀ and EC₅₀ determination) or in sterile water at 5 mg/ml (*in vivo* experiments). Hamamelis bark and leaf full extract as well as ultrafiltration fractions and the EPs® 7630-derived oligo-/polymeric fraction were dissolved in DMSO. If needed for solubilization, 1h sonication at 25 kHz was applied. Tannin-free extracts were prepared at CRP Santé by depleting tannins from extract or single compound solutions in PBS under continuous stirring with 25 mg/ml (antiviral efficacy experiments) or 50 mg/ml (hemagglutination/neuraminidase assay) of hide powder for 1h at room temperature. In this process, tannins bind to the hide proteins, precipitate and can be removed by filtration over Whatman cellulose filters grade 1.

4.4.1.2 Quantification of phenols and condensed tannins

Phenolics, the main constituting moieties of both hydrolysable and condensed tannins, were quantified before and after hide powder treatment by Folin-Ciocalteu's phenol reagent. This is the standard method of the European Pharmacopoeia (Ainsworth & Gillespie 2007, European Directorate for the Quality of Medicines & Healthcare 2008) for quantification of total phenolics based on their reducing capacities. Briefly, 2 volumes of pyrogallol standard or sample, 1 volume Folin-Ciocalteu reagent, 10 volumes of water were mixed and 12 volumes Na_2CO_3 (290 g/L) were added. After 30 minutes of incubation at room temperature, absorbance was read at 760 nm on a SpectraMax Plus plate reader. Phenol content was determined using a pyrogallol standard curve, expressed as pyrogallol equivalents (PGE) and PGE of hide powder treated samples was normalized to PGE of untreated samples, corresponding to 100%. To estimate reproducibility of the Hamamelis bark extract and UF-fraction preparation, the amount of only condensed tannins was determined at Dr. Willmar Schwabe GmbH & Co KG, using the acid-butanol method (Bate-Smith 1975) as used in a previous publication with Hamamelis UF-fractions (Erdelmeier et al. 1996). Therefore, the drugs were heated for 2h at 95°C with 5% concentrated hydrochloric acid in n-butanol and absorbance was measured at 550 nm.

4.4.1.3 Cytotoxicity assay

Cytotoxicity was assessed in 96-well plates with 3×10^4 A549 cells per well incubated for 24h with 2-fold serial drug dilutions using the Cell Proliferation Kit II. The kit is based on the conversion of XTT to an orange formazan salt by metabolically active cells. XTT reagent was added after 24h, the plate was incubated for 2h at 37°C and absorbance was read at 450 nm and 650 nm (subtracted background) on a SpectraMax plus plate reader.

4.4.1.4 Antiviral efficacy determination against a GFP-reporter virus

A549 cells grown in black clear bottom plates were infected with a GFP-reporter virus (H1N1 A/Puerto Rico/8/34-NS116-GFP) at a MOI of 0.01 (EPs® 7630), 0.04 (oligo-/polymeric fraction and isolated catechins) or 0.4 (Hamamelis extracts, fractions and hydrolysable tannins). These MOIs were selected since they provided optimal fluorescent readout of the respective used virus batches. Serial drug dilutions were added immediately after virus

inoculation. After 24h, GFP fluorescence was read (excitation 485 nm, emission 535 nm) on a Tecan Genios plus Reader and the background (drug treated uninfected cells) was subtracted.

4.4.1.5 Selectivity index determination

The half maximal cytotoxic concentration (CC50) and the half maximal antiviral concentration EC50 were determined using SigmaPlot; the selectivity index (SI) was calculated as $SI = CC50/EC50$.

4.4.1.6 Antiviral efficacy determination against wild type viruses

A549 (0.1 MOI IAV except if mentioned otherwise, 0.05 MOI adenovirus) or A549Slam (0.01 MOI measles virus) cells were infected in at least triplicates and the drugs were added immediately after the virus unless stated otherwise. After 24, 48 or 72h of incubation as indicated in the respective Result Sections, supernatants were titered on MDCK (IAV), A549 (adenovirus) or VeroSlam (measles virus) cells. Time of addition studies as well as virus and cell preincubation experiments were performed similarly, with the modifications described in the corresponding Result Section.

4.4.1.7 Hemagglutination inhibition assay

IAV has the capacity to agglutinate erythrocytes by interaction of viral hemagglutinin with cellular sialic acid. Such hemagglutination is visible by a diffuse distribution of erythrocytes in a round-bottom plate, while non-agglutinated erythrocytes settle to the bottom of the plate and appear as a red dot. Blood group 0 human erythrocytes were diluted to 0.75% in PBS. 30 μ l of the lowest agglutinating concentration of H1N1 A/Puerto Rico/8/34 (EPs® 7630, 1.2×10^5 TCID50), H1N1 A/Luxembourg/46/2009 (Hamamelis, 2.4×10^5 TCID50) or PBS were mixed with 20 μ l drug serial dilutions or PBS and 50 μ l erythrocyte solution in round-bottom wells and scored after 60 min. If needed, the half maximal hemagglutination inhibiting concentration (HIC50) was calculated using ID-50 5.0.

4.4.1.8 Neuraminidase inhibition assay

50 μ l of virus-free assay buffer, H1N1 A/Puerto Rico/8/34 (EPs® 7630, 2.6×10^5 TCID50) or H1N1 A/Luxembourg/46/2009 virus (Hamamelis, 2.4×10^5 TCID50) in assay buffer supplemented with 0.1 % IGEPAL® non-ionic surfactant were mixed in a 96-well black

clear-bottom plate with 50 μ l of drug serial dilutions or assay buffer and incubated for 45 minutes at room temperature. 50 μ l 0.3mM 2'-(4-methylumbelliferyl)- α -D-N-acetylneuraminic acid were added and incubated for 1h at 37°C. After addition of stop solution, fluorescence was read at 488 nm (excitation at 360 nm) on an Infinite® M200 plate reader and background fluorescence (no virus) was subtracted. The half maximal neuraminidase inhibiting concentration (NIC50) was calculated using SigmaPlot.

4.4.1.9 Resistance development assay

To monitor the development of resistance against EPs® 7630 after repeated treatment, a multi passage protocol comparable to previously published protocols was used (Ludwig et al. 2004, Ehrhardt et al. 2007, Pleschka et al. 2009). Triplicates of A549 cells in 6-well plates were infected with H1N1 A/Puerto Rico/8/34 (0.2 MOI) and incubated with 0 or 10 μ g/ml EPs® 7630 for 24 h. Then, fresh A549 cells were inoculated with 100 μ l of supernatant and left untreated for 24 h to allow virus to re-expand, before 0 or 10 μ g/ml EPs® 7630 were added again for 24 h. Four passages were performed, supernatants being titered after each passage.

4.4.1.10 Apoptosis induction and unspecific effects on host cell receptors

Metabolic activity of A549 cells was determined in triplicates using the Cell proliferation kit II 24 h after adding the compounds. Caspase 3/7 activity of A549 cells after 24 h of incubation with the drugs, with 2.5 μ M staurosporine or with DMSO was measured using Caspase-Glo® 3/7 Assay according to the manufacturer's instructions. The assay is based on cleavage of a substrate by caspase 3 or 7 to luminogenic aminoluciferin.

Interference of the drugs with cellular TNF- α signalling was investigated as previously described (Ehrhardt et al. 2007). Briefly, 30 ng/ml TNF- α were added to A549 cells 30 minutes before or at the same time than drug treatment. Total proteins were extracted 15 minutes later using CHAPS buffer, boiled for 5 min in LDS sample buffer with DTT, loaded on a 4-12% Bis-Tris gel and run in a protein electrophoresis chamber (15 min – 90 V – 125 mA – 200 W, then 60 min – 180 V – 250 mA – 200 W). Proteins were blotted on an activated Hybond™ ECL membrane in transfer buffer in transfer chamber at 45 mA for 90 min. After blocking, I κ B- α was detected by using a primary rabbit anti-I κ B- α antibody. As a loading control, β -actin was detected using a mouse anti- β -actin antibody. Cy-5 and Cy-3 labelled appropriate secondary antibodies were used and fluorescence was detected on a Typhoon™ TRIO+ scanner. All washing steps were made with TBS or TBS with 0.3% TWEEN® 20.

4.4.2 Antiviral drug testing *in vivo*

4.4.2.1 Ethical statement

CRP-Santé is authorized by the Luxembourg Ministry of Agriculture, Viticulture and Rural Development to conduct animal experiments for scientific reasons (Authorization dated January 1st 2012, according to Article 12 of the Animal Welfare and Protection Law dated March 15th 1983 and the Règlement Grand-Ducal dated August 6th 1999). All animal experiments were performed in accordance with the Directive 2010/63/EU of the European Parliament and of the Council of 22/09/2010 on the protection of animals used for scientific purposes.

4.4.2.2 Mouse infections with IAV

Pathogen-free female 7 week old BALB/c mice were used for all experiments. Infections were performed on day 1 by intranasal instillation of 1 or 4 half maximal mouse lethal doses (MLD50) of A/Puerto Rico/8/34 (Results Part 2) or between 10^3 and 10^7 TCID₅₀ of pH1N1 NS reassortants (Results Part 1) in 50 μ l PBS to mice under light isoflurane anesthesia.

4.4.2.3 Antiviral drug treatment by peroral gavage

5 mg/kg of EPs® 7630 suspension in 0.2 % agar (or 0.2% agar only) were administered by peroral gavage three times a day over 10 days to mice infected with 4 MLD50 of A/Puerto Rico/8/34. A pretreatment was done 6 h before infection.

4.4.2.4 Antiviral drug treatment by inhalation

Inhalation was performed using two PARI Boy® SX aerosol nebulizers on opposite sides of a 3.9 L inhalation chamber. Excess aerosol could escape from narrow gaps evenly distributed around the cage, allowing exposition of the whole cage volume to freshly nebulized drug under steady state conditions. The nebulizers produce a particle average mass median aerodynamic diameter 2.2 μ m at a total output rate 450 mg/min. Inhalation chambers with PARI nebulizers have been used previously (Droebner et al. 2007). On day 1, 10 mice per group were pretreated by inhalation with EPs® 7630 (5 mg/ml) or water and infected intranasally with 1 or 4 MLD50 of A/Puerto Rico/8/34. Then, mice were treated three times a day for 10 minutes by inhalation with EPs® 7630 or water during 10 days.

4.4.2.5 Mouse monitoring and tissue handling

Rectal body temperature and body weight were monitored daily for 14 days for drug testing experiments and MLD50 determinations. Mice were sacrificed when their body weight loss exceeded 25 % or on day 14. Lungs were explanted and homogenized in virus growth medium on a TissueLyserII for 12 min at 25 Hz, followed by a 10 minutes centrifugation at 11000 rpm and supernatant titration.

4.5 Statistical methods

Results are represented as means \pm standard deviations. SigmaPlot was used for CC50 and EC50 determination for the cytotoxicity assay, the antiviral assay using GFP reporter virus and the neuraminidase assay. Statistical analysis was done in SigmaPlot using Student's t-test (Results Part 1), Mann-Whitney Rank Sum test (Results Part 2 and 3) or Pearson correlation. Survival analysis was performed using Gehan-Breslow test. $p < 0.05$ was considered as significant.

5 Results and Discussion

Part 1

5.1 Characterization of pandemic H1N1/2009 IAV reassortants carrying heterologous NS genes reveals a role of a naturally occurring NS1 five amino acid deletion in host gene regulation

A manuscript to this study is in preparation for publication as: Linda L. Theisen, Sandra Gohrbandt, Sophie A. Kirschner, Aurélie Sausy, Regina Brunnhöfer, Jürgen Stech, Claude P. Muller; Characterization of pandemic H1N1/2009 influenza A virus reassortants carrying heterologous NS genes reveals a role of a naturally occurring NS1 five amino acid deletion in host gene regulation.

L. Theisen contributed the major part to conception and design of the study, experimental work, data analysis and interpretation and writing of the manuscript.

Pandemic H1N1 (pH1N1) virus emerged in 2009 by reassortment between a North American triple reassortant and Eurasian swine IAVs (Garten et al. 2009, Smith et al. 2009). After its global spread it continues to circulate nowadays as seasonal H1N1. In addition to infecting humans, pH1N1 has also been detected in pigs (Ducatez et al. 2011, Yan et al. 2012), poultry (Mathieu et al. 2010, Reid et al. 2012) and other host species (Fiorentini et al. 2011, Goldstein et al. 2013), probably by spill-overs from humans. Its broad host range is a risk for co-infections of pH1N1 virus with other circulating human, avian or swine strains and thereby the development of new reassortants. Several natural pH1N1 reassortments have been detected (Vijaykrishna et al. 2010, Nelson et al. 2012), including the prominent reassortment

of the matrix gene from pH1N1 with a swine origin H3N2 in North American swine. This reassortant virus seems to have an increased human tropism. Moreover, reassortments were at the origin of the IAV pandemics of 1957, 1968 and 2009 (Taubenberger & Kash 2010). Thus, pH1N1 co-circulates with IAV strains from several host species and has the propensity to generate reassortants with new properties in terms of growth, pathogenicity, infectivity, host range or pandemic potential.

Reassortment of IAV genes in a pH1N1 background can induce to differences in viral fitness: insertion of polymerase genes from different IAV strains could lead to an increase or decrease in viral replication (Song et al. 2011). The pH1N1 background seems compatible with several genes from other subtypes. A reassortant of pH1N1 with avian H9 HA remained transmissible in ferrets (Kimble et al. 2011). Reassortants between HPAIV H5N1 and pH1N1 could be obtained by co-infection *in vitro* (Octaviani et al. 2010) or by reverse genetics (Cline et al. 2011). Similar to hemagglutinin or the viral polymerase genes, NS1 is a virulence determinant (Tscherne & Garcia-Sastre 2011) that influences viral fitness *in vitro* and *in vivo* (Seo et al. 2002, Zhu et al. 2008, Ma et al. 2010). It is therefore essential to investigate with which NS genes of human, avian and swine strains pH1N1 can reassort and how this influences viral fitness.

Here, eight different pH1N1 reassortants carrying NS genes of human, avian or swine strains were constructed by reverse genetics to characterize their viral fitness *in vitro* and for the most interesting candidates also *in vivo*. Such characterization enables a first evaluation of the probability to naturally emerge as well as of the threat posed by such NS reassortants. By NS1 sequence comparison of reassortants with differential fitness, amino acids involved in fitness were indentified and their function was investigated. By this strategy, a naturally occurring deletion of five amino acids in NS1 was shown to be involved in viral fitness at least *in vitro* and to regulate general host gene expression.

5.1.1 Results

5.1.1.1 Characterization of reassortant pH1N1 strains carrying NS genes of human, avian and swine origin *in vitro*

During and after the 2009 pandemic, pH1N1 was also detected in birds and swine, providing ample opportunities to reassort with IAV strains from these species. By reverse genetics, we constructed eight reassortants consisting of a background of seven genes from pH1N1 and NS genes from human seasonal H3N2, four avian strains (HPAIV H5N1 isolated from a bird, HPAIV H5N1 isolated from a human, LPAIV H5N1, LPAIV H9N2) and three swine strains (European H1N1, European H3N2, American H1N1). All reassortants could be successfully rescued and propagated on MDCK cells with only small differences in viral titer (< 18-fold, data not shown), demonstrating compatibility of the gene segments. Since NS is a virulence factor and involved in host adaptation, we compared the viral fitness of the NS reassortants to wildtype (wt) pH1N1 by their growth kinetics on human A549, avian DF-1 and swine ST cells. All reassortants grew to similar titers in ST cells (< 8-fold difference at 48h p.i., Fig. 13A), and 6 of 8 reassortants showed a growth only marginally lower than pH1N1 wt in A549 cells (< 13-fold difference at 48h p.i., Fig. 13B). However, pronounced differences in titer were observed in A549 and DF-1 cells between pH1N1 wt and the reassortants carrying NS genes from HPAIV strains. The H5-av or H5-hum reassortants' titers were > 1700 or > 700-fold lower in A549 cells (Fig. 13BC) and > 60- or > 170-fold lower on DF-1 (Fig. 13D) as compared to wt at 48h p.i. ($p < 0.05$). In view of these fitness differences in human and avian cells, pH1N1 reassortants carrying NS from HPAIV H5N1 were selected for further characterization.

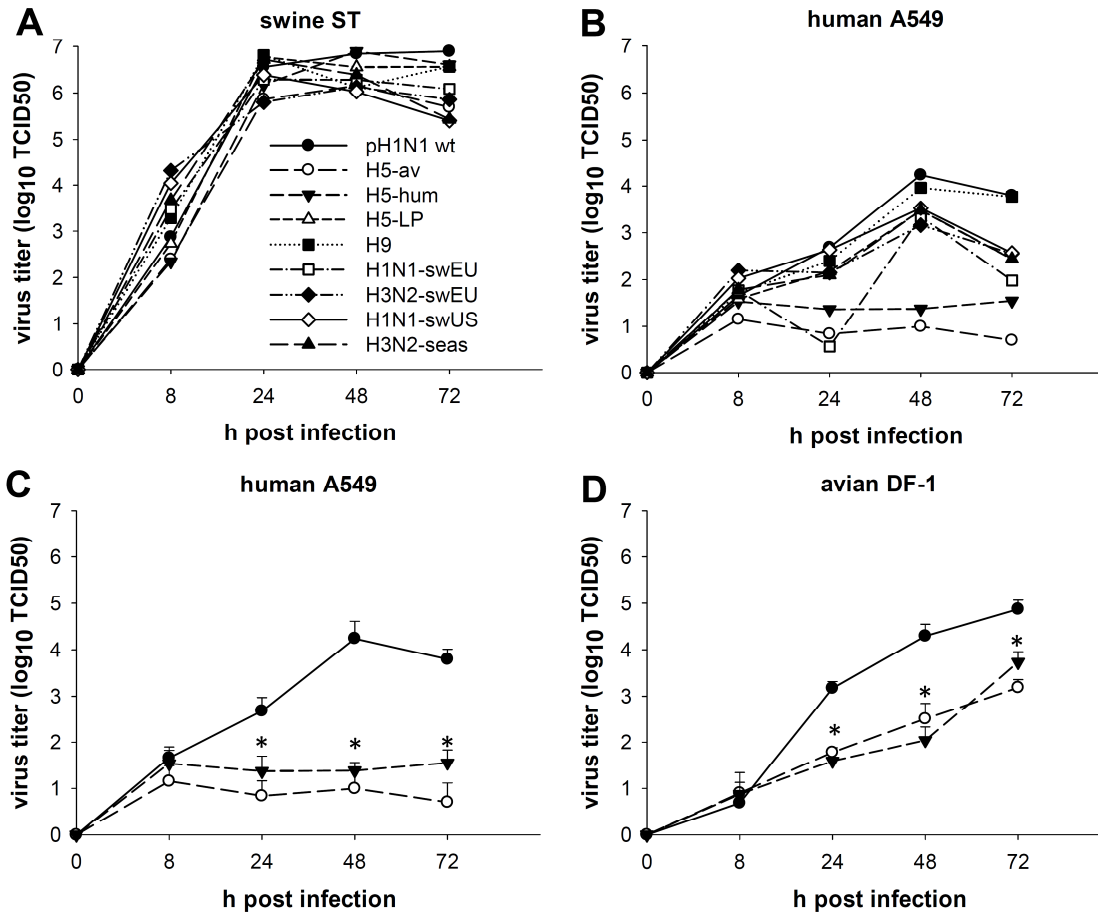


Figure 13: Fitness of NS reassortants *in vitro*. Growth kinetics of pH1N1 wt and the different NS reassortants on swine testis (ST) cells (A), human lung epithelial cells (A549) (B, C) and chicken embryo fibroblasts (DF-1) (D) after cell infection with an MOI of 0.01, as measured by TCID₅₀ determination. * indicates a significant difference ($p < 0.05$) to pH1N1 wt at the indicated time point. Statistical analysis and error bars of (A) and (B) were omitted in order not to overload the Figure.

5.1.1.2 Characterization of reassortant pH1N1 strains with NS genes of HPAIV H5N1 *in vivo*

Groups of ≥ 4 mice were infected with dilution series of pH1N1 wt and H5 NS reassortants to determine their MLD₅₀s. While at a viral dose of 10^6 TCID₅₀, all mice infected with pH1N1 wt were dead within 6 days, 25% or 75% of the mice infected with H5-hum or H5-av reassortants survived the complete 14 days of the observation period (data not shown). All mice infected with 10^5 TCID₅₀ of pH1N1 wt died on day 6, while the mice infected with the reassortants showed signs of sickness (ruffled fur, loss of body weight up to 15%, loss of body temperature up to 6%) but all survived (Fig. 14A-C). In line with our results in A549 cells, a reduced virulence of H5-av (MLD₅₀ = $10^{6.0}$ TCID₅₀) and H5-hum (MLD₅₀ = $10^{5.7}$

TCID50) reassortants was also observed in mice as a > 60- or > 25-fold increase in MLD50 in comparison to pH1N1 wt ($10^{4.3}$ TCID50).

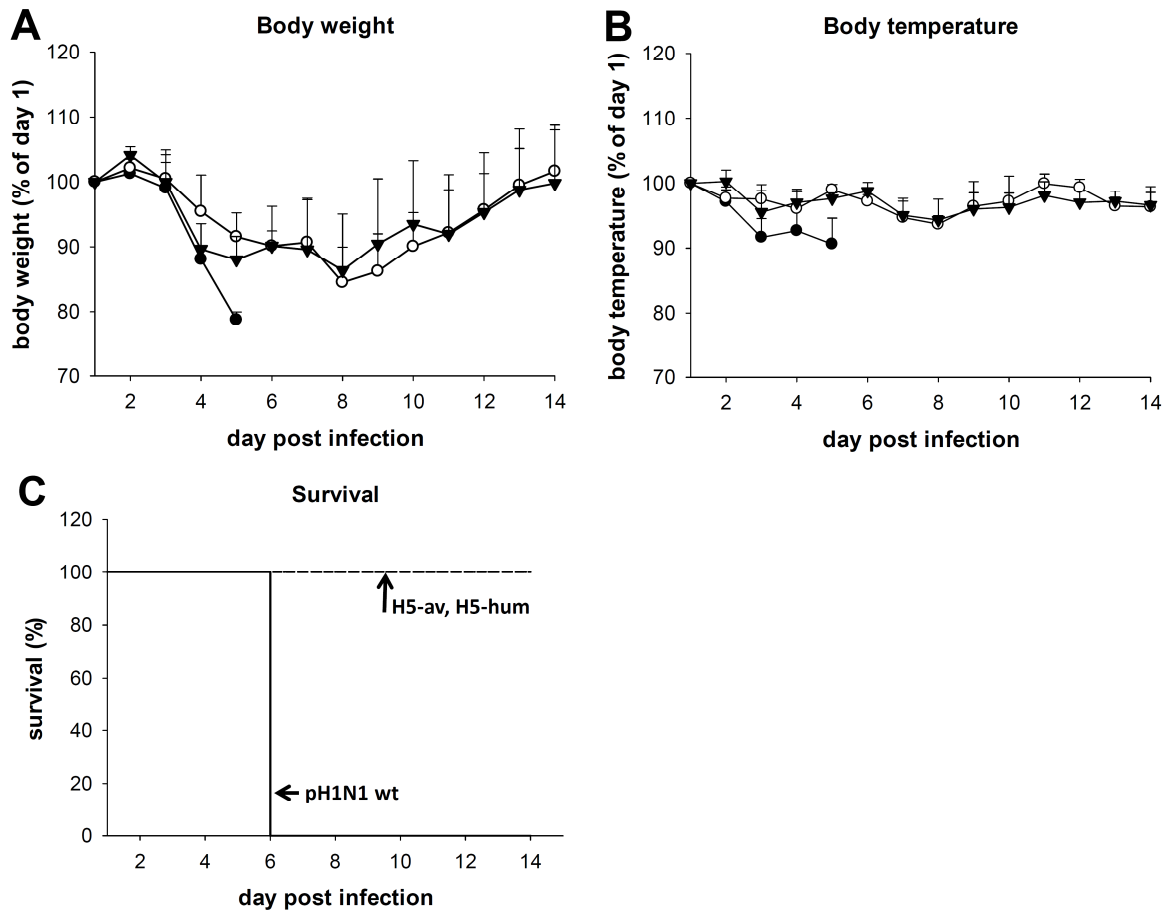


Figure 14: Pathogenicity of NS reassortants *in vivo*. Four mice per group were infected with 10^5 TCID50 of pH1N1 wt (●), H5-av (○) and H5-hum (▼) reassortants on day 1 and monitored daily for body weight (A), body temperature (B) and survival (C). Mice were sacrificed when their body weight loss exceeded 25% of the initial weight. (C) pH1N1 wt is represented by a solid line, H5-av and H5-hum reassortants by broken lines (both 100% survival).

5.1.1.3 Characterization of the role of amino acids 80-84 of NS1 in viral fitness *in vitro* and *in vivo*

By sequence comparison (Fig. 15) of the NS1 proteins, three loci of aa differences were identified between strains reaching high titers on A549 cells and the attenuated HPAIV reassortants: R118K, P212L and a deletion of 5 aa in position 80-84.

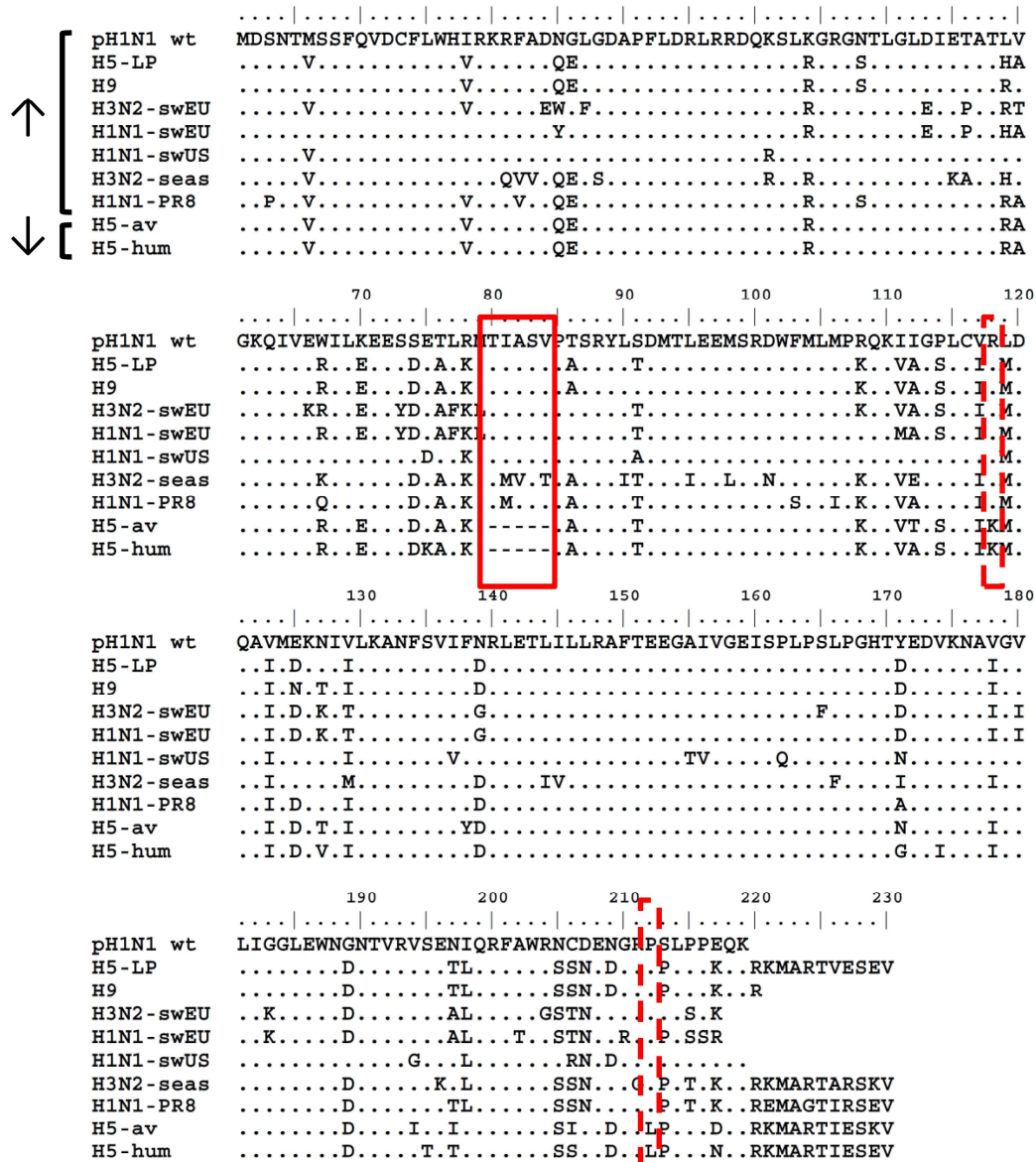


Figure 15: NS1 sequence analysis. ↑: NS reassortants with high titer growth kinetics on A549 cells; ↓: NS reassortants attenuated on A549 cells; boxes show amino acid differences between high and low replicating strains; solid box: chosen for characterization.

When the same strains were tested *in vivo*, mice infected with 10^5 or 10^6 TCID₅₀ of pH1N1 wt, H5-av-ins or H5-hum-ins died a bit earlier and somewhat more frequently than mice infected with pH1N1 wt-del, H5-av or H5-hum, suggesting that TIASV in position 80-84 slightly increased virulence (data not shown). However, these differences were too small to be reflected by an important change in the MLD₅₀s: Between an IAV strain carrying TIASV in position 80-84 and the corresponding strain without TIASV, the maximal change in MLD₅₀ was < 3.5-fold.

5.1.1.4 Effect of NS reassortment and aa 80-84 on cytokine expression

NS1 is a key player in the downregulation of the host cells' antiviral immune response and different NS gene segments in the same viral background can differentially induce the IFN response (Geiss et al. 2002, Twu et al. 2007, Kuo et al. 2010). A549 cells stably transfected with a reporter plasmid containing a luciferase gene under the control of an IFN- β promoter (Hayman et al. 2006) were infected with the different H5 NS reassortants with and without TIASV in position 80-84 for 8 or 24h. Uninfected or polyI:C transfected cells served as a negative or positive control, respectively. While all reassortants showed lower IFN- β expression than the polyI:C positive control, IFN- β expression was highest in pH1N1 wt infected cells. IFN levels in cells infected with H5 NS reassortants were similar to the uninfected negative control (Fig. 17AB). Interestingly, the deletion of aa 80-84 in pH1N1 wt significantly decreased IFN- β expression. Nevertheless, insertion of aa 80-84 did not result in IFN- β upregulation in the H5 reassortants (Fig. 17AB). Viral titers at 8h post infection showed only minimal differences (< 3-fold, Fig.17C), demonstrating that differences in viral growth were not the reason for the differential cytokine expression. The differential IFN- β expression can be clearly attributed to NS, since transfection of NS expression plasmids had a similar effect on IFN- β than infection with the corresponding NS reassortants (Fig. 17D).

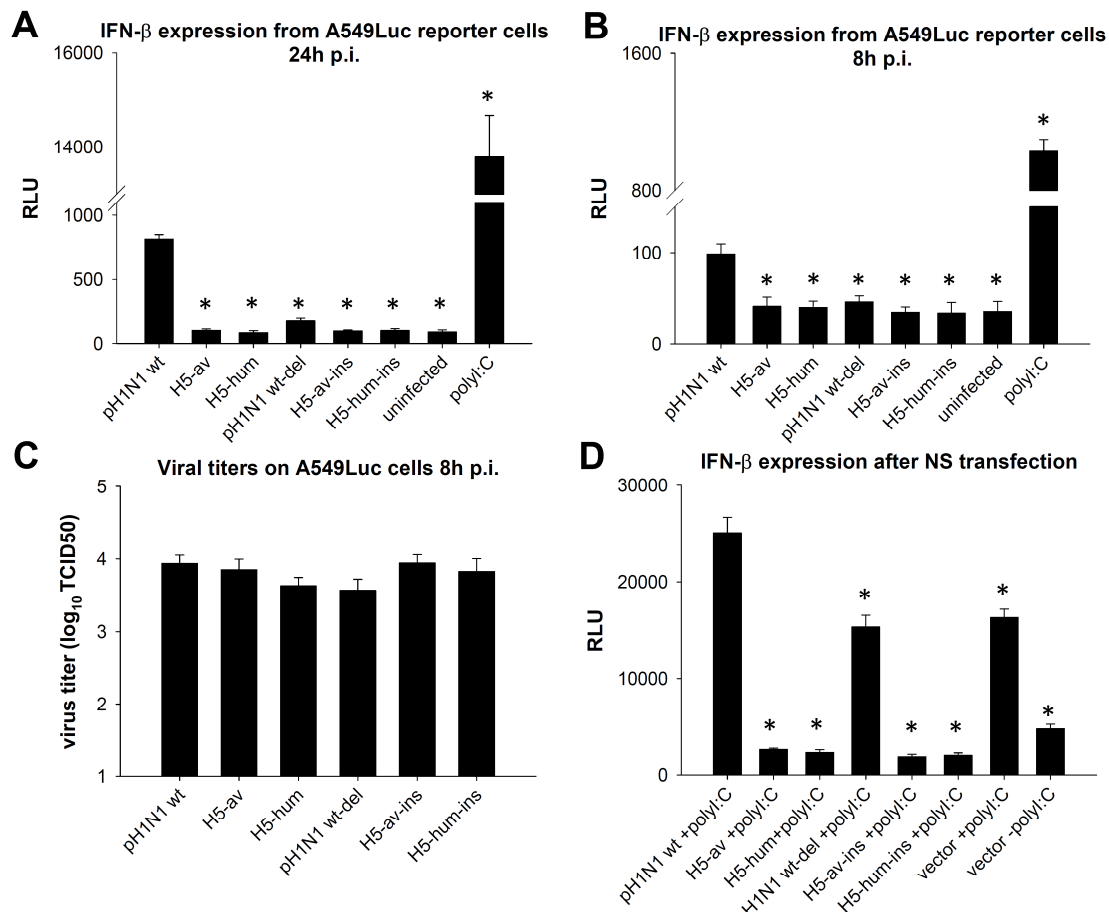


Figure 17: Effect of NS reassortment and aa 80-84 deletion/insertion on IFN-β expression. (A, B) IFN-β expression after IAV infection. A549 cells stably expressing a firefly luciferase reporter plasmid (A549Luc) under the control of an IFN-β promoter were infected with NS reassortants or aa 80-84 deletion/insertion mutants (MOI 3) or transfected with 50 ng of polyI:C. Luminescence was read after 24h (A) or 8h (B). (C) TCID₅₀ of A549Luc cell supernatants were determined 8h after infection with an MOI of 3. (D) IFN-β expression after NS transfection. HEK293T cells were transfected with 0.25 μg of the IFN-β reporter plasmid IFN-βLuc and 0.75 μg of NS plasmid or empty vector for 48h. Then, IFN-β expression was stimulated by transfection of 0.2 μg of polyI:C and 6h later luminescence was read. * indicates a significant difference ($p < 0.05$) to pH1N1 wt.

A similar expression profile of IFN-β was maintained on the mRNA level, as detected by real-time PCR (Fig. 18A). This observation was also extended to other cytokines. For four of the six cytokines analysed (IFN-β, TNF-α, IP-10, IL-6), mRNA expression in A549 cells 24h p.i. was highest for pH1N1 wt and significantly lower for both H5 NS reassortants. Also, deletion of aa 80-84 in pH1N1 wt decreased mRNA expression for five of six cytokines, three of them showing a statistically significant difference (IFN-β, TNF-α, IL-6, Fig. 18A-D, F).

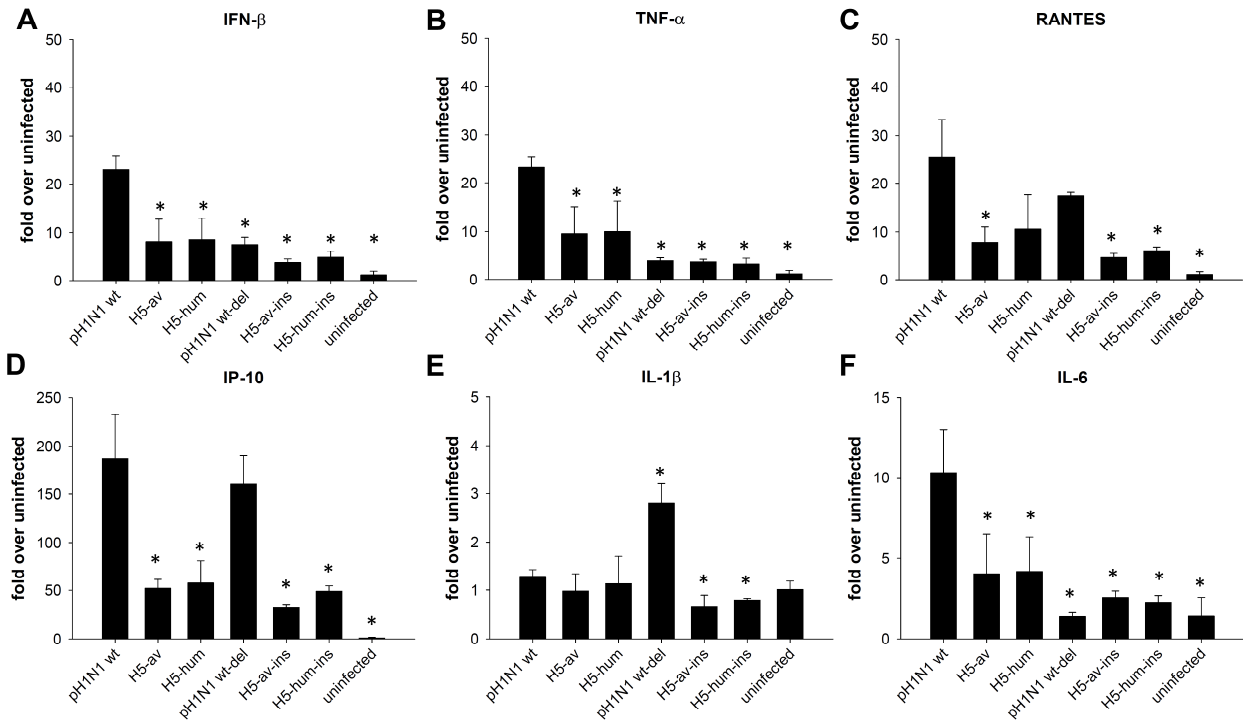


Figure 18: Effect of NS reassortment and aa 80-84 deletion/insertion on cytokine mRNA expression. Total RNA extracted from A549 cells 24 h after infection (MOI 1) was reverse transcribed using dT₂₀ primers and mRNA levels of IFN- β (A), TNF- α (B), RANTES (C), IP-10 (D), IL-1 β (E) and IL-6 (F) were quantified by real-time PCR. Changes in gene expression were calculated using the $2^{-\Delta\Delta C_t}$ method and expressed as fold over uninfected. * indicates a significant difference ($p < 0.05$) to pH1N1 wt.

Moreover, the differential expression of 84 antiviral response genes after infection with pH1N1 wt, the H5-hum reassortant or their respective aa 80-84 deletion/insertion mutants was investigated using a PCR array. Nine genes were upregulated > 5-fold (CCL5/RANTES, CXCL10/IP-10, CCL11/IP-9, FOS, IL12A, ISG15, JUN, MX1, OAS2) and 8 genes were upregulated 3- to 5-fold (CASP1, DDX58/RIG-I, DHX58/LGP-2, IFIH1/MDA-5, IFNB1, IL8, IRF7, TLR3) after pH1N1 wt infection at 24 h p.i. of A549 cells as compared to H5-hum reassortants (Fig. 19A, Table 1). Three genes were upregulated >5-fold (CD80, FOS, PYDC1) and 5 genes 3- to 5-fold (CCL3/MIP-1 α , CXCL9/MIG, IL6, TLR8, TNF) after pH1N1 wt infection as compared to pH1N1 wt-del (Fig. 19B, Table 1). In comparison to both H5 reassortants and pH1N1 wt-del, pH1N1 showed higher expression of genes encoding cytokines and chemokines, but also members of pattern recognition receptor signalling cascades (RIG-I, MDA5, LGP2, TLR3, IRF7 for H5-hum, TLR8 for wt-del), interferon stimulated genes (MX1, OAS2, ISG15 for H5-hum), components of the AP-1 transcription factor (FOS, JUN for H5-hum, FOS for wt-del) or the inflammasome (CASP1 for H5-hum, PYDC1 for wt-del). No differences > 3-fold were detected between the H5-hum and the H5-

hum-ins reassortants (Fig. 19C, Table 1). These data confirm that pH1N1 wt infection induces a higher expression of antiviral host genes than H5-hum reassortants and pH1N1 wt-del infection, while insertion of TIASV into H5-hum NS1 has no effect.

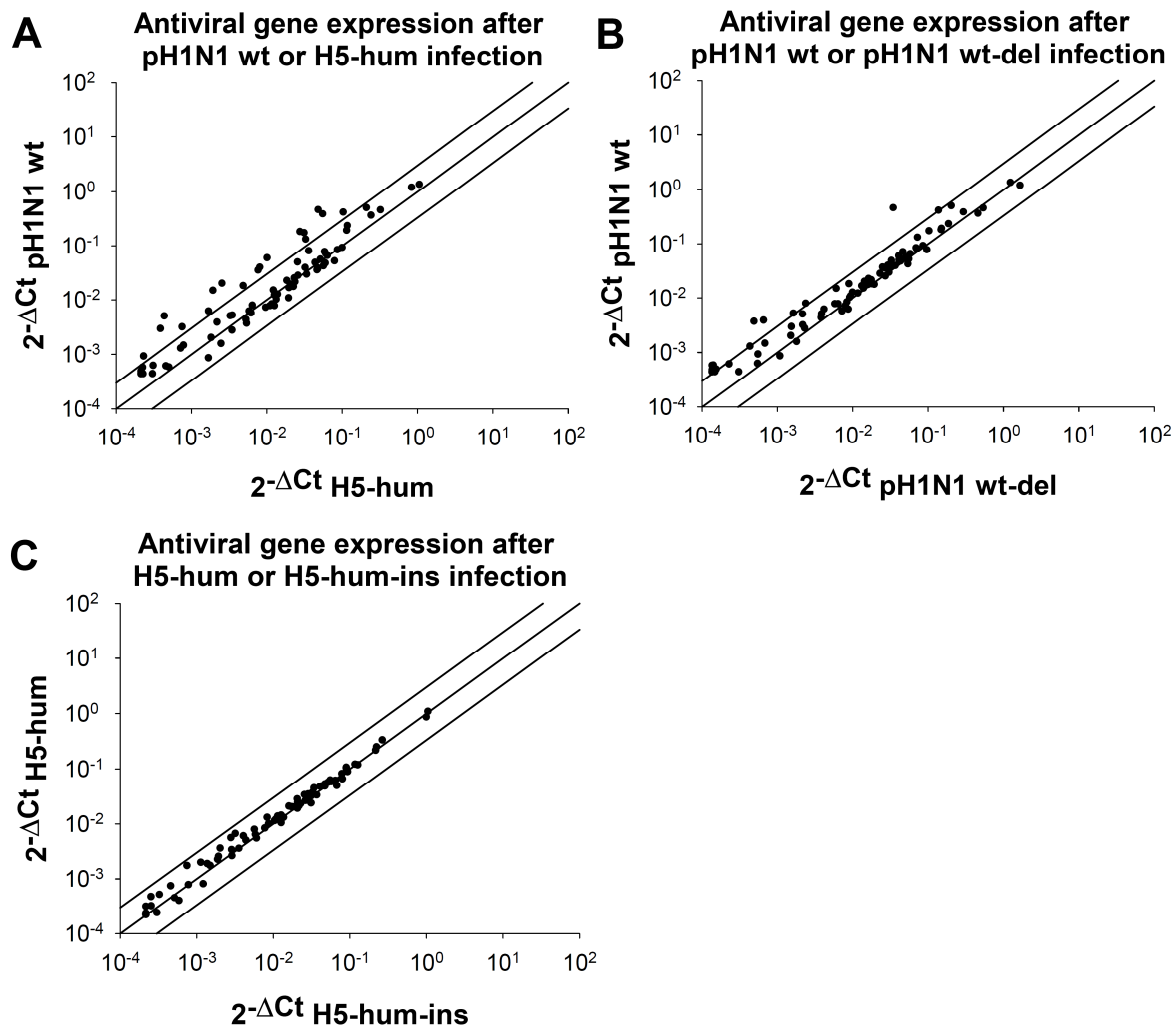


Figure 19: Effect of NS reassortment and aa 80-84 deletion/insertion on expression of 84 genes involved in the human antiviral host response, investigated by PCR array. (A-C) DNA-free total RNA was extracted from A549 cells 24h after infection (MOI 1) and reverse transcribed using the RT² First Strand Kit. Human Antiviral Response PCR Arrays were performed and changes in gene expression between the gene of interest and housekeeping genes (ΔCt) were plotted as $2^{-\Delta Ct}$. The main diagonal indicates gene expression fold changes ($2^{-\Delta Ct}$) of 1. The top and bottom lines indicate fold-changes of 3. Differences in gene expression between pH1N1 wt and its H5-hum NS reassortant (A), pH1N1 wt and its amino acid 80-84 deletion mutant (wt-del, B) and H5-hum and its amino acid 80-84 TIASV insertion mutant (H5-hum-ins, C) are shown.

Table 1: Human antiviral host response PCR array data

Human antiviral host gene expression after infection with NS reassortants or aa 80-84 deletion/insertion mutants

fold up- or downregulation			gene	gene full name
pH1N1 wt/ H5-hum	pH1N1 wt/ wt-del	H5-hum/ H5-hum- ins		
1,88			AIM2	Absent in melanoma 2
-1,17	-1,06	1,18	ATG5	ATG5 autophagy related 5 homolog
1,28	-1,28	-1,08	AZI2	5-azacytidine induced 2
1,49			CARD9	Caspase recruitment domain family, member 9
3,87	1,63		CASP1	Caspase 1, apoptosis-related cysteine peptidase (interleukin 1, beta, convertase)
-1,68	1,17	1,51	CASP10	Caspase 10, apoptosis-related cysteine peptidase
1,08	1,46	1,28	CASP8	Caspase 8, apoptosis-related cysteine peptidase
	4,12		CCL3	MIP-1 α , Chemokine (C-C motif) ligand 3
5,73	1,42	-1,26	CCL5	RANTES, Chemokine (C-C motif) ligand 5
	7,27	1,92	CD80	CD80 molecule
1,06	1,19	-1,05	CHUK	Conserved helix-loop-helix ubiquitous kinase
-1,37	-1,31	-1,02	CTSB	Cathepsin B
1,39	-1,43	-1,20	CTSL1	Cathepsin L1
1,19	1,36	-1,12	CTSS	Cathepsin S
7,35			CXCL10	IP-10, Chemokine (C-X-C motif) ligand 10
11,09	2,24		CXCL11	IP-9, Chemokine (C-X-C motif) ligand 11
	3,11		CXCL9	MIG, Chemokine (C-X-C motif) ligand 9
-1,36	1,08	1,16	CYLD	Cylindromatosis (turban tumor syndrome)
-1,09	1,31	-1,06	DAK	Dihydroxyacetone kinase 2 homolog (<i>S. cerevisiae</i>)
1,39	-1,20	1,21	DDX3X	DEAD (Asp-Glu-Ala-Asp) box polypeptide 3, X-linked
3,89	1,77	1,28	DDX58	RIG-I, DEAD (Asp-Glu-Ala-Asp) box polypeptide 58
4,46	1,27	1,35	DHX58	LGP-2, DEXH (Asp-Glu-X-His) box polypeptide 58
1,13	1,49	1,09	FADD	Fas (TNFRSF6)-associated via death domain
9,39	13,11	-1,41	FOS	FBJ murine osteosarcoma viral oncogene homolog
1,24	1,06	1,01	HSP90A A1	Heat shock protein 90kDa alpha (cytosolic), class A member 1
4,79	1,33	1,04	IFIH1	MDA-5, Interferon induced with helicase C domain 1
-1,62			IFNA1	Interferon, alpha 1
1,80			IFNA2	Interferon, alpha 2
-1,32	1,44	1,09	IFNAR1	Interferon (alpha, beta and omega) receptor 1
3,52			IFNB1	Interferon, beta 1, fibroblast
-1,44	-1,03	1,08	IKBKB	Inhibitor of kappa light polypeptide gene enhancer in B-cells, kinase beta
7,43	2,38		IL12A	Interleukin 12A (natural killer cell stimulatory factor 1, cytotoxic lymphocyte maturation factor 1, p35)
		2,25	IL12B	Interleukin 12B (natural killer cell stimulatory factor 2, cytotoxic lymphocyte maturation factor 2, p40)
-1,47	1,30	1,06	IL15	Interleukin 15

-1,12	1,04	1,11	IL18	Interleukin 18 (interferon-gamma-inducing factor)
	3,22	2,01	IL6	Interleukin 6 (interferon, beta 2)
3,93	2,96	1,15	IL8	Interleukin 8
-1,06	1,17	-1,08	IRAK1	Interleukin-1 receptor-associated kinase 1
-1,30	1,07	-1,09	IRF3	Interferon regulatory factor 3
-1,38	-1,14	1,11	IRF5	Interferon regulatory factor 5
3,62	1,98		IRF7	Interferon regulatory factor 7
6,84	1,29	1,06	ISG15	ISG15 ubiquitin-like modifier
5,35	1,63	-1,01	JUN	Jun proto-oncogene
1,89	1,17	-1,03	MAP2K1	MEK1, Mitogen-activated protein kinase kinase 1
1,18	1,04	-1,15	MAP2K3	Mitogen-activated protein kinase kinase 3
	-1,46	1,42	MAP3K1	Mitogen-activated protein kinase kinase kinase 1
1,06	-1,11	-1,35	MAP3K7	Mitogen-activated protein kinase kinase kinase 7
-1,56	-1,09	1,00	MAPK1	Mitogen-activated protein kinase 1
-1,22	1,22	1,14	MAPK14	Mitogen-activated protein kinase 14
-1,33	1,07	-1,01	MAPK3	Mitogen-activated protein kinase 3
-1,23	-1,01	1,00	MAPK8	Mitogen-activated protein kinase 8
-1,87	1,11	1,07	MAVS	Mitochondrial antiviral signaling protein
1,13			MEFV	Mediterranean fever
6,41	1,18	1,33	MX1	Myxovirus (influenza virus) resistance 1, interferon-inducible protein p78 (mouse)
2,16	1,10	1,10	MYD88	Myeloid differentiation primary response gene (88)
-1,07	1,00	-1,08	NFKB1	Nuclear factor of kappa light polypeptide gene enhancer in B-cells 1
2,35	2,43	-1,04	NFKBIA	Nuclear factor of kappa light polypeptide gene enhancer in B-cells inhibitor, alpha
7,66	1,36		OAS2	2'-5'-oligoadenylate synthetase 2, 69/71kDa
-1,14	1,23	1,09	PIN1	Peptidylprolyl cis/trans isomerase, NIMA-interacting 1
-1,26	1,18	-1,00	PYCARD	PYD and CARD domain containing
1,71	5,69		PYDC1	PYD (pyrin domain) containing 1
1,06	1,08	1,08	RELA	V-rel reticuloendotheliosis viral oncogene homolog A (avian)
	-1,31		RIPK1	Receptor (TNFRSF)-interacting serine-threonine kinase 1
1,47	-1,29	1,08	SPP1	Secreted phosphoprotein 1
1,94	1,22	1,00	STAT1	Signal transducer and activator of transcription 1, 91kDa
-1,00	1,10	-1,26	SUGT1	SGT1, suppressor of G2 allele of SKP1 (S. cerevisiae)
-1,14	1,19	1,14	TBK1	TANK-binding kinase 1
1,19	1,05	1,01	TICAM1	Toll-like receptor adaptor molecule 1
4,08			TLR3	Toll-like receptor 3
	2,90		TLR7	Toll-like receptor 7
2,16	3,40		TLR8	Toll-like receptor 8
	3,07	1,72	TNF	Tumor necrosis factor
-1,34	1,23	1,13	TRAF3	TNF receptor-associated factor 3
-1,18	-1,13	1,26	TRAF6	TNF receptor-associated factor 6
1,62	1,24	-1,11	TRIM25	Tripartite motif containing 25

> 5-fold upregulations are indicated in **bold red**, between 3 and 5-fold upregulations are indicated in **bold green**

5.1.1.5 Effect of NS reassortment and amino acids 80-84 on general host gene expression

The above results showed that the expression of a wide variety of cytokines and genes involved in the antiviral host response was higher after pH1N1 wt infection than after infection with the H5-av or H5-hum reassortant as well as pH1N1 wt-del. Thus, we investigated if this was due to differential regulation of general host gene expression, rather than to differential expression regulation of specific genes (e.g. cytokines). Therefore, a Renilla luciferase reporter gene under the control of a constitutively active SV40 promoter was co-transfected with plasmids expressing NS from different IAV strains. Again, gene expression was highest in cells transfected with NS from pH1N1 wt and significantly lower after transfection of NS from H5 and wt-del (Fig. 20A), similar to the predominant gene expression pattern observed above (Fig. 17-19). This suggests that differential regulation of general host gene expression causes the above differences in antiviral gene expression. Interestingly, NS from avian and seasonal H3N2 origin showed low reporter gene expression compared to swine origin and H1N1-PR8 NS (Fig. 20A). We mutated the splice acceptor site of NS, leading to inhibition of NS splicing and thereby to inhibition of NS2/NEP expression, while the unspliced NS1 mRNA was still expressed. This resulted in essentially the same gene expression profiles (Fig. 20B as compared to Fig. 20A), showing that NS1 but not NS2 is involved in this regulation. Importantly, deletion of aa 80-84 in NS1 wt led to a significant decrease in general host gene expression. This was confirmed for two other strains, H1N1-swEU and H1N1-PR8, regardless of NS2 expression (Fig. 20C), suggesting a role of NS1 aa 80-84 in the regulation of general host gene expression. Finally, to rule out an influence of the pHWS plasmid used, we repeated the experiment using a different plasmid backbone, pIRES2-AcGFP1. This plasmid expresses GFP (previously used to optimize transfections) and NS wt or wt-del. Also in a different plasmid backbone, transfection of NS wt-del induced significantly lower gene expression than NS wt (Fig. 20D).

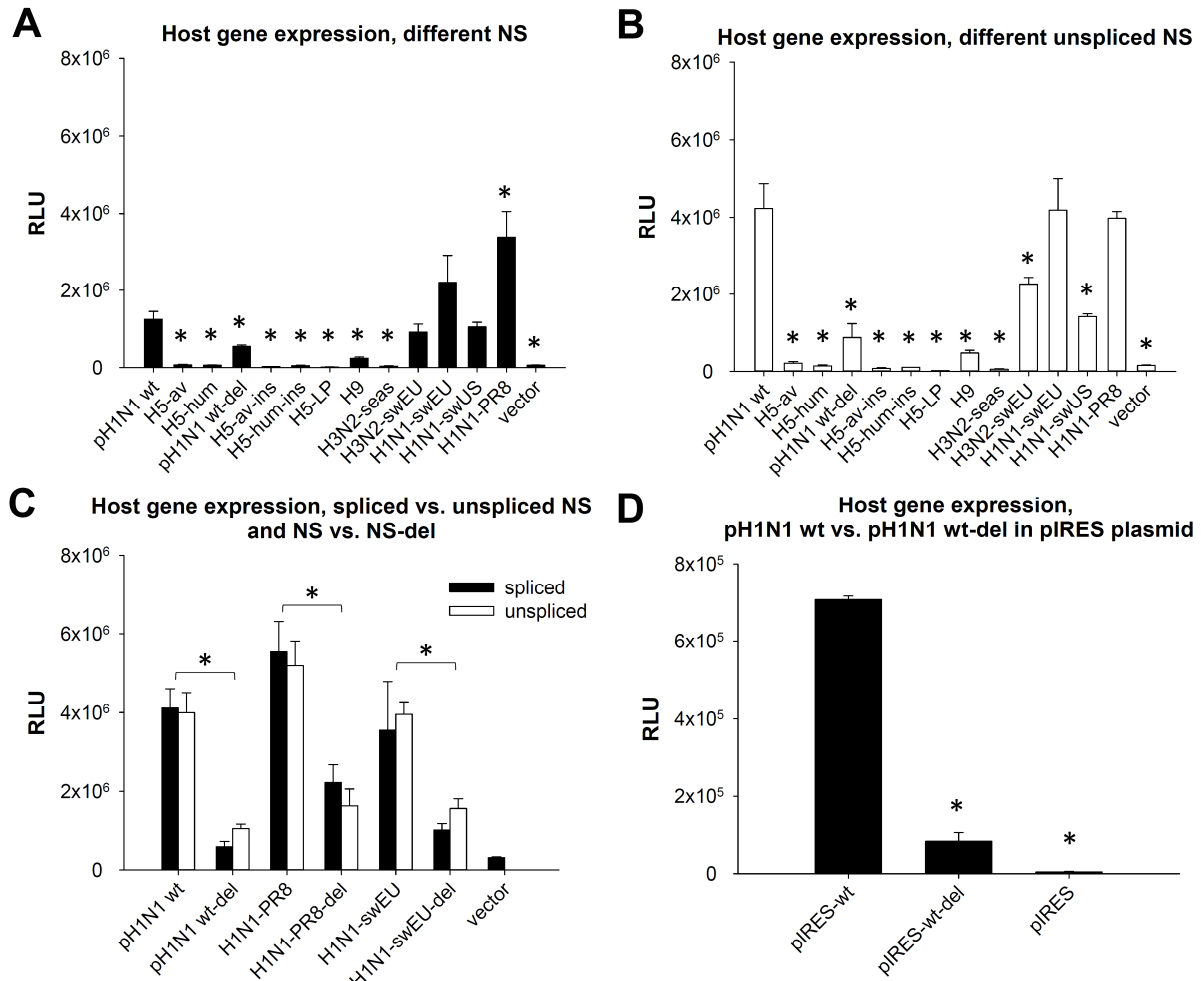


Figure 20: Effect of NS reassortment and aa 80-84 deletion/insertion on general host gene expression. (A-D) 0.75 μ g of NS containing pHWS (A-C) or pIRES (D) plasmid or empty vector and 12.5 ng of a plasmid encoding Renilla luciferase under control of a constitutively active SV40 promoter were co-transfected into HEK293T cells and luminescence was read after 48h. Closed bars: transfection of NS plasmids expressing both NS1 and NS2 proteins (normal splicing); open bars: transfection of NS plasmids expressing only NS1 but not NS2 proteins, due to mutation of the splice acceptor site and thereby inhibition of splicing. RLU, relative luminescence units. * indicates a significant difference ($p < 0.05$) to pH1N1 wt.

5.1.1.6 Effect of NS reassortment and amino acids 80-84 on pre-mRNA maturation

Since luciferase expression under a constitutively active promoter was differentially regulated by NS1 proteins from different viral strains (Fig. 20AB), and by deletion of the NS1 aa 80-84 (Fig. 20C), it was investigated which posttranscriptional step is involved in this regulation. Since both proteins (e.g. Fig. 17A, B, D) and mRNAs (Fig. 18 A-D, F) showed similar expression patterns (wt > H5-hum or H5-av, wt > wt-del), we examined pre-mRNA levels by real time PCR 24h after infection with an MOI of 1 of the corresponding reassortants. To

quantify pre-mRNA only, primer pairs where one primer (F or R) targets an exon and the other an intron were used on DNase-treated total RNA after reverse transcription with random hexamers. Indeed, on the pre-mRNA level, the expression pattern we found for proteins (luciferase, Fig. 17&20) and mRNA (Fig. 18A-D, F), wt > H5-hum or H5-av, wt > wt-del, was disrupted: pre-mRNA expression after pH1N1 wt infection was not significantly different or even significantly lower than pre-mRNA expression after H5-hum or H5-av reassortant infection (Fig. 21), suggesting that regulation by NS1 occurs at the level of pre-mRNA maturation. The regulation of gene expression by the deletion of aa 80-84 in pH1N1 NS1 seemed to also occur between the pre-mRNA and the mRNA level, since the major expression pattern found on the protein and mRNA level, wt > wt-del, was only found in one of four cytokines tested on the pre-mRNA level (Fig. 21).

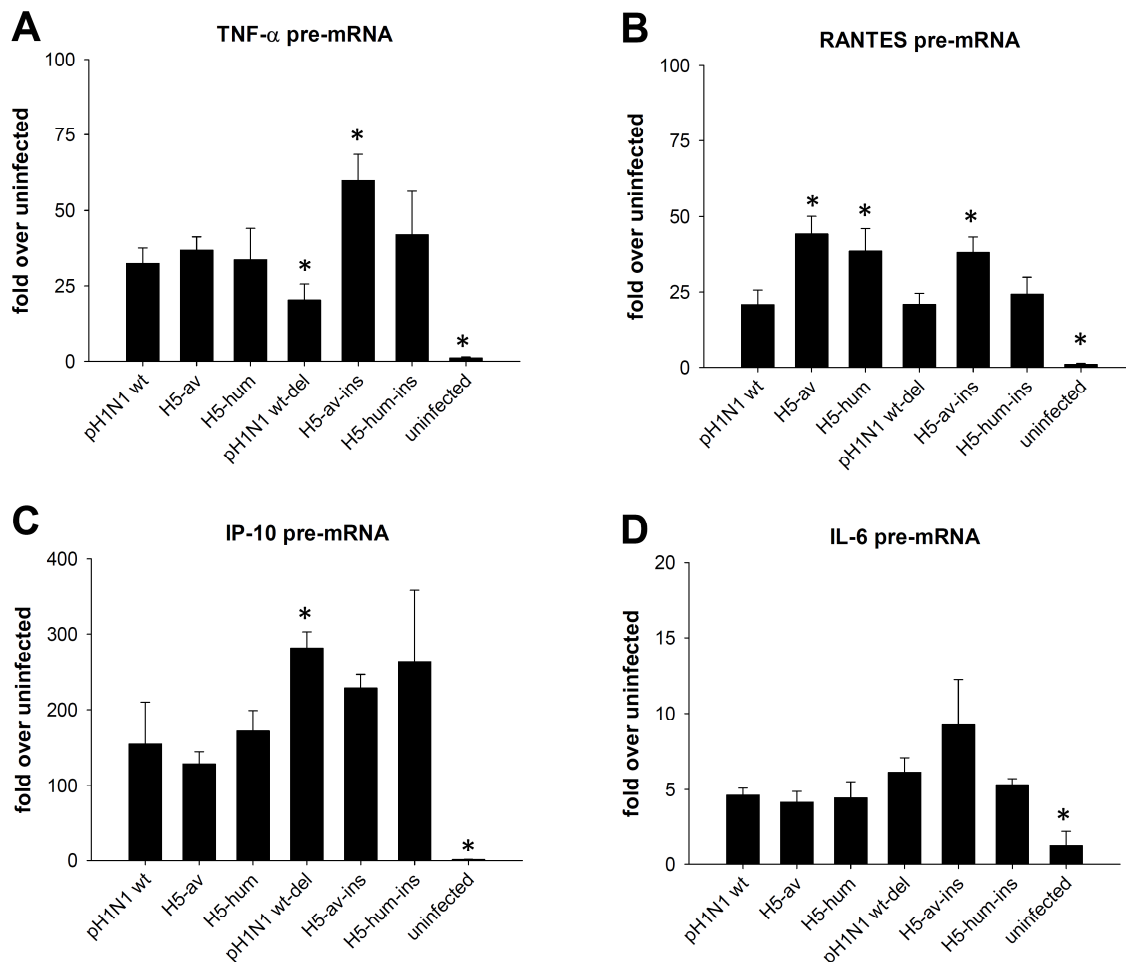


Figure 21: Effect of NS reassortment and aa 80-84 deletion/insertion on pre-mRNA expression. Total DNase-treated RNA extracted from A549 cells 24 h after infection (MOI 1) was reverse transcribed using random hexamers and pre-mRNA levels of TNF- α (A), RANTES (B), IP-10 (C) and IL-6 (D) were quantified by real-time PCR using one primer complementary to the exon and 1 primer complementary to the intron. Changes in gene expression were calculated using the $2^{-\Delta\Delta C_t}$ method and expressed as fold of uninfected.

5.1.2 Discussion

pH1N1 circulates globally since 2009 and has been detected in several host species, providing multiple possibilities to reassort with other co-circulating IAV strains. As a result, multiple pH1N1 reassortants have already naturally emerged, especially in swine (Nelson et al., 2012; Vijaykrishna et al., 2010). Our experiments demonstrated a high genetic compatibility of the pH1N1 background with NS genes of all strains tested irrespective of their human, swine or avian origin: all reassortants productively replicated at least in MDCK and ST cells. Genetic compatibility of pH1N1 and NS from H9N2 or seasonal H3N2 has been previously observed (Sun et al. 2011, Shelton et al. 2012). Thus, natural NS reassortment with circulating pH1N1 seems to be a likely scenario and requires monitoring, in particular since NS is an important pathogenicity factor. Despite the high genetic compatibility of NS from different species with the pH1N1 background, pH1N1 wt was one of the fittest viruses in swine, avian and human cell cultures. Thus, viral fitness of pH1N1 is unlikely to increase after reassortment with NS genes of other IAV strains. It also suggests a high level of adaptation of pH1N1 NS to the pH1N1 background genes and perhaps even a role of NS in the development of this pandemic virus.

Distinct NS reassortments between well proliferating wild type IAV strains strongly decreased fitness of the reassortant. For instance, wildtype strains of pH1N1 and the HPAIV H5N1 strains grew to high titers on A549 cells and in mice (Fig. 13BC and (Bogs et al. 2011, Matthaei et al. 2013, Mänz, Dornfeld, et al. 2013)). However, the introduction of HPAIV H5N1 NS into the pH1N1 background severely attenuated growth in A549 or DF-1 cells and in mice. Thus, the higher pathogenicity of HPAIV could not be transferred to pH1N1 by NS reassortment. Interestingly, the attenuation was not observed in MDCK and ST cells, suggesting that the loss of fitness was due to differential interactions of NS with host cell proteins, rather than to a general reduction in fitness due to gene incompatibility or the production of non-infective viral particles.

Despite the stronger antiviral host response induced by pH1N1 wt, this virus was considerably fitter on A549 cells than the H5-av and H5-hum NS reassortants or pH1N1 wt-del. Since all strains showed a titer reduction upon type I IFN treatment (data not shown), this was not due to type I interferon resistance. While several studies found that IAVs inducing high antiviral host responses were attenuated (Garcia-Sastre et al. 1998, Donelan et al. 2003, Solórzano et al. 2005), more recent studies also reported examples of the opposite. In general, pH1N1 NS1

binds CPSF30 only weakly (Hale et al. 2010). However, a pH1N1 strain that more efficiently suppressed the antiviral host response due to three mutations increasing CPSF30 binding was attenuated in mice and ferrets (Hale et al. 2010). The direct interaction of NS1 with the viral polymerase (Marión et al. 1997) and CPSF30 (Nemeroff et al. 1998) could be a possible explanation. In line with this, temperature sensitivity of IAV strains by NS mutations was suppressed by exchanging polymerase genes (Scholtissek & Spring 1982) and it was proposed that strong interactions between NS1 and CPSF30 could impair the activity of the viral polymerase and thereby viral replication (Shelton et al. 2012). Although the exact mechanism causing the reduced viral fitness of H5 NS reassortants or pH1N1 wt-del in our study has not been determined, the above observations suggest a direct role of NS1 in the regulation of the viral polymerase, possibly depending on its binding strength to CPSF30.

Sequence comparison of the well-proliferating NS reassortants and pH1N1 wt to the attenuated NS reassortants on A549 (Fig. 15) identified the NS1 deletion of aa 80-84 to decrease viral fitness in a pH1N1 background on A549 cells (Fig. 16). Conversely, a small but significant fitness improvement was observed when TIASV was inserted in position 80-84 into the H5-hum NS1, suggesting that aa 80-84 contribute to viral fitness in the pH1N1 background. The viral fitness of H5-av was not improved by this insertion. This differential effect could be due to one of 12 aa differences (Fig 15), possibly corresponding to accessory mutations acquired by NS from the human H5N1 isolate during its replication in the human host. The significance of these aa for viral fitness or host adaptation requires further attention. The obtained results showed that, in general, deleting aa 80-84 in pH1N1 NS1 resulted in larger differences both in viral growth and regulation of host gene expression than inserting these aa into H5 NS1. One explanation could be that NS1 positions 80-84 act in concert with other amino acids. For instance, at least six amino acids have been described to influence NS1 binding to CPSF30 (Li et al. 2001, Twu et al. 2006, Kochs et al. 2007, Hale et al. 2010). In this case, the effect of additional NS1 mutations on CPSF30 binding would depend on the constellation of these six amino acids.

The identified 5 aa deletion of position 80-84 was absent in all IAV strains before 2000 and emerged in HPAIV H5N1 in China in 2000 (Guan et al. 2002). By 2004, already most of the H5N1 strains had this deletion (Zhou et al. 2006, Long et al. 2008). Between 2011 and 2013, it was found in 95 % of 207 H5N1 NS1 sequences but was rarely detected in non-H5 IAV subtypes: only 8 out of > 20 000 non-H5 NS1 proteins had this deletion (NIAID Influenza

Research Database, <http://www.fludb.org>, (Squires et al. 2012) accessed on November 10, 2013). Five H9N2 strains carrying the deletion after an NS reassortment with HPAIV H5N1 in Pakistan (2005-2007) showed no difference in pathogenicity in chicken (Iqbal et al. 2009). Here, we demonstrated that in a pH1N1 background, deletion of aa 80-84 in NS1 impairs viral growth in A549 cells, but does not affect the MLD50. In a H1N1 PR8 background, NS reassortants from H5N1 naturally carrying the deletion of aa 80-84 were attenuated as compared to reassortants carrying NS from another H5N1 strain without deletion (Lipatov et al. 2005)). In contrast, in a background of HPAIV H5N1, the deletion increased virulence in mice and chicken (Long et al. 2008). Although in these studies, the contribution of other mutations cannot be totally excluded, the effect of aa 80-84 seems to depend on the viral background. The reduced fitness associated with this deletion in a human IAV background may explain its absence in NS1 of naturally circulating human IAV strains.

Throughout the study, we consistently observed a markedly lower host gene and protein expression mediated by H5 NS and pH1N1 wt-del NS compared to pH1N1 wt NS. Importantly, this allowed us to assign a previously unknown role in host gene regulation to aa 80-84 in pH1N1. However, from the present experiments, it is difficult to conclude whether this was due to a differential upregulation or a differential downregulation of the host gene expression. We observed a downregulation of luciferase expression relative to polyI:C stimulation in the infection experiments (Fig. 17AB). However, the level of IFN induced by polyI:C is not comparable to IFN levels after IAV infection. The ideal positive control, a NS deficient pH1N1, does not replicate in IFN-competent systems such as the A549Luc reporter cells. The low Renilla luciferase expression after empty vector transfection (Fig. 20) is indicative of differential upregulation by distinct NS's or a general upregulation followed by a differential downregulation by distinct NS's. Finally, irrespective of whether this is caused by a host gene expression up- or downregulation, we consistently observed lower host gene expression in presence of H5 NS or pH1N1 wt-del NS relative to pH1N1 wt NS.

The regulation of the antiviral host response differed between NS from distinct species. Interestingly, in addition to the well-established PR8 NS1 (Kochs et al. 2007), pH1N1- and swine-origin NS1 allowed considerably higher general host gene expression than avian and human seasonal NS1, as reflected by higher luciferase expression from an SV40-promoter driven plasmid (Fig. 20AB). It has been proposed previously that NS1 proteins from both classical swine IAV and H1N1 PR8 bind inefficiently to CPSF30 (Kochs et al. 2007, Hale et

al. 2010), thereby allowing a high antiviral host response. We showed that also NS1 proteins from European swine IAV H1N1 and H3N2 strains allow high levels of general host gene expression (Fig. 20AB). Since the NS gene of pH1N1 is ultimately derived from classical swine IAV, this property seems inherent to NS1 proteins of swine origin. Notably, it seems only possible to observe the effect of the aa 80-84 deletion on general host gene expression in an NS1 protein allowing high enough host gene expression in the first place. This possibly explains why this function of the aa 80-84 deletion has not been previously detected for avian NS1.

Finally, we investigated at which step the NS reassortments and aa 80-84 deletions regulated general host gene expression. While on the protein (Fig. 17ABD) and mRNA level (Fig. 18A-D, F), infection with H5 NS reassortants as well as pH1N1 wt-del consistently led to lower cytokine expression as compared to pH1N1 wt, this was not the case on the pre-mRNA level for H5 NS reassortants and only in one of four cytokine pre-mRNAs for pH1N1 wt del (Fig. 21). This may indicate that regulation of general host gene expression occurs at the level of pre-mRNA maturation. Mechanisms of pre-mRNA maturation include splicing, capping and polyadenylation, followed by nuclear export of the mature mRNA (Hocine et al. 2010). Differential regulation of splicing by NS1 is not responsible for modulating gene expression (Fig. 18A, Fig. 20), since neither the IFN- β nor the Renilla luciferase gene are spliced during pre-mRNA maturation. Also, differential inhibition of nuclear export does not seem implicated, since RNA for real time PCR quantification of cytokines was extracted independently of its intracellular location. While NS1 has not been shown previously to influence capping, its inhibition of polyadenylation by binding to CPSF30 and PABPII is widely accepted (Nemeroff et al. 1998, Chen et al. 1999, Twu et al. 2006, Hale et al. 2010). Whether binding to these proteins plays a role for NS1 from European swine IAV strains or pH1N1 wt-del remains to be determined.

In conclusion, we showed by introducing NS genes from various IAV host species and subtypes into the pH1N1 background that (i) pH1N1 largely tolerates different NS genes with only minor fitness losses in 6 out of 8 reassortants, (ii) reassortment with NS from HPAIV H5N1 led to attenuation on A549 and DF-1 cells and in mice, (iii) a naturally occurring deletion of amino acid positions 80-84 in NS1 attenuated the reassortant *in vitro* and (iv) this deletion plays a previously unknown role in the regulation of the general host gene expression, possibly at the level of pre-mRNA maturation.

Part 2:

5.2 EPs® 7630 (Umckaloabo®), an extract from *Pelargonium sidoides* roots, exerts anti-influenza virus activity *in vitro* and *in vivo*

This study has been published as: Linda L. Theisen, Claude P. Muller (2012), EPs® 7630 (Umckaloabo®), an extract from *Pelargonium sidoides* roots, exerts anti-influenza virus activity *in vitro* and *in vivo*, Antiviral Research 94: 147–56, and was adapted therefrom.

L. Theisen contributed the major part to conception and design of the study, experimental work, data analysis and interpretation and wrote the manuscript. Plant extracts, fractions and single compounds used in this study were produced and provided by Dr. Willmar Schwabe GmbH & Co. KG, Karlsruhe.

Pelargonium sidoides DC (Geraniaceae) has widely been used as a traditional indigenous medicine in South Africa against dysentery, fever and respiratory diseases (Brendler & van Wyk 2008). In 2005, an ethanolic root extract (drug to extraction solvent ratio 1:8-10), referred to as EPs® 7630 (Umckaloabo®), received full marketing authorization by the German drug regulatory agency (Conrad et al. 2007). To date, the extract is mainly used to treat acute bronchitis and has shown good tolerability in multiple clinical trials in both adults and children (Matthys et al. 2003, Matthys & Heger 2007, Agbabiaka et al. 2008, Kamin et al. 2010). Utilization of this already licensed and well characterized drug to treat a new indication therefore has advantages over the development of a drug with scarce previous characterization and an unknown safety profile.

EPs® 7630 mainly consists of polyphenolic compounds (Schötz & Nöldner 2007, Schoetz et al. 2008). Oligo- and polymeric condensed tannins based on gallicocatechin and epigallocatechin moieties account for about 40% of the dry extract. These compounds are present in an enormous structural variety (from monomers to at least 16-mers, A- and B-type bonding and different stereoisomers) (Schoetz et al. 2008).

Here the antiviral efficacy of EPs® 7630 and its constituents against a variety of IAV strains, the step of the virus life cycle affected and the propensity of EPs® 7630 to induce resistance were investigated. Importantly, active compounds were characterized and an antiviral effect of EPs® 7630 *in vivo* was demonstrated.

5.2.1 Results

5.2.1.1 Anti-IAV activity of EPs® 7630 is exerted at non-toxic concentrations *in vitro*

Cytotoxicity was tested by adding serial dilutions of EPs® 7630 to A549 cells. After 24h of incubation, cell viability was measured by XTT test. The half maximal cytotoxic concentration of EPs® 7630 (CC50) was 557 µg/ml (Fig. 22A).

To assess its antiviral activity, serial dilutions of EPs® 7630 were added to A549 cells infected with 0.01 MOI (giving an optimal fluorescent readout) of a reporter virus containing a NS1-GFP fusion protein (A/Puerto Rico/8/34-NS116-GFP) (Kittel et al. 2004). After 24h, the half maximal antiviral concentration of EPs® 7630 (EC50) was determined as 6.6 µg/ml (Fig. 22A), corresponding to a selectivity index (SI=CC50/EC50) of 84.4.

The anti-influenza activity of EPs® 7630 was further demonstrated for five wild type IAV strains, which all showed a dose-dependent titer reduction. TCID50 determination of wild type pandemic H1N1 (A/Luxembourg/46/2009) confirmed the fluorescent readout and resulted in an EC50 of 5.4 µg/ml (Fig. 22B), corresponding to an SI of 103.1. The H1N1 strain A/Puerto Rico/8/34 showed complete virus growth inhibition at 50 µg/ml, similarly after 8, 24 and 48h post infection (Fig. 22C). The concentrations required for complete virus clearance varied from 16 µg/ml (pandemic H1N1 A/Luxembourg/46/2009, Fig. 22B) up to 300 µg/ml for seasonal Oseltamivir resistant H1N1 A/Luxembourg/572/2008 (Fig. 22F). Intermediate values were found for A/Puerto Rico/8/34 (50 µg/ml, Fig. 22C), seasonal H3N2

A/Luxembourg/01/2005 (50 $\mu\text{g/ml}$, Fig. 22D) and seasonal Oseltamivir-sensitive H1N1 A/Luxembourg/663/2008 (100 $\mu\text{g/ml}$, Fig. 22E). In contrast, EPs® 7630 had no antiviral activity against the unenveloped adenovirus type 5 (ATCC reference strain, Fig. 22G) or against the enveloped measles virus (Rimevax vaccine strain) at non toxic concentrations (Fig. 22H).

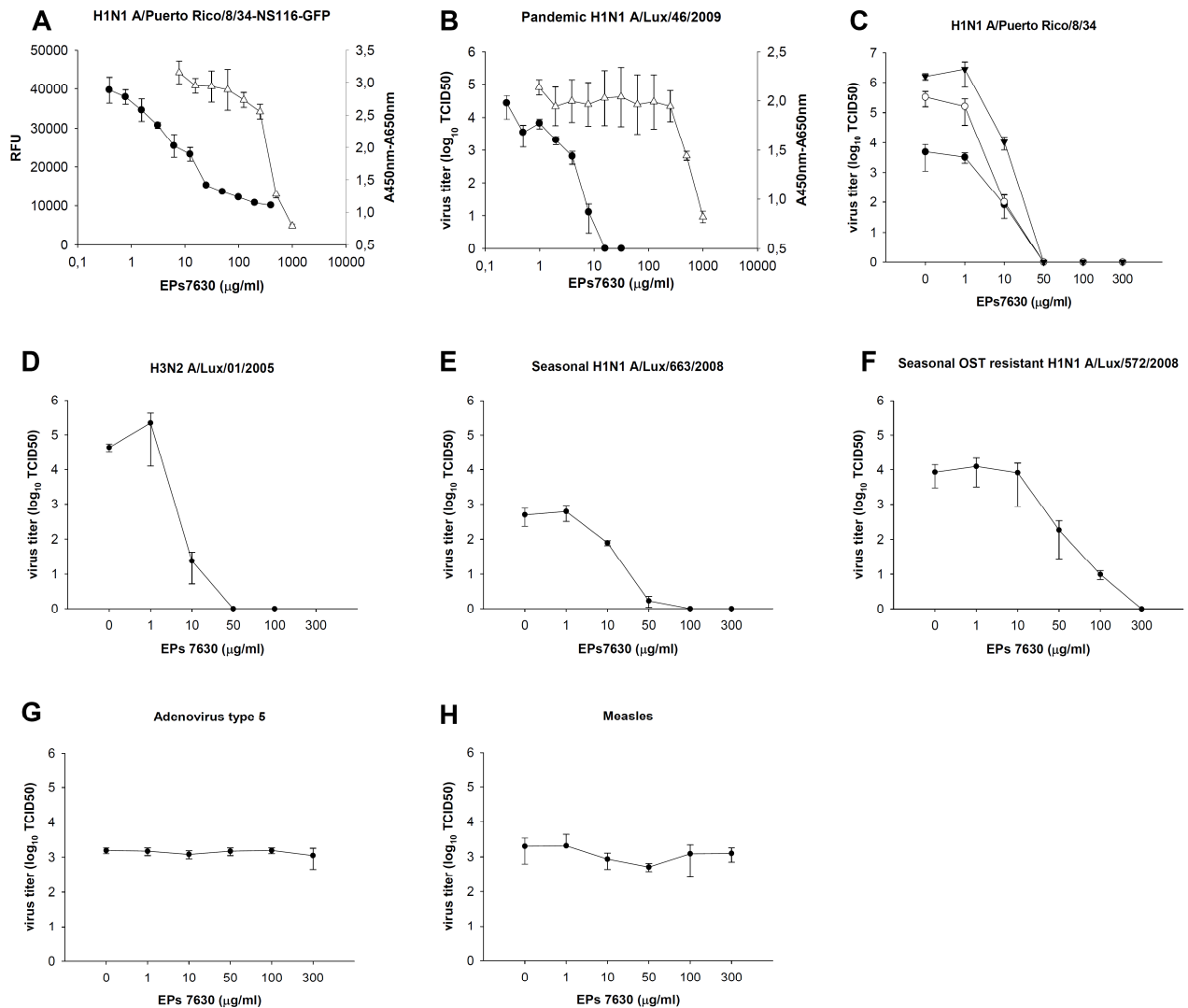


Figure 22: Cytotoxicity and antiviral efficacy of EPs® 7630 *in vitro*. (A) A/Puerto Rico/8/34-NS116-GFP reporter virus-associated fluorescence expressed as RFU (relative fluorescence units, ●) measured 24h after infection of A549 cells with GFP-virus (MOI 0.01) in presence of serial dilutions of EPs® 7630. (B) pH1N1 A/Luxembourg/46/2009 titer measured 24h after infection of A549 cells (0.1 MOI, ●). (A-B) Δ : A549 cell viability determined by XTT assay 24h after EPs® 7630 addition. Background absorbance (650 nm) was subtracted from reagent absorbance (450 nm). (C-H) EPs® 7630 activity against different virus strains. A549 cells were infected with 0.1 MOI of (C) A/Puerto Rico/8/34 (titered after 8h (●), 24h (○) or 48h (▼)), (D) seasonal H3N2 A/Luxembourg/01/2005, (E) Oseltamivir (OST) sensitive seasonal H1N1 A/Luxembourg/663/2008, (F) Oseltamivir resistant seasonal H1N1 A/Luxembourg/572/2008, (G) adenovirus

type 5 (ATCC reference strain, MOI 0.05) or **(H)** A549Slam infected with measles virus (Schwarz vaccine strain, MOI 0.01) in presence of EPs® 7630, titrated 24 or 48h **(E, F, H)** post infection by TCID50 determination.

5.2.1.2 EPs® 7630 affects an early step in the influenza virus life cycle

Next, we investigated at which step of the virus life cycle EPs® 7630 exerts its antiviral activity. A549 cells were infected with A/Puerto Rico/8/34 (MOI 0.1) and 50 µg/ml of EPs® 7630 was added at different time points (-2, 0, +2, +4, +6 h) before or after infection. TCID50 in the supernatant was determined 8h or 24h post infection (corresponding to approximately 1 or 3 virus life cycles).

In the one life cycle experiment, the EPs® 7630 containing medium was replaced by EPs® 7630-free medium at 8h post infection to allow proliferation of intracellular virus for another 24h before titration. No virus was detectable in the supernatant when treatment with EPs® 7630 was started before or at the time of inoculation (Fig. 23A). However, when the plant extract was added 2, 4 or 6h post infection, no effect on virus proliferation was observed (Fig. 23A), suggesting that the extract inhibited an early step of viral infection, presumably viral entry into the host cell.

When EPs® 7630 was allowed for 24h (instead of 8h) on the culture, no virus was detectable in the supernatant, irrespective of the start of the treatment (-2, 0, +2, +4, +6 hours post infection) (Fig 23B). Thus, EPs® 7630 efficiently prevented virus released from host cells after the first life cycle (i.e. 8h post infection) to re-enter new host cells and complete its next life cycles.

5.2.1.3 EPs® 7630 inhibits hemagglutination and neuraminidase activity of influenza virus

The effect of EPs® 7630 on H1N1 A/Puerto Rico/8/34 virus binding to its receptor was tested by hemagglutination inhibition assay. EPs® 7630 prevented virus-mediated hemagglutination from 100 µg/ml (data not shown). In absence of virus, EPs® 7630 had no effect on hemagglutination. In a standard fluorescence based neuraminidase inhibition assay, 121.7 µg/ml EPs® 7630 reduced neuraminidase activity of A/Puerto Rico/8/34 by 50% (Fig. 23C). Thus, EPs® 7630 interferes with virus binding to its host cell receptors (attachment) as well as neuraminidase activity.

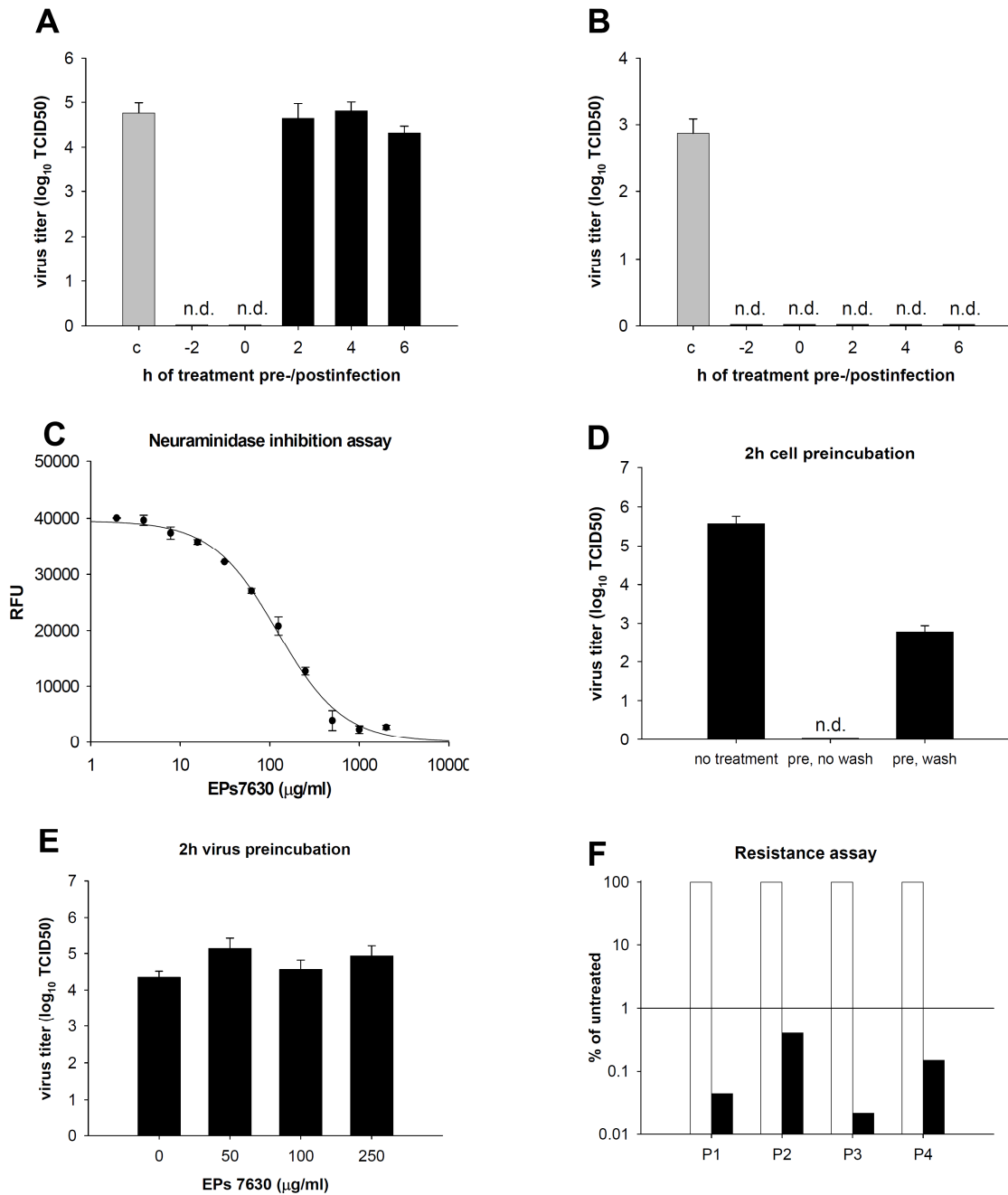


Figure 23: Anti-IAV mechanism of EPs® 7630. (A-B) PBS (c, control) or 50 $\mu\text{g/ml}$ of EPs® 7630 was added to A549 cells 2h before infection or 0, 2, 4, or 6h after infection with A/Puerto Rico/8/34 (MOI 0.1). (A) Supernatant replacement 8h post infection (1 virus life cycle) by EPs® 7630-free supernatant. TCID₅₀ determination 24h after medium change. (B) TCID₅₀ determination after 24h of incubation (3 virus life cycles). (C) Effect of EPs® 7630 dilutions (duplicates) on neuraminidase activity of A/Puerto Rico/8/34 expressed as relative fluorescence units (RFU) of a fluorogenic substrate of the neuraminidase, 2-(4-methylumbelliferyl)- α -D-N-acetylneuraminic acid. (D) Preincubation (pre) of A549 cells with EPs® 7630 (0 or 50 $\mu\text{g/ml}$) 2h before infection, with and without washing step before infection with A/Puerto Rico/8/34. TCID₅₀ determination after 24h. (E) Preincubation of A/Puerto Rico/8/34 for 2h with EPs® 7630 (0, 50, 100 or 250 $\mu\text{g/ml}$) before infection of A549 cells (MOI 0.1). TCID₅₀ determination 24h after infection. (F) Resistance assay: infection of A549 cells with 0.2 MOI H1N1 A/Puerto Rico/8/34 cells in presence of 0 (open bars) or 10 $\mu\text{g/ml}$ (closed bars) of

EPs® 7630. After 24h, fresh A549 cells were inoculated with 100 µl of supernatant and left untreated for 24h, before that 0 or 10 µg/ml EPs® 7630 were added again for 24h. Four passages (P1-P4) were performed. Supernatants were titered on MDCK cells and titers are expressed in % of titer of untreated cells, which was set to 100%. All experiments done in triplicates unless otherwise indicated. n.d., not detectable.

5.2.1.4 Effect of preincubation of cells or virus with EPs® 7630

A549 cells were preincubated for 2h with 50 µg/ml of extract or PBS and then infected with 0.1 MOI of A/Puerto Rico/8/34. As already shown in Fig. 23A, continuous treatment with EPs® 7630 prevented virus growth. When EPs® 7630 was washed out before infection, the virus was inhibited by more than 2 log to an average titer of 6×10^2 TCID₅₀ compared to 3.7×10^5 TCID₅₀ in EPs® 7630-free cultures (Fig. 23D). Thus, the effect of EPs® 7630 on the host cells impairs viral infection. Washing out EPs® 7630 from the cells prior to infection allowed only partial virus growth, suggesting that the extract's effect is partially irreversible.

To assess a direct virucidal effect of EPs® 7630, virus stock was preincubated with up to 250 µg/ml of EPs® 7630 for 2h before infection. At inoculation, virus was diluted 1:200 fold, corresponding to 0.1 MOI and a negligible final concentration of EPs® 7630 of < 1.25 µg/ml. 24h post infection, supernatants were titered and no difference in virus growth was observed between cultures infected with EPs® 7630 treated and untreated virus (Fig. 23E). A direct virucidal activity of EPs® 7630, at least up to concentrations of 250 µg/ml, can therefore be excluded.

5.2.1.5 EPs® 7630 shows no propensity to generate resistant viruses

H1N1 A/Puerto Rico/8/34 was passaged four times in presence of 0 or 10 µg/ml EPs® 7630, a concentration reducing virus growth without completely inhibiting it (see Fig. 22C). In every passage, 10 µg/ml of EPs® 7630 constantly reduced the viral titer well below 1% of the untreated controls (P1 0.04%, P2 0.40%, P3 0.02%, P4 0.15%, Fig. 23F), showing that, at least over 4 passages, the susceptibility of the virus to EPs® 7630 did essentially not change. Thus, EPs® 7630 did not show propensity to induce resistant viruses.

5.2.1.6 Anti-influenza activity of EPs® 7630 is mediated by tannins

Since tannins in EPs® 7630 have been shown to impair adhesion of streptococci to epithelial cells (Janecki et al. 2011), we examined whether they were also involved in its antiviral activity. Therefore, tannins were removed from EPs® 7630 by precipitation with hide powder, a standardized procedure from the European Pharmacopoeia (European Directorate for the Quality of Medicines & Healthcare 2008). While full EPs® 7630 extract abolished growth of 0.05 MOI of H1N1 A/Puerto Rico/8/34 above a concentration of 10 µg/ml, the tannin-free extract did not show any antiviral effect at least up to 100 µg/ml (Fig. 24), indicating that tannins represent the active principle of EPs® 7630 against IAV.

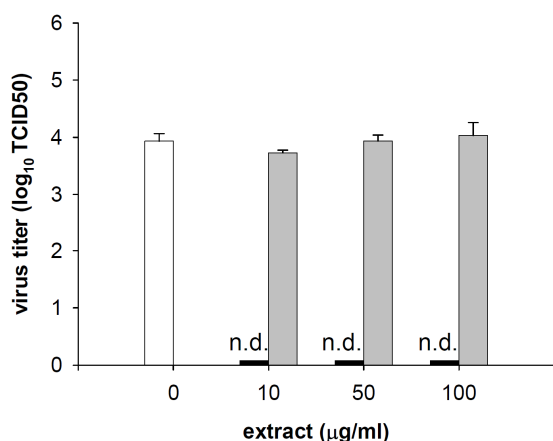


Figure 24: Anti-IAV activity of tannins from EPs® 7630. Effect of tannins on H1N1 A/Puerto Rico/8/34 (0.05 MOI). Infection of A549 cells in triplicates and incubation with dilutions of full extract (closed bars), tannin-free extract (grey bars) or PBS (no treatment, open bar) for 24h. n.d., not detected.

5.2.1.7 Chain length of (pseudo)tannins influences antiviral activity

Gallocatechin and its stereoisomer epigallocatechin are the main moieties of condensed tannins, the predominating constituents of EPs® 7630 (Schoetz et al. 2008). To assess the minimal chain length requirement for antiviral activity, we studied monomers (see Fig. 25 for structure), dimers of these two main compounds (Fig. 25) and an oligo-/polymeric fraction (containing trimeric up to high molecular weight condensed tannins) isolated from EPs® 7630 full extract by fractionation over a Sephadex LH20 column (Vennat et al. 1992).

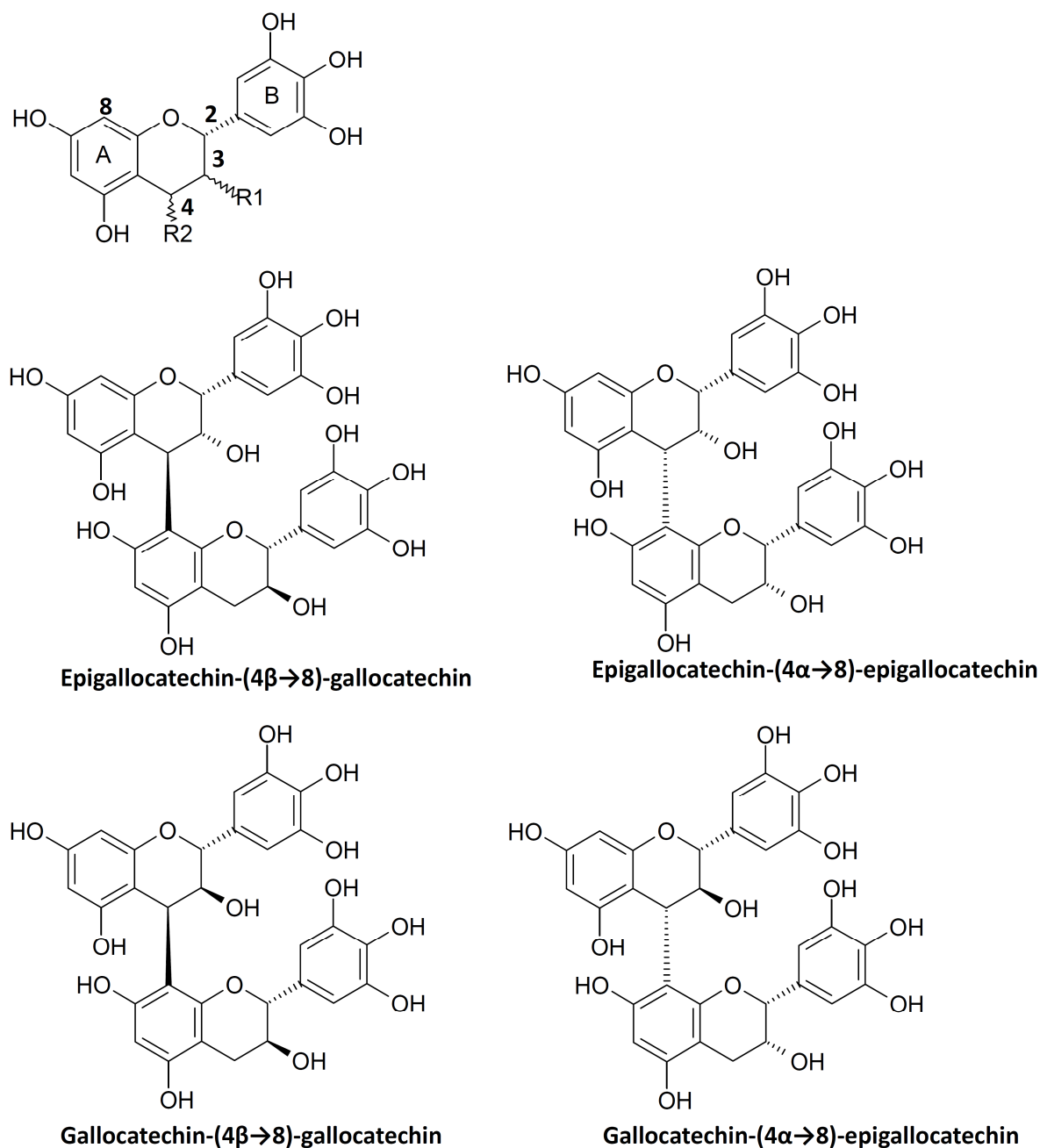


Figure 25: Structures of EPs® 7630 constituents with anti-IAV activity. Structures of the main moieties of condensed tannins, gallocatechin and epigallocatechin, as well as isolated dimers tested for antiviral efficacy. R1: \blacktriangleleft OH, gallocatechin, $\bullet\bullet$ OH, epigallocatechin; R2: oligomerization site.

Interestingly, both monomers had similar efficacy against H1N1 A/Puerto Rico/8/34-NS116-GFP (1.5 fold difference, Table 2). The antiviral activity of the four homo- and heterodimers (epigallocatechin-(4 β →8)-gallocatechin, epigallocatechin-(4 α →8)-epigallocatechin, gallocatechin-(4 β →8)-gallocatechin, gallocatechin-(4 α →8)-epigallocatechin) was 2 to 7-

fold higher than that of the monomers, as shown by their EC₅₀ values and the oligo-/polymeric fraction was over 10-fold or 2-5-fold more active than the monomers or dimers, respectively, on a weight basis (Table 2, column “EC₅₀, μg/ml”). Calculated on a molar basis, dimers were 4 to 13-fold more active than monomers (Table 2, column “EC₅₀, μM”). Under the identical conditions than in the antiviral assay (24h incubation), the oligo-/polymeric fraction had a CC₅₀ of 116.1 μg/ml. The monomers and dimers did not exhibit any cytotoxic effects on A549 cells up to > 160 μg/ml, in a way that it was not possible to determine the exact CC₅₀ (Table 2). Thus, anti-IAV efficacy depends on the polyphenolic chain length: gallic catechin and its stereoisomer have comparable efficacy and exert antiviral activity in their monomeric form, but dimeric and oligo-/polymeric (epi-)gallic catechins are more effective.

Table 2: Cytotoxic and anti-IAV activities of catechin monomers, dimers and oligo-/polymers present in EPs® 7630

	CC ₅₀		EC ₅₀		SI	PG
	μM	μg/ml	μM	μg/ml		
Epigallocatechin	> 522.4	> 160	138.8	42.5	> 3.7	1
Gallic catechin	> 522.4	> 160	92.7	28.4	> 5.6	1
Epigallocatechin- (4β→8)-gallic catechin	> 261.2	> 160	10.3	6.3	> 25.4	2
Epigallocatechin- (4α→8)- epigallocatechin	ND	ND	23.2	14.2		2
Gallic catechin-(4β→8)- gallic catechin	ND	ND	11.9	7.3		2
Gallic catechin-(4α→8)- epigallocatechin	> 261.2	> 160	21.2	13.0	> 12.3	2
Oligo-/polymeric fraction	Not applicable	116.1	Not applicable	2.8	41.5	3- ≥9

CC₅₀, half maximal cytotoxic concentration; EC₅₀, half maximal antiviral concentration; SI, selectivity index; PG, polymerization grade; ND, not determined.

5.2.1.8 EPs® 7630 exerts anti-influenza activity in mice by inhalation

When mice were infected with 4 MLD50 of H1N1 A/Puerto Rico/8/34 and were treated by oral gavage with vehicle only or EPs® 7630 (5 mg/kg three times a day, corresponding to the human recommended dose recalculated for mice) (Reagan-Shaw et al. 2008), no difference in survival, body weight or temperature was observed (data not shown). The absence of antiviral effect after oral administration was in contrast to a clear anti-influenza effect observed in the following inhalation experiments. For the inhalation protocol, groups of 10 mice were infected with 1 or 4 MLD50 of H1N1 A/Puerto Rico/8/34 and treated with EPs® 7630 or water by inhalation three times a day. For both virus doses, EPs® 7630 significantly increased survival of virus-infected mice ($p < 0.003$). All 10 mock treated animals infected with 4 MLD50 were euthanized between day 6 and 8 because of a $> 25\%$ loss in body weight, while the first mouse of the EPs® 7630 treated group was euthanized only on day 8. 3 of the 4MLD50 infected and 9 of the 1MLD50 infected EPs® 7630 treated animals did not show any sign of disease after day 10 and survived until the end of the monitoring period (day 14), while none (4 MLD50) or only 2 (1 MLD50) untreated mice survived (Fig. 26AB).

Body weights (Fig. 26C) of EPs® 7630 treated mice were significantly higher as compared to the untreated group as of day 5, and body temperature as of day 6 (Fig. 26D). Surviving mice completely cleared the virus, while euthanized mock treated mice had an average lung titer of 5.9×10^5 TCID50 (4 MLD50) or 3×10^3 TCID50 (1 MLD50) (Fig. 26E, F). Sacrificed EPs® 7630 treated mice showed a lower average lung titer (4×10^3 TCID50 in the 4 MLD50 group, 7.41 TCID50 in the 1 MLD50 group) as compared to the untreated group, but the difference was not significant (Fig. 26E, F). The only sacrificed treated mouse in the 1 MLD50 group may have recovered, as its lung titer was remarkably low. Thus, inhalative treatment with EPs® 7630 induced a robust improvement of survival, lower lung titers and less signs of disease, demonstrating a clear benefit of the treatment of influenza with EPs® 7630 in the mouse model.

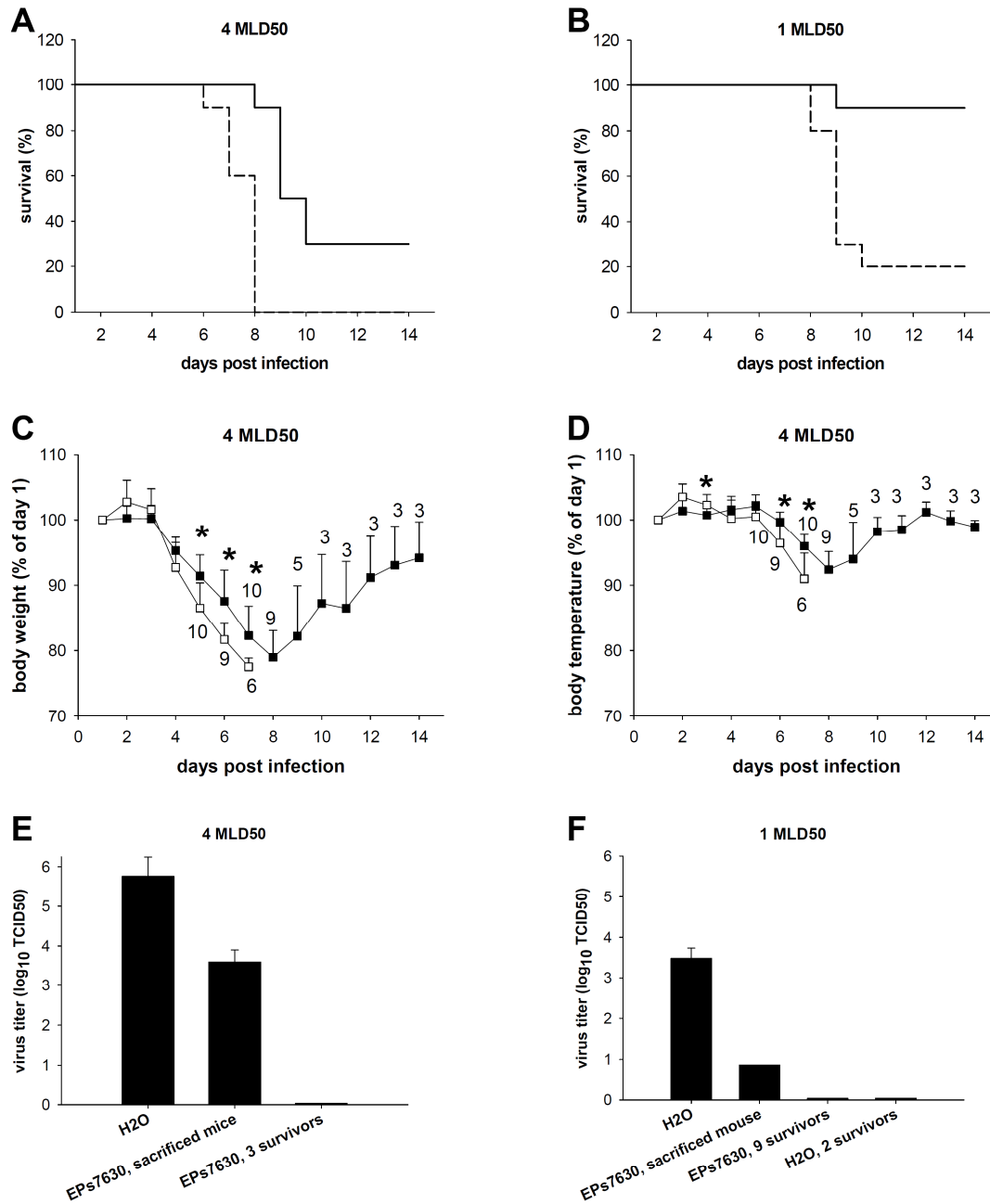


Figure 26: Anti-IAV activity of EPs® 7630 *in vivo*. (A-F) Infection of 10 mice per group with 4 MLD50 (A, C, D, E) or 1 MLD50 (B, F) of A/Puerto Rico/8/34, treatment with EPs® 7630 or water by inhalation three times a day for 10 days. (A-B) Survival analysis of EPs® 7630 (solid line) or water (broken line) treated animals. (C, D) Evolution of body weight (C) or body temperature (D) of EPs® 7630 (■) or water (□) treated animals. Numbers represent surviving animals from a group of 10. * indicates a significant difference between the EPs® 7630- and mock-treated group. (E-F) Influence of EPs® 7630 treatment on virus lung titers. Lungs were removed on the day when less than 75% bodyweight was reached or on day 14 for surviving mice; homogenization and titration on MDCK cells. MLD50, half maximal mouse lethal dose.

5.2.1.9 EPs® 7630 has no apparent toxic effect in mice

Groups of five mice were treated by the same regimen as the *in vivo* inhalative efficacy study. Daily monitoring of body weight (Fig. 27A) and body temperature (Fig. 27B) showed no significant toxicity of EPs® 7630 between both groups. Thus, EPs® 7630 did not produce obvious toxic effects in mice and had a good safety profile when used by inhalation.

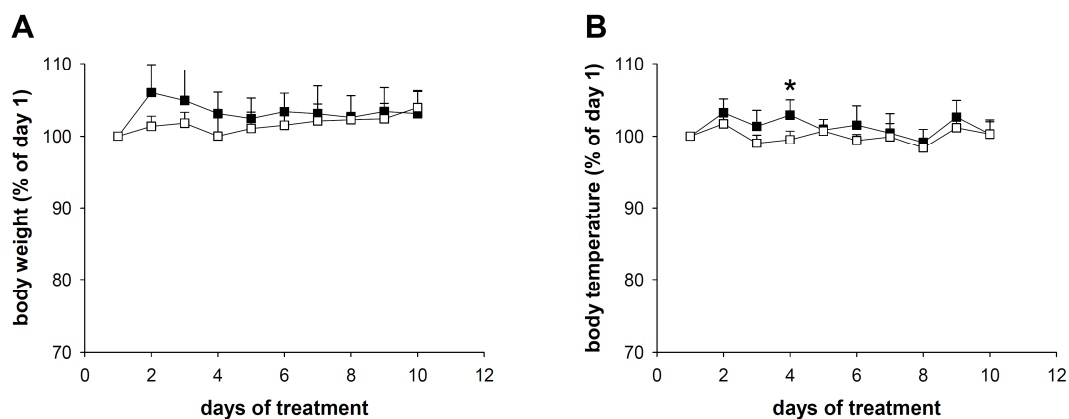


Figure 27: Toxicity of EPs® 7630 *in vivo*. (A, B) Five mice per group were mock infected with 50 μ l PBS and treated with EPs® 7630 or water by inhalation three times a day for 10 days with daily monitoring of body weight and temperature. Evolution of body weight (A) and body temperature (B) for EPs® 7630 (■) or water (□) treated animals. * indicates a significant difference between the EPs® 7630- and mock-treated group.

5.2.2 Discussion

Our study confirmed the antiviral activity of tannin-rich plant extracts against several IAV strains, in contrast to non-enveloped adenovirus, as was reported before (Gescher, Kuhn, et al. 2011, Michaelis et al. 2011). However, EPs® 7630 does not exclusively inhibit enveloped viruses, as it was also effective against the non-enveloped coxsackie virus (Michaelis et al. 2011). Also, the extract seemed to inhibit several paramyxoviridae (respiratory syncytial virus, parainfluenza) (Michaelis et al. 2011), but in our hands failed to inhibit measles virus proliferation. Also, some IAV strains were inhibited at an up to 30-fold lower concentration than others. Differential sensitivity of IAV strains to tannin-rich plant extracts has also been previously observed (Ehrhardt et al. 2007, Sundararajan et al. 2010). While it was believed for a long time that tannin-protein interactions are a largely unspecific process, our observations are in line with some selectivity of the tannins. It was previously shown that binding affinity correlates with protein size, structure and amino acid composition, and is pH-dependent (Hagerman & Butler 1981). Especially, the specificity of the binding of a series of tannins and pseudotannins was demonstrated, as epigallocatechin was shown to bind to the 5HT1-receptor while it had no affinity for the 5HT2 or adenosine 1 receptor (Zhu et al. 1997). Therefore, we suggest a differential anti-IAV effect depending on the content or composition of (viral or cellular) surface proteins.

EPs® 7630 had no direct virucidal effect on the virus but inhibited hemagglutination and neuraminidase activity. This is in line with a reversible effect of EPs® 7630 activity on hemagglutination and neuraminidase inhibition, suggesting that EPs® 7630 inhibits host cell infection by interfering with the action of these two surface glycoproteins. The concentrations at which EPs® 7630 interfered with receptor binding and neuraminidase activity of H1N1 A/Puerto Rico/8/34 (complete inhibition at 100 and 500 µg/ml, respectively) were 2- to 10-fold higher than those required for complete growth inhibition. This shows that, beyond its effect on viral hemagglutination and neuraminidase activity, the effect of EPs® 7630 on the host cell plays an important role, as demonstrated in the cell preincubation experiments. In addition to an effect on the host cell surface proteins, EPs® 7630 has been reported to activate the innate immune response, inducing macrophages and other cells to release interferons (Kolodziej et al. 2003, Kolodziej & Kiderlen 2007) and intracellular nitric oxide (Thäle et al. 2008), which impairs influenza virus proliferation (Rimmelzwaan et al. 1999). EPs® 7630 did not increase the induction of interferon-β in IAV infected A549 cells by ELISA (data not

shown). This may be due to the interferon inhibiting properties of the IAV NS1 protein (Hale et al. 2008). It also does not exclude an effect of EPs® 7630 on other cytokines or components of the immune system.

This study showed that virus released from host cells after one life cycle is also efficiently prevented from entering new host cells to initiate its next life cycle. This suggests that in addition to a preventive effect, EPs® 7630 may have a therapeutic effect, limiting the spread of infection. Also, it was demonstrated that over 4 passages in presence of EPs® 7630 no resistant virus mutants emerged, while resistance can develop already after 2-4 passages against oseltamivir or amantadine (Ludwig et al. 2004, Ehrhardt et al. 2007, Pleschka et al. 2009). As the extract inhibits IAV at an early stage of its life cycle and acts on both the virus and host cell, the development of resistances may be less likely, as has been shown also for other polyphenol-rich plant extracts (Ehrhardt et al. 2007, Pleschka et al. 2009).

EPs® 7630 consists of about 40% condensed tannins, more precisely of oligo- and polymeric prodelphinidins, which are composed of gallicocatechin and epigallocatechin (Schoetz et al. 2008). When EPs® 7630 was depleted of tannins by precipitating them with hide powder, the antiviral effect was abolished (Fig. 24), showing that tannins represent the active antiviral principle. This study showed the anti-IAV activity of selected tannins and pseudotannins, such as gallicocatechin and epigallocatechin in their monomeric, dimeric or oligo-/polymeric form.

Lately, it has been shown that condensed tannins and pseudotannins from EPs® 7630 inhibit adhesion of group A streptococci to human epithelial cells (Janecki & Kolodziej 2010). For this activity, a minimal structure of a trihydroxylated B-ring was required (see Fig. 25 for chemical nomenclature), as is present in epigallocatechin and gallicocatechin. The antiviral activity of tannins from *Rumex acetosa* L. against herpes simplex has also been shown (Gescher, Hensel, et al. 2011), as condensed tannins galloylated in position 3 blocked viral attachment to the host cell. Epigallocatechin gallate, which is galloylated in position 3, is effective against a broad range of viruses (reviewed by Steinmann (Steinmann et al. 2013)). Against IAV, compounds carrying only trihydroxylation at the B-ring, but no galloylation in position 3, showed a weaker antiviral effect against IAV than their galloylated homologs (Song et al. 2005). Nevertheless, since we demonstrated an antiviral effect of ungalloylated monomers and dimers, our study shows that galloylation in position 3 is not required for anti-

IAV efficacy, although it is likely to potentiate the antiviral effect. Also, our results showed that on a molar and on a weight basis, monomers are less active than dimers and oligo-/polymers, which is in line to previous data on herpes simplex virus (Takechi et al. 1985).

EPs® 7630 has shown good antiviral efficacy *in vivo* when administered as an aerosol of particle size 2.2 µm by inhalation. Under these conditions, the predicted deposition will be about 5% in the tracheobronchial system and 8-15% in the lungs (Raabe et al. 1988, Oldham & Robinson 2007), but it is difficult to provide an estimate of the EPs® 7630 dose delivered. Mice treated by oral administration of 5 mg/kg three times a day had no advantage when compared to mock treated controls. After oral uptake, polyphenols are cleaved into their mono- or dimeric moieties (Spencer et al. 2000), before being absorbed through the gut (Deprez et al. 2001). As monomers and dimers retain antiviral activity (although less pronounced than oligo-/polymers), an antiviral effect after oral application would be possible, but could not be demonstrated in mice at the calculated human equivalent dose of EPs® 7630. Uptake of at least low molecular weight catechins over the mucosa of the oral cavity (Yang et al. 1999) is possible when EPs® 7630 is taken orally, but not when the drug is delivered by gavage as in the present experiments. Application by inhalation delivers the complete spectrum of EPs® 7630 polyphenols directly to the site of the respiratory infection and may therefore be more effective than peroral application. Thus, testing of EPs® 7630 in humans by inhalation would be of interest.

Part 3:

5.3 Tannins from *Hamamelis virginiana* bark extract: Characterization and improvement of the antiviral efficacy against influenza A virus

This study has been published as: Linda L. Theisen, Clemens A. J. Erdelmeier, Gilles A. Spoden, Fatima Boukhallouk, Aurélie Sausy, Luise Florin, Claude P. Muller (2014), Tannins from *Hamamelis virginiana* bark extract: Characterization and improvement of the antiviral efficacy against influenza A virus and human papillomavirus, PLOS ONE 9: e88062, and was adapted therefrom.

L. Theisen contributed the major part to conception and design of the study, experimental work, data analysis and interpretation and wrote the manuscript. The plant extracts and fractions used in this study were produced and provided by Dr. Willmar Schwabe GmbH & Co. KG, Karlsruhe.

Antiviral activity has been demonstrated for selected tannins. However, different classes and molecular weights of tannins are often found together in plant extracts, and may differ in their antiviral activities. Nevertheless, there are only few systematic comparisons of their anti-IAV structure-activity relations. For condensed tannins, we have previously shown that the anti-IAV effect increases with their polymeric chain length (Part 2 of this study and (Theisen & Muller 2012)), and the importance of the 3-galloyl group was shown for monomeric catechins (Song et al. 2005). A better understanding of the antiviral activity of different tannin categories and structures against IAV is warranted to optimize plant-based antivirals in view of higher selectivity indices.

To investigate differential antiviral activities of tannins, *Hamamelis virginiana* L. (Hamamelidaceae) extracts were chosen as model extracts. This shrub-like deciduous tree originates from the Eastern part of North America. Pharmaceutical extracts or distillates are primarily obtained from the bark or leaves. Due to their antiphlogistic and astringent properties, these extracts are widely used in skin care, to treat small wounds, local inflammations (Laux & Oschmann 1993, Deters et al. 2001, Wolff & Kieser 2007), or hemorrhoids (MacKay 2001). In addition, antimutagenic as well as antioxidant properties have been described (Dauer et al. 1998, Pereira da Silva et al. 2000, Touriño et al. 2008).

Hamamelis bark extract is an ideal candidate to investigate differential antiviral activities because it is rich in tannins, which account for as much as 8-12% of the bark weight (European Medicines Agency 2009), and its tannins and pseudotannins are diverse and well characterized (see Figure 12 in the Introduction for an overview of Hamamelis tannins and pseudotannins). Ethanolic bark extract contains about 31% of condensed tannins (Erdelmeier et al. 1996), which are mainly composed of (epi)catechin and (epi)gallocatechin moieties, linked preferably by 4→8 interflavan bonds (Dauer et al. 2003). Up to 29-mers have been detected in the extract and while the terminal catechin units are not galloylated, chain extender units are completely galloylated at position 3 (Dauer et al. 2003). In addition to condensed tannins, Hamamelis bark contains various hydrolysable tannins and pseudotannins. Besides the major compound hamamelitannin, gallic acid as well as carbohydrates with up to 10 galloyl moieties, such as pentagalloylglucose (5 galloylations) or tannic acid (≤ 10 galloylations), have been identified (Vennat et al. 1988, Wang et al. 2003, González et al. 2010, Sánchez-Tena et al. 2012).

Antiviral activity of Hamamelis extracts has so far been demonstrated only against herpes simplex virus (Erdelmeier et al. 1996). This is the first report on the efficacy of Hamamelis extracts against IAV. We compared the antiviral effect against IAV of bark and leaf extracts, fractions enriched in tannins of different molecular weights and individual tannins of defined structures, including pseudotannins. The anti-IAV structure-activity relations, cytotoxic effects and antiviral mechanisms of (pseudo)tannins were investigated, highlighting differences between tannins from different classes and molecular weights. A highly potent fraction inhibiting early virus life cycle steps was identified and characterized. This fraction was obtained by enrichment of high molecular weight condensed tannins using ultrafiltration, a simple, reproducible and easily upscalable method.

5.3.1 Results

5.3.1.1 Antiviral activity of Hamamelis bark and leaf extract

Hamamelis bark and leaf full extracts were tested for their antiviral activity against IAV using a GFP reporter virus and their cytotoxic effect by XTT assay on A549 cells. Both had approximately the same antiviral efficacy against the H1N1 strain A/Puerto Rico/8/34-NS116-GFP (EC50=5.2 or 3.9 $\mu\text{g/ml}$ respectively), but the bark extract showed a lower cytotoxicity. Therefore, the bark extract had a SI of 94.7 compared to 57.1 for the leaf extract (Fig. 28AB, Table 3) and was chosen for further investigation.

Table 3: Cytotoxic and anti-IAV activities of Hamamelis extracts

	CC50, $\mu\text{g/ml}$	EC50, $\mu\text{g/ml}$	SI (CC50/EC50)
Bark extract	495.1	5.2	94.7
Leaf extract	223.6	3.9	57.1

CC50, Half maximal cytotoxic concentration; EC50, half maximal antiviral concentration, SI, selectivity index.

The bark extract showed a dose-dependent reduction in titers on all IAV strains tested. Viral growth was completely abolished at 24h post infection at $\geq 50 \mu\text{g/ml}$ for the H1N1 laboratory strain A/Puerto Rico/8/34 (Fig. 28C), the currently circulating pandemic H1N1 (Fig. 28D) and seasonal H3N2 strains (Fig. 28E) and was reduced > 400 -fold for the recently emerged avian H7N9 IAV (Fig. 28F). The antiviral effect persisted at 48 and 72h post infection (Fig. 28C). At the same concentrations, the bark extract had no substantial effect on measles (Schwarz strain, Fig. 28G) or type 5 adenovirus (ATCC reference strain, Fig. 28H).

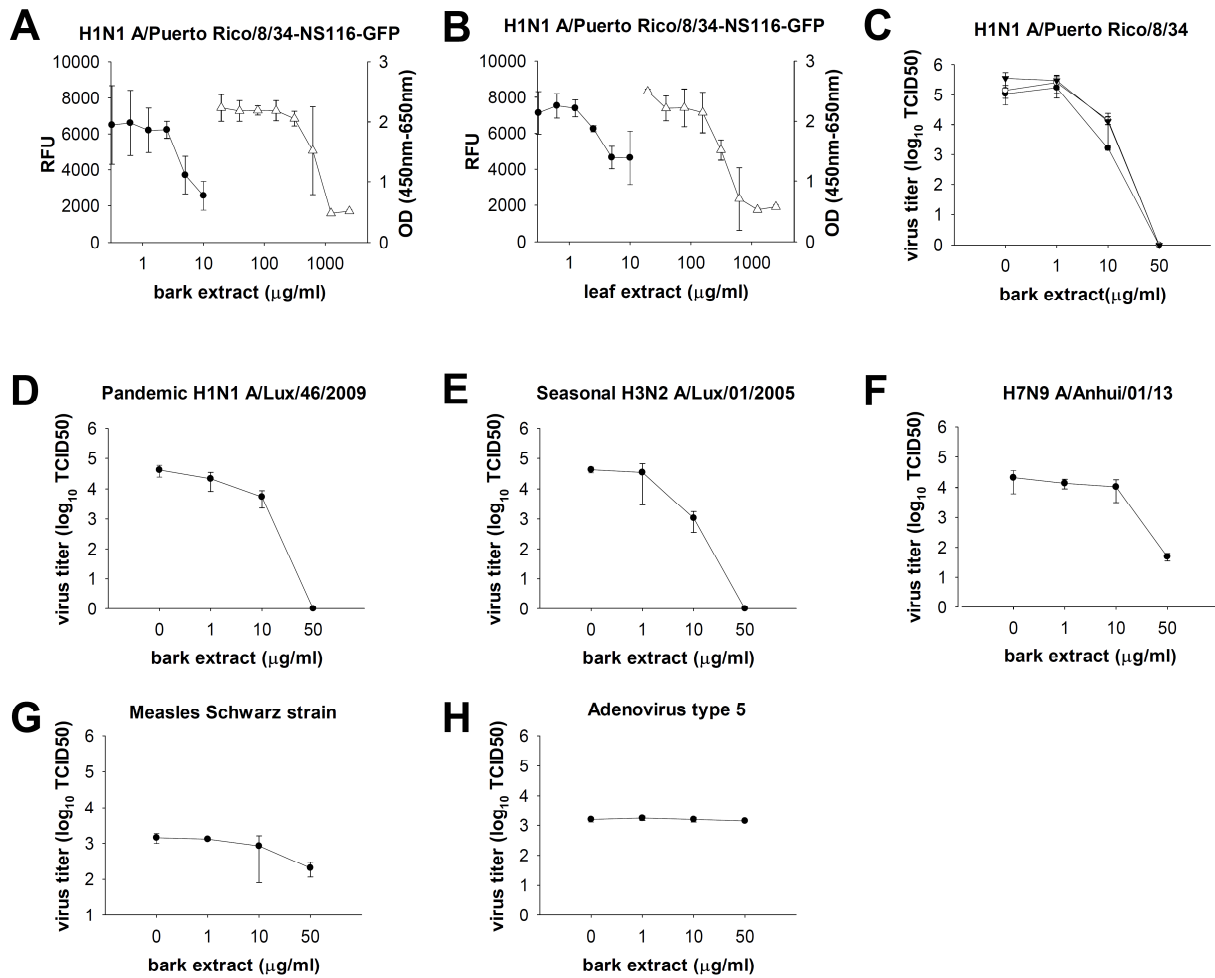


Figure 28: Antiviral activity of Hamamelis bark extract. (A-B) Selectivity index determination. Fluorescence of an H1N1 reporter virus A/Puerto Rico/8/34-NS116-GFP (MOI 0.4 on A549 cells) after 24h of treatment with Hamamelis bark (A) or leaf (B) extract, expressed in relative fluorescent units (RFU, ●). Cytotoxicity of bark (A) or leaf (B) extract on A549 cells after 24h as determined by XTT assay (Δ). Background absorbance at 650 nm has been subtracted from XTT absorbance at 450 nm. A representative of at least two independent experiments is shown. (C-H) Antiviral activity of the bark extract against wild type strains. A549 cells (or A549Slam for measles) were infected with an MOI of 0.1 for H1N1 A/Puerto Rico/8/34 (C), pandemic H1N1 A/Lux/46/2009 (D), seasonal H3N2 A/Lux/01/2005 (E), H7N9 A/Anhui/01/2013 (F), a MOI of 0.01 for measles Schwarz strain/Rimevax (G) or a MOI of 0.05 for adenovirus type 5 ATCC reference strain (H) in presence of Hamamelis bark extract serial dilutions. TCID₅₀ was determined after 24h (C-F, H, ●), 48h (C, ○; G), or 72h (C, ▼).

5.3.1.2 Antiviral structure-activity relations of hydrolysable tannins and pseudotannins

Tannins are major constituents of Hamamelis bark and the antiviral potential of tannin-rich extracts or single tannins has been described (Mantani et al. 1999, Liu et al. 2011, Lin et al. 2013, Ueda et al. 2013). However, a direct systematic comparison of the anti-IAV effects of hydrolysable tannins and pseudotannins is of interest. After 24h of incubation with H1N1 A/Puerto Rico/8/34-NS116-GFP, the EC50s of gallic acid, pentagalloylglucose (5 galloylations) and tannic acid (≤ 10 galloylations, see Fig. 12 for structures) were determined as 50.8 μM , 19.5 μM and 4.3 μM respectively. Thus, the anti-IAV effect increased with the number of galloylations for these compounds on a molar basis (Table 4). Hamamelitannin did not show any anti-IAV activity up to 10 mM (Table 4). With CC50s of 770.5 μM for gallic acid, 779.4 μM for pentagalloylglucose and 132 μM for tannic acid, SIs of 15.2, 40.0 and 30.7 were determined (Table 4). EGCG, a monomeric condensed tannin carrying one galloylation was chosen for comparison to hydrolysable tannins and showed a higher SI (85.0) than any other single (pseudo)tannin (Table 4). Comparison to a polymeric condensed tannin was not possible due to the unavailability of an isolated, well defined high molecular weight compound. Interestingly, the bark extract showed a higher SI (94.7, Table 3) than any of the single compounds (Table 4).

Table 4: Cytotoxic and anti-IAV activities of hydrolysable tannins and pseudotannins

	CC50		EC50		SI	Gall.	Mmol g/mol
	μM	$\mu\text{g/ml}$	μM	$\mu\text{g/ml}$			
Hamamelitannin			>10mM				
Gallic acid	770.5	144.9	50.8	9.6	15.2	1	188.1
Pentagalloylglucose	779.4	733.1	19.5	18.3	40.0	5	940.7
Tannic acid	132.0	224.4	4.3	7.3	30.7	≤ 10	1701.2
EGCG	1029.1	471.8	12.1	5.6	85.0	1	458.4

CC50, half maximal cytotoxic concentration; EC50, half maximal antiviral concentration, SI, selectivity index; Gall., number of galloylations; Mmol, molecular weight. Molar mass of tannic acid calculated as carrying 10 galloylations.

5.3.1.3 Antiviral activity of Hamamelis bark extract enriched in high molecular weight tannins by ultrafiltration

In order to remove the antivirally inactive hamamelitannin (Table 4, (Erdelmeier et al. 1996)) and because it has been shown that the effect of condensed tannins increases with molecular weight (Part 2 of this study), the bark extract was fractionated by ultrafiltration (UF) through a 3 kDa membrane. In a previous publication (Erdelmeier et al. 1996), the acid butanol method (Bate-Smith 1975) was used for condensed tannin quantification in similar UF-fractions. Using the same method, Dr Willmar Schwabe GmbH & Co KG determined the overall condensed tannin content as 33.2% (bark extract), 66.2% (UF-concentrate) and 17.1% (UF-filtrate). The comparison with the previously published contents (30.9%, 62.3%, 14.6%, respectively, (Erdelmeier et al. 1996) shows good reproducibility of the extraction and fractionation procedure. The UF-filtrate (< 3 kDa) was shown to be enriched in low molecular weight tannins (monomers, dimers, trimers) and the UF-concentrate (\geq 3 kDa) in tetrameric and longer condensed tannins (Erdelmeier et al. 1996). Importantly, UF-concentration nearly doubled the condensed tannin content and increased the SI from 94.7 for the bark extract to 325.5 for the UF-concentrate (Table 5), which corresponded to the highest SI of all compounds tested. In contrast, the SI of the UF-filtrate (fraction < 3kDa) decreased by more than three-fold to 26.7 (Table 5).

Table 5: Cytotoxic and anti-IAV activities of Hamamelis extracts and UF-fractions

	CC50, $\mu\text{g/ml}$	EC50, $\mu\text{g/ml}$	SI (CC50/EC50)	Enriched in
Bark extract	495.1	5.2	94.7	/
UF-concentrate	349.3	1.1	325.5	\geq tetrameric CT
UF-filtrate	968.9	36.2	26.7	HT, < tetrameric CT

CC50, half maximal cytotoxic concentration; EC50, half maximal antiviral concentration; SI, selectivity index; CT, condensed tannins, HT, hydrolysable tannins.

The high anti-IAV activity of the UF-concentrate was confirmed on wild type IAV strains: after 24h of treatment, 10 $\mu\text{g/ml}$ of UF-concentrate reduced viral titers of pandemic H1N1 as well as of H1N1 A/Puerto Rico/8/34 strains by > 3 or > 5 logs, respectively, on A549 cells (Fig. 29AB, closed circles), while 50 $\mu\text{g/ml}$ of bark extract were needed to achieve comparable titer reductions (Fig. 28CD). While in parallel to a 4.7-fold increase in anti-IAV

efficacy, also a 1.4-fold increase in cytotoxicity was observed on A549 cells for the UF-concentrate as compared to the bark full extract (Table 5, Fig. 28A, Fig. 29A, open triangles), there was no cytotoxicity detectable by XTT assay at antiviral concentrations (Fig. 29A, open triangles). Thus, for Hamamelis bark extract, concentration of high molecular weight tannins by ultrafiltration is a convenient and reproducible method to increase the antiviral SI.

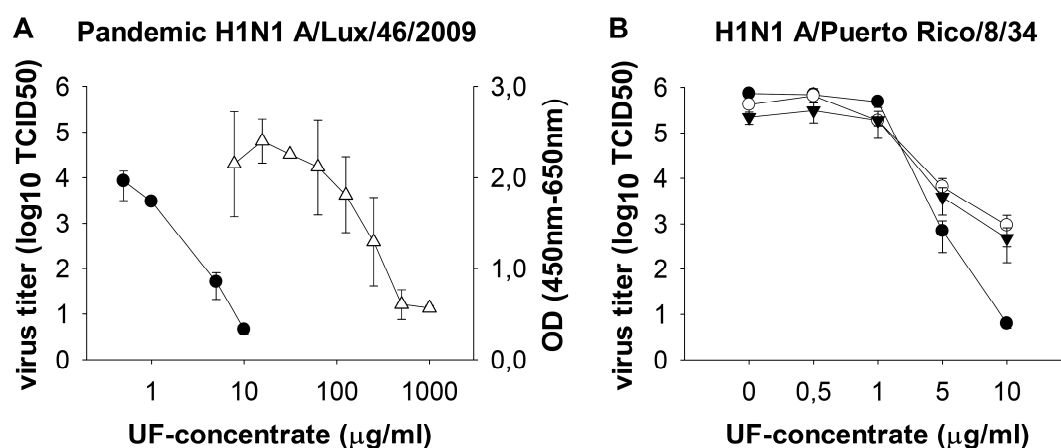


Figure 29: Anti-IAV activity of UF-concentrate. A549 cells were infected in triplicates at a MOI of 0.1 with pandemic H1N1 A/Lux/46/2009 (**A**) or H1N1 A/Puerto Rico/8/34 (**B**) and serial dilutions of UF-concentrate were added at the same time. TCID₅₀ was determined at 24h (**A**, **B**, ●), 48h (**B**, ○) or 72h (**B**, ▼) post infection. (**A**) Cytotoxicity of UF-concentrate on A549 (Δ) was determined after 24h by XTT assay. Background absorbance at 650 nm has been subtracted from XTT absorbance at 450 nm. OD, optical density.

5.3.1.4 Determination of the active antiviral principle in Hamamelis extracts

The results from Part 2 of this study and the comparison of the Hamamelis extracts and UF-fractions have shown that the anti-IAV effect increases in parallel to the molecular weight of their condensed tannins. Similarly, the binding efficiency of tannins to proteins increases with their molecular size (Haslam 1996). To see if (i) tannins are the antiviral principle of the Hamamelis extracts and (ii) tanning (protein precipitating) activity is needed for antiviral efficacy, we removed tannins from the bark extract using hide powder (European Directorate for the Quality of Medicines & Healthcare 2008). By incubation of a drug solution with hide powder, compounds with tanning activity bind to the collagen in the hide powder, precipitate, and can be removed by filtration. In general, tannins with molecular weight from 500-3000 g/mol precipitate proteins (Wagner 1999). Therefore, monomeric catechins or gallic acid (< 500 g/mol) can normally not or only incompletely be removed from plant extracts by hide powder. Phenols, the main constituting moieties of both hydrolysable and condensed tannins,

were quantified before and after hide powder treatment by Folin-Ciocalteu's phenol reagent (Ainsworth & Gillespie 2007, European Directorate for the Quality of Medicines & Healthcare 2008). Tannins were efficiently removed (remaining phenol content < 1% or < 10% of untreated) from the long molecular weight tannin containing UF-concentrate and tannic acid, but not from gallic acid or the UF-filtrate rich in low molecular weight constituents (89% or 60% remained, Fig. 30A). Phenols in bark extract, containing both high and low molecular weight tannins, and EGCG showed intermediate reduction (Fig. 30A). In the anti-IAV assay, ≥ 10 $\mu\text{g/ml}$ of the bark extract completely abolished growth of pandemic H1N1 (MOI 0.05) after 24h of incubation, but even 50 $\mu\text{g/ml}$ of tannin-depleted extract did not have a similar effect (Fig. 30B). Also for the UF-fractions and the single compounds, the antiviral effect was abolished after successful tannin removal, but not if large amounts of low molecular weight polyphenols remained in solution (gallic acid, EGCG, Fig. 30C). Thus, tannins do mediate the antiviral effect, while the tanning activity *per se* is not absolutely required, as can be seen by the remaining antiviral effect of tannin-free gallic acid and EGCG.

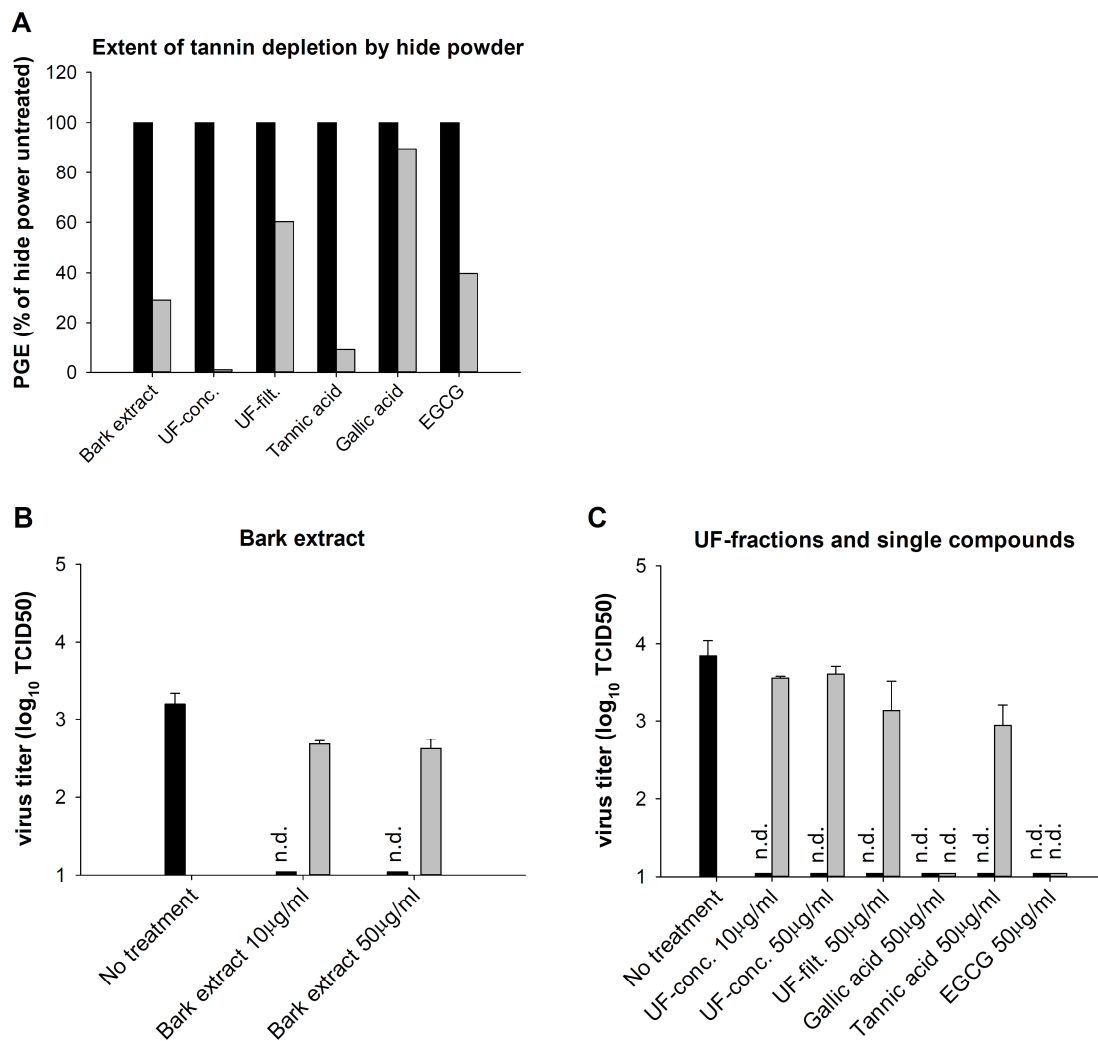


Figure 30: Anti-IAV activity of Hamamelis tannins. (A) Extent of tannin depletion by precipitation with hide powder. Tannins were depleted from drug solutions by stirring with hide powder for 1h at room temperature followed by filtration. Phenolics, the main constituting moieties of tannins, were photometrically quantified before (black bars) and after (grey bars) hide powder treatment by Folin-Ciocalteu's phenol reagent. Pyrogallol equivalents (PGE) of hide powder treated samples were determined using a standard curve and normalized to PGE of untreated samples, set to 100%. (B-C) Antiviral effect of tannins. A549 cells were infected in triplicates with pandemic H1N1 A/Lux/46/2009 (MOI 0.05) and were left untreated or treated for 24h with bark extract (B), UF-fractions or isolated (pseudo)tannins (C) which had been (grey bars) or had not been (black bars) treated with hide powder. Titers were determined at 24h post infection by TCID₅₀. n.d., not detectable or TCID₅₀ < 1.

5.3.1.5 Determination of the affected step of the viral life cycle

To determine the step of the IAV life cycle affected by the bark extract and the UF-concentrate, A549 cells were infected with an MOI of 0.1 of pandemic H1N1, accompanied by treatment with 50 $\mu\text{g/ml}$ of bark extract or 10 $\mu\text{g/ml}$ of UF-concentrate 2h before infection, at the time of infection or 2, 4 and 6h after infection. The medium was replaced with drug-free medium 8h post infection, which approximately corresponds to one IAV life cycle, to allow proliferation of intracellular virus to sufficient titers for another 24h before titration. When drug treatment was started before or at the time of infection, no virus was detectable, while treatment starting at 2h, 4h or 6h post infection induced slightly reduced but detectable virus titers as compared to the untreated control (Fig. 31AB). Therefore, an early step in the viral life cycle such as viral attachment or entry is inhibited. Treatment up to 6h post infection also induced a decreased titer, suggesting that intermediary or late steps might be inhibited to a minor extent.

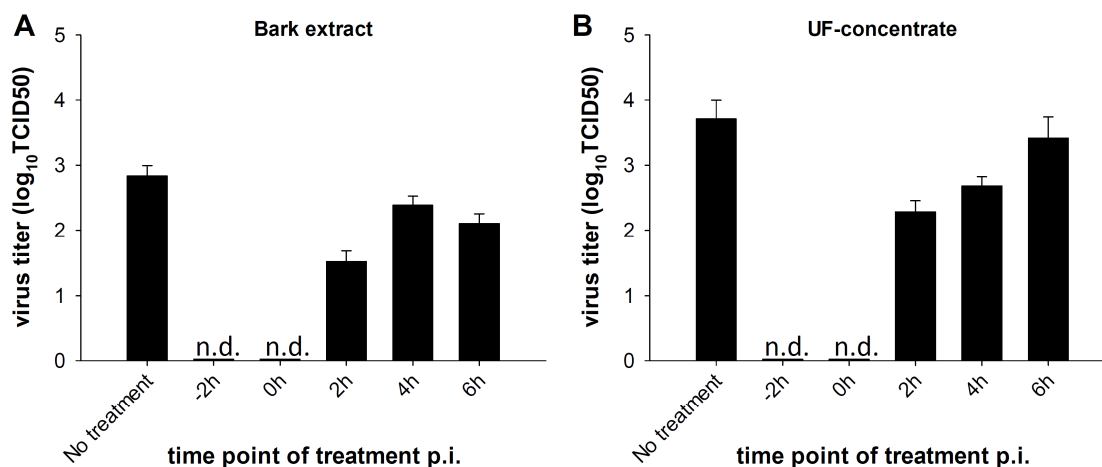


Figure 31: Effect of bark extract and UF-concentrate on different IAV life cycle steps. A549 cells were infected with pandemic H1N1 (MOI 0.1), and treated with 50 $\mu\text{g/ml}$ of bark extract (A) or 10 $\mu\text{g/ml}$ of UF-concentrate (B) starting 2h before infection or 0, 2, 4 or 6 h after infection. TCID₅₀s were determined 24h post infection (p.i.).

5.3.1.6 Effect of tannins and pseudotannins on viral surface protein interactions

Since at least an early and a later step of the IAV life cycle seem to be inhibited and tannins are known to interact with proteins, we investigated the effect of the extracts and single compounds on the activity of the IAV surface proteins hemagglutinin and neuraminidase, involved in viral attachment and entry (Hamilton et al. 2012) or cleavage of nascent virions from the host cell (Seto & Rott 1966). In a hemagglutination inhibition assay, the UF-concentrate and the bark extract were the most active, while gallic acid, EGCG and hamamelitannin did not inhibit hemagglutination at concentrations up to > 400 µg/ml (Table 6). Of note, the drugs also induced hemagglutination of virus-free erythrocytes at concentrations of at least > 3.5-fold above HIC50 (data not shown), suggesting that they also interfere with cell surface proteins. After hide powder treatment of the active compounds, the hemagglutination inhibition disappeared at the tested concentrations, showing involvement of protein precipitating tannins in receptor binding inhibition. Interestingly, all tested extracts and compounds inhibited neuraminidase activity (Table 6), even in absence of tanning activity (gallic acid) or antiviral effect (hamamelitannin).

Table 6: Hemagglutination and neuraminidase inhibition of Hamamelis extracts, UF-fractions and individual compounds

	HIC50 (µg/ml)	NIC50 (µg/ml)	NIC50/HIC50
Bark extract	4.4	136.5	31.0
UF-concentrate	2.2	138.9	63.1
UF-filtrate	89.1	202.2	2.3
Tannic acid	14	125.3	9.0
Gallic acid	>400	106.6	<1
EGCG	>400	97.1	<1
Hamamelitannin	>400	147.8	<1

HIC50, half maximal hemagglutination inhibiting concentration; NIC50, half maximal neuraminidase inhibiting concentration.

5.3.1.7 Effect of preincubation of virus or cells with Hamamelis extracts or single compounds

After 2h of preincubation at room temperature of pandemic H1N1 with Hamamelis bark extract, the UF-fractions or single compounds, A549 cells were infected with an MOI of 0.1 (1/100 dilution resulting in negligible drug concentrations). Virus preincubation with 50 $\mu\text{g/ml}$ of UF-concentrate or EGCG resulted in a roughly 20- or 7-fold lower viral titer, indicating an irreversible effect on IAV virus particles. The other extracts or single compounds did not notably influence IAV growth (Fig. 32AB).

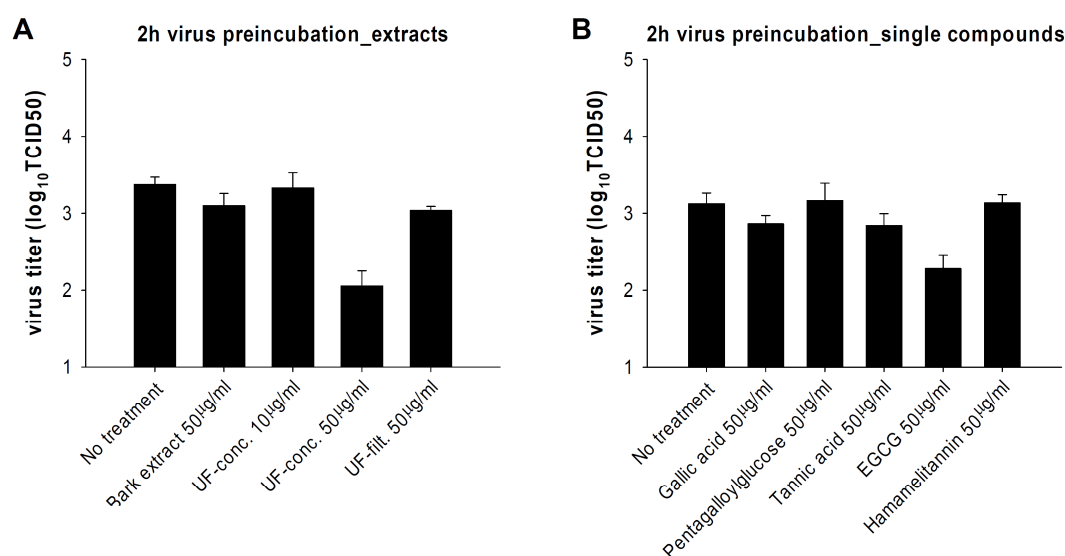


Figure 32: IAV preincubation with Hamamelis extracts or individual compounds. Preincubation of pandemic H1N1 A/Lux/46/2009 for 2h with virus growth medium (“no treatment”) or bark extract / UF-fractions (A) or individual compounds (B) before infection of A549 cells (MOI 0.1) and titration 24 h post infection.

Titers were significantly decreased (36- or 20-fold, respectively) when A549 cells were preincubated for 2h with 50 $\mu\text{g/ml}$ of bark extract or UF-concentrate, washed three times with PBS and infected with an MOI of 0.1 of pandemic H1N1 for 24h (Fig. 33AB), indicating an irreversible effect of these compounds on the host cells.

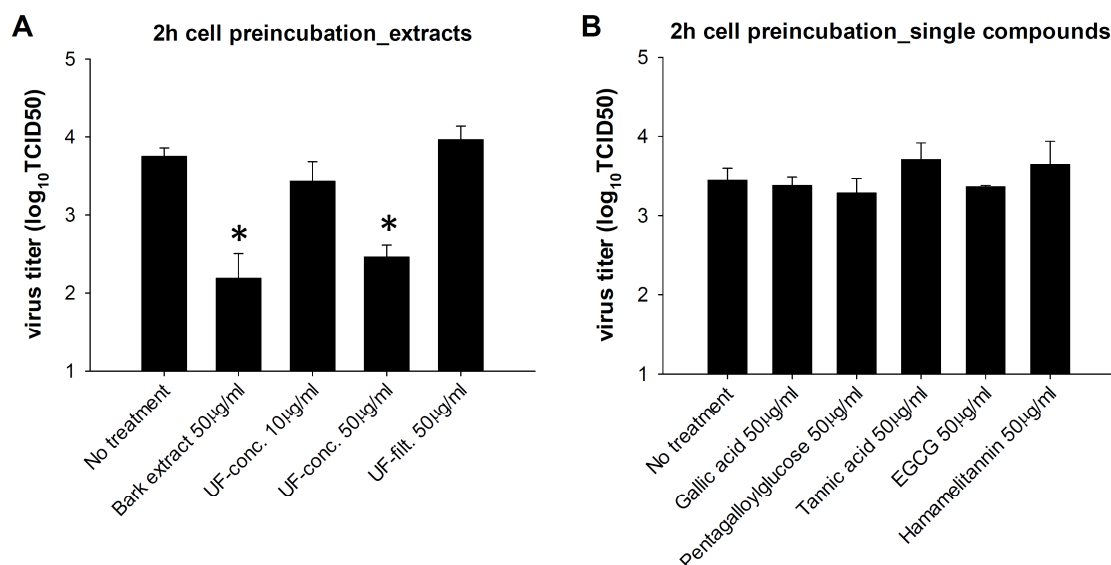


Figure 33: Cell preincubation with Hamamelis extracts or individual compounds. Preincubation of A549 cells for 2h with virus growth medium (“no treatment”) or bark extract / UF-fractions (A) or single compounds (B) before three washes with PBS, infection with pandemic H1N1 (MOI 0.1) and titration 24h p.i.. *, significant difference ($p < 0.05$) as compared to “no treatment”.

5.3.1.8 Determination of cytotoxicity or unspecific host cell receptor inhibition

Antiviral drugs can mediate adverse effects by induction of cytotoxicity at antivirally active concentrations. In order to investigate this possibility, we determined CC50s using serial drug dilutions as described above (Fig. 28AB, Fig. 29A, Tables 3-5) and compared cell metabolic capacity of all extracts and compounds used in the study at 50 µg/ml or 10 µg/ml (UF-concentrate) by XTT assay. No important downregulation was found after 24h of incubation, except for 2.5 µM staurosporine, a known apoptosis inducer used as a positive control (Fig. 34A). Apoptosis induction was monitored by luminescence quantification of a caspase 3/7 cleavage product. No significant caspase 3/7 upregulation was detected up to 50 µg/ml or 10 µg/ml (UF-concentrate) after 24h of treatment, except for the positive control (Fig. 34B). In addition, A549 cells were infected by adenovirus type 5 (MOI 0.05) and incubated for 24h in presence of different bark extract or UF-concentrate dilutions. The extracts did not affect adenoviral growth (Fig. 28H, Fig. 34C), showing that the cellular machinery (at least the part needed for adenoviral replication) was still functional. Thus, the extracts did not seem to exert cytotoxic or unspecific effects on the cell that would inhibit viral growth in general.

Since bark extract and UF-concentrate were shown to inhibit hemagglutinin interaction with its cellular receptor, we tested whether host cell surface proteins such as TNF- α were blocked

unspecifically (Ehrhardt et al. 2007). When TNF- α binds to its receptor, it induces the NF κ B cascade and degradation of the NF κ B inhibitor I κ B- α . Treatment with bark extract or UF-concentrate starting 30 minutes before or at the time of A549 cell treatment with 30 ng/ml TNF- α did not influence I κ B- α degradation (Fig. 34D). Thus, the bark extract and UF-concentrate do not inhibit activation of the TNF- α receptor as a model of an unrelated cellular receptor.

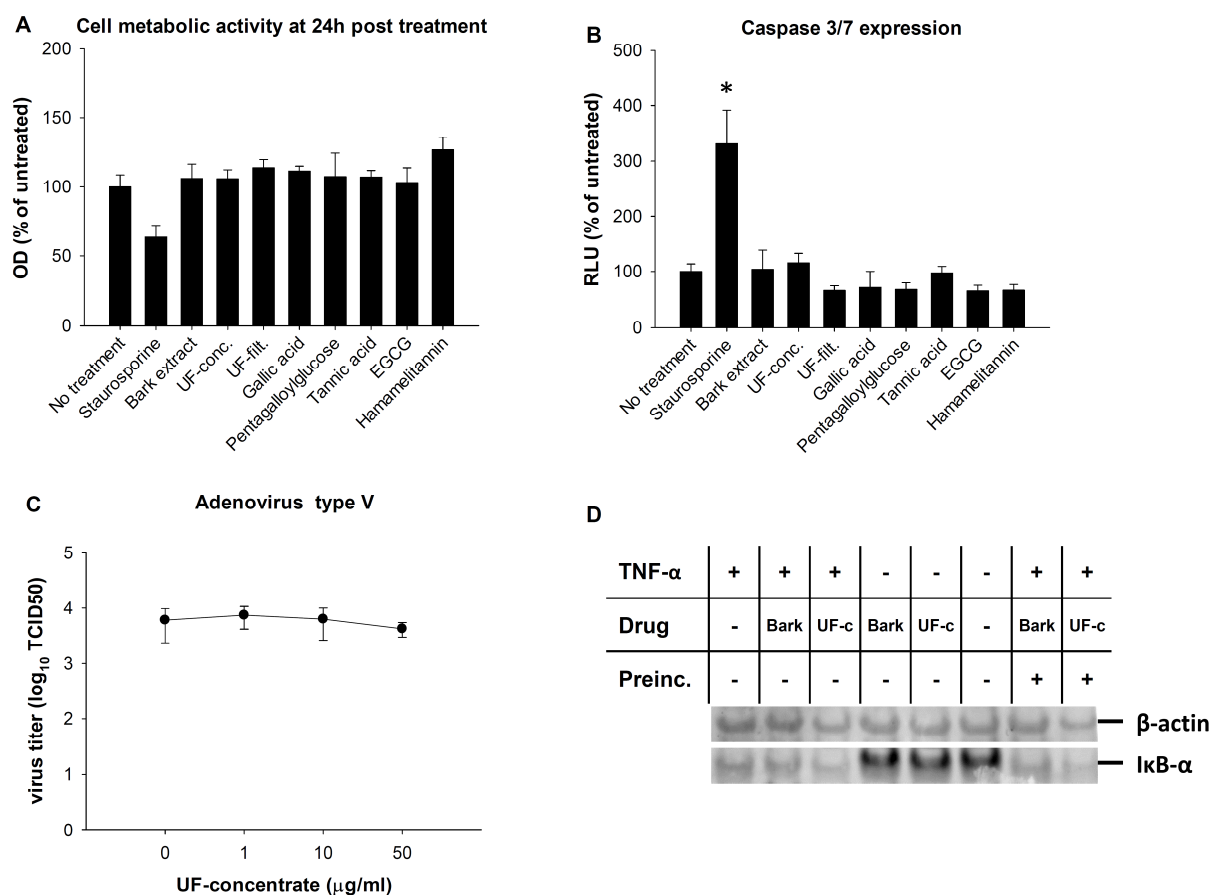


Figure 34: Cytotoxicity or unspecific host cell receptor inhibition of Hamamelis extracts or individual compounds. (A) Cell metabolic activity after 24h of incubation of A549 cells with DMSO (no treatment), 2.5 μ M of staurosporine, 10 μ g/ml of UF-concentrate or 50 μ g/ml of the remaining drugs was determined in triplicates using XTT assay. Optical density (OD) was determined at 450 nm after background (650 nm) subtraction and expressed as % of the untreated samples. (B) Caspase 3/7 activity after 24h of A549 cell incubation with DMSO (no treatment), 2.5 μ M of staurosporine, 10 μ g/ml of UF-concentrate or 50 μ g/ml of the remaining drugs was assayed in at least triplicates using detection of a luminogenic caspase 3/7 cleavage product. (C) A549 cells were infected in triplicates with adenovirus type 5 (MOI of 0.05) and simultaneously treated with UF-concentrate. TCID₅₀ was determined at 24h post infection. (D) Interference of the drugs with cellular TNF- α signaling. A549 cells were preincubated for 30 or 0 minutes (“Preinc.” + or -, respectively) with 50 μ g/ml of bark extract (“Bark”) or UF-concentrate (“UF-c”). Then, 0 or 30 ng/ml TNF- α were and 15 minutes

later, total proteins were extracted. I κ B- α and the loading control β -actin were detected on a Western blot using specific primary and Cy-5 and Cy-3 labeled secondary antibodies. * significantly elevated caspase expression ($p < 0.05$) as compared to “No treatment”.

5.3.2 Discussion

The study demonstrates the antiviral activity of Hamamelis bark extract against different IAV subtypes, systematically compares the activity of different tannin classes and structures and is the first report showing that a tannin-rich extract inhibits H7N9 subtype infection. Importantly, the antiviral efficacy was considerably increased in the UF-concentrate, an extract where high molecular weight condensed tannins were enriched by ultrafiltration. Interestingly, the results showed an increased benefit of the bark extract and especially the UF-concentrate, (SI of 94.7 and 325.5, respectively) compared to any of the individual hydrolysable (pseudo)tannins (SIs ranging from 15.2-40) or monomeric EGCG (SI 85). Since plant extracts normally contain different types of tannins, these observations are important for the development and improvement of plant-based antivirals.

The increased SI of the UF-concentrate above those of isolated compounds suggests a pronounced effect of the high molecular weight condensed tannins. For the bark extract, a synergistic effect of the different tannins in the extract could play a role. A similar effect has been demonstrated against some multiresistant nosocomial bacteria or *Streptococcus mutans* (Sasaki et al. 2004, Betts et al. 2011). Alternatively, the antiviral efficacy of the bark extract could be partially mediated by EGCG. However, it cannot be solely mediated by EGCG, since the bark extract and EGCG have approximately the same EC₅₀, but the bark extract contains only 31% condensed tannins (Erdelmeier et al. 1996). Also, the strong antiviral effect (SI 325.5) of the UF-concentrate is independent of EGCG, as it mainly contains tetrameric and longer condensed tannins. Of note, EGCG showed a roughly 2- to 6-fold higher SI than other single pseudotannins or tannic acid. The UF-concentrate showed by far the highest SI, although the 4.7-fold increase in anti-IAV efficacy was concomitant with a 1.4-fold increase in cytotoxicity, as compared to the bark extract (Table 5). Since UF-concentration of a *Pelargonium sidoides* extract induced essentially no SI increase (84.4 to 86.3, data not shown) due to a concomitant increase of antiviral and cytotoxic effects, the

benefit of fractionation by ultrafiltration (as well as the cut-off size of the ultrafiltration membrane) should be evaluated individually for every plant extract.

When single hydrolysable tannins were tested, their anti-IAV activity (on a molar basis) increased with the number of galloylations and cytotoxicity increased from pentagalloylglucose to highly galloylated tannic acid, resulting in the highest SI (SI = 40) for pentagalloylglucose. This effect of galloylation on antiviral efficacy has also been observed for herpes simplex virus (Takechi et al. 1985, Gescher, Hensel, et al. 2011). However, while tannic acid is nearly 12-fold more active than gallic acid on a molar basis, EC50s of both compounds are similar when expressed in $\mu\text{g/ml}$ (1.3-fold difference, Table 4, in italics). Thus, the total number of galloyl residues determines the antiviral effect of hydrolysable tannins, irrespective of whether they are on the same or on different molecules.

We have shown that tannins are the active antiviral principle of Hamamelis-based extracts, as their depletion by hide powder abolishes antiviral activity (Fig. 30BC). Interestingly, tanning activity in *sensu stricto* (i.e. the ability to precipitate protein) is not essential for the anti-IAV activity as gallic acid does not precipitate hide protein but has antiviral activity (Fig. 30AC). Also, catechin monomers usually have only weak protein precipitating activity (Wagner 1999) but are well known for their antiviral efficacy (Nakayama et al. 1993, Song et al. 2005, Theisen & Muller 2012, Steinmann et al. 2013).

The bark extract and the UF-concentrate were shown to inhibit both an early and, to a lesser extent, a late step of the IAV life cycle (Fig. 31AB), and lost their anti-IAV activity when depleted of tannins (Fig. 30). While an effect of tannin-rich extracts on viral neuraminidase and hemagglutination has been observed before (Ehrhardt et al. 2007, Haidari et al. 2009, Theisen & Muller 2012), the role of different (pseudo)tannins was not clear. Interestingly, the extracts and compounds rich in high molecular weight tannins and with a strong tanning activity upon incubation with hide powder (bark extract, UF-concentrate, tannic acid) inhibited hemagglutination at HIC50s as low as 4.4, 2.2 or 14 $\mu\text{g/ml}$, respectively. Their 9- to 63-fold higher NIC50s (Table 6) together with the strong inhibition of early steps in the IAV life cycle (Fig. 31AB) suggest that their effect on attachment contributes more to the antiviral activity than their effect on neuraminidase. In line with this, a significant correlation between EC50 and HIC50 ($R^2=0.997$), but not NIC50 values, was observed for drugs inhibiting hemagglutination/neuraminidase activity in our assay. We have shown that gallic acid and

EGCG, which do not inhibit hemagglutination, interfere with neuraminidase activity (Table 6). However, this inhibition is unlikely to play a role in the antiviral activity of gallic acid and EGCG, since also the antivirally inactive hamamelitannin inhibits neuraminidase at similar concentrations. Thus, it seems like the high molecular weight tannins tested in this study inhibit viral attachment by their tanning effects, while the antiviral activity of EGCG and gallic acid relies on different mechanisms. Previously proposed antiviral mechanisms for EGCG include inhibition of viral attachment (Steinmann et al. 2013), inhibition of endosomal acidification (Imanishi et al. 2002), membrane damage (Hashimoto et al. 1999) or virus aggregation (Nakayama et al. 1993). The anti-IAV mechanism of gallic acid remains to be determined. For herpes simplex virus, its virucidal activity was shown at concentrations below those that interfered with attachment and penetration (Kratz et al. 2008).

In the preincubation experiments (Fig. 32A, Fig. 33A), an irreversible effect of high molecular weight tannins of the UF-concentrate on the virus particle as well as on the host cell at 50 µg/ml was observed. In contrast, the UF-filtrate (rich in low molecular weight tannins) and single hydrolysable tannins seem to have either no or only a reversible effect in this assay. In line with this observation, the protein binding efficiency of tannins increases with molecular size (Haslam 1996) and the number of galloyl residues (Minoda et al. 2010, Ishii et al. 2011), suggesting a tighter binding of high molecular weight tannins to target proteins. In addition to interfering with surface proteins, a virucidal activity (e.g. by membrane damage) has been proposed for EGCG (Ikigai et al. 1993, Hashimoto et al. 1999) and could explain the 7-fold decrease in titer after virus preincubation with EGCG. Our preincubation experiment did not allow discriminating between a virucidal activity and an irreversible inhibition of viral proteins. Interestingly, cell but not virus preincubation with the bark extract led to reduced viral titers (Fig. 32A, Fig. 33A), which may be due to a higher affinity of bark extract tannins to cellular over viral surface proteins.

Titers $> 10^2$ TCID₅₀ of pandemic H1N1 virus were still detected (Fig. 32A, Fig. 33A) upon preincubation of either the virus or the cell with 50 µg/ml of UF-concentrate, while viral growth was minimal when only 10 µg/ml of UF-concentrate were added at the time of infection (Fig. 29A). This suggests that in addition to irreversible effects, reversible effects play a role, e.g. reversible inhibition of surface proteins or surface-independent effects. For instance, tannins stimulated innate immunity in infected PBMCs in the case of dengue virus (Kimmel et al. 2011).

While inhibiting different IAV strains, the effect of the bark extract and UF-concentrate was nevertheless not unspecific, since for example adenovirus was not inhibited up to $> 50 \mu\text{g/ml}$. Also, the hemagglutination assay showed that the bark extract and UF-concentrate inhibited IAV binding to the host cell receptor (Table 6), but not the TNF- α receptor activity (Fig. 34D), demonstrating some level of specificity.

This study describes for the first time the anti-influenza activity of *Hamamelis virginiana* L. Importantly, we directly compared the anti-IAV effects of full extracts, fractions enriched in tannins of different molecular weights and single defined tannins or pseudotannins. Further insight into the structural basis of the anti-IAV activity of tannins and into the affected steps of the viral life cycle was provided. We also showed interesting structure-related differences in receptor binding inhibition capacities and pointed out the probably low contribution of neuraminidase inhibition to the antiviral activity. Finally, a highly potent fraction against IAV that was enriched in high molecular weight tannins by simple and reproducible ultrafiltration was identified.

6 Conclusions and perspectives

In the present study, different aspects of IAV preparedness were investigated. Due to global travel and trade of animals, new IAV strains can spread extremely fast, as exemplified by pH1N1 in 2009. In the event of an emerging potentially pandemic IAV strain, a fast and accurate assessment of the virus' characteristics is essential to develop prompt and adequate response measures and reduce the impact of the new strain on society. Pandemic preparedness can be greatly facilitated by a thorough knowledge of previously characterized virulence markers or experimental reassortants.

The co-circulation of pH1N1 and other human, avian or swine IAV strains highlights the risk of IAV gene reassortment to form viruses with new, potentially dangerous characteristics. By investigating a panel of gene reassortants carrying NS from human, avian and swine strains in the pH1N1 genetic background, the high propensity of pH1N1 to undergo NS reassortment was demonstrated. These findings highlight the need for continuous surveillance. In cell culture, most reassortants grew similarly to pH1N1 wt or were only minorly attenuated. Thus, also naturally occurring NS reassortment seems to have little probability to increase the fitness of pH1N1. Although it will be impossible to predict the behaviour of a new IAV strain with 100% certitude, effective IAV surveillance in combination with characterization of reassortments or mutations are of great importance for global public health.

Investigation of differential viral fitness can lead to identification of involved relevant amino acids and give important insights into their biological function. In this study, reassortants carrying NS from highly pathogenic H5N1 were severely attenuated both *in vitro* and *in vivo*. NS1 sequence comparison led to the identification of a naturally occurring deletion of NS1 amino acids at position 80-84 that contributed to this attenuation at least *in vitro*.

Mechanistically, a previously unknown role of this five amino acid deletion in regulation of the general host gene expression was identified.

In addition to a reliable risk assessment and prevention of IAV infections, public health is dependent on safe and effective antiviral drugs. Considering the high variability of IAV strains by reassortments and point mutations, development of drug resistance on the long run is very likely. Widespread resistance has already been detected against matrix protein inhibitors, in a way that neuraminidase inhibitors remain the only class of recommended fully licensed IAV antivirals. Therefore, development of new classes of antivirals is urgently needed.

This study contributed to a better understanding of tannins and pseudotannins as antiviral agents. The antiviral activity of tannin-rich plant extracts from *Pelargonium sidoides* and *Hamamelis virginiana* was demonstrated against several IAV strains *in vitro*, most strongly affecting an early step of the viral life cycle. EPs® 7630, which is licensed for acute bronchitis treatment, showed good *in vivo* efficacy and did not induce antiviral resistance at least over four passages. Importantly, the established antiviral structure-activity relations of tannins and pseudotannins from *Pelargonium sidoides* and *Hamamelis virginiana* are of interest for developing and improving plant-based antivirals.

There are several advantages of (pseudo)tannin-rich extracts as antivirals:

- (i) Due to the complexity of tannin-rich extracts, they target different steps of the IAV life cycle at a time which makes them more effective and less likely to induce resistance.
- (ii) Among others, they target viral entry, a target step distinct from those of currently licensed IAV drugs. Therefore, they could possibly be used in combination with matrix or neuraminidase inhibitors to minimize drug doses and adverse effects, or they could be effective against M/NA inhibitor-resistant IAV strains.
- (iii) The presence of (pseudo)tannins in a large variety of plants and their relatively easy extraction makes them an accessible drug.
- (iv) Tannin-rich plant extracts that are already licensed and therefore well characterized concerning their safety profile (e.g. EPs® 7630) could be adapted to be used as antivirals.

However, disadvantages such as the natural variability of the tannin content of the plants as well as the complex characterization of the extracts need to be taken into account when developing (pseudo)tannin-rich extracts as antivirals.

In conclusion, this dissertation contributed to two issues of IAV preparedness, specifically to the characterization of currently circulating and possibly emerging IAV strains and to the development and optimization of plant-based antivirals. Considering the recent creation of ferret-to-ferret transmissible HPAIVs, the emergence of avian H7N9 which has infected more than 130 people in 2013 and not less seasonal IAV epidemics, IAV surveillance and drug development should remain a public health priority.

7 References

1. Adar Y, Singer Y, Levi R, Tzehoval E, Perk S, Banet-Noach C, Nagar S, Arnon R, Ben-Yedidia T (2009) A universal epitope-based influenza vaccine and its efficacy against H5N1. *Vaccine* 27:2099–2107
2. Agbabiaka TB, Guo R, Ernst E (2008) *Pelargonium sidoides* for acute bronchitis: a systematic review and meta-analysis. *Phytomedicine* 15:378–385
3. Ainsworth EA, Gillespie KM (2007) Estimation of total phenolic content and other oxidation substrates in plant tissues using Folin-Ciocalteu reagent. *Nat Protoc* 2:875–7
4. Altstein AD, Gitelman AK, Smirnov YA, Piskareva LM, Zakharova LG, Pashvykina G, Shmarov MM, Zhirnov OP, Varich NP, Ilyinskii PO, Shneider AM (2006) Immunization with influenza A NP-expressing vaccinia virus recombinant protects mice against experimental infection with human and avian influenza viruses. *Arch Virol* 151:921–931
5. Anthony SJ, St Leger JA, Pugliares K, Ip HS, Chan JM, Carpenter ZW, Navarrete-Macias I, Sanchez-Leon M, Saliki JT, Pedersen J, Karesh W, Daszak P, Rabadan R, Rowles T, Lipkin WI (2012) Emergence of fatal avian influenza in New England harbor seals. *MBio* 3:e00166–12
6. Aragón, Luna S dela, Novoa I, Carrasco L, Ortín J, Nieto A (2000) Eukaryotic translation initiation factor 4GI is a cellular target for NS1 protein, a translational activator of influenza virus. *Mol Cell Biol* 20:6259–68
7. Balgi AD, Wang J, Cheng DYH, Ma C, Pfeifer TA, Shimizu Y, Anderson HJ, Pinto LH, Lamb RA, DeGrado WF, Roberge M (2013) Inhibitors of the influenza A virus M2 proton channel discovered using a high-throughput yeast growth restoration assay. *PLoS One* 8:e55271
8. Basler CF, Reid AH, Dybing JK, Janczewski TA, Fanning TG, Zheng H, Salvatore M, Perdue ML, Swayne DE, Garcia-Sastre A, Palese P, Taubenberger JK (2001) Sequence of the 1918 pandemic influenza virus nonstructural gene (NS) segment and characterization of recombinant viruses bearing the 1918 NS genes. *Proc Natl Acad Sci U S A* 98:2746–2751
9. Basu D, Walkiewicz MP, Frieman M, Baric RS, Auble DT, Engel DA (2009) Novel influenza virus NS1 antagonists block replication and restore innate immune function. *J Virol* 83:1881–91
10. Bate-Smith E (1975) Phytochemistry of proanthocyanidins. *Phytochemistry* 14:1107–1113

11. Baum A, Sachidanandam R, García-Sastre A (2010) Preference of RIG-I for short viral RNA molecules in infected cells revealed by next-generation sequencing. *Proc Natl Acad Sci U S A* 107:16303–8
12. Baz M, Abed Y, Papenburg J, Bouhy X, Hamelin ME, Boivin G (2009) Emergence of oseltamivir-resistant pandemic H1N1 virus during prophylaxis. *N Engl J Med* 361:2296–7
13. Bertram S, Glowacka I, Steffen I, Köhl A, Pöhlmann S (2010) Novel insights into proteolytic cleavage of influenza virus hemagglutinin. *Rev Med Virol* 20:298–310
14. Betts JW, Kelly SM, Haswell SJ (2011) Antibacterial effects of theaflavin and synergy with epicatechin against clinical isolates of *Acinetobacter baumannii* and *Stenotrophomonas maltophilia*. *Int J Antimicrob Agents* 38:421–5
15. Beveridge WI (1991) The chronicle of influenza epidemics. *Hist Philos Life Sci* 13:223–34
16. Bogs J, Kalthoff D, Veits J, Pavlova S, Schwemmle M, Mänz B, Mettenleiter TC, Stech J (2011) Reversion of PB2-627E to -627K during replication of an H5N1 Clade 2.2 virus in mammalian hosts depends on the origin of the nucleoprotein. *J Virol* 85:10691–8
17. Bornholdt ZA, Prasad BVV (2006) X-ray structure of influenza virus NS1 effector domain. *Nat Struct Mol Biol* 13:559–60
18. Boulo S, Akarsu H, Ruigrok RWH, Baudin F (2007) Nuclear traffic of influenza virus proteins and ribonucleoprotein complexes. *Virus Res* 124:12–21
19. Brendler T, Wyk BE van (2008) A historical, scientific and commercial perspective on the medicinal use of *Pelargonium sidoides* (Geraniaceae). *J Ethnopharmacol* 119:420–433
20. Bright RA, Shay DK, Shu B, Cox NJ, Klimov AI (2006) Adamantane resistance among influenza A viruses isolated early during the 2005-2006 influenza season in the United States. *JAMA* 295:891–4
21. Bui M, Whittaker G, Helenius A (1996) Effect of M1 protein and low pH on nuclear transport of influenza virus ribonucleoproteins. *J Virol* 70:8391–401
22. Burgui I (2003) PABP1 and eIF4GI associate with influenza virus NS1 protein in viral mRNA translation initiation complexes. *J Gen Virol* 84:3263–3274
23. Butt KM, Smith GJD, Chen H, Zhang LJ, Leung YHC, Xu KM, Lim W, Webster RG, Yuen KY, Peiris JSM, Guan Y (2005) Human infection with an avian H9N2 influenza A virus in Hong Kong in 2003. *J Clin Microbiol* 43:5760–7
24. Carson RS, Frisch AW (1953) The inactivation of influenza viruses by tannic acid and related compounds. *J Bacteriol* 66:572–5
25. Carter NJ, Curran MP (2011) Live attenuated influenza vaccine (FluMist®; Fluenz™): a review of its use in the prevention of seasonal influenza in children and adults. *Drugs* 71:1591–622
26. Cass LM, Efthymiopoulos C, Bye A (1999) Pharmacokinetics of zanamivir after intravenous, oral, inhaled or intranasal administration to healthy volunteers. *Clin Pharmacokinet* 36 Suppl 1:1–11
27. Centers for Disease Control and Prevention CDC (2009) Update: Influenza activity—United States, September 28, 2008–January 31, 2009. *MMWR Morb Mortal Wkly Rep*:115–9

28. Centers for Disease Control and Prevention (2011) Limited human-to-human transmission of novel influenza A (H3N2) virus--Iowa, November 2011. *MMWR Morb Mortal Wkly Rep* 60:1615–7
29. Centers for Disease Control and Prevention (2012a) Update: Influenza A (H3N2)v transmission and guidelines - five states, 2011. *MMWR Morb Mortal Wkly Rep* 60:1741–4
30. Centers for Disease Control and Prevention (2012b) Update: Influenza Activity — United States, 2011–12 Season and Composition of the 2012–13 Influenza Vaccine. *MMWR Morb Mortal Wkly Rep* 61:414–20
31. Centers for Disease Control and Prevention (2013a) Case Count: Detected U.S. Human Infections with H3N2v by State since August 2011. <http://www.cdc.gov/flu/swineflu/h3n2v-case-count.htm>, accessed December 16, 2013
32. Centers for Disease Control and Prevention (2013b) Use of Antivirals. Guidance on the Use of Influenza Antiviral Agents. <http://www.cdc.gov/flu/professionals/antivirals/antiviral-use-influenza.htm>, accessed July 21, 2013
33. Centers for Disease Control and Prevention (2013c) Influenza activity--United States, 2012-13 season and composition of the 2013-14 influenza vaccine. *MMWR Morb Mortal Wkly Rep* 62:473–9
34. Chen Z, Li Y, Krug RM (1999) Influenza A virus NS1 protein targets poly(A)-binding protein II of the cellular 3'-end processing machinery. *EMBO J* 18:2273–83
35. Chen W, Calvo PA, Malide D, Gibbs J, Schubert U, Bacik I, Basta S, O'Neill R, Schickli J, Palese P, Henklein P, Bennink JR, Yewdell JW (2001) A novel influenza A virus mitochondrial protein that induces cell death. *Nat Med* 7:1306–1312
36. Chen Y, Liang W, Yang S, Wu N, Gao H, Sheng J, Yao H, Wo J, Fang Q, Cui D, Li Y, Yao X, Zhang Y, Wu H, Zheng S, Diao H, Xia S, Zhang Y, Chan KH, Tsoi HW, Teng JLL, Song W, Wang P, Lau SY, Zheng M, Chan JFW, To KKW, Chen H, Li L, Yuen KY (2013) Human infections with the emerging avian influenza A H7N9 virus from wet market poultry: clinical analysis and characterisation of viral genome. *Lancet* 381:1916–25
37. Cho EJ, Xia S, Ma LC, Robertus J, Krug RM, Anslyn E V, Montelione GT, Ellington AD (2012) Identification of influenza virus inhibitors targeting NS1A utilizing fluorescence polarization-based high-throughput assay. *J Biomol Screen* 17:448–59
38. Ciesek S, Hahn T von, Colpitts CC, Schang LM, Friesland M, Steinmann J, Manns MP, Ott M, Wedemeyer H, Meuleman P, Pietschmann T, Steinmann E (2011) The green tea polyphenol, epigallocatechin-3-gallate, inhibits hepatitis C virus entry. *Hepatology* 54:1947–55
39. Cline TD, Karlsson EA, Freiden P, Seufzer BJ, Rehg JE, Webby RJ, Schultz-Cherry S (2011) Increased pathogenicity of a reassortant 2009 pandemic H1N1 influenza virus containing an H5N1 hemagglutinin. *J Virol* 85:12262–70
40. Conrad A, Kolodziej H, Schulz V (2007) Pelargonium sidoides-extract (EPs 7630): registration confirms efficacy and safety. *Wien Med Wochenschr* 157:331–336
41. Cowan MM (1999) Plant products as antimicrobial agents. *Clin Microbiol Rev* 12:564–82
42. Daly JM, MacRae S, Newton JR, Watrang E, Elton DM (2011) Equine influenza: a review of an unpredictable virus. *Vet J* 189:7–14

43. Dauer A, Metzner P, Schimmer O (1998) Proanthocyanidins from the bark of *Hamamelis virginiana* exhibit antimutagenic properties against nitroaromatic compounds. *Planta Med* 64:324–7
44. Dauer A, Rimpler H, Hensel A (2003) Polymeric proanthocyanidins from the bark of *Hamamelis virginiana*. *Planta Med* 69:89–91
45. Dawood FS, Iuliano D, Reed C, Meltzer MI, Shay DK, Cheng PY, Bandaranayake D, Breiman RF, Brooks WA, Buchy P, Feikin DR, Fowler KB, Gordon A, Hien NT, Horby P, Huang QS, Katz MA, Krishnan A, Lal R, Montgomery JM, Mølbak K, Pebody R, Presanis AM, Razuri H, Steens A, Tinoco YO, Wallinga J, Yu H, Vong S, Bresee J, Widdowson MA (2012) Estimated global mortality associated with the first 12 months of 2009 pandemic influenza A H1N1 virus circulation: a modelling study. *Lancet Infect Dis* 12:687–95
46. DeBruyne T, Pieters L, Witvrouw M, Clercq E De, Berghe D Vanden, Vlietinck AJ (1999) Biological evaluation of proanthocyanidin dimers and related polyphenols. *J Nat Prod* 62:954–958
47. Decroly E, Ferron F, Lescar J, Canard B (2012) Conventional and unconventional mechanisms for capping viral mRNA. *Nat Rev Microbiol* 10:51–65
48. Deprez S, Mila I, Huneau JF, Tome D, Scalbert A (2001) Transport of proanthocyanidin dimer, trimer, and polymer across monolayers of human intestinal epithelial Caco-2 cells. *Antioxid Redox Signal* 3:957–967
49. Deters A, Dauer A, Schnetz E, Fartasch M, Hensel A (2001) High molecular compounds (polysaccharides and proanthocyanidins) from *Hamamelis virginiana* bark: influence on human skin keratinocyte proliferation and differentiation and influence on irritated skin. *Phytochemistry* 58:949–58
50. DeVeer MJ, Holko M, Frevel M, Walker E, Der S, Paranjape JM, Silverman RH, Williams BR (2001) Functional classification of interferon-stimulated genes identified using microarrays. *J Leukoc Biol* 69:912–20
51. Dias A, Bouvier D, Crépin T, McCarthy AA, Hart DJ, Baudin F, Cusack S, Ruigrok RWH (2009) The cap-snatching endonuclease of influenza virus polymerase resides in the PA subunit. *Nature* 458:914–8
52. Dixit E, Kagan JC (2013) Intracellular pathogen detection by RIG-I-like receptors. *Adv Immunol* 117:99–125
53. Donelan NR, Basler CF, Garcia-Sastre A (2003) A recombinant influenza A virus expressing an RNA-binding-defective NS1 protein induces high levels of beta interferon and is attenuated in mice. *J Virol* 77:13257–66
54. Droebner K, Ehrhardt C, Poetter A, Ludwig S, Planz O (2007) CYSTUS052, a polyphenol-rich plant extract, exerts anti-influenza virus activity in mice. *Antivir Res* 76:1–10
55. Ducatez MF, Hause B, Stigger-Rosser E, Darnell D, Corzo C, Juleen K, Simonson R, Brockwell-Staats C, Rubrum A, Wang D, Webb A, Crumpton JC, Lowe J, Gramer M, Webby RJ (2011) Multiple Reassortment between Pandemic (H1N1) 2009 and Endemic Influenza Viruses in Pigs, United States. *Emerg Infect Dis* 17:1624–1629
56. Dundon WG, Capua I (2009) A Closer Look at the NS1 of Influenza Virus. *Viruses* 1:1057–72

57. Ehrhardt C, Hrinčius ER, Korte V, Mazur I, Droebner K, Poetter A, Dreschers S, Schmolke M, Planz O, Ludwig S (2007) A polyphenol rich plant extract, CYSTUS052, exerts anti influenza virus activity in cell culture without toxic side effects or the tendency to induce viral resistance. *Antiviral Res* 76:38–47
58. Ehrhardt C, Seyer R, Hrinčius ER, Eierhoff T, Wolff T, Ludwig S (2010) Interplay between influenza A virus and the innate immune signaling. *Microbes Infect* 12:81–87
59. Enami M, Luytjes W, Krystal M, Palese P (1990) Introduction of site-specific mutations into the genome of influenza virus. *Proc Natl Acad Sci U S A* 87:3802–3805
60. Engelhardt OG, Fodor E (2006) Functional association between viral and cellular transcription during influenza virus infection. *Rev Med Virol* 16:329–45
61. Erdelmeier CA, Cinatl J, Rabenau H, Doerr HW, Biber A, Koch E (1996) Antiviral and antiphlogistic activities of Hamamelis virginiana bark. *Planta Med* 62:241–245
62. European Directorate for the Quality of Medicines & Healthcare (2008) Bestimmung des Gerbstoffgehalts pflanzlicher Drogen. In: *European Pharmacopoeia* 6.0.p 328
63. European Medicines Agency (2009) Assessment report on Hamamelis virginiana L., cortex, Hamamelis virginiana L. folium, Hamamelis virginiana L., folium et cortex aut ramunculus destillatum. EMA/HMPC/1
64. European Medicines Agency (2012) EPAR summary for the public Fluenz influenza vaccine. http://www.ema.europa.eu/docs/en_GB/document_library/EPAR_-_Summary_for_the_public/human/001101/WC500103712.pdf, accessed January 15, 2014
65. Falcón AM, Fortes P, Marión RM, Beloso A, Ortín J (1999) Interaction of influenza virus NS1 protein and the human homologue of Staufen in vivo and in vitro. *Nucleic Acids Res* 27:2241–7
66. Falcón AM, Fernandez-Sesma A, Nakaya Y, Moran TM, Ortín J, Garcia-Sastre A (2005) Attenuation and immunogenicity in mice of temperature-sensitive influenza viruses expressing truncated NS1 proteins. *J Gen Virol* 86:2817–21
67. Fiers W, Filette M De, Bakkouri K El, Schepens B, Roose K, Schotsaert M, Birkett A, Saelens X (2009) M2e-based universal influenza A vaccine. *Vaccine* 27:6280–6283
68. Fiorentini L, Taddei R, Moreno A, Gelmetti D, Barbieri I, Marco MA De, Tosi G, Cordioli P, Massi P (2011) Influenza A Pandemic (H1N1) 2009 Virus Outbreak in a Cat Colony in Italy. *Zoonoses Public Heal* 58:573–81
69. Fodor E, Devenish L, Engelhardt OG, Palese P, Brownlee GG, Garcia-Sastre A (1999) Rescue of influenza A virus from recombinant DNA. *J Virol* 73:9679–9682
70. Fouchier RAM, Schneeberger PM, Rozendaal FW, Broekman JM, Kemink SAG, Munster V, Kuiken T, Rimmelzwaan GF, Schutten M, Doornum GJJ Van, Koch G, Bosman A, Koopmans M, Osterhaus ADME (2004) Avian influenza A virus (H7N7) associated with human conjunctivitis and a fatal case of acute respiratory distress syndrome. *Proc Natl Acad Sci U S A* 101:1356–61
71. Frazier RA, Deaville ER, Green RJ, Stringano E, Willoughby I, Plant J, Mueller-Harvey I (2010) Interactions of tea tannins and condensed tannins with proteins. *J Pharm Biomed Anal* 51:490–5
72. Fujiyoshi Y, Kume NP, Sakata K, Sato SB (1994) Fine structure of influenza A virus observed by electron cryo-microscopy. *EMBO J* 13:318–26

73. Furuta Y, Takahashi K, Shiraki K, Sakamoto K, Smee DF, Barnard DL, Gowen BB, Julander JG, Morrey JD (2009) T-705 (favipiravir) and related compounds: Novel broad-spectrum inhibitors of RNA viral infections. *Antiviral Res* 82:95–102
74. Gack MU, Albrecht RA, Urano T, Inn KS, Huang IC, Carnero E, Farzan M, Inoue S, Jung JU, Garcia-Sastre A (2009) Influenza A virus NS1 targets the ubiquitin ligase TRIM25 to evade recognition by the host viral RNA sensor RIG-I. *Cell Host Microbe* 5:439–49
75. Gale M, Katze MG (1998) Molecular mechanisms of interferon resistance mediated by viral-directed inhibition of PKR, the interferon-induced protein kinase. *Pharmacol Ther* 78:29–46
76. Gammelin M, Altmüller A, Reinhardt U, Mandler J, Harley VR, Hudson PJ, Fitch WM, Scholtissek C (1990) Phylogenetic analysis of nucleoproteins suggests that human influenza A viruses emerged from a 19th-century avian ancestor. *Mol Biol Evol* 7:194–200
77. Gao R, Cao B, Hu Y, Feng Z, Wang D, Hu W, Chen J, Jie Z, Qiu H, Xu K, Xu X, Lu H, Zhu W, Gao Z, Xiang N, Shen Y, He Z, Gu Y, Zhang Z, Yang Y, Zhao X, Zhou L, Li X, Zou S, Zhang Y, Li X, Yang L, Guo J, Dong J, Li Q, Dong L, Zhu Y, Bai T, Wang S, Hao P, Yang W, Zhang Y, Han J, Yu H, Li D, Gao GF, Wu G, Wang Y, Yuan Z, Shu Y (2013) Human infection with a novel avian-origin influenza A (H7N9) virus. *N Engl J Med* 368:1888–97
78. Gao X, Wang W, Li Y, Zhang S, Duan Y, Xing L, Zhao Z, Zhang P, Li Z, Li R, Wang X, Yang P (2013) Enhanced Influenza VLP vaccines comprising matrix-2 ectodomain and nucleoprotein epitopes protects mice from lethal challenge. *Antiviral Res* 98:4–11
79. García M, Crawford JM, Latimer JW, Rivera-Cruz E, Perdue ML (1996) Heterogeneity in the haemagglutinin gene and emergence of the highly pathogenic phenotype among recent H5N2 avian influenza viruses from Mexico. *J Gen Virol* 77:1493–504
80. Garcia-Sastre A, Egorov A, Matassov D, Brandt S, Levy DE, Durbin JE, Palese P, Muster T (1998) Influenza A virus lacking the NS1 gene replicates in interferon-deficient systems. *Virology* 252:324–330
81. Garfinkel MS, Katze MG (1993) Translational control by influenza virus. Selective translation is mediated by sequences within the viral mRNA 5'-untranslated region. *J Biol Chem* 268:22223–6
82. Garten RJ, Davis CT, Russell CA, Shu B, Lindstrom S, Balish A, Sessions WM, Xu X, Skepner E, Deyde V, Okomo-Adhiambo M, Gubareva L, Barnes J, Smith CB, Emery SL, Hillman MJ, Rivaller P, Smagala J, Graaf M de, Burke DF, Fouchier RAM, Pappas C, Alpuche-Aranda CM, Lopez-Gatell H, Olivera H, Lopez I, Myers CA, Faix D, Blair PJ, Yu C, Keene KM, Dotson Jr. PD, Boxrud D, Sambol AR, Abid SH, St George K, Bannerman T, Moore AL, Stringer DJ, Blevins P, Demmler-Harrison GJ, Ginsberg M, Kriner P, Waterman S, Smole S, Guevara HF, Belongia EA, Clark PA, Beatrice ST, Donis R, Katz J, Finelli L, Bridges CB, Shaw M, Jernigan DB, Uyeki TM, Smith DJ, Klimov AI, Cox NJ (2009) Antigenic and genetic characteristics of swine-origin 2009 A(H1N1) influenza viruses circulating in humans. *Science* 325:197–201
83. Garten W, Klenk HD (1999) Understanding influenza virus pathogenicity. *Trends Microbiol* 7:99–100
84. Ge S, Wang Z (2011) An overview of influenza A virus receptors. *Crit Rev Microbiol* 37:157–65

85. Geiss GK, Salvatore M, Tumpey TM, Carter VS, Wang X, Basler CF, Taubenberger JK, Bumgarner RE, Palese P, Katze MG, Garcia-Sastre A (2002) Cellular transcriptional profiling in influenza A virus-infected lung epithelial cells: the role of the nonstructural NS1 protein in the evasion of the host innate defense and its potential contribution to pandemic influenza. *Proc Natl Acad Sci U S A* 99:10736–10741
86. Gescher K, Hensel A, Hafezi W, Derksen A, Kühn J (2011) Oligomeric proanthocyanidins from *Rumex acetosa* L. inhibit the attachment of herpes simplex virus type-1. *Antiviral Res* 89:9–18
87. Gescher K, Kuhn J, Lorentzen E, Hafezi W, Derksen A, Deters A, Hensel A (2011) Proanthocyanidin-enriched extract from *Myrothamnus flabellifolia* Welw. exerts antiviral activity against herpes simplex virus type 1 by inhibition of viral adsorption and penetration. *J Ethnopharmacol* 134:468–474
88. Ginsberg M, Hopkins J, Maroufi A, Dunne G (2009) Swine influenza A (H1N1) infection in two children--Southern California, March-April 2009. *MMWR Morb Mortal Wkly Rep* 58:400–2
89. Gohrbandt S, Veits J, Hundt J, Bogs J, Breithaupt A, Teifke JP, Weber S, Mettenleiter TC, Stech J (2011) Amino acids adjacent to the haemagglutinin cleavage site are relevant for virulence of avian influenza viruses of subtype H5. *J Gen Virol* 92:51–9
90. Goldstein T, Mena I, Anthony SJ, Medina R, Robinson PW, Greig DJ, Costa DP, Lipkin WI, Garcia-Sastre A, Boyce WM (2013) Pandemic H1N1 influenza isolated from free-ranging Northern Elephant Seals in 2010 off the central California coast. *PLoS One* 8:e62259
91. Gómez-Puertas P, Albo C, Pérez-Pastrana E, Vivo A, Portela A (2000) Influenza virus matrix protein is the major driving force in virus budding. *J Virol* 74:11538–47
92. González MJ, Torres JL, Medina I (2010) Impact of thermal processing on the activity of gallotannins and condensed tannins from *Hamamelis virginiana* used as functional ingredients in seafood. *J Agric Food Chem* 58:4274–83
93. Gorman OT, Bean WJ, Kawaoka Y, Webster RG (1990) Evolution of the nucleoprotein gene of influenza A virus. *J Virol* 64:1487–97
94. Gottschalk A (1957) Neuraminidase: the specific enzyme of influenza virus and *Vibrio cholerae*. *Biochim Biophys Acta* 23:645–6
95. Greenspan D, Palese P, Krystal M (1988) Two nuclear location signals in the influenza virus NS1 nonstructural protein. *J Virol* 62:3020–6
96. Gu RX, Liu LA, Wang YH, Xu Q, Wei DQ (2013) Structural comparison of the wild-type and drug-resistant mutants of the influenza A M2 proton channel by molecular dynamics simulations. *J Phys Chem B* 117:6042–51
97. Guan Y, Shortridge KF, Krauss S, Webster RG (1999) Molecular characterization of H9N2 influenza viruses: were they the donors of the “internal” genes of H5N1 viruses in Hong Kong? *Proc Natl Acad Sci U S A* 96:9363–7
98. Guan Y, Peiris JSM, Lipatov AS, Ellis TM, Dyrting KC, Krauss S, Zhang LJ, Webster RG, Shortridge KF (2002) Emergence of multiple genotypes of H5N1 avian influenza viruses in Hong Kong SAR. *Proc Natl Acad Sci U S A* 99:8950–5
99. Guilligay D, Tarendeau F, Resa-Infante P, Coloma R, Crepin T, Sehr P, Lewis J, Ruigrok RWH, Ortin J, Hart DJ, Cusack S (2008) The structural basis for cap binding by influenza virus polymerase subunit PB2. *Nat Struct Mol Biol* 15:500–6

100. Guillot L, LeGoffic R, Bloch S, Escriou N, Akira S, Chignard M, Si-Tahar M (2005) Involvement of toll-like receptor 3 in the immune response of lung epithelial cells to double-stranded RNA and influenza A virus. *J Biol Chem* 280:5571–80
101. Hagerman AE, Butler LG (1981) The specificity of proanthocyanidin-protein interactions. *J Biol Chem* 256:4494–7
102. Hagerman AE (1992) Tannin-protein interactions. *ACS Symp Ser* 506:236–47
103. Haidari M, Ali M, Ward Casscells S 3rd, Madjid M (2009) Pomegranate (*Punica granatum*) purified polyphenol extract inhibits influenza virus and has a synergistic effect with oseltamivir. *Phytomedicine* 16:1127–1136
104. Hale BG, Randall RE, Ortin J, Jackson D (2008) The multifunctional NS1 protein of influenza A viruses. *J Gen Virol* 89:2359–2376
105. Hale BG, Steel J, Medina R, Manicassamy B, Ye J, Hickman D, Hai R, Schmolke M, Lowen AC, Perez DR, Garcia-Sastre A (2010) Inefficient control of host gene expression by the 2009 pandemic H1N1 influenza A virus NS1 protein. *J Virol* 84:6909–22
106. Hall T (1999) BioEdit: a user-friendly biological sequence alignment editor and analysis program for Windows 95/98/NT. *Nucleic Acids Symp Ser* 41:95–98
107. Hamilton BS, Whittaker GR, Daniel S (2012) Influenza virus-mediated membrane fusion: determinants of hemagglutinin fusogenic activity and experimental approaches for assessing virus fusion. *Viruses* 4:1144–68
108. Hashimoto T, Kumazawa S, Nanjo F, Hara Y, Nakayama T (1999) Interaction of tea catechins with lipid bilayers investigated with liposome systems. *Biosci Biotechnol Biochem* 63:2252–5
109. Haslam E (1996) Natural polyphenols (vegetable tannins) as drugs: possible modes of action. *J Nat Prod* 59:205–15
110. Haslam E (2007) Vegetable tannins - lessons of a phytochemical lifetime. *Phytochemistry* 68:2713–21
111. Hatada E, Saito S, Fukuda R (1999) Mutant influenza viruses with a defective NS1 protein cannot block the activation of PKR in infected cells. *J Virol* 73:2425–33
112. Hayman A, Comely S, Lackenby A, Murphy S, McCauley J, Goodbourn S, Barclay W (2006) Variation in the ability of human influenza A viruses to induce and inhibit the IFN-beta pathway. *Virology* 347:52–64
113. Herfst S, Schrauwen EJ, Linster M, Chutinimitkul S, Wit E de, Munster VJ, Sorrell EM, Bestebroer TM, Burke DF, Smith DJ, Rimmelzwaan GF, Osterhaus ADME, Fouchier RAM (2012) Airborne transmission of influenza A/H5N1 virus between ferrets. *Science* 336:1534–41
114. Hinshaw VS, Bean WJ, Geraci J, Fiorelli P, Early G, Webster RG (1986) Characterization of two influenza A viruses from a pilot whale. *J Virol* 58:655–6
115. Hocine S, Singer RH, Grünwald D (2010) RNA processing and export. *Cold Spring Harb Perspect Biol* 2:a000752
116. Hoffmann E, Neumann G, Kawaoka Y, Hobom G, Webster RG (2000) A DNA transfection system for generation of influenza A virus from eight plasmids. *Proc Natl Acad Sci U S A* 97:6108–13

117. Horimoto T, Kawaoka Y (2005) Influenza: lessons from past pandemics, warnings from current incidents. *Nat Rev Microbiol* 3:591–600
118. Hornung V, Ellegast J, Kim S, Brzózka K, Jung A, Kato H, Poeck H, Akira S, Conzelmann KK, Schlee M, Endres S, Hartmann G (2006) 5'-Triphosphate RNA is the ligand for RIG-I. *Science* 314:994–7
119. Hovanessian AG (1991) Interferon-induced and double-stranded RNA-activated enzymes: a specific protein kinase and 2',5'-oligoadenylate synthetases. *J Interferon Res* 11:199–205
120. Howell AB, Vorsa N, Marderosian A Der, Foo LY (1998) Inhibition of the adherence of P-fimbriated *Escherichia coli* to uroepithelial-cell surfaces by proanthocyanidin extracts from cranberries. *N Engl J Med* 339:1085–1086
121. Hull Vance S, Tucci M, Benghuzzi H (2011) Evaluation of the antimicrobial efficacy of green tea extract (egcg) against *Streptococcus pyogenes* in vitro - biomed 2011. *Biomed Sci Instrum* 47:177–82
122. Hurt AC, Hardie K, Wilson NJ, Deng YM, Osbourn M, Gehrig N, Kelso A (2011) Community transmission of oseltamivir-resistant A(H1N1)pdm09 influenza. *N Engl J Med* 365:2541–2542
123. Ichinohe T (2010) Respective roles of TLR, RIG-I and NLRP3 in influenza virus infection and immunity: impact on vaccine design. *Expert Rev Vaccines* 9:1315–24
124. Ikigai H, Nakae T, Hara Y, Shimamura T (1993) Bactericidal catechins damage the lipid bilayer. *Biochim Biophys Acta* 1147:132–6
125. Imai M, Watanabe T, Hatta M, Das SC, Ozawa M, Shinya K, Zhong G, Hanson A, Katsura H, Watanabe S, Li C, Kawakami E, Yamada S, Kiso M, Suzuki Y, Maher EA, Neumann G, Kawaoka Y (2012) Experimental adaptation of an influenza H5 HA confers respiratory droplet transmission to a reassortant H5 HA/H1N1 virus in ferrets. *Nature* 486:420–8
126. Imanishi N, Tuji Y, Katada Y, Maruhashi M, Konosu S, Mantani N, Terasawa K, Ochiai H (2002) Additional inhibitory effect of tea extract on the growth of influenza A and B viruses in MDCK cells. *Microbiol Immunol* 46:491–4
127. Inglis SC, Brown CM (1981) Spliced and unspliced RNAs encoded by virion RNA segment 7 of influenza virus. *Nucleic Acids Res* 9:2727–40
128. International Committee on Taxonomy of Viruses (2012) ICTV Master Species List V3. http://talk.ictvonline.org/files/ictv_documents/m/msl/4440.aspx, accessed January 13, 2014
129. Iqbal M, Yaqub T, Reddy K, McCauley JW (2009) Novel genotypes of H9N2 influenza A viruses isolated from poultry in Pakistan containing NS genes similar to highly pathogenic H7N3 and H5N1 viruses. *PLoS One* 4:e5788
130. Ishii T, Ichikawa T, Minoda K, Kusaka K, Ito S, Suzuki Y, Akagawa M, Mochizuki K, Goda T, Nakayama T (2011) Human serum albumin as an antioxidant in the oxidation of (-)-epigallocatechin gallate: participation of reversible covalent binding for interaction and stabilization. *Biosci Biotechnol Biochem* 75:100–6
131. Ito T, Okazaki K, Kawaoka Y, Takada A, Webster RG, Kida H (1995) Perpetuation of influenza A viruses in Alaskan waterfowl reservoirs. *Arch Virol* 140:1163–72

132. Ito T, Couceiro JN, Kelm S, Baum LG, Krauss S, Castrucci MR, Donatelli I, Kida H, Paulson JC, Webster RG, Kawaoka Y (1998) Molecular basis for the generation in pigs of influenza A viruses with pandemic potential. *J Virol* 72:7367–73
133. Ito T, Goto H, Yamamoto E, Tanaka H, Takeuchi M, Kuwayama M, Kawaoka Y, Otsuki K (2001) Generation of a highly pathogenic avian influenza A virus from an avirulent field isolate by passaging in chickens. *J Virol* 75:4439–43
134. Itzstein M von, Wu WY, Kok GB, Pegg MS, Dyason JC, Jin B, Phan T Van, Smythe ML, White HF, Oliver SW (1993) Rational design of potent sialidase-based inhibitors of influenza virus replication. *Nature* 363:418–23
135. Jablonski JJ, Basu D, Engel DA, Geysen HM (2012) Design, synthesis, and evaluation of novel small molecule inhibitors of the influenza virus protein NS1. *Bioorg Med Chem* 20:487–97
136. Jagger BW, Wise HM, Kash JC, Walters KA, Wills NM, Xiao YL, Dunfee RL, Schwartzman LM, Ozinsky A, Bell GL, Dalton RM, Lo A, Efstathiou S, Atkins JF, Firth AE, Taubenberger JK, Digard P (2012) An overlapping protein-coding region in influenza A virus segment 3 modulates the host response. *Science* 337:199–204
137. Janecki A, Kolodziej H (2010) Anti-adhesive activities of flavan-3-ols and proanthocyanidins in the interaction of group A-streptococci and human epithelial cells. *Molecules* 15:7139–7152
138. Janecki A, Conrad A, Engels I, Frank U, Kolodziej H (2011) Evaluation of an aqueous-ethanolic extract from *Pelargonium sidoides* (EPs((R)) 7630) for its activity against group A-streptococci adhesion to human HEp-2 epithelial cells. *J Ethnopharmacol* 133:147–152
139. Jöbstl E, Howse JR, Fairclough JP, Williamson MP (2006) Noncovalent cross-linking of casein by epigallocatechin gallate characterized by single molecule force microscopy. *J Agric Food Chem* 54:4077–81
140. Johnson NP, Mueller J (2002) Updating the accounts: global mortality of the 1918–1920 “Spanish” influenza pandemic. *Bull Hist Med* 76:105–15
141. Kageyama T, Fujisaki S, Takashita E, Xu H, Yamada S, Uchida Y, Neumann G, Saito T, Kawaoka Y, Tashiro M (2013) Genetic analysis of novel avian A(H7N9) influenza viruses isolated from patients in China, February to April 2013. *Euro Surveill* 18:20453
142. Kamin W, Maydannik V, Malek FA, Kieser M (2010) Efficacy and tolerability of EPs 7630 in children and adolescents with acute bronchitis - a randomized, double-blind, placebo-controlled multicenter trial with a herbal drug preparation from *Pelargonium sidoides* roots. *Int J Clin Pharmacol Ther* 48:184–191
143. Katze MG, Krug RM (1984) Metabolism and expression of RNA polymerase II transcripts in influenza virus-infected cells. *Mol Cell Biol* 4:2198–206
144. Kawaoka Y, Krauss S, Webster RG (1989) Avian-to-human transmission of the PB1 gene of influenza A viruses in the 1957 and 1968 pandemics. *J Virol* 63:4603–8
145. Kerkhove MD van, Mumford E, Mounts AW, Bresee J, Ly S, Bridges CB, Otte J (2011) Highly pathogenic avian influenza (H5N1): pathways of exposure at the animal-human interface, a systematic review. *PLoS One* 6:e14582
146. Kim CU, Lew W, Williams MA, Liu H, Zhang L, Swaminathan S, Bischofberger N, Chen MS, Mendel DB, Tai CY, Laver WG, Stevens RC (1997) Influenza neuraminidase inhibitors possessing a novel hydrophobic interaction in the enzyme active site: design,

- synthesis, and structural analysis of carbocyclic sialic acid analogues with potent anti-influenza activity. *J Am Chem Soc* 119:681–90
147. Kimble JB, Sorrell E, Shao H, Martin PL, Perez DR (2011) Compatibility of H9N2 avian influenza surface genes and 2009 pandemic H1N1 internal genes for transmission in the ferret model. *Proc Natl Acad Sci U S A* 108:12084–12088
148. Kimmel EM, Jerome M, Holderness J, Snyder D, Kemoli S, Jutila MA, Hedges JF (2011) Oligomeric procyanidins stimulate innate antiviral immunity in dengue virus infected human PBMCs. *Antiviral Res* 90:80–6
149. Kittel C, Sereinig S, Ferko B, Stasakova J, Romanova J, Wolkerstorfer A, Katinger H, Egorov A (2004) Rescue of influenza virus expressing GFP from the NS1 reading frame. *Virology* 324:67–73
150. Klenk HD, Rott R, Orlich M, Blödorn J (1975) Activation of influenza A viruses by trypsin treatment. *Virology* 68:426–39
151. Klenk HD, Garten W (1994) Host cell proteases controlling virus pathogenicity. *Trends Microbiol* 2:39–43
152. Kochs G, Garcia-Sastre A, Martínez-Sobrido L (2007) Multiple anti-interferon actions of the influenza A virus NS1 protein. *J Virol* 81:7011–21
153. Kolodziej H, Kayser O, Radtke OA, Kiderlen AF, Koch E (2003) Pharmacological profile of extracts of *Pelargonium sidoides* and their constituents. *Phytomedicine* 10 Suppl 4:18–24
154. Kolodziej H, Kiderlen AF (2007) In vitro evaluation of antibacterial and immunomodulatory activities of *Pelargonium reniforme*, *Pelargonium sidoides* and the related herbal drug preparation EPs 7630. *Phytomedicine* 14 Suppl 6:18–26
155. Kratz JM, Andrighetti-Fröhner CR, Kolling DJ, Leal PC, Cirne-Santos CC, Yunes RA, Nunes RJ, Trybala E, Bergström T, Frugulhetti ICPP, Barardi CRM, Simões CMO (2008) Anti-HSV-1 and anti-HIV-1 activity of gallic acid and pentyl gallate. *Mem Inst Oswaldo Cruz* 103:437–42
156. Krug RM, Etkind PR (1973) Cytoplasmic and nuclear virus-specific proteins in influenza virus-infected MDCK cells. *Virology* 56:334–348
157. Krug RM (1981) Priming of influenza viral RNA transcription by capped heterologous RNAs. *Curr Top Microbiol Immunol* 93:125–49
158. Kuntz-Simon G, Madec F (2009) Genetic and antigenic evolution of swine influenza viruses in Europe and evaluation of their zoonotic potential. *Zoonoses Public Heal* 56:310–325
159. Kuo RL, Zhao C, Malur M, Krug RM (2010) Influenza A virus strains that circulate in humans differ in the ability of their NS1 proteins to block the activation of IRF3 and interferon- β transcription. *Virology* 408:146–58
160. Lackenby A, Hungnes O, Dudman SG, Meijer A, Paget WJ, Hay AJ, Zambon MC (2008) Emergence of resistance to oseltamivir among influenza A(H1N1) viruses in Europe. *Euro Surveill* 13
161. Lackenby A, Moran Gilad J, Pebody R, Miah S, Calatayud L, Bolotin S, Vipond I, Muir P, Guiver M, McMenamin J, Reynolds A, Moore C, Gunson R, Thompson C, Galiano M, Bermingham A, Ellis J, Zambon M (2011) Continued emergence and

- changing epidemiology of oseltamivir-resistant influenza A(H1N1)2009 virus, United Kingdom, winter 2010/11. *Eurosurveillance* 16:1–6
162. Lamb RA, Choppin PW (1979) Segment 8 of the influenza virus genome is unique in coding for two polypeptides. *Proc Natl Acad Sci U S A* 76:4908–12
163. Lamb RA, Choppin PW, Chanock RM, Lai CJ (1980) Mapping of the two overlapping genes for polypeptides NS1 and NS2 on RNA segment 8 of influenza virus genome. *Proc Natl Acad Sci U S A* 77:1857–61
164. Lamb RA, Horvath CM (1991) Diversity of coding strategies in influenza viruses. *Trends Genet* 7:261–6
165. Laux P, Oschmann R (1993) Die Zaubernuss - *Hamamelis virginiana* L. *Zeitschrift für Phyther* 14:155–166
166. Lazarowitz SG, Compans RW, Choppin PW (1971) Influenza virus structural and nonstructural proteins in infected cells and their plasma membranes. *Virology* 46:830–43
167. Lazarowitz SG, Compans RW, Choppin PW (1973) Proteolytic cleavage of the hemagglutinin polypeptide of influenza virus. Function of the uncleaved polypeptide HA. *Virology* 52:199–212
168. Li KS, Guan Y, Wang J, Smith GJD, Xu KM, Duan L, Rahardjo AP, Puthavathana P, Buranathai C, Nguyen TD, Estoe pangestie ATS, Chaisingh A, Auewarakul P, Long HT, Hanh NTH, Webby RJ, Poon LLM, Chen H, Shortridge KF, Yuen KY, Webster RG, Peiris JSM (2004) Genesis of a highly pathogenic and potentially pandemic H5N1 influenza virus in eastern Asia. *Nature* 430:209–13
169. Li M, Hagerman AE (2013) Interactions between plasma proteins and naturally occurring polyphenols. *Curr Drug Metab* 14:432–45
170. Li Q, Zhou L, Zhou M, Chen Z, Li F, Wu H, Xiang N, Chen E, Tang F, Wang D, Meng L, Hong Z, Tu W, Cao Y, Li L, Ding F, Liu B, Wang M, Xie R, Gao R, Li X, Bai T, Zou S, He J, Hu J, Xu Y, Chai C, Wang S, Gao Y, Jin L, Zhang Y, Luo H, Yu H, Gao L, Pang X, Liu G, Shu Y, Yang W, Uyeki TM, Wang Y, Wu F, Feng Z (2013) Preliminary Report: Epidemiology of the Avian Influenza A (H7N9) Outbreak in China. *N Engl J Med*:1–11
171. Li S, Min JY, Krug RM, Sen GC (2006) Binding of the influenza A virus NS1 protein to PKR mediates the inhibition of its activation by either PACT or double-stranded RNA. *Virology* 349:13–21
172. Li W, Escarpe PA, Eisenberg EJ, Cundy KC, Sweet C, Jakeman KJ, Merson J, Lew W, Williams M, Zhang L, Kim CU, Bischofberger N, Chen MS, Mendel DB (1998) Identification of GS 4104 as an orally bioavailable prodrug of the influenza virus neuraminidase inhibitor GS 4071. *Antimicrob Agents Chemother* 42:647–53
173. Li Y, Yamakita Y, Krug RM (1998) Regulation of a nuclear export signal by an adjacent inhibitory sequence: the effector domain of the influenza virus NS1 protein. *Proc Natl Acad Sci U S A* 95:4864–9
174. Li Y, Chen ZY, Wang W, Baker CC, Krug RM (2001) The 3'-end-processing factor CPSF is required for the splicing of single-intron pre-mRNAs in vivo. *RNA* 7:920–31
175. Lin LT, Chen TY, Lin SC, Chung CY, Lin TC, Wang GH, Anderson R, Lin CC, Richardson CD (2013) Broad-spectrum antiviral activity of chebulagic acid and punicalagin against viruses that use glycosaminoglycans for entry. *BMC Microbiol* 13:187

176. Lipatov AS, Andreansky S, Webby RJ, Hulse DJ, Rehg JE, Krauss S, Perez DR, Doherty PC, Webster RG, Sangster MY (2005) Pathogenesis of Hong Kong H5N1 influenza virus NS gene reassortants in mice: the role of cytokines and B- and T-cell responses. *J Gen Virol* 86:1121–30
177. Liu G, Xiong S, Xiang YF, Guo CW, Ge F, Yang CR, Zhang YJ, Wang YF, Kitazato K (2011) Antiviral activity and possible mechanisms of action of pentagalloylglucose (PGG) against influenza A virus. *Arch Virol* 156:1359–69
178. Livak KJ, Schmittgen TD (2001) Analysis of relative gene expression data using real-time quantitative PCR and the 2(-Delta Delta C(T)) Method. *Methods* 25:402–8
179. Long JX, Peng DX, Liu YL, Wu YT, Liu XF (2008) Virulence of H5N1 avian influenza virus enhanced by a 15-nucleotide deletion in the viral nonstructural gene. *Virus Genes* 36:471–8
180. Ludwig S, Wolff T, Ehrhardt C, Wurzer WJ, Reinhardt J, Planz O, Pleschka S (2004) MEK inhibition impairs influenza B virus propagation without emergence of resistant variants. *FEBS Lett* 561:37–43
181. Luna S dela, Fortes P, Beloso A, Ortín J (1995) Influenza virus NS1 protein enhances the rate of translation initiation of viral mRNAs. *J Virol* 69:2427–33
182. Lund JM, Alexopoulou L, Sato A, Karow M, Adams NC, Gale NW, Iwasaki A, Flavell RA (2004) Recognition of single-stranded RNA viruses by Toll-like receptor 7. *Proc Natl Acad Sci U S A* 101:5598–603
183. Luo GX, Luytjes W, Enami M, Palese P (1991) The polyadenylation signal of influenza virus RNA involves a stretch of uridines followed by the RNA duplex of the panhandle structure. *J Virol* 65:2861–7
184. Luytjes W, Krystal M, Enami M, Parvin JD, Palese P (1989) Amplification, expression, and packaging of foreign gene by influenza virus. *Cell* 59:1107–1113
185. Ma W, Brenner D, Wang Z, Dauber B, Ehrhardt C, Hogner K, Herold S, Ludwig S, Wolff T, Yu K, Richt JA, Planz O, Pleschka S (2010) The NS segment of an H5N1 highly pathogenic avian influenza virus (HPAIV) is sufficient to alter replication efficiency, cell tropism, and host range of an H7N1 HPAIV. *J Virol* 84:2122–2133
186. MacKay D (2001) Hemorrhoids and varicose veins: a review of treatment options. *Altern Med Rev* 6:126–40
187. Maeda T, Ohnishi S (1980) Activation of influenza virus by acidic media causes hemolysis and fusion of erythrocytes. *FEBS Lett* 122:283–7
188. Maeda T, Kawasaki K, Ohnishi SI (1981) Interaction of influenza virus hemagglutinin with target membrane lipids is a key step in virus-induced hemolysis and fusion at pH 5.2. *Proc Natl Acad Sci U S A* 78:4133–7
189. Malakhov MP, Aschenbrenner LM, Smee DF, Wandersee MK, Sidwell RW, Gubareva L V, Mishin VP, Hayden FG, Kim DH, Ing A, Campbell ER, Yu M, Fang F (2006) Sialidase fusion protein as a novel broad-spectrum inhibitor of influenza virus infection. *Antimicrob Agents Chemother* 50:1470–9
190. Mantani N, Andoh T, Kawamata H, Terasawa K, Ochiai H (1999) Inhibitory effect of Ephedrae herba, an oriental traditional medicine, on the growth of influenza A/PR/8 virus in MDCK cells. *Antiviral Res* 44:193–200

191. Mänz B, Dornfeld D, Götz V, Zell R, Zimmermann P, Haller O, Kochs G, Schwemmle M (2013) Pandemic influenza A viruses escape from restriction by human MxA through adaptive mutations in the nucleoprotein. *PLoS Pathog* 9:e1003279
192. Mänz B, Schwemmle M, Brunotte L (2013) Adaptation of avian influenza A virus polymerase in mammals to overcome the host species barrier. *J Virol* 87:7200–9
193. Marión RM, Zürcher T, Luna S dela, Ortín J (1997) Influenza virus NS1 protein interacts with viral transcription-replication complexes in vivo. *J Gen Virol* 78:2447–51
194. Maroto M, Fernandez Y, Ortin J, Pelaez F, Cabello MA (2008) Development of an HTS assay for the search of anti-influenza agents targeting the interaction of viral RNA with the NS1 protein. *J Biomol Screen* 13:581–90
195. Martin K, Helenius A (1991) Transport of incoming influenza virus nucleocapsids into the nucleus. *J Virol* 65:232–44
196. Mathieu C, Moreno V, Retamal P, Gonzalez A, Rivera A, Fuller J, Jara C, Lecocq C, Rojas M, Garcia A, Vasquez M, Agredo M, Gutiérrez C, Escobar H, Fasce R, Mora J, Garcia J, Fernández J, Ternicier C, Avalos P (2010) Pandemic (H1N1) 2009 in breeding turkeys, Valparaiso, Chile. *Emerg Infect Dis* 16:709–11
197. Matrosovich MN, Gambaryan AS, Teneberg S, Piskarev VE, Yamnikova SS, Lvov DK, Robertson JS, Karlsson K a (1997) Avian influenza A viruses differ from human viruses by recognition of sialyloligosaccharides and gangliosides and by a higher conservation of the HA receptor-binding site. *Virology* 233:224–34
198. Matthaei M, Budt M, Wolff T (2013) Highly pathogenic H5N1 influenza A virus strains provoke heterogeneous IFN- α/β responses that distinctively affect viral propagation in human cells. *PLoS One* 8:e56659
199. Matthys H, Eisebitt R, Seith B, Heger M (2003) Efficacy and safety of an extract of *Pelargonium sidoides* (EPs 7630) in adults with acute bronchitis. A randomised, double-blind, placebo-controlled trial. *Phytomedicine* 10 Suppl 4:7–17
200. Matthys H, Heger M (2007) Treatment of acute bronchitis with a liquid herbal drug preparation from *Pelargonium sidoides* (EPs 7630): a randomised, double-blind, placebo-controlled, multicentre study. *Curr Med Res Opin* 23:323–331
201. Mibayashi M, Martínez-Sobrido L, Loo YM, Cárdenas WB, Gale M, Garcia-Sastre A (2007) Inhibition of retinoic acid-inducible gene I-mediated induction of beta interferon by the NS1 protein of influenza A virus. *J Virol* 81:514–24
202. Michaelis M, Doerr HW, Cinatl J (2011) Investigation of the influence of EPs® 7630, a herbal drug preparation from *Pelargonium sidoides*, on replication of a broad panel of respiratory viruses. *Phytomedicine* 18:384–6
203. Min JY, Krug RM (2006) The primary function of RNA binding by the influenza A virus NS1 protein in infected cells: Inhibiting the 2'-5' oligo (A) synthetase/RNase L pathway. *Proc Natl Acad Sci U S A* 103:7100–5
204. Minoda K, Ichikawa T, Katsumata T, Onobori KI, Mori T, Suzuki Y, Ishii T, Nakayama T (2010) Influence of the galloyl moiety in tea catechins on binding affinity for human serum albumin. *J Nutr Sci Vitaminol (Tokyo)* 56:331–4
205. Mo IP, Brugh M, Fletcher OJ, Rowland GN, Swayne DE (1997) Comparative pathology of chickens experimentally inoculated with avian influenza viruses of low and high pathogenicity. *Avian Dis* 41:125–36

-
206. Moltedo B, López CB, Pazos M, Becker MI, Hermesh T, Moran TM (2009) Cutting edge: stealth influenza virus replication precedes the initiation of adaptive immunity. *J Immunol* 183:3569–73
 207. Monto AS, McKimm-Breschkin JL, Macken C, Hampson AW, Hay A, Klimov A, Tashiro M, Webster RG, Aymard M, Hayden FG, Zambon M (2006) Detection of influenza viruses resistant to neuraminidase inhibitors in global surveillance during the first 3 years of their use. *Antimicrob Agents Chemother* 50:2395–402
 208. Moscona A (2009) Global transmission of oseltamivir-resistant influenza. *N Engl J Med* 360:953–6
 209. Mosley VM, Wyckoff RWG (1946) Electron micrography of the virus of influenza. *Nature* 157:263
 210. Moss RB, Hansen C, Sanders RL, Hawley S, Li T, Steigbigel RT (2012) A phase II study of DAS181, a novel host directed antiviral for the treatment of influenza infection. *J Infect Dis* 206:1844–51
 211. Mössler C, Groiss F, Wolzt M, Wolschek M, Seipelt J, Muster T (2013) Phase I/II trial of a replication-deficient trivalent influenza virus vaccine lacking NS1. *Vaccine* 31:6194–200
 212. Müller KH, Kainov DE, Bakkouri K El, Saelens X, Brabander JK De, Kittel C, Sasm E, Muller CP (2011) The proton translocation domain of cellular vacuolar ATPase provides a target for the treatment of influenza A virus infections. *Br J Pharmacol* 164:344–57
 213. Munster VJ, Schrauwen EJ, Wit E de, Brand JMA van den, Bestebroer TM, Herfst S, Rimmelzwaan GF, Osterhaus ADME, Fouchier R a M (2010) Insertion of a multibasic cleavage motif into the hemagglutinin of a low-pathogenic avian influenza H6N1 virus induces a highly pathogenic phenotype. *J Virol* 84:7953–60
 214. Nakajima K, Desselberger U, Palese P (1978) Recent human influenza A (H1N1) viruses are closely related genetically to strains isolated in 1950. *Nature* 274:334–9
 215. Nakayama M, Suzuki K, Toda M, Okubo S, Hara Y, Shimamura T (1993) Inhibition of the infectivity of influenza virus by tea polyphenols. *Antiviral Res* 21:289–99
 216. Nance CL, Shearer WT (2003) Is green tea good for HIV-1 infection? *J Allergy Clin Immunol* 112:851–3
 217. Nayak DP, Hui EKW, Barman S (2004) Assembly and budding of influenza virus. *Virus Res* 106:147–65
 218. Nelson MI, Vincent AL, Kitikoon P, Holmes EC, Gramer MR (2012) Evolution of novel reassortant A/H3N2 influenza viruses in North American swine and humans, 2009–2011. *J Virol* 86:8872–8
 219. Nemeroff ME, Qian XY, Krug RM (1995) The influenza virus NS1 protein forms multimers in vitro and in vivo. *Virology* 212:422–8
 220. Nemeroff ME, Barabino SM, Li Y, Keller W, Krug RM (1998) Influenza virus NS1 protein interacts with the cellular 30 kDa subunit of CPSF and inhibits 3' end formation of cellular pre-mRNAs. *Mol Cell* 1:991–1000
 221. Neumann G, Zobel A, Hobom G (1994) RNA polymerase I-mediated expression of influenza viral RNA molecules. *Virology* 202:477–9

222. Neumann G, Watanabe T, Ito H, Watanabe S, Goto H, Gao P, Hughes M, Perez DR, Donis R, Hoffmann E, Hobom G, Kawaoka Y (1999) Generation of influenza A viruses entirely from cloned cDNAs. *Proc Natl Acad Sci U S A* 96:9345–9350
223. Neumann G, Kawaoka Y (2002) Generation of influenza A virus from cloned cDNAs—historical perspective and outlook for the new millenium. *Rev Med Virol* 12:13–30
224. Neumann G, Noda T, Kawaoka Y (2009) Emergence and pandemic potential of swine-origin H1N1 influenza virus. *Nature* 459:931–9
225. Nguyen JT, Hoopes JD, Le MH, Smee DF, Patick AK, Faix DJ, Blair PJ, Jong MD de, Prichard MN, Went GT (2010) Triple combination of amantadine, ribavirin, and oseltamivir is highly active and synergistic against drug resistant influenza virus strains in vitro. *PLoS One* 5:e9332
226. Notka F, Meier G, Wagner R (2004) Concerted inhibitory activities of *Phyllanthus amarus* on HIV replication in vitro and ex vivo. *Antiviral Res* 64:93–102
227. O’Neill RE, Talon J, Palese P (1998) The influenza virus NEP (NS2 protein) mediates the nuclear export of viral ribonucleoproteins. *EMBO J* 17:288–296
228. Octaviani CP, Ozawa M, Yamada S, Goto H, Kawaoka Y (2010) High level of genetic compatibility between swine-origin H1N1 and highly pathogenic avian H5N1 influenza viruses. *J Virol* 84:10918–10922
229. Oldham MJ, Robinson RJ (2007) Predicted tracheobronchial and pulmonary deposition in a murine asthma model. *Anat Rec* 290:1309–1314
230. Olsen B, Munster VJ, Wallensten A, Waldenström J, Osterhaus ADME, Fouchier RAM (2006) Global patterns of influenza a virus in wild birds. *Science* 312:384–8
231. Olsen CW (2002) The emergence of novel swine influenza viruses in North America. *Virus Res* 85:199–210
232. Ono N, Tatsuo H, Hidaka Y, Aoki T, Minagawa H, Yanagi Y (2001) Measles viruses on throat swabs from measles patients use signaling lymphocytic activation molecule (CDw150) but not CD46 as a cellular receptor. *J Virol* 75:4399–401
233. Ostrowsky B, Huang A, Terry W, Anton D, Brunagel B, Traynor L, Abid S, Johnson G, Kacica M, Katz JM, Edwards L, Lindstrom S, Klimov A, Uyeki TM (2012) Low pathogenic avian influenza A (H7N2) virus infection in immunocompromised adult, New York, USA, 2003. *Emerg Infect Dis* 18:1128–31
234. Oxford JS (2000) Influenza A pandemics of the 20th century with special reference to 1918: virology, pathology and epidemiology. *Rev Med Virol* 10:119–33
235. Palese P, Tobita K, Ueda M, Compans RW (1974) Characterization of temperature sensitive influenza virus mutants defective in neuraminidase. *Virology* 61:397–410
236. Palese P, Compans RW (1976) Inhibition of influenza virus replication in tissue culture by 2-deoxy-2,3-dehydro-N-trifluoroacetylneuraminic acid (FANA): mechanism of action. *J Gen Virol* 33:159–63
237. Pastene E, Speisky H, García A, Moreno J, Troncoso M, Figueroa G, Garcia A (2010) In vitro and in vivo effects of apple peel polyphenols against *Helicobacter pylori*. *J Agric Food Chem* 58:7172–7179
238. Peiris M, Yuen KY, Leung CW, Chan KH, Ip PL, Lai RW, Orr WK, Shortridge KF (1999) Human infection with influenza H9N2. *Lancet* 354:916–7

-
239. Peiris JSM, Yu WC, Leung CW, Cheung CY, Ng WF, Nicholls JM, Ng TK, Chan KH, Lai ST, Lim WL, Yuen KY, Guan Y (2004) Re-emergence of fatal human influenza A subtype H5N1 disease. *Lancet* 363:617–9
240. Pensaert M, Ottis K, Vandeputte J, Kaplan MM, Bachmann PA (1981) Evidence for the natural transmission of influenza A virus from wild ducts to swine and its potential importance for man. *Bull World Health Organ* 59:75–8
241. Pereira da Silva A, Rocha R, Silva CM, Mira L, Duarte MF, Florêncio MH (2000) Antioxidants in medicinal plant extracts. A research study of the antioxidant capacity of *Crataegus*, *Hamamelis* and *Hydrastis*. *Phytother Res* 14:612–6
242. Perez-Padilla R, la Rosa-Zamboni D de, Ponce de Leon S, Hernandez M, Quiñones-Falconi F, Bautista E, Ramirez-Venegas A, Rojas-Serrano J, Ormsby CE, Corrales A, Higuera A, Mondragon E, Cordova-Villalobos JA (2009) Pneumonia and respiratory failure from swine-origin influenza A (H1N1) in Mexico. *N Engl J Med* 361:680–9
243. Pica N, Hai R, Krammer F, Wang TT, Maamary J, Eggink D, Tan GS, Krause JC, Moran T, Stein CR, Banach D, Wrammert J, Belshe RB, Garcia-Sastre A, Palese P (2012) Hemagglutinin stalk antibodies elicited by the 2009 pandemic influenza virus as a mechanism for the extinction of seasonal H1N1 viruses. *Proc Natl Acad Sci U S A* 109:2573–8
244. Pichlmair A, Schulz O, Tan CP, Näslund TI, Liljeström P, Weber F, Reis e Sousa C (2006) RIG-I-mediated antiviral responses to single-stranded RNA bearing 5'-phosphates. *Science* 314:997–1001
245. Pinto LH, Lamb RA (2007) Controlling influenza virus replication by inhibiting its proton channel. *Mol Biosyst* 3:18–23
246. Plataniias LC (2005) Mechanisms of type-I- and type-II-interferon-mediated signalling. *Nat Rev Immunol* 5:375–86
247. Pleschka S, Wolff T, Ehrhardt C, Hobom G, Planz O, Rapp UR, Ludwig S (2001) Influenza virus propagation is impaired by inhibition of the Raf/MEK/ERK signalling cascade. *Nat Cell Biol* 3:301–5
248. Pleschka S, Stein M, Schoop R, Hudson JB (2009) Anti-viral properties and mode of action of standardized *Echinacea purpurea* extract against highly pathogenic avian influenza virus (H5N1, H7N7) and swine-origin H1N1 (S-OIV). *Virology* 6:197
249. Plotch SJ, Bouloy M, Ulmanen I, Krug RM (1981) A unique cap(m7GpppXm)-dependent influenza virion endonuclease cleaves capped RNAs to generate the primers that initiate viral RNA transcription. *Cell* 23:847–58
250. Potter CW (2001) A history of influenza. *J Appl Microbiol* 91:572–9
251. Qi X, Qian YH, Bao C, Guo XL, Cui LB, Tang FY, Ji H, Huang Y, Cai PQ, Lu B, Xu K, Shi C, Zhu FC, Zhou MH, Wang H (2013) Probable person to person transmission of novel avian influenza A (H7N9) virus in Eastern China, 2013: epidemiological investigation. *BMJ* 347:f4752
252. Qian XY, Chien CY, Lu Y, Montelione GT, Krug RM (1995) An amino-terminal polypeptide fragment of the influenza virus NS1 protein possesses specific RNA-binding activity and largely helical backbone structure. *RNA* 1:948–56
253. Raabe O, Al-Bayati M, Teague S, Rasolt A (1988) Regional deposition of inhaled monodisperse coarse and fine aerosol particles in small laboratory animals. *Ann Occ Hyg* 32 inhaled:53–63

254. Rajsbaum R, Albrecht RA, Wang MK, Maharaj NP, Versteeg G a, Nistal-Villán E, Garcia-Sastre A, Gack MU (2012) Species-specific inhibition of RIG-I ubiquitination and IFN induction by the influenza A virus NS1 protein. *PLoS Pathog* 8:e1003059
255. Reagan-Shaw S, Nihal M, Ahmad N (2008) Dose translation from animal to human studies revisited. *FASEB J* 22:659–661
256. Reeth K van (2007) Avian and swine influenza viruses: our current understanding of the zoonotic risk. *Vet Res* 38:243–60
257. Reid SM, Cox WJ, Ceeraz V, Sutton D, Essen SC, Howard WA, Slomka MJ, Irvine RM, Brown IH (2012) First reported detection of influenza A (H1N1)pdm09 in turkeys in the United Kingdom. *Avian Dis* 56:1062–7
258. Richardson JC, Akkina RK (1991) NS2 protein of influenza virus is found in purified virus and phosphorylated in infected cells. *Arch Virol* 116:69–80
259. Rimmelzwaan GF, Baars MM, Lijster P de, Fouchier RAM, Osterhaus AD (1999) Inhibition of influenza virus replication by nitric oxide. *J Virol* 73:8880–8883
260. Roberts WK, Hovanessian A, Brown RE, Clemens MJ, Kerr IM (1976) Interferon-mediated protein kinase and low-molecular-weight inhibitor of protein synthesis. *Nature* 264:477–80
261. Rogers GN, Paulson JC (1983) Receptor determinants of human and animal influenza virus isolates: differences in receptor specificity of the H3 hemagglutinin based on species of origin. *Virology* 127:361–73
262. Romanova J, Krenn BM, Wolschek M, Ferko B, Romanovskaja-Romanko E, Morokutti A, Shurygina AP, Nakowitsch S, Ruthsatz T, Kiefmann B, König U, Bergmann M, Sachet M, Balasingam S, Mann A, Oxford J, Slais M, Kiselev O, Muster T, Egorov A (2009) Preclinical evaluation of a replication-deficient intranasal DeltaNS1 H5N1 influenza vaccine. *PLoS One* 4:e5984
263. Rossignol J-F, Kabil SM, El-Gohary Y, Younis AM (2006) Effect of nitazoxanide in diarrhea and enteritis caused by *Cryptosporidium* species. *Clin Gastroenterol Hepatol* 4:320–4
264. Rossignol JF, Frazia S La, Chiappa L, Ciucci A, Santoro MG (2009) Thiazolides, a new class of anti-influenza molecules targeting viral hemagglutinin at the post-translational level. *J Biol Chem* 284:29798–808
265. Rossman JS, Lamb RA (2011) Influenza virus assembly and budding. *Virology* 411:229–36
266. Sánchez-Tena S, Fernández-Cachón ML, Carreras A, Mateos-Martín ML, Costoya N, Moyer MP, Nuñez MJ, Torres JL, Cascante M (2012) Hamamelitannin from witch hazel (*Hamamelis virginiana*) displays specific cytotoxic activity against colon cancer cells. *J Nat Prod* 75:26–33
267. Sarni-Manchado P, Cheynier V, Moutounet M (1999) Interactions of grape seed tannins with salivary proteins. *J Agric Food Chem* 47:42–7
268. Sasaki H, Matsumoto M, Tanaka T, Maeda M, Nakai M, Hamada S, Ooshima T (2004) Antibacterial activity of polyphenol components in oolong tea extract against *Streptococcus mutans*. *Caries Res* 38:2–8

-
269. Satterly N, Tsai PL, Deursen J van, Nussenzweig DR, Wang Y, Faria PA, Levay A, Levy DE, Fontoura BMA (2007) Influenza virus targets the mRNA export machinery and the nuclear pore complex. *Proc Natl Acad Sci U S A* 104:1853–8
270. Schnitzler P, Schneider S, Stintzing FC, Carle R, Reichling J (2008) Efficacy of an aqueous *Pelargonium sidoides* extract against herpesvirus. *Phytomedicine* 15:1108–1116
271. Schoetz K, Erdelmeier CA, Germer S, Hauer H (2008) A detailed view on the constituents of EPs 7630. *Planta Med* 74:667–674
272. Scholtissek C, Rohde W, Hoyningen V Von, Rott R (1978) On the origin of the human influenza virus subtypes H2N2 and H3N2. *Virology* 87:13–20
273. Scholtissek C, Spring SB (1982) Extragenic suppression of temperature-sensitive mutations in RNA segment 8 by replacement of different rna segments with those of other influenza A virus prototype strains. *Virology* 118:28–34
274. Scholtissek C, Bürger H, Kistner O, Shortridge KF (1985) The nucleoprotein as a possible major factor in determining host specificity of influenza H3N2 viruses. *Virology* 147:287–94
275. Scholtissek C (1990) Pigs as mixing vessels for the creation of new pandemic influenza A viruses. *Med Princ Pr* 2:65–71
276. Schötz K, Nöldner M (2007) Mass spectroscopic characterisation of oligomeric proanthocyanidins derived from an extract of *Pelargonium sidoides* roots (EPs 7630) and pharmacological screening in CNS models. *Phytomedicine* 14 Suppl 6:32–39
277. Schulman JL, Kilbourne ED (1969) Independent variation in nature of hemagglutinin and neuraminidase antigens of influenza virus: distinctiveness of hemagglutinin antigen of Hong Kong-68 virus. *Proc Natl Acad Sci U S A* 63:326–33
278. Selman M, Dankar SK, Forbes NE, Jia JJ, Brown EG (2012) Adaptive mutation in influenza A virus non-structural gene is linked to host switching and induces a novel protein by alternative splicing. *Emerg Microbes Infect* 1:e42
279. Seo SH, Hoffmann E, Webster RG (2002) Lethal H5N1 influenza viruses escape host anti-viral cytokine responses. *Nat Med* 8:950–954
280. Seong BL, Brownlee GG (1992) A new method for reconstituting influenza polymerase and RNA in vitro: a study of the promoter elements for cRNA and vRNA synthesis in vitro and viral rescue in vivo. *Virology* 186:247–60
281. Seto JT, Rott R (1966) Functional significance of sialidase during influenza virus multiplication. *Virology* 30:731–7
282. Shapiro GI, Gurney T, Krug RM (1987) Influenza virus gene expression: control mechanisms at early and late times of infection and nuclear-cytoplasmic transport of virus-specific RNAs. *J Virol* 61:764–73
283. Shelton H, Smith M, Hartgroves L, Stilwell P, Roberts K, Johnson B, Barclay W (2012) An influenza reassortant with polymerase of pH1N1 and NS gene of H3N2 influenza A virus is attenuated in vivo. *J Gen Virol* 93:998–1006
284. Sheu TG, Fry AM, Garten RJ, Deyde VM, Shwe T, Bullion L, Peebles PJ, Li Y, Klimov AI, Gubareva L V (2011) Dual resistance to adamantanes and oseltamivir among seasonal influenza A(H1N1) viruses: 2008-2010. *J Infect Dis* 203:13–17
285. Shinya K, Ebina M, Yamada S, Ono M, Kasai N, Kawaoka Y (2006) Avian flu: influenza virus receptors in the human airway. *Nature* 440:435–6

286. Shinya K, Makino a, Kawaoka Y (2010) Emerging and reemerging influenza virus infections. *Vet Pathol* 47:53–7
287. Shope RE (1931) Swine Influenza: III. Filtration experiments and etiology. *J Exp Med* 54:373–85
288. Skehel JJ, Hay AJ (1978) Nucleotide sequences at the 5' termini of influenza virus RNAs and their transcripts. *Nucleic Acids Res* 5:1207–19
289. Slemons RD, Johnson DC, Osborn JS, Hayes F (1974) Type-A influenza viruses isolated from wild free-flying ducks in California. *Avian Dis* 18:119–24
290. Smee DF, Hurst BL, Wong M-H, Tarbet EB, Babu YS, Klumpp K, Morrey JD (2010) Combinations of oseltamivir and peramivir for the treatment of influenza A (H1N1) virus infections in cell culture and in mice. *Antiviral Res* 88:38–44
291. Smith GJD, Vijaykrishna D, Bahl J, Lycett SJ, Worobey M, Pybus OG, Ma SK, Cheung CL, Raghvani J, Bhatt S, Peiris JSM, Guan Y, Rambaut A (2009) Origins and evolutionary genomics of the 2009 swine-origin H1N1 influenza A epidemic. *Nature* 459:1122–5
292. Solórzano A, Webby RJ, Lager KM, Janke BH, Garcia-Sastre A, Richt JA (2005) Mutations in the NS1 protein of swine influenza virus impair anti-interferon activity and confer attenuation in pigs. *J Virol* 79:7535–43
293. Solorzano A, Song H, Hickman D, Perez DR (2007) Pandemic influenza: preventing the emergence of novel strains and countermeasures to ameliorate its effects. *Infect Disord Drug Targets* 7:304–317
294. Song JM, Lee KH, Seong BL (2005) Antiviral effect of catechins in green tea on influenza virus. *Antivir Res* 68:66–74
295. Song MS, Pascua PN, Lee JH, Baek YH, Park KJ, Kwon HI, Park SJ, Kim CJ, Kim H, Webby RJ, Webster RG, Choi YK (2011) Virulence and genetic compatibility of polymerase reassortant viruses derived from the pandemic (H1N1) 2009 influenza virus and circulating influenza A viruses. *J Virol* 85:6275–6286
296. Spencer JP, Chaudry F, Pannala AS, Srail SK, Debnam E, Rice-Evans C (2000) Decomposition of cocoa procyanidins in the gastric milieu. *Biochem Biophys Res Commun* 272:236–241
297. Squires RB, Noronha J, Hunt V, Garcia-Sastre A, Macken C, Baumgarth N, Suarez D, Pickett BE, Zhang Y, Larsen CN, Ramsey A, Zhou L, Zaremba S, Kumar S, Deitrich J, Klem E, Scheuermann RH (2012) Influenza research database: an integrated bioinformatics resource for influenza research and surveillance. *Influenza Other Respi Viruses* 6:404–16
298. Stech J, Stech O, Herwig A, Altmeyen H, Hundt J, Gohrbandt S, Kreibich A, Weber S, Klenk HD, Mettenleiter TC (2008) Rapid and reliable universal cloning of influenza A virus genes by target-primed plasmid amplification. *Nucleic Acids Res* 36:e139
299. Stech O, Veits J, Weber S, Deckers D, Schröer D, Vahlenkamp TW, Breithaupt A, Teifke J, Mettenleiter TC, Stech J (2009) Acquisition of a polybasic hemagglutinin cleavage site by a low-pathogenic avian influenza virus is not sufficient for immediate transformation into a highly pathogenic strain. *J Virol* 83:5864–8
300. Steel J, Lowen AC, Wang TT, Yondola M, Gao Q, Haye K, Garcia-Sastre A, Palese P (2010) Influenza virus vaccine based on the conserved hemagglutinin stalk domain. *MBio* 1:e00018–10

301. Steinmann J, Buer J, Pietschmann T, Steinmann E (2013) Anti-infective properties of epigallocatechin-3-gallate (EGCG), a component of green tea. *Br J Pharmacol* 168:1059–73
302. Stieneke-Gröber A, Vey M, Angliker H, Shaw E, Thomas G, Roberts C, Klenk HD, Garten W (1992) Influenza virus hemagglutinin with multibasic cleavage site is activated by furin, a subtilisin-like endoprotease. *EMBO J* 11:2407–14
303. Subbarao EK, London W, Murphy BR (1993) A single amino acid in the PB2 gene of influenza A virus is a determinant of host range. *J Virol* 67:1761–4
304. Subbarao K (1998) Characterization of an Avian Influenza A (H5N1) Virus Isolated from a Child with a Fatal Respiratory Illness. *Science* (80-) 279:393–396
305. Sun Y, Qin K, Wang J, Pu J, Tang Q, Hu Y, Bi Y, Zhao X, Yang H, Shu Y, Liu J (2011) High genetic compatibility and increased pathogenicity of reassortants derived from avian H9N2 and pandemic H1N1/2009 influenza viruses. *Proc Natl Acad Sci U S A* 108:4164–4169
306. Sundararajan A, Ganapathy R, Huan L, Dunlap JR, Webby RJ, Kotwal GJ, Sangster MY (2010) Influenza virus variation in susceptibility to inactivation by pomegranate polyphenols is determined by envelope glycoproteins. *Antivir Res* 88:1–9
307. Takechi M, Tanaka Y, Takehara M, Nonaka GI, Nishioka I (1985) Structure and antiherpetic activity among the tannins. *Phytochemistry* 24:2245–2250
308. Takeda M, Ohno S, Seki F, Nakatsu Y, Tahara M, Yanagi Y (2005) Long untranslated regions of the measles virus M and F genes control virus replication and cytopathogenicity. *J Virol* 79:14346–54
309. Talon J, Salvatore M, O’Neill RE, Nakaya Y, Zheng H, Muster T, Garcia-Sastre A, Palese P (2000) Influenza A and B viruses expressing altered NS1 proteins: A vaccine approach. *Proc Natl Acad Sci U S A* 97:4309–14
310. Tam JS (2002) Influenza A (H5N1) in Hong Kong: an overview. *Vaccine* 20 Suppl 2:S77–81
311. Tan SL, Katze MG (1998) Biochemical and genetic evidence for complex formation between the influenza A virus NS1 protein and the interferon-induced PKR protein kinase. *J Interferon Cytokine Res* 18:757–66
312. Taubenberger JK, Reid AH, Lourens RM, Wang R, Jin G, Fanning TG (2005) Characterization of the 1918 influenza virus polymerase genes. *Nature* 437:889–93
313. Taubenberger JK, Kash JC (2010) Influenza virus evolution, host adaptation, and pandemic formation. *Cell Host Microbe* 7:440–51
314. Thäle C, Kiderlen A, Kolodziej H (2008) Anti-infective mode of action of EPs 7630 at the molecular level. *Planta Med* 74:675–81
315. Theisen LL, Muller CP (2012) EPs® 7630 (Umckaloabo®), an extract from *Pelargonium sidoides* roots, exerts anti-influenza virus activity in vitro and in vivo. *Antiviral Res* 94:147–56
316. Thomas PG, Dash P, Aldridge JR, Ellebedy AH, Reynolds C, Funk AJ, Martin WJ, Lamkanfi M, Webby RJ, Boyd KL, Doherty PC, Kanneganti TD (2009) The intracellular sensor NLRP3 mediates key innate and healing responses to influenza A virus via the regulation of caspase-1. *Immunity* 30:566–75

317. Tong S, Li Y, Rivaviller P, Conrardy C, Castillo DAA, Chen LM, Recuenco S, Ellison JA, Davis CT, York IA, Turmelle AS, Moran D, Rogers S, Shi M, Tao Y, Weil MR, Tang K, Rowe LA, Sammons S, Xu X, Frace M, Lindblade KA, Cox NJ, Anderson LJ, Rupprecht CE, Donis RO (2012) A distinct lineage of influenza A virus from bats. *Proc Natl Acad Sci U S A* 109:4269–74
318. Tong S, Zhu X, Li Y, Shi M, Zhang J, Bourgeois M, Yang H, Chen X, Recuenco S, Gomez J, Chen L-M, Johnson A, Tao Y, Dreyfus C, Yu W, McBride R, Carney PJ, Gilbert AT, Chang J, Guo Z, Davis CT, Paulson JC, Stevens J, Rupprecht CE, Holmes EC, Wilson I a, Donis RO (2013) New world bats harbor diverse influenza A viruses. *PLoS Pathog* 9:e1003657
319. Touriño S, Lizárraga D, Carreras A, Lorenzo S, Ugartondo V, Mitjans M, Vinardell MP, Juliá L, Cascante M, Torres JL (2008) Highly galloylated tannin fractions from witch hazel (*Hamamelis virginiana*) bark: electron transfer capacity, in vitro antioxidant activity, and effects on skin-related cells. *Chem Res Toxicol* 21:696–704
320. Treanor JJ, Snyder MH, London WT, Murphy BR (1989) The B allele of the NS gene of avian influenza viruses, but not the A allele, attenuates a human influenza A virus for squirrel monkeys. *Virology* 171:1–9
321. Tscherne DM, Garcia-Sastre A (2011) Virulence determinants of pandemic influenza viruses. *J Clin Invest* 121:6–13
322. Tumpey TM, Basler CF, Aguilar P V, Zeng H, Solórzano A, Swayne DE, Cox NJ, Katz JM, Taubenberger JK, Palese P, Garcia-Sastre A (2005) Characterization of the reconstructed 1918 Spanish influenza pandemic virus. *Science* 310:77–80
323. Tweed SA, Skowronski DM, David ST, Larder A, Petric M, Lees W, Li Y, Katz JM, Kraiden M, Tellier R, Halpert C, Hirst M, Astell C, Lawrence D, Mak A (2004) Human illness from avian influenza H7N3, British Columbia. *Emerg Infect Dis* 10:2196–9
324. Twu KY, Noah DL, Rao P, Kuo RL, Krug RM (2006) The CPSF30 binding site on the NS1A protein of influenza A virus is a potential antiviral target. *J Virol* 80:3957–65
325. Twu KY, Kuo RL, Marklund J, Krug RM (2007) The H5N1 influenza virus NS genes selected after 1998 enhance virus replication in mammalian cells. *J Virol* 81:8112–8121
326. Ueda K, Kawabata R, Irie T, Nakai Y, Tohya Y, Sakaguchi T (2013) Inactivation of pathogenic viruses by plant-derived tannins: strong effects of extracts from persimmon (*Diospyros kaki*) on a broad range of viruses. *PLoS One* 8:e55343
327. Veits J, Weber S, Stech O, Breithaupt A, Gräber M, Gohrbandt S, Bogs J, Hundt J, Teifke JP, Mettenleiter TC, Stech J (2012) Avian influenza virus hemagglutinins H2, H4, H8, and H14 support a highly pathogenic phenotype. *Proc Natl Acad Sci U S A* 109:2579–84
328. Vennat B, Pourrat H, Pouget MP, Gross D, Pourrat A (1988) Tannins from *Hamamelis virginiana*: identification of proanthocyanidins and hamamelitannin quantification in leaf, bark, and stem extracts. *Planta Med* 54:454–7
329. Vennat B, Gross D, Pourrat A, Pourrat H (1992) *Hamamelis virginiana*: identification and assay of proanthocyanidins, phenolic acids and flavonoids in leaf extracts. *Pharm Acta Helv* 67:11–14
330. Vey M, Orlich M, Adler S, Klenk HD, Rott R, Garten W (1992) Hemagglutinin activation of pathogenic avian influenza viruses of serotype H7 requires the protease recognition motif R-X-K/R-R. *Virology* 188:408–13

-
331. Vijaykrishna D, Poon LLM, Zhu HC, Ma SK, Li OTW, Cheung CL, Smith GJD, Peiris JSM, Guan Y (2010) Reassortment of pandemic H1N1/2009 influenza A virus in swine. *Science* 328:1529
332. Vries E van der, Stelma FF, Boucher CAB (2010) Emergence of a multidrug-resistant pandemic influenza A (H1N1) virus. *N Engl J Med* 363:1381–2
333. Wacheck V, Egorov A, Groiss F, Pfeiffer A, Fuereder T, Hoeflmayer D, Kundi M, Popow-Kraupp T, Redlberger-Fritz M, Mueller CA, Cinatl J, Michaelis M, Geiler J, Bergmann M, Romanova J, Roethl E, Morokutti A, Wolschek M, Ferko B, Seipelt J, Dick-Gudenus R, Muster T (2010) A novel type of influenza vaccine: safety and immunogenicity of replication-deficient influenza virus created by deletion of the interferon antagonist NS1. *J Infect Dis* 201:354–62
334. Wagner H (1999) *Pharmazeutische Biologie Band 2; Arzneidrogen und ihre Inhaltsstoffe*. Wissenschaftliche Verlagsgesellschaft Stuttgart, Stuttgart
335. Wagner R, Matrosovich M, Klenk HD (2002) Functional balance between haemagglutinin and neuraminidase in influenza virus infections. *Rev Med Virol* 12:159–66
336. Wahle E, Kühn U (1997) The mechanism of 3' cleavage and polyadenylation of eukaryotic pre-mRNA. *Prog Nucleic Acid Res Mol Biol* 57:41–71
337. Wahle E, Rügsegger U (1999) 3'-End processing of pre-mRNA in eukaryotes. *FEMS Microbiol Rev* 23:277–95
338. Walkiewicz MP, Basu D, Jablonski JJ, Geysen HM, Engel DA (2011) Novel inhibitor of influenza non-structural protein 1 blocks multi-cycle replication in an RNase L-dependent manner. *J Gen Virol* 92:60–70
339. Wang C, Wang J, Su W, Gao S, Luo J, Zhang M, Xie L, Liu S, Liu X, Chen Y, Jia Y, Zhang H, Ding H, He H (2014) Relationship Between Domestic and Wild Birds in Live Poultry Market and a Novel Human H7N9 Virus in China. *J Infect Dis* 209:34–7
340. Wang H, Provan GJ, Helliwell K (2003) Determination of hamamelitannin, catechins and gallic acid in witch hazel bark, twig and leaf by HPLC. *J Pharm Biomed Anal* 33:539–544
341. Wang J, Wu Y, Ma C, Fiorin G, Wang J, Pinto LH, Lamb RA, Klein ML, Degrado WF (2013) Structure and inhibition of the drug-resistant S31N mutant of the M2 ion channel of influenza A virus. *Proc Natl Acad Sci U S A* 110:1315–20
342. Wang TT, Tan GS, Hai R, Pica N, Ngai L, Ekiert DC, Wilson IA, Garcia-Sastre A, Moran TM, Palese P (2010) Vaccination with a synthetic peptide from the influenza virus hemagglutinin provides protection against distinct viral subtypes. *Proc Natl Acad Sci U S A* 107:18979–18984
343. Webster RG, Laver WG (1972) The origin of pandemic influenza. *Bull World Health Organ* 47:449–52
344. Webster RG, Bean WJ, Gorman OT, Chambers TM, Kawaoka Y (1992) Evolution and ecology of influenza A viruses. *Microbiol Rev* 56:152–79
345. Weis W, Brown JH, Cusack S, Paulson JC, Skehel JJ, Wiley DC (1988) Structure of the influenza virus haemagglutinin complexed with its receptor, sialic acid. *Nature* 333:426–31

346. Williamson MP, McCormick TG, Nance CL, Shearer WT (2006) Epigallocatechin gallate, the main polyphenol in green tea, binds to the T-cell receptor, CD4: Potential for HIV-1 therapy. *J Allergy Clin Immunol* 118:1369–74
347. Wise HM, Foeglein A, Sun J, Dalton RM, Patel S, Howard W, Anderson EC, Barclay WS, Digard P (2009) A complicated message: Identification of a novel PB1-related protein translated from influenza A virus segment 2 mRNA. *J Virol* 83:8021–8031
348. Wise HM, Hutchinson EC, Jagger BW, Stuart AD, Kang ZH, Robb N, Schwartzman LM, Kash JC, Fodor E, Firth AE, Gog JR, Taubenberger JK, Digard P (2012) Identification of a novel splice variant form of the influenza A virus M2 ion channel with an antigenically distinct ectodomain. *PLoS Pathog* 8:e1002998
349. Wolff HH, Kieser M (2007) Hamamelis in children with skin disorders and skin injuries: results of an observational study. *Eur J Pediatr* 166:943–8
350. Woo HM, Kim KS, Lee JM, Shim HS, Cho SJ, Lee WK, Ko HW, Keum YS, Kim SY, Pathinayake P, Kim CJ, Jeong YJ (2013) Single-stranded DNA aptamer that specifically binds to the influenza virus NS1 protein suppresses interferon antagonism. *Antiviral Res* 100:337–45
351. World Health Organization (2009a) Seasonal, animal and pandemic influenza: an overview. <http://influenzatraining.org/collect/whoinfluenza/files/s15546e/s15546e.ppt>, accessed January 14, 2014
352. World Health Organization (2009b) Fact sheet influenza (seasonal). <http://www.who.int/mediacentre/factsheets/fs211/en/index.html>, accessed February 14, 2013
353. World Health Organization (2013a) Cumulative number of confirmed human cases for avian influenza A(H5N1) reported to WHO, 2003-2013. http://www.who.int/influenza/human_animal_interface/EN_GIP_20131008CumulativeNumberH5N1cases.pdf, accessed December 16, 2013
354. World Health Organization (2013b) Number of confirmed human cases of avian influenza A(H7N9) reported to WHO. http://www.who.int/influenza/human_animal_interface/influenza_h7n9/10u_ReportWebH7N9Number.pdf, accessed December 16, 2013
355. World Health Organization (2013c) WHO Regional Office for Europe recommendations on influenza vaccination during the 2013/2014 winter season. http://www.euro.who.int/__data/assets/pdf_file/0009/217485/EURO_2013_2014-flu-vacc-rec-for-winter.pdf, accessed January 15, 2014
356. World Health Organization (2014) WHO Risk Assessment: Human infections with avian influenza A(H7N9) virus. http://www.who.int/influenza/human_animal_interface/RiskAssessment_H7N9_21Jan14.pdf, accessed January 29, 2014
357. Wurzer WJ, Ehrhardt C, Pleschka S, Berberich-Siebelt F, Wolff T, Walczak H, Planz O, Ludwig S (2004) NF-kappaB-dependent induction of tumor necrosis factor-related apoptosis-inducing ligand (TRAIL) and Fas/FasL is crucial for efficient influenza virus propagation. *J Biol Chem* 279:30931–7
358. Xu X, Subbarao, Cox NJ, Guo Y (1999) Genetic characterization of the pathogenic influenza A/Goose/Guangdong/1/96 (H5N1) virus: similarity of its hemagglutinin gene to those of H5N1 viruses from the 1997 outbreaks in Hong Kong. *Virology* 261:15–9

-
359. Yamashita M, Tomozawa T, Kakuta M, Tokumitsu A, Nasu H, Kubo S (2009) CS-8958, a prodrug of the new neuraminidase inhibitor R-125489, shows long-acting anti-influenza virus activity. *Antimicrob Agents Chemother* 53:186–92
360. Yan JH, Xiong Y, Yi CH, Sun XX, He QS, Fu W, Xu XK, Jiang JX, Ma L, Liu Q (2012) Pandemic (H1N1) 2009 virus circulating in pigs, Guangxi, China. *Emerg Infect Dis* 18:357–9
361. Yang CS, Lee MJ, Chen L (1999) Human salivary tea catechin levels and catechin esterase activities: implication in human cancer prevention studies. *Cancer Epidemiol Biomarkers Prev* 8:83–89
362. Yodsheewan R, Maneewatch S, Srimanote P, Thueng-In K, Songserm T, Dong-Din-On F, Bangphoomi K, Sookrung N, Choowongkamon K, Chaicumpa W (2013) Human monoclonal ScFv specific to NS1 protein inhibits replication of influenza viruses across types and subtypes. *Antiviral Res* 100:226–37
363. Zamarin D, Ortigoza MB, Palese P (2006) Influenza A virus PB1-F2 protein contributes to viral pathogenesis in mice. *J Virol* 80:7976–83
364. Zell R, Krumbholz A, Eitner A, Krieg R, Halbhuber K-J, Wutzler P (2007) Prevalence of PB1-F2 of influenza A viruses. *J Gen Virol* 88:536–46
365. Zhao J, Hyman L, Moore C (1999) Formation of mRNA 3' ends in eukaryotes: mechanism, regulation, and interrelationships with other steps in mRNA synthesis. *Microbiol Mol Biol Rev* 63:405–45
366. Zheng H, Lee HA, Palese P, Garcia-Sastre A (1999) Influenza A virus RNA polymerase has the ability to stutter at the polyadenylation site of a viral RNA template during RNA replication. *J Virol* 73:5240–3
367. Zhou H, Jin M, Chen H, Huag Q, Yu Z (2006) Genome-sequence analysis of the pathogenic H5N1 avian influenza A virus isolated in China in 2004. *Virus Genes* 32:85–95
368. Zhou NN, Senne DA, Landgraf JS, Swenson SL, Erickson G, Rossow K, Liu L, Yoon KJ, Krauss S, Webster RG (1999) Genetic reassortment of avian, swine, and human influenza A viruses in American pigs. *J Virol* 73:8851–6
369. Zhu M, Phillipson JD, Greengrass PM, Bowery NE, Cai Y (1997) Plant polyphenols: biologically active compounds or non-selective binders to protein? *Phytochemistry* 44:441–447
370. Zhu Q, Yang H, Chen W, Cao W, Zhong G, Jiao P, Deng G, Yu K, Yang C, Bu Z, Kawaoka Y, Chen HC-2224367 (2008) A naturally occurring deletion in its NS gene contributes to the attenuation of an H5N1 swine influenza virus in chickens. *J Virol* 82:220–228

8 Annexe

8.1 Publications

- Kainov DE, Müller KH, **Theisen LL**, Anastasina M, Kaloinen M, Muller CP (2011). Differential effects of NS1 proteins of human pandemic H1N1/2009, avian highly pathogenic H5N1, and low pathogenic H5N2 influenza A viruses on cellular pre-mRNA polyadenylation and mRNA translation. *J Biol Chem* 286: 7239-47.
- **Theisen LL**, Muller CP (2012). EPs® 7630 (Umckaloabo®), an extract from *Pelargonium sidoides* roots, exerts anti-influenza virus activity *in vitro* and *in vivo*, *Antiviral Research* 94: 147–56.
- **Theisen LL**, Erdelmeier CAJ, Spoden GA, Boukhallouk F, Sausy A, Florin L, Muller CP (2014). Tannins from *Hamamelis virginiana* bark extract: Characterization and improvement of the antiviral efficacy against influenza A virus and human papillomavirus. *PLOS ONE* 9: e88062.
- Denisova OV, Virtanen S, Von Schantz-Fant C, Bychkov D, Desloovere J, Soderholm S, **Theisen LL**, Tynell J, Ikonen N, Vashchinkina E, Nyman T, Matikainen S, Kallioniemi O, Julkunen I, Muller CP, Saelens X, Verkhusha V, Kainov DE (2014). Akt inhibitor MK2206 inhibits influenza A(H1N1)pdm2009 virus infection in vitro. Submitted.
- **Theisen LL**, Gohrbandt S, Kirschner SA, Sausy A, Brunnhöfer R, Stech J, Muller CP Characterization of pandemic H1N1/2009 influenza A virus reassortants carrying heterologous NS genes reveals a role of a naturally occurring NS1 five amino acid deletion in host gene regulation. In preparation.

8.2 Conference participations:

8.2.1 Oral presentations

- Theisen LL et al., “EPs® 7630, an extract from *Pelargonium sidoides* roots inhibits influenza A virus *in vitro* and *in vivo*”
15th SaarLorLux meeting on Virus Research, September 7, 2011, Remich, Luxembourg
- Theisen LL et al., “EPs® 7630 (Umckaloabo®), an extract from roots of *Pelargonium sidoides*, exerts anti-influenza virus activity *in vitro* and *in vivo*”
Société des Sciences Médicales Luxembourg, Séance de communications courtes, November 16, 2011, Luxembourg
- Theisen LL et al., “EPs® 7630 (Umckaloabo®), a root extract from *Pelargonium sidoides*, exerts anti-influenza virus activity *in vitro* and *in vivo*.”
University of Luxembourg Life Sciences PhD days 2012, September 11-12, 2012, Luxembourg
- Theisen LL et al., “Anti-influenza effect and structure-activity relations of polyphenols from *Hamamelis virginiana* bark.”
16th SaarLorLux Meeting on Virus Research, November 28, 2012, Nancy, France
- Theisen LL et al., “Construction and characterization of reassortant pandemic H1N1 influenza virus strains with NS genes of human, avian and pig origin.”
University of Luxembourg Life Sciences PhD days 2013, September 9-10, 2013, Luxembourg

8.2.2 Posters

- Theisen LL et al., “Strain-specific activities of NS1 proteins from three influenza A virus strains in cellular pre-mRNA polyadenylation and mRNA translation”

EMBO workshop viruses and innate immunity, May 5-7, 2010, Dublin, Ireland

- Theisen LL et al., “EPs® 7630 (Umckaloabo®), an extract from roots of *Pelargonium sidoides*, exerts anti-influenza virus activity *in vitro* and *in vivo*”

University of Luxembourg Life Sciences PhD days 2011, September 13-14, 2011, Luxembourg

- Theisen LL et al., “EPs® 7630 (Umckaloabo®), an extract from roots of *Pelargonium sidoides*, exerts anti-influenza virus activity *in vitro* and *in vivo*”

22nd Annual Meeting of the Society for Virology, March 14-17, 2012, Essen, Germany

- Theisen LL et al., “EPs® 7630 (Umckaloabo®), an extract from roots of *Pelargonium sidoides*, exerts anti-influenza virus activity *in vitro* and *in vivo*”

Third International Influenza Meeting, September 2-4, 2012, Münster, Germany

8.3 Acknowledgements

I would like to thank Prof. Dr. Claude P. Muller and Prof. Dr. Martina Sester for giving me the opportunity to do my PhD studies under their supervision. I am very grateful to Prof. Muller for his valuable scientific guidance, support and confidence throughout my whole PhD.

I especially thank Dr Sandra Gohrbandt for introducing me into the fascinating reverse genetics technique and for all her support, expertise, discussions and positiveness!

I would like to thank the Fonds National de la Recherche Luxembourg for financially supporting this study by an AFR PhD grant (Reference 2903120).



Moreover, I am grateful to Dr. Willmar Schwabe GmbH & Co. KG for financially supporting the studies on the antiviral efficacy of natural extracts. I would particularly like to thank Dr Clemens Erdelmeier and Dr Egon Koch for their enthusiastic involvement in this fruitful collaboration. I also thank all our collaborators and people who kindly provided materials, especially Dr Jürgen Stech, who contributed reverse genetics expression plasmids.

I would like to thank all my colleagues from the Department of Immunology at the CRP Santé for their support and always available advice, and not less for making our lab a fun place to work!

Special thanks go to Aurélie, Regina and Ombeline for their perfect technical assistance and more: with you, the pipetting marathons in the BSL2 were much more fun! I am grateful to Sophie F, Steph W, Nathalie and Vitor for all their help with the mice. Big thanks also to Nina, Anna, Sandra and Chantal for their helpful comments and corrections on this manuscript and for always having a funny story to tell!

I especially want to thank Chantal, the best office mate, for the great four years in office 2. Thanks for all the early morning “papotage” and your scientific and non-scientific support: both were invaluable!

Danke Stefan dass du selbst über die Entfernung immer für mich da bist. Deine Nerven wie Drahtseile waren Gold wert. Du hast mich immer wieder motiviert, aufgebaut und bestätigt. Gut dass du dir das Ganze bald aus der Nähe anhören kannst!

Als lescht géif ech gär mengen Elteren merci soen. Merci dass dir mech ennerstetzt an allem wat ech maachen an dass ech emmer op iech ziele kann. Ech ka mer keng besser Elteren virstellen ewéi iech!

Curriculum vitae

Linda Theisen

Personal details

Date of birth March 11, 1984
Place of birth Bad Pyrmont, Germany
Nationality Luxembourgish and German

Education

1996-2003 Secondary school
 Athénée de Luxembourg, Luxembourg

2003-2009 Pharmacy studies
 Albert-Ludwigs-Universität Freiburg, Germany

Sept 2006-Feb 2007 ERASMUS program
 University of Montpellier 1, France

May-Nov 2008 Pharmacy internship
 Apotheke am Theater, Freiburg, Germany

Nov 2008-May 2009 Research internship
 Topic: "Gene therapy of type I diabetes mediated by adeno-associated
 virus"
 University of Florida, Gainesville, USA

July 2009 Graduation as a pharmacist
 Albert-Ludwigs-Universität Freiburg, Germany

Sept 2009-Nov 2013 PhD studies

Department of Immunology,

Centre de Recherche Public de la Santé, Luxembourg

and

Universität des Saarlandes, Homburg/Saar, Germany

Topic: Influenza A Virus Preparedness: Characterization of NS Gene

Reassortants and the Antiviral Efficacy of Tannin-rich Plant Extracts